Universität Bonn

Helmholtz-Institut für Strahlen- und Kernphysik

Phenomenology of the QCD θ-angle and axions in nuclear and particle physics

Thomas Vonk

Helmholtz-Institut für
Strahlen- und Kernphysik
Universität Bonn
Nussallee 14–16
D-53115 Bonn

Phenomenology of the QCD θ-angle and axions in nuclear and particle physics

Dissertation

zur

Erlangung des Doktorgrades (Dr. rer. nat.)

der

Mathematisch-Naturwissenschaftlichen Fakultät

der

Rheinischen Friedrich-Wilhelms-Universität Bonn

von

Thomas Vonk

aus

Tönisvorst

Bonn, 2022

Zusammenfassung/Abstract

Zusammenfassung

Diese Dissertation ist eine Sammlung von Studien, welche sich mit der Phänomenologie des θ-Winkels der Quantenchromodynamik (QCD) im Wertebereich $0 < \theta < \pi$, sowie des Axions in der Kern- und Teilchenphysik befassen. Im ersten Teil werden die Auswirkungen eines von Null verschiedenen θ-Winkels auf die Nukleonmassen, die Bindungsenergien leichter Kerne und den Prozess der Nukleosynthese erforscht. In den darauf folgenden Studien werden die Wechselwirkungen des Axions mit Photonen und Baryonen mit den Mitteln der Chiralen Störungstheorie – der effektiven Feldtheorie der starken Wechselwirkung im Niedrigenergiebereich – untersucht. Die Ergebnisse werden schließlich verwendet, um den Wirkungsquerschnitt der Pionerzeugung durch Axion-Nukleon-Wechselwirkung mit Beiträgen der Δ-Resonanz zu bestimmen. All diese Studien stehen somit im Zusammenhang mit dem als "Strong CP Problem" bekannten Makel des Standardmodells der Teilchenphysik, wobei insbesondere die letztgenannten Studien auch Beiträge zur Axionsuche darstellen.

Abstract

This thesis is a collection of studies concerned with the phenomenology of the θ-angle of quantum chromodynamics (QCD) at values $0 < \theta < \pi$, and of the axion in nuclear and particle physics. In the first part, the consequences of a non-vanishing θ-angle for nuclear physics are determined with respect to the nucleon masses, the binding energies of light nuclei, and the process of nucleosynthesis. In the second part, the interaction of axions with photons and baryons is examined making use of chiral perturbation theory, the low-energy effective field theory of the strong interaction part of the Standard Model. Finally, these insights are used to determine the cross section of pion axioproduction with contributions from the Δ resonance. All these studies hence are related to a flaw of the Standard Model of Particle Physics known in the literature as the "strong CP problem". In particular, the latter studies are contributions to the search of axions.

Contents

Introduction

1.1 You got a problem?

The Standard Model (SM) of particle physics is the outcome of decades of tremendous research efforts comprising milestone events on both experimental and theoretical side. The last century has seen the prediction and discovery of numerous elementary particles that like pieces of a puzzle led to the emergence of a coherent picture. On the experimental side this includes the discovery of antiparticles such as the positron [1], the discovery of heavy partners of the electron, i.e. the muon [2] and the tau [3], the discovery of parity violation in the weak interaction [4], the discovery of new generations of neutrinos [5], and the detection of the Z and W vector gauge bosons [6–10]. Starting with the quark hypothesis (see below) and deep inelastic scattering experiments [11, 12] accessing the substructure of nucleons, quarks finally have been identified as the elementary constituents of hadrons systematizing the ever-growing number of experimentally produced mesons and baryons, which culminated in the discovery of the top quark at the end of the last century [13, 14].

These great moments of experimental physics were accompanied and in fact most often preceded by equally great hours of theoretical physics which includes the derivation of a relativistic field equation for spin-$\frac{1}{2}$ particles including the prediction of antimatter by Dirac [15], the development of quantum electrodynamics [16–22] (QED), the extension of gauge theories to non-Abelian groups [23–25] now being called Yang–Mills theory, the electroweak unification [26–28], the Higgs mechanism [29–31] (Englert–Brout–Higgs–Guralnik–Hagen–Kibble mechanism to be precise), the development of quantum chromodynamics [32–38] (QCD), and the verification of the renormalizability of such gauge theories [39, 40].[1]

The last great highlight of this unprecedented human endeavor was the discovery of the Higgs boson [41, 42], the period of the last sentence of a book with a large number of instructive chapters. This model with its story of success has proven to be both highly explanatory and predictive, and in terms of its mathematical formulation, its realized exact and approximate symmetries, it can be considered an elegant building of modern architecture.

And it has proven to be, say, unpleasant.

One of the most unpleasant things about the SM is the large number of input parameters, which is

---

[1] The list of "milestones" is of course incomplete and rather a personal collection of works the author considers fundamental. In reality, the Standard Model is not the completed picture of a puzzle consisting of, say, fifty pieces, but rather consisting of a puzzle of hundreds or even thousands of pieces.

surprising considering the fact that the fermionic matter fields clearly show a pattern in terms of their charges and their masses (generations). Currently, no mechanism neither within nor beyond the SM is known to explain this pattern. In fact, the SM with massless neutrinos requires the manual input of 19 parameters.[2] Further phenomena that currently cannot be explained within the SM are, for instance, neutrino oscillations implying massive (though very light) neutrinos [44–50],[3] the possible existence of particle dark matter (see, e.g., the reviews [55–58]), or possibly the recently measured anomalous magnetic dipole moment of the muon [59] (however, with 4.2 standard deviations this finding currently does not meet the 5σ criterion).

Another example of an unpleasant feature in the SM is the appearance of a CP non-conserving term in the strong interaction part of the SM Lagrangian, the θ-term. As will be explained in more detail in the next section, this term arises as a consequence of the instanton solution [60–62], but as opposed to this, no such CP violation has ever been observed within the strong interaction.[4] The associated QCD θ-angle, which determines the strength of this strong CP violation, turns out to be $\theta \lesssim 10^{-11}$ permitting that $\theta = 0$.[5] So on the one hand, there is the theoretical existence of the θ-term without any restriction to the value of θ (which means that given the periodicity of this angle, it might take on any value between $-\pi$ and $+\pi$), but on the other hand, in our real world, $\theta \approx 0$ of all things. This goes by the name of "strong CP problem".

In order to ponder the meaning of this problem, one might take a look at how this problem might be solved (or not solved), as it is related to the question of why certain aspects of the SM are considered "unsatisfying". Basically, there are four possibilities:

1. There might be some mechanism *within* the SM yet to be unraveled that shows that θ actually is restricted to a value of exactly or approximately zero.

2. It might be that the SM is incomplete and that an *extended* SM provides an explanation of the observed value of θ (this might include that $\theta \neq 0$ at earlier stages of the universe, but is then relaxed to its present value).

3. It might turn out that a new theory *beyond* the SM explains why θ is restricted to a value of exactly or approximately zero (including the possibility that $\theta \neq 0$ at earlier stages of the universe).

4. It might be the case that the observed value of θ is just accidental meaning there is no problem in the strict sense.

This list shows that a problem such as the "strong CP problem" (and the several other outstanding challenges of the SM mentioned above) is in any case the point of departure to fresh research leading to a deeper understanding of the physical world and the theories describing it. This even applies for the latter point: Taking the "accidental universe" as a starting point might stimulate the questions "What if θ had another value than the one we measure? Would a world with, for example, $\theta = \frac{\pi}{2}$ look different from ours?" The answers to such questions undoubtedly would deepen the understanding of the connection between the SM

---

[2] 9 fermion masses, 3 mixing angles and one CP-violating phase of the Cabibbo–Kobayashi–Maskawa matrix, the mass and vacuum expectation value of the Higgs, 3 gauge coupling constants, and θ (after Ref. [43]). If one includes neutrino masses and oscillations, 7 additional parameters appear: the 3 neutrino masses, and 3 mixing angles and one CP-violating phase of the Pontecorvo–Maki–Nakagawa–Sakata matrix.

[3] A possible extension of the SM explaining the origin of such tiny neutrino masses is the seesaw mechanism [51–54].

[4] In contrast to that, CP violation indeed is a feature of the weak interaction part of the SM [63, 64].

[5] This will be elaborated in more detail below. The actual observable parameter is usually denoted $\bar{\theta}$, but in this introduction, I simply write θ and refer to the next section for the details.

parameter θ and the observables of our world. Additionally, such considerations might give insights in terms of another, related question, that is: Is it *necessary* from an anthropic viewpoint that the quantity θ has exactly the observed value (or at least lies within a certain range), because otherwise there would be no human posing this question, e.g. if θ alters nuclear physics in such a way that element formation is seriously impaired.

As stated already, this also applies to all challenges of the SM, meaning that in principle any of the issues might be solved (or not solved) by one of the four points listed above (and possibly a single solution might solve more than one SM problem). But what would all that mean for the SM, this great model with its overwhelming success and its predictive and explanatory power? Without doubt, the SM as it stands will certainly never be entirely replaced by a theory beyond it. This is comparable to the case of Newtonian gravity and its successor general relativity: the new theory then simply shows the limits of validity of the old one.

Turning now to the topic of the present thesis, it is the above-mentioned "strong CP problem" that constitutes the starting point for the six studies presented in the main chapters of this thesis. In particular, we followed two paths, one of which has already been indicated above, namely the question of how $\theta \neq 0$ affects nuclear physics (ch. 2 and 3). The second of these two paths is related to the second possibility in the list above and is based on a solution to the "strong CP problem" that possibly can at the same time provide a solution to the question of the nature of dark matter (ch. 4–7). This solution is the famous Peccei–Quinn mechanism [65, 66], which naturally leads to a vanishing θ-angle, but also to a light boson called the axion.

This thesis is thus concerned with the *phenomenology* of the QCD θ-angle at values $\neq 0$, in particular its consequences for nuclear physics, and of the axion in nuclear and particle physics. The latter is performed in the context of chiral perturbation theory [67–73], the low-energy effective field theory of the strong interaction part of the SM. In particular, we studied its interaction with photons (ch. 4) and with baryonic matter (ch. 5 and ch. 6), where we used the insights from the latter to finally study pion axioproduction[6]. The results of these studies hence can be regarded as contributions to the search of axions and – in a greater context – to the question of how to solve (or not solve) one (or two) open problems of the SM, that is the unpleasant "strong CP problem".

1.2 Short theoretical overview

The following theoretical overview focuses on the origin of the QCD θ-vacuum and gives an introduction to the "strong CP problem" and possible solutions including the Peccei–Quinn mechanism and the axion. Other aspects such as the models and methods used in the several studies, are not presented here, but are each part of the respective papers, where in any case appropriate theoretical information is given.

1.2.1 Instantons and QCD vacuum structure

The QCD θ-vacuum is a consequence of the famous instanton solution in classical, non-linear gauge field theories [60].[7] Consider a non-Abelian pure Yang–Mills gauge theory with gauge group $\mathscr{G}$ [23] in

---

[6] The term axioproduction has been proposed by Ulf-G. Meißner in analogy to terms like electroproduction or photoproduction. Pion axioproduction hence means pion production induced by axions.

[7] This chapter is freely based on Refs. [74–76].

four-dimensional Euclidean space E^4 with action

$$\mathscr{S} = \int \mathrm{d}^4 x \, \frac{1}{2} \operatorname{Tr}\left[G_{\mu\nu}G_{\mu\nu}\right], \tag{1.1}$$

where

$$G_{\mu\nu} = \frac{1}{2}\tau^a G^a_{\mu\nu} = \partial_\mu A_\nu - \partial_\nu A_\mu - ig\left[A_\mu, A_\nu\right] \tag{1.2}$$

is the field strength tensor in matrix notation, τ^a are the generators of the group $\mathscr{G}$ with group index a, $A_\mu = \frac{1}{2}\tau^a A^a_\mu$ are the gauge potentials, and g is the coupling constant of the gauge field. The commutators $[\,,\,]$ are determined by the corresponding Lie algebra of the group $\mathscr{G}$. The dual of $G_{\mu\nu}$ is defined by

$$\tilde{G}_{\mu\nu} = \frac{1}{2}\epsilon_{\mu\nu\rho\sigma}G_{\rho\sigma}, \tag{1.3}$$

where $\epsilon_{\mu\nu\rho\sigma}$ is the four-dimensional Levi-Civita symbol with $\epsilon_{1234} = 1$ for Euclidean space-time indexes $1 \dots 4$. The involved objects transform under a gauge transformation $U \in \mathscr{G}$ as

$$\begin{aligned}
A_\mu &\to U A_\mu U^{-1} - \frac{i}{g}(\partial_\mu U)U^{-1},\\
G_{\mu\nu} &\to U G_{\mu\nu} U^{-1},\\
\tilde{G}_{\mu\nu} &\to U \tilde{G}_{\mu\nu} U^{-1}.
\end{aligned} \tag{1.4}$$

Minimization of the action (1.1) leads to the classical field equations

$$D_\mu G_{\mu\nu} = 0 \tag{1.5}$$

with the covariant derivative

$$D_\mu G_{\mu\nu} = \partial_\mu G_{\mu\nu} - ig\left[A_\mu, G_{\mu\nu}\right]. \tag{1.6}$$

A solution to the field equation is found when $G_{\mu\nu}$ is self-dual or anti-self-dual, i.e.

$$G_{\mu\nu} = \pm\tilde{G}_{\mu\nu} \tag{1.7}$$

with the boundary condition

$$\lim_{x\to\infty} G_{\mu\nu}(x) = 0. \tag{1.8}$$

Of course, the field equation (1.5) is trivially satisfied if $A_\mu(x) = 0 \ \forall \ x \in E^4$, which one would identify with the vacuum of the theory. However, as it turns out there is another class of solutions that drastically changes the notion of the vacuum. These solutions arise when the mapping from an element of the boundary of Euclidean space E^4 into the group space $\mathscr{G}$ fall into distinct homotopy classes, that is if the homotopy group $\pi_n(\mathscr{G})$ is non-trivial. As the boundary of E^4 is clearly isomorphic to the three-sphere S^3, this is indeed the case for gauge groups such as SU(2) or SU(3),[8] for which

$$\pi_3(\mathscr{G}) = \mathbb{Z}. \tag{1.9}$$

---

[8] But not for U(1) in four-dimensional space, in which case the third homotopy group is trivial. Things are, however, different in two dimensions [62].

The consequence is thus that the solution $A_\mu(x) = 0$ at the boundary is just one solution among an infinite number of topologically distinct solutions that are characterized by an integer $\nu \in \mathbb{Z}$. As these fall into different homotopy classes, these solutions are non-deformable into each other. In order to determine the consequences, note that the boundary condition (1.8) actually does not imply $A_\mu(x) = 0$ at the boundary, but rather

$$\lim_{x \to \infty} A_\mu(x) = -\frac{i}{g}(\partial_\mu U)U^{-1}, \qquad U \in \mathcal{G}. \tag{1.10}$$

Noting furthermore that the action is minimized by self-dual and anti-self-dual field configuration $G_{\mu\nu} = \pm \tilde{G}_{\mu\nu}$ and using Eq. (1.10) as the boundary condition, the classical action Eq. (1.1) can then be calculated explicitly. The result is [61, 62]

$$\mathcal{S} = \frac{8\pi^2}{g^2}|\nu|, \tag{1.11}$$

where the Pontryagin index ν is just given by

$$\nu = \frac{g^2}{16\pi^2} \int d^4x \, \text{Tr}\left[G_{\mu\nu}\tilde{G}_{\mu\nu}\right]. \tag{1.12}$$

However, things become even more interesting when proceeding to the quantum theory. To that end, it is instructive to use the gauge freedom to set $A_0 = 0$ and concentrate on the time boundary of four dimensional space-time, i.e. $t \to \pm\infty$, and see what happens in between. Imagine that the fields at these boundaries belong to different homotopy classes with index $n, m \in \mathbb{Z}$, that is

$$\lim_{t \to -\infty} A_i(x) = -\frac{i}{g}(\partial_i U_n)U_n^{-1},$$
$$\lim_{t \to +\infty} A_i(x) = -\frac{i}{g}(\partial_i U_m)U_m^{-1}, \tag{1.13}$$

In the quantum theory, a field configuration corresponds to an eigenstate of the field operator, which in the case of the two boundary states Eq. (1.13) might be labeled $|n\rangle$ and $|m\rangle$. Then the functional integral

$$\langle m| \exp(-i\mathcal{H}t)|n\rangle = \int [\mathcal{D}A_\mu]_{(m-n)} e^{-\mathcal{S}} \tag{1.14}$$

describes the transition amplitude from vacuum $|n\rangle$ to $|m\rangle$, which is thus of order $\exp(-\mathcal{S})$ with $\mathcal{S}$ given by Eq. (1.11) and $\nu = m - n$. This means that the instanton with winding number ν describes a transition from vacuum $|n\rangle$ to vacuum $|m\rangle = |n + \nu\rangle$. If such instantaneous transitions between different vacuum states of different homotopy class are hence allowed in the quantum theory, the true vacuum cannot be $|0\rangle$ or any other vacuum $|n\rangle$, but must be a superposition of all these states up to a phase θ

$$|\theta\rangle = \sum_n e^{in\theta}|n\rangle, \tag{1.15}$$

which is the θ vacuum (this particular form ensures invariance under gauge transformations). Asking now for the vacuum-to-vacuum transition amplitude, one gets [61, 62]

$$\langle \theta'| \exp(-i\mathcal{H}t)|\theta\rangle = \delta(\theta' - \theta) \sum_\nu \int [\mathcal{D}A_\mu]_\nu e^{-i\nu\theta - \mathcal{S}} \tag{1.16}$$

where the expression in the exponential function corresponds to an integral over the Lagrange density

$$\mathscr{L} = -\frac{1}{2}\,\mathrm{Tr}\left[G_{\mu\nu}G^{\mu\nu}\right] - \theta\frac{g^2}{16\pi^2}\,\mathrm{Tr}\left[G_{\mu\nu}\tilde{G}^{\mu\nu}\right] \tag{1.17}$$

which finally shows the notorious θ-term (note that this expression now is rotated back to Minkowski space).[9] As QCD as part of the SM is a gauge theory with gauge group SU(3), this θ-term also shows up in the full QCD Lagrangian causing the "strong CP problem". As the object $\mathrm{Tr}\left[G_{\mu\nu}\tilde{G}^{\mu\nu}\right]$ is not invariant under P (parity) and T (time reversal) transformations and given the CPT theorem [81–83], the θ-term implies that QCD violates CP symmetry unless $\theta = 0$.[10] It is clear from the derivation that θ is a 2π periodic angle [61, 87], but also that it otherwise is not determined from the theory, meaning that it has to be measured for our world (note that the δ-distribution in Eq. (1.16) means that θ does not transit to another vacuum with $\theta' \neq \theta$).

Now it is of course interesting to see what happens when matter fields are present. It is known that QCD with N_f light quark flavors (realistic choices are of course only $N_f = 2$ and $N_f = 3$) is approximately invariant under global $U(N_f)_R \times U(N_f)_L \simeq SU(N_f)_R \times SU(N_f)_L \times U(1)_V \times U(1)_A$. While the spontaneous breakdown of the subgroup $SU(N_f)_R \times SU(N_f)_L$ to $SU(N_f)_V$ leads to the observed pattern of $N_f^2 - 1$ light mesons, the pseudo-Nambu–Goldstone bosons of the spontaneous symmetry breaking, the $U(1)_A$ part of the symmetry group does not persist in the quantum theory as a consequence of the invariance of the functional integral measure [88, 89], which is known as Adler–Bell–Jackiw anomaly [90, 91]. In the presence of a mass term, which explicitly breaks chiral symmetry, a $U(1)_A$ transformation on a quark field q_f with flavor f

$$q_f \to q_f' = e^{i\frac{\phi_f}{2}\gamma_5}q_f \tag{1.18}$$

has two effects: it shifts the θ-angle by $\phi = \sum_f \phi_f$ (as a consequence of the anomaly) and it adds a complex phase to the quark mass matrix

$$\theta\frac{g^2}{16\pi^2}\,\mathrm{Tr}\left[G_{\mu\nu}\tilde{G}^{\mu\nu}\right] \to (\theta - \phi)\frac{g^2}{16\pi^2}\,\mathrm{Tr}\left[G_{\mu\nu}\tilde{G}^{\mu\nu}\right] \tag{1.19}$$

$$\bar{q}\mathscr{M}q \to \bar{q}U\mathscr{M}_q Uq, \quad U_{ij} = \delta_{ij}e^{i\frac{\phi_i}{2}\gamma_5} \tag{1.20}$$

where q is the quark vector in flavor space and $\mathscr{M}_q = \mathrm{diag}\{m_f\}$ is the quark mass matrix. This means that there exists a rather straightforward solution to the "strong CP problem", that is if one quark were massless, say the up quark, one might simply choose $\phi_u = \theta$ and $\phi_f = 0$ otherwise, then the θ-term cancels and CP symmetry is restored.[11] However, it appears that the massless up quark solution is ruled out [92], which is implied by the current determinations of the quark mass ratios [93, 94] and is also suggested by Lattice QCD calculations [95–97]. Consequently, any transformation (1.18) eliminating the θ-term, effectively just shifts the problem to the mass term, which then acquires a CP-violating phase.

---

[9] It can be shown that $\mathrm{Tr}\left[G_{\mu\nu}\tilde{G}^{\mu\nu}\right]$ can be written as a total derivative thus one may think that such a surface term stemming from the anomaly can be dropped from the Lagrangian, but the instanton solution clearly proved that this is not the case in the presence of instantons [77–79]. This provided a solution to the $U(1)_A$ problem [80].

[10] Or $\theta = \pi$, for $\theta = \pi \xrightarrow{CP} -\pi$. However, it turns out that as a consequence of Dashen's mechanism [84] CP is then spontaneously broken due to the appearance of two vacuum states. The interesting physics when θ approaches π is investigated in [85, 86].

[11] To be more precise, the shift symmetry of Eq. (1.19) becomes an exact symmetry if one quark is massless, which renders θ an unphysical quantity.

The extent of this CP-violation is measurable, because the θ-term causes an electric dipole moment of the neutron $\propto \bar{\theta}$ [98, 99], where $\bar{\theta}$ is the effective θ-angle to be introduced below. Theoretical estimations of this quantity roughly vary between $|d_n| \approx 10^{-16} \bar{\theta} \, e \, \text{cm}$ and $|d_n| \approx 10^{-15} \bar{\theta} \, e \, \text{cm}$, see e.g. Refs. [92, 100–102], while the upper limit for its physical value determined in experiments is $|d_n| < 1.8 \times 10^{-26} \, e \, \text{cm}$ (90 % C.L.) [103], which taken together implies

$$\bar{\theta} \lesssim 10^{-11} \,, \tag{1.21}$$

which is the estimation mentioned already in the introduction.

To sum up, it can be said that there is a deep connection between the θ vacuum and the quark masses – a connection that persists when turning to hadron physics. In fact, the masses of the pseudo-Nambu–Goldstone bosons of chiral perturbation theory are θ-dependent quantities. In particular, the leading order θ-dependent pion mass in SU(2) chiral perturbation theory is known analytically (see ch. 2 and 3), which in turn causes higher order effects on quantities such as the nucleon masses (including the proton-neutron mass difference) or the pion-nucleon coupling constant. Note that the leading order effects are CP-even, while CP-odd effects are subleading.

Before proceeding to the Peccei–Quinn solution of the "strong CP problem", there is one subtlety regarding the observable θ-angle that should be mentioned. Above, the quark mass matrix $\mathcal{M}_q$ has been assumed real, positive, and γ_5-free. However, the most general form of the quark mass matrix is not as a consequence of electroweak CP-violating phases [76, 104]. For the case of such a general mass matrix, it is convenient to decompose the quark fields into left- and right-handed parts,

$$q_{R/L} = \frac{1}{2} \left(\mathbb{1} \pm \gamma_5 \right). \tag{1.22}$$

Then the mass term can be rewritten into the form

$$\mathscr{L}_{\mathscr{M}} = \bar{q}_L \mathscr{M} q_R + \bar{q}_R \mathscr{M}^\dagger q_L \tag{1.23}$$

where the mass matrix now is $\mathscr{M} = \text{diag}\{m_f \exp(i\phi_f)\}$. This implies that the actual observable is not the bare θ-angle, but [76]

$$\bar{\theta} = \theta + \text{Arg} \det \mathscr{M} = \theta + \theta_{\text{weak}}. \tag{1.24}$$

This is the effective angle $\bar{\theta}$ mentioned above. In what follows, θ has to be understood as the effective, physical $\bar{\theta}$.

1.2.2 Peccei–Quinn solution of the "strong CP problem" and axions

In the previous section, the δ-distribution in Eq. (1.16) has been interpreted as a superselection rule following Refs. [61, 62], as there is no transition from one θ-vacuum to another, meaning that if θ has its value once, it has its value forever, and different worlds with different θ clearly have different physical properties [105].

To be more precise, all that only applies if the theory has no classically exact global $U(1)_A$ symmetry. So the shrewd solution to the "strong CP problem" proposed by Peccei and Quinn [65, 66] is based on the introduction of another global chiral $U(1)_A$ symmetry, which ever since Weinberg's follow-up article [106] has been labeled $U(1)_{\text{PQ}}$. As in the case of the chiral $U(1)_A$ symmetry of QCD with at least one massless quark described above, the quantum anomaly associated with such symmetries can be used to eliminate

the θ-term via a shift symmetry similar to the one in Eq. (1.19).

However, as QCD as it stands in the SM does not possess such a symmetry, it must be hidden, meaning that the symmetry must be realized in the Nambu–Goldstone mode in contrast to the chiral $U(1)_A$ symmetry of massless QCD which is realized in Wigner–Weyl mode. The spontaneous breakdown of $U(1)_{PQ}$ symmetry is therefore associated with the appearance of a massless Nambu–Goldstone boson, which received the name *axion*.[12] This offers another view on the mechanism that eliminates θ: Let $a(x)$ denote the axion field, then due to the anomaly one gets

$$\mathscr{L}_{a\theta} = -\left(\theta + \frac{a(x)}{f_a}\right)\frac{g^2}{16\pi^2}\,\mathrm{Tr}\left[G_{\mu\nu}\tilde{G}^{\mu\nu}\right] \tag{1.25}$$

where f_a is a parameter to be introduced below. Setting $\theta_{\mathrm{eff}}(x) = \theta + a(x)/f_a$, this means that one effectively has made the substitution from the fixed parameter θ of the original model to the dynamical field $\theta(x)$ in the new model. Now consider the path integral formula for the ground state energy $E(\theta_{\mathrm{eff}})$ in a Euclidean volume V

$$e^{-VE(\theta_{\mathrm{eff}})} = \int [\mathscr{D}A_\mu]\det(\not{D} + \mathscr{M})$$
$$\times \exp\left(-\frac{1}{2}\int \mathrm{d}^4x\,\mathrm{Tr}\left[G_{\mu\nu}G_{\mu\nu}\right] + i\theta_{\mathrm{eff}}(x)\frac{g^2}{16\pi^2}\int \mathrm{d}^4x\,\mathrm{Tr}\left[G_{\mu\nu}\tilde{G}_{\mu\nu}\right]\right). \tag{1.26}$$

As has been shown by Vafa and Witten [108], if θ_{eff} is a dynamical variable, then the QCD vacuum energy is minimized at $\theta_{\mathrm{eff}} = 0$ thus eliminating any CP-violation from the QCD Lagrangian.

Though being formally a massless Nambu–Goldstone boson, the axion's intimate linking to the QCD vacuum and the quark masses leads to a small, but non-vanishing mass [106, 109, 110]. A current estimate of this mass is given by (see the study of ch. 4 for a derivation)

$$m_a \approx 5.7\left(\frac{10^{12}\,\mathrm{GeV}}{f_a}\right)\times 10^{-6}\,\mathrm{eV} \tag{1.27}$$

which shows a dependence on the parameter f_a, the axion decay constant, which is related to the vaccum expectation value of the scalar field/fields that enter typical axion models as discussed below. This quantity also sets the scale for the spontaneous breakdown of the PQ symmetry and presumably is at least of $\mathscr{O}(10^9\,\mathrm{GeV})$ (see below).

Now that it is clear that the $U(1)_{PQ}$ symmetry dynamically leads to CP-conservation, one has to extend the SM in such a way that this symmetry is manifest above a certain scale but spontaneously broken below it. The arguably simplest model is the Kim–Shifman–Vainshtein–Zakharov axion model (KSVZ) [111, 112]. In this model, one simply introduces an entire new sector that almost completely decouples from the SM – except for the axion. Consider a hypothetical, exotic quark Q and a complex scalar particle σ, the former being a singlet with respect to the weak interaction but might be a color triplet and carry hypercharge, the latter being a singlet with respect to the full SM gauge group $SU(3)_c \times SU(2)_{I_{ew}} \times U(1)_Y$. A possible Lagrangian of this sector then is

$$\mathscr{L}_{\mathrm{KSVZ}} = \bar{Q}i\not{D}Q + \partial_\mu\sigma\partial^\mu\sigma^* - Y\left(\sigma\bar{Q}_LQ_R + \sigma^*\bar{Q}_RQ_L\right) - V(\sigma), \tag{1.28}$$

---

[12] At first sight, this name is just natural as the axion is the Nambu–Goldstone boson associated with the spontaneous symmetry breaking of the *axial* U(1) symmetry. However, as "Axion" is also the brand name of a laundry detergent, it also fits in the sense that the axion cleans up QCD from the obstinate stain the θ-term represents. In fact, Wilczek, who coined this name, saw this product a few years before in a supermarket noting that this might be a good name for a particle [107].

where the third term represents a Yukawa interaction with coupling constant Y and the potential is given by

$$V(\sigma) = \mu^2 \sigma^* \sigma + \lambda \left(\sigma^* \sigma\right)^2.$$ (1.29)

This Lagrangian is indeed classically invariant under the chiral U(1) transformation

$$Q_{L/R} \to e^{\pm i \frac{1}{2} \alpha} Q_{L/R}, \quad \sigma \to e^{i\alpha} \sigma.$$ (1.30)

Here the PQ charges $\pm \frac{1}{2}$ and $+1$ have been assigned to the left- and right-handed quark and σ, respectively. The potential $V(\sigma)$ is minimized by

$$\sigma = \sqrt{-\frac{\mu^2}{2\lambda}} \equiv \frac{v_\sigma}{\sqrt{2}}$$ (1.31)

if $\mu^2 < 0$. Expanding σ as usual around its vacuum expectation value

$$\sigma = \frac{1}{\sqrt{2}} \left(v_\sigma + \rho\right) e^{i \frac{a}{v_\sigma}}$$ (1.32)

indeed leads to a pseudoscalar massless Nambu–Goldstone boson a, present in the complex phase of σ. The real scalar ρ as well as Q achieve masses $\propto v_\sigma$ and there appear interactions among the involved particles. The point is, if $v_\sigma \propto f_a$ is very large, ρ and Q are extraordinarily heavy particles and can thus be integrated out from the theory. They are just phantoms [112] to fit the needs of the model.[13]

However, it can be argued that the introduction of an entire new sector into the model just to ensure CP-invariance is somehow artificial, if not as unpleasant as the original θ-term itself. Therefore, the original approach by Weinberg [106] and Wilczek [110] after the proposal of the Peccei–Quinn mechanism was to directly integrate this solution of the "strong CP problem" into the already existing Glashow–Salam–Weinberg model [26–28] of the electroweak interaction, which is known by the name PQWW axion model. The inclusion of the U(1)$_{PQ}$ symmetry, however, required the addition of at least one additional Higgs doublet. Let ϕ_u, ϕ_d be two Higgs doublets, q_L a left-handed quark doublet, and u_R, d_R the corresponding right-handed up-type and down-type singlets, and let furthermore i, j be quark generation indexes, then a possible Lagrangian of this sector is (omitting kinetic terms) (see also [76, 113])

$$\mathscr{L}_{PQWW} = Y_{ij}^u \bar{q}_{Li} \phi_u u_{Rj} + Y_{ij}^d \bar{q}_{Li} \phi_d d_{Rj} + \text{h.c.} - V(\phi_u, \phi_d),$$ (1.33)

where the coefficients $Y_{ij}^{u/d}$ are the Yukawa coupling constants and h.c. denotes the Hermitian conjugate. As can be seen in this Lagrangian, the two Higgs doublets restrictively couple either to right-handed up-type quarks or to right-handed down-type quarks. The inclusion of leptons can in principle be achieved by introducing Yukawa couplings between leptons and either ϕ_u, ϕ_d, or another Higgs doublet ϕ_l, leading to slightly different phenomenology (see [76]). Depending on the assignment of PQ charges, the Lagrangian (1.33) can be made invariant under U(1)$_{PQ}$, which ensures the desired shift symmetry. In its simplest form, the potential $V(\phi_u, \phi_d)$ is just given by two distinct potentials of the same form as Eq. (1.29), one for each Higgs doublet, where now one has $\phi_{u/d}$ and $\phi_{u/d}^\dagger$ instead of σ and σ^* (in more sophisticated models, also couplings among the Higgs doublets might appear). Let the vacuum expectation values be

---

[13] The quark Q thus has an expected mass of $\mathcal{O}\left(10^{10}\,\text{GeV}\right)$ based on usual estimations of f_a. The need for such large values of f_a is discussed below.

$\langle \phi_u \rangle = v_1/\sqrt{2}$ and $\langle \phi_d \rangle = v_2/\sqrt{2}$, and $v = \sqrt{v_1^2 + v_2^2}$, then one can expand the scalar fields according to

$$\phi_u^0 = \frac{1}{\sqrt{2}} (v_1 + \rho_1)\, e^{i\frac{a_1}{v_1}}$$
$$\phi_d^0 = \frac{1}{\sqrt{2}} (v_2 + \rho_2)\, e^{i\frac{a_2}{v_2}} \tag{1.34}$$

where ρ_1 and ρ_2 are two real Higgs fields. One of the two possible orthogonal linear combinations of a_1 and a_2 is absorbed by the Z boson via the Higgs mechanism, whereas

$$a = \frac{v_2 a_1 + v_1 a_2}{v} \tag{1.35}$$

is the massless Nambu–Goldstone boson, the axion field. If $x = v_1/v_2$ denotes the ratio of the vacuum expectation values, then this produces tree-level couplings of the axion to SM quarks $\propto 1/(xv)$ in the case of up-type quarks, and $\propto x/v$ in the case of down-type quarks (couplings to leptons depend on the type of lepton-Higgs Yukawa couplings). Finally, the decay constant f_a is also of the order v. The quantity v itself is determined by the electroweak scale,

$$v = (\sqrt{2} G_F)^{-\frac{1}{2}} \approx 246 \, \text{GeV}, \tag{1.36}$$

where G_F is the Fermi constant. According to Eq. (1.27), this would correspond to an axion with a mass of $\mathcal{O}(10^2)$ keV. However, already shortly after its proposal, the PQWW axion could be ruled out experimentally [92, 114–116].

Such axions that were readily accessible to experiments already at the time of their proposal are labeled "visible" axions, and the fact that they could be ruled out then led to the idea of the "invisible" axion and the KSVZ axion above is such a model by simply requiring that v_σ is "large". Another approach of constructing an invisible axion that does not require the inclusion of exotic heavy quarks, is the Dine–Fischler–Srednicki–Zhitnitsky (DFSZ) axion model [117, 118] that can be regarded as an extension of the PQWW axion. Just as the latter, the DFSZ model comes with two Higgs doublets ϕ_u and ϕ_d, where the former restrictively couples to right-handed up-type quarks and the latter only to right-handed down-type quarks and right-handed leptons. The key innovation is the inclusion of a complex scalar σ coupling to these Higgses, which allows one to separate the PQ scale from the electroweak scale. As in the KSVZ, σ is a singlet under the full SM gauge group. The main mechanisms are basically the same as the ones discussed above for the KSVZ and the PQWW models. After the fields ϕ_u, ϕ_d, and σ acquire non-trivial vacuum expectation values, where again $\langle \sigma \rangle = v_\sigma/\sqrt{2}$, $\langle \phi_u \rangle = v_1/\sqrt{2}$ and $\langle \phi_d \rangle = v_2/\sqrt{2}$, and $v = \sqrt{v_1^2 + v_2^2}$, the quarks and vector bosons achieve their masses by the Higgs mechanism leaving a massless Nambu–Goldstone boson appearing as a linear combination of the complex components of the Higgs doublets and the σ. If $v_\sigma \gg v$, which is of course needed for this axion being "invisible", then it can be shown that the axion is dominantly composed of the σ. As in the PQWW model, the DFSZ model leads to tree-level couplings of axions with quarks and leptons of $\mathcal{O}(f_a)$, where in the case of the DFSZ model [117]

$$f_a \propto \frac{\sqrt{4 v_1^2 v_2^2 + v^2 v_\sigma^2}}{v} \tag{1.37}$$

thus roughly $f_a \propto v_\sigma$ for $v_\sigma \gg v$.

The models presented so far, the PQWW, KSVZ, and DFSZ models, are often considered the prototypical axion models. In fact, each of these models leave considerable freedom of how certain aspects are finally realized. Besides these variant models, there is a large number of different axions and axion-like particles on the market, see, e.g., Refs. [92, 119–124].

So far, the relation between f_a and the involved vacuum expectation values always was shown as a proportionality relation. The reason is that there is indeed a model dependent proportionality constant that has been omitted up to now. As has been shown by Sikivie [125], in many models, a discrete subgroup Z_N of $U(1)_{\mathrm{PQ}}$ is left unbroken resulting in a degeneracy of the vacuum in the range of $[0, 2\pi f_a]$ and domain walls.[14] The degeneracy is characterized by the domain wall number N_{DW}, which is also known as color anomaly coefficient $\mathscr{C}$. If one hence considers

$$\mathscr{L}_a = -\frac{a(x)}{f_a} \frac{g^2}{16\pi^2} \operatorname{Tr}\left[G_{\mu\nu}\tilde{G}^{\mu\nu}\right] \tag{1.38}$$

as the definition of f_a such that

$$a \to a + 2\pi f_a \tag{1.39}$$

leaves Eq. (1.38) invariant, then $1/N_{\mathrm{DW}}$ must be added as a proportionality constant when relating f_a to the vacuum expectation values of the model. Formally, N_{DW} can be calculated via

$$N_{\mathrm{DW}} = \sum_i Q_{\mathrm{PQ}}(q_i)T^2, \tag{1.40}$$

where the sum runs over all fermions q_i carrying (normalized) PQ charge $Q_{\mathrm{PQ}}(q_i)$, and T^2 is related to the generators of $SU(3)_c$ in a given representation via $\operatorname{Tr}\left[T_a T_b\right] = T^2/2\delta_{ab}$ [76, 128].

After rotating away the $a \operatorname{Tr}\left[\tilde{G}_{\mu\nu}G^{\mu\nu}\right]$ term, the QCD axion effectively couples to quarks and – depending on the axion model – might have tree-level couplings to quarks and leptons (if there is no tree-level coupling to leptons, it is called "hadronic"). Additionally, it couples to photons through the electromagnetic axial anomaly, analogously to pions (the determination of the coupling strength is part of the study in ch. 4). Thus the axion might decay into two photons, but the lifetime is extremely large [124]

$$\tau_a \approx \left(\frac{f_a}{10^{12}\,\mathrm{GeV}}\right)^5 \times 10^{50}\,\mathrm{s}\,, \tag{1.41}$$

thus (almost stable) axions might populate the universe making it a dark matter candidate [57, 130–135]. Cosmological considerations lead to the traditional axion window [92, 104, 130–132]

$$10^9\,\mathrm{GeV} \lesssim f_a \lesssim 10^{12}\,\mathrm{GeV}\,, \tag{1.42}$$

corresponding to a mass of a few μeV and 10^{-1} eV. As all couplings to SM particles and hadronic matter are of $\mathcal{O}(1/f_a)$, the axion would indeed be "dark" matter, and consequently it has not been detected hitherto (a summary of the recent experimental status can be found in Ref. [124]; main experimental approaches are described, e.g., in [76, 92, 136]).

---

[14] The appearance of domain walls in the early universe is problematic, which is known as the domain wall problem [104, 125–129].

1.3 Overview over the studies performed

The six studies presented in the next chapters can be classified as follows: The first two studies, ch. 2 and ch. 3, are devoted to the question of how a non-vanishing θ-angle would alter nuclear physics with respect to nucleon masses, binding energies of light nuclei, and nucleosynthesis. The third study, ch. 4, is related to the structure of the QCD θ-vacuum and its relation to the axion mass and includes a determination of the axion-photon coupling. The last three studies, ch. 5–7, deal with the interaction of axions with baryonic matter. In this section, a brief summery of these studies is given.

The first study, "θ-dependence of light nuclei and nucleosynthesis" [137], grew out of an unpublished part of the Master's thesis [138], where it has been shown that the only previous study devoted to that topic [139] improperly focused on subleading CP-odd effects and that a more thorough study must consider first and foremost the leading order effects stemming from the θ-dependence of the pion mass. The topic therefore was revived by Ulf-G. Meißner, Mikhail Shifman, and Dean Lee, who invited me to pursue this question anew. The central idea was to implement a one-boson exchange model for the two-nucleon potential and collect the knowledge of the θ-dependence of the involved quantities. The θ-dependence of the σ, ω, and ρ, have been adopted from [140]. As an additional effect of varying θ, the strong part of the proton-neutron mass difference has been considered. According to our model, the diproton and dineutron become bound states and in general the binding energies of the few-nucleon system increases as θ is varied from 0 to π. At the same time the proton-neutron mass difference becomes larger. This has considerable consequences for Big Bang nucleosyntheses (as seen, for instance, in a drop-off of the Helium mass fraction) and stellar evolution (suppression of ^{16}O production in stars). This last part of the study, has been worked out in collaboration with Keith Olive.

The second study, "Alpha-alpha scattering in the Multiverse" [141], updates two previous studies, Ref. [142, 143], in which the the ground state energies of ^{4}He , ^{8}Be and ^{12}C, as well as the ground state energy of the Hoyle state are determined in dependence of the light quark masses and the electromagnetic fine-structure constant α_{em} including an estimation of the sensitivity of the triple-alpha process in terms of a variation of these quantities. Besides being an update of this work, the new study additionally is extended to also include the θ-dependence of these objects. The main work has been performed by Serdar Elhatisari as part of the Nuclear Lattice Effective Field Theory (NLEFT) Collaboration using the computational method of the same name NLEFT. My contribution was to show that the results for the light quark mass dependence at the same time can be used to estimate the θ-dependence. To that end, it is demonstrated that to first order any θ-dependence is primarily driven by the varying pion mass. The results are then valid for a variation of $0 < \theta \lesssim 0.9$.

The third study, "QCD θ-vacuum energy and axion properties" [144], started as a project of Zhen-Yan Lu, Meng-Lin Du, and Feng-Kun Guo, who invited me to contribute and to cross-check the calculations performed. As the QCD θ-vacuum energy and the axion mass are intimately linked, a more precise knowledge of the vacuum energy density automatically leads to a more precise determination of the axion mass. In this study, the topological susceptibility and the fourth cumulant of the QCD topological charge distribution of the θ-vacuum, which can directly be mapped to the axion mass and the axion quartic self-coupling, are determined using chiral perturbation theory up to $\mathcal{O}(p^4)$ in the chiral power counting. The main derivation of the vacuum energy density is performed for the general SU(N_f) case with non-degenerate quark masses, while the final results of the quantities mentioned above are calculated for the case of $N_f = 3$. As an addition, the axion-photon coupling is determined in SU(3) chiral perturbation theory up to $\mathcal{O}(p^6)$. The latter is relevant as many axion searches are based on this axion-photon coupling, for example, cavity haloscopes [145–151], axion helioscopes [145, 146, 152–156], or light shining through

a wall experiments [157–159].

In the fourth study, "Precision calculation of the axion-nucleon coupling in chiral perturbation theory" [86], we study the coupling of axions to the proton and neutron. While the leading order coupling has been calculated numerous times since the development of the first axion models [114, 160–164], it is the first study in which it is determined up to $\mathcal{O}(p^3)$ in SU(2) baryon chiral perturbation theory. As in the case of the axion-photon coupling, the relevance of the axion-nucleon coupling is related to axion searches. In particular, the axion-nucleon bremsstrahlung process $NN \rightarrow NNa$ might contribute to the cooling of proto-neutron stars. Determining the axion production rate in such stellar objects and relating it to the cooling rate due to neutrinos and the observed cooling rate results in constraints for the axion decay constant f_a [165–178] (see also the overviews [136, 179]).

The fifth study, "The axion-baryon coupling in SU(3) heavy baryon chiral perturbation theory" [180], extends to previous study to the case of three light flavors. It is shown that the axion not only couples to protons and neutrons, but to any baryon of the the full ground state baryon octet with a similar strength. This has further phenomenological implications, because it has been suggested that hyperons might exist in the cores of neutron stars [181–199]. As the above-mentioned constraints for the axion decay constant from the cooling of neutron stars are based on the coupling to nucleons alone, this new finding might lead to considerable corrections to these constraints.

The idea to the sixth study, "Pion axioproduction: The Delta resonance contribution" [200], was brought to us by Alessandro Mirizzi, Pierluca Carenza, and Maurizio Giannotti. They proposed that there might be an enhancement of axion emission in neutron stars by the process $\pi N \rightarrow aN$ due to the appearance of resonances, in particular the Δ resonance [201, 202]. The reverse process, pion axioproduction $aN \rightarrow \pi N$ might then be a candidate for a new experimental search of axions, in particular using underground water Cherenkov detectors. It is exactly this process that we have investigated in this last study demonstrating that there is indeed a region of enhancement. However, due to the fact that the process is a isospin violating process, this enhancement is suppressed by a factor of $\mathcal{O}(10^{-1})$ up to $\mathcal{O}(10^{-5})$, depending on the underlying axion model.

References

[1] C. D. Anderson, *The Positive Electron*, Phys. Rev. **43** (1933) 491.

[2] J. C. Street and E. C. Stevenson, *New Evidence for the Existence of a Particle of Mass Intermediate Between the Proton and Electron*, Phys. Rev. **52** (1937) 1003.

[3] M. L. Perl et al., *Evidence for Anomalous Lepton Production in e+ - e- Annihilation*, Phys. Rev. Lett. **35** (1975) 1489.

[4] C. S. Wu, E. Ambler, R. W. Hayward, D. D. Hoppes, and R. P. Hudson, *Experimental Test of Parity Conservation in β Decay*, Phys. Rev. **105** (1957) 1413.

[5] G. Danby et al., *Observation of High-Energy Neutrino Reactions and the Existence of Two Kinds of Neutrinos*, Phys. Rev. Lett. **9** (1962) 36.

[6] F. J. Hasert et al., *Observation of Neutrino Like Interactions Without Muon Or Electron in the Gargamelle Neutrino Experiment*, Phys. Lett. B **46** (1973) 138.

[7] G. Arnison et al., *Experimental Observation of Isolated Large Transverse Energy Electrons with Associated Missing Energy at $\sqrt{s}$ = 540 GeV*, Phys. Lett. B **122** (1983) 103.

[8] G. Arnison et al., *Experimental Observation of Lepton Pairs of Invariant Mass Around 95-GeV/c**2 at the CERN SPS Collider*, Phys. Lett. B **126** (1983) 398.

[9] P. Bagnaia et al., *Evidence for $Z^0 \to e^+ e^-$ at the CERN $\bar{p}p$ Collider*, Phys. Lett. B **129** (1983) 130.

[10] M. Banner et al., *Observation of Single Isolated Electrons of High Transverse Momentum in Events with Missing Transverse Energy at the CERN anti-p p Collider*, Phys. Lett. B **122** (1983) 476.

[11] E. D. Bloom et al., *High-Energy Inelastic e p Scattering at 6-Degrees and 10-Degrees*, Phys. Rev. Lett. **23** (1969) 930.

[12] M. Breidenbach et al., *Observed behavior of highly inelastic electron-proton scattering*, Phys. Rev. Lett. **23** (1969) 935.

[13] S. Abachi et al., *Observation of the top quark*, Phys. Rev. Lett. **74** (1995) 2632, arXiv: `hep-ex/9503003`.

[14] F. Abe et al., *Observation of top quark production in $\bar{p}p$ collisions*, Phys. Rev. Lett. **74** (1995) 2626, arXiv: `hep-ex/9503002`.

[15] P. A. M. Dirac, *The quantum theory of the electron*, Proc. Roy. Soc. Lond. A **117** (1928) 610.

[16] S. Tomonaga, *On a relativistically invariant formulation of the quantum theory of wave fields*, Prog. Theor. Phys. **1** (1946) 27.

[17] J. S. Schwinger, *Quantum electrodynamics. I A covariant formulation*, Phys. Rev. **74** (1948) 1439, ed. by K. A. Milton.

[18] J. S. Schwinger, *On Quantum electrodynamics and the magnetic moment of the electron*, Phys. Rev. **73** (1948) 416.

[19] R. P. Feynman, *Space - time approach to quantum electrodynamics*, Phys. Rev. **76** (1949) 769, ed. by L. M. Brown.

[20] R. P. Feynman, *Mathematical formulation of the quantum theory of electromagnetic interaction*, Phys. Rev. **80** (1950) 440, ed. by L. M. Brown.

[21] F. J. Dyson, *The Radiation theories of Tomonaga, Schwinger, and Feynman*, Phys. Rev. **75** (1949) 486.

[22] F. J. Dyson, *The S matrix in quantum electrodynamics*, Phys. Rev. **75** (1949) 1736.

[23] C.-N. Yang and R. L. Mills, *Conservation of Isotopic Spin and Isotopic Gauge Invariance*, Phys. Rev. **96** (1954) 191, ed. by J.-P. Hsu and D. Fine.

[24] J. J. Sakurai, *Theory of strong interactions*, Annals Phys. **11** (1960) 1.

[25] S. L. Glashow and M. Gell-Mann, *Gauge Theories of Vector Particles*, Annals Phys. **15** (1961) 437.

[26] S. L. Glashow, *The renormalizability of vector meson interactions*, Nucl. Phys. **10** (1959) 107.

[27] A. Salam and J. C. Ward, *Weak and electromagnetic interactions*, Nuovo Cim. **11** (1959) 568.

[28] S. Weinberg, *A Model of Leptons*, Phys. Rev. Lett. **19** (1967) 1264.

[29] F. Englert and R. Brout, *Broken Symmetry and the Mass of Gauge Vector Mesons*,
Phys. Rev. Lett. **13** (1964) 321, ed. by J. C. Taylor.

[30] P. W. Higgs, *Broken Symmetries and the Masses of Gauge Bosons*,
Phys. Rev. Lett. **13** (1964) 508, ed. by J. C. Taylor.

[31] G. S. Guralnik, C. R. Hagen, and T. W. B. Kibble,
Global Conservation Laws and Massless Particles,
Phys. Rev. Lett. **13** (1964) 585, ed. by J. C. Taylor.

[32] M. Gell-Mann, *The Eightfold Way: A Theory of strong interaction symmetry*, (1961).

[33] Y. Ne'eman, *Derivation of strong interactions from a gauge invariance*,
Nucl. Phys. **26** (1961) 222, ed. by R. Ruffini and Y. Verbin.

[34] M. Gell-Mann, *A Schematic Model of Baryons and Mesons*, Phys. Lett. **8** (1964) 214.

[35] G. Zweig, *An SU(3) model for strong interaction symmetry and its breaking. Version 1*, (1964).

[36] O. W. Greenberg,
Spin and Unitary Spin Independence in a Paraquark Model of Baryons and Mesons,
Phys. Rev. Lett. **13** (1964) 598.

[37] M. Y. Han and Y. Nambu, *Three Triplet Model with Double SU(3) Symmetry*,
Phys. Rev. **139** (1965) B1006, ed. by T. Eguchi.

[38] H. Fritzsch, M. Gell-Mann, and H. Leutwyler, *Advantages of the Color Octet Gluon Picture*,
Phys. Lett. B **47** (1973) 365.

[39] G. 't Hooft, *Renormalizable Lagrangians for Massive Yang-Mills Fields*,
Nucl. Phys. B **35** (1971) 167, ed. by J. C. Taylor.

[40] G. 't Hooft and M. J. G. Veltman, *Regularization and Renormalization of Gauge Fields*,
Nucl. Phys. B **44** (1972) 189.

[41] G. Aad et al., *Observation of a new particle in the search for the Standard Model Higgs boson
with the ATLAS detector at the LHC*, Phys. Lett. B **716** (2012) 1,
arXiv: `1207.7214 [hep-ex]`.

[42] S. Chatrchyan et al.,
Observation of a New Boson at a Mass of 125 GeV with the CMS Experiment at the LHC,
Phys. Lett. B **716** (2012) 30, arXiv: `1207.7235 [hep-ex]`.

[43] P. Langacker, *The Standard Model and Beyond*, Taylor & Francis, 2017.

[44] B. Pontecorvo, *Mesonium and anti-mesonium*, Sov. Phys. JETP **6** (1957) 429.

[45] Z. Maki, M. Nakagawa, and S. Sakata, *Remarks on the unified model of elementary particles*,
Prog. Theor. Phys. **28** (1962) 870.

[46] B. Pontecorvo, *Neutrino Experiments and the Problem of Conservation of Leptonic Charge*,
Zh. Eksp. Teor. Fiz. **53** (1967) 1717.

[47] V. N. Gribov and B. Pontecorvo, *Neutrino astronomy and lepton charge*,
Phys. Lett. B **28** (1969) 493.

[48] J. Schechter and J. W. F. Valle, *Neutrino Masses in SU(2) x U(1) Theories*,
Phys. Rev. D **22** (1980) 2227.

[49] Y. Fukuda et al., *Evidence for oscillation of atmospheric neutrinos*,
Phys. Rev. Lett. **81** (1998) 1562, arXiv: `hep-ex/9807003`.

[50] Q. R. Ahmad et al., *Direct evidence for neutrino flavor transformation from neutral current interactions in the Sudbury Neutrino Observatory*, Phys. Rev. Lett. **89** (2002) 011301,
arXiv: `nucl-ex/0204008`.

[51] T. Yanagida, *Horizontal gauge symmetry and masses of neutrinos*,
Conf. Proc. C **7902131** (1979) 95, ed. by O. Sawada and A. Sugamoto.

[52] M. Gell-Mann, P. Ramond, and R. Slansky, *Complex Spinors and Unified Theories*,
Conf. Proc. C **790927** (1979) 315, arXiv: `1306.4669 [hep-th]`.

[53] Y. Chikashige, R. N. Mohapatra, and R. D. Peccei,
Are There Real Goldstone Bosons Associated with Broken Lepton Number?
Phys. Lett. B **98** (1981) 265.

[54] R. Foot, H. Lew, X. G. He, and G. C. Joshi,
Seesaw Neutrino Masses Induced by a Triplet of Leptons, Z. Phys. C **44** (1989) 441.

[55] G. Bertone, D. Hooper, and J. Silk, *Particle dark matter: Evidence, candidates and constraints*,
Phys. Rept. **405** (2005) 279, arXiv: `hep-ph/0404175`.

[56] J. L. Feng, *Dark Matter Candidates from Particle Physics and Methods of Detection*,
Ann. Rev. Astron. Astrophys. **48** (2010) 495, arXiv: `1003.0904 [astro-ph.CO]`.

[57] D. J. E. Marsh, *Axion Cosmology*, Phys. Rept. **643** (2016) 1,
arXiv: `1510.07633 [astro-ph.CO]`.

[58] G. Bertone and D. Hooper, *History of dark matter*, Rev. Mod. Phys. **90** (2018) 045002,
arXiv: `1605.04909 [astro-ph.CO]`.

[59] B. Abi et al., *Measurement of the Positive Muon Anomalous Magnetic Moment to 0.46 ppm*,
Phys. Rev. Lett. **126** (2021) 141801, arXiv: `2104.03281 [hep-ex]`.

[60] A. A. Belavin, A. M. Polyakov, A. S. Schwartz, and Y. S. Tyupkin,
Pseudoparticle Solutions of the Yang-Mills Equations,
Phys. Lett. B **59** (1975) 85, ed. by J. C. Taylor.

[61] C. G. Callan Jr., R. F. Dashen, and D. J. Gross, *The Structure of the Gauge Theory Vacuum*,
Phys. Lett. B **63** (1976) 334, ed. by J. C. Taylor.

[62] C. G. Callan Jr., R. F. Dashen, and D. J. Gross, *Toward a Theory of the Strong Interactions*,
Phys. Rev. D **17** (1978) 2717, ed. by M. A. Shifman.

[63] J. H. Christenson, J. W. Cronin, V. L. Fitch, and R. Turlay,
Evidence for the 2π Decay of the K_2^0 Meson, Phys. Rev. Lett. **13** (1964) 138.

[64] M. Kobayashi and T. Maskawa,
CP Violation in the Renormalizable Theory of Weak Interaction,
Prog. Theor. Phys. **49** (1973) 652.

[65] R. D. Peccei and H. R. Quinn, *CP Conservation in the Presence of Instantons*,
Phys. Rev. Lett. **38** (1977) 1440.

[66] R. D. Peccei and H. R. Quinn,
Constraints Imposed by CP Conservation in the Presence of Instantons,
Phys. Rev. D **16** (1977) 1791.

[67] S. Weinberg, *Phenomenological Lagrangians*, Physica A **96** (1979) 327, ed. by S. Deser.

[68] J. Gasser and H. Leutwyler, *Chiral Perturbation Theory to One Loop*,
Annals Phys. **158** (1984) 142.

[69] J. Gasser and H. Leutwyler,
Chiral Perturbation Theory: Expansions in the Mass of the Strange Quark,
Nucl. Phys. B **250** (1985) 465.

[70] J. Gasser, M. E. Sainio, and A. Svarc, *Nucleons with Chiral Loops*,
Nucl. Phys. B **307** (1988) 779.

[71] E. E. Jenkins and A. V. Manohar,
Baryon chiral perturbation theory using a heavy fermion Lagrangian,
Phys. Lett. B **255** (1991) 558.

[72] G. Ecker, *Chiral perturbation theory*, Prog. Part. Nucl. Phys. **35** (1995) 1,
arXiv: `hep-ph/9501357`.

[73] V. Bernard, N. Kaiser, and U.-G. Meißner, *Chiral dynamics in nucleons and nuclei*,
Int. J. Mod. Phys. E **4** (1995) 193, arXiv: `hep-ph/9501384`.

[74] R. Rajaraman, *Solitons and Instantons*, North Holland, 1982.

[75] L. H. Ryder, *Quantum Field Theory*, Cambridge University Press, 1996.

[76] J. E. Kim, *Light Pseudoscalars, Particle Physics and Cosmology*, Phys. Rept. **150** (1987) 1.

[77] G. 't Hooft, *Symmetry Breaking Through Bell-Jackiw Anomalies*,
Phys. Rev. Lett. **37** (1976) 8, ed. by M. A. Shifman.

[78] G. 't Hooft, *Computation of the Quantum Effects Due to a Four-Dimensional Pseudoparticle*,
Phys. Rev. D **14** (1976) 3432, ed. by M. A. Shifman, [Erratum: Phys.Rev.D 18, 2199 (1978)].

[79] G. 't Hooft, *How Instantons Solve the U(1) Problem*, Phys. Rept. **142** (1986) 357.

[80] S. Weinberg, *The U(1) Problem*, Phys. Rev. D **11** (1975) 3583.

[81] J. S. Schwinger, *The Theory of quantized fields. 1.*,
Phys. Rev. **82** (1951) 914, ed. by K. A. Milton.

[82] G. Lüders, *On the Equivalence of Invariance under Time Reversal and under
Particle-Antiparticle Conjugation for Relativistic Field Theories*,
Kong. Dan. Vid. Sel. Mat. Fys. Med. **28N5** (1954) 1.

[83] G. Lüders, *Proof of the TCP theorem*, Annals Phys. **2** (1957) 1.

[84] R. F. Dashen, *Some features of chiral symmetry breaking*, Phys. Rev. D **3** (1971) 1879.

[85] A. V. Smilga, *QCD at theta similar to pi*, Phys. Rev. D **59** (1999) 114021,
arXiv: `hep-ph/9805214`.

[86] T. Vonk, F.-K. Guo, and U.-G. Meißner, *Aspects of the QCD θ-vacuum*,
JHEP **06** (2019) 106, [Erratum: JHEP 10, 028 (2019)], arXiv: `1905.06141 [hep-th]`.

[87] R. Jackiw and C. Rebbi, *Vacuum Periodicity in a Yang-Mills Quantum Theory*, Phys. Rev. Lett. **37** (1976) 172, ed. by J. C. Taylor.

[88] K. Fujikawa, *Path Integral Measure for Gauge Invariant Fermion Theories*, Phys. Rev. Lett. **42** (1979) 1195.

[89] K. Fujikawa, *Path Integral for Gauge Theories with Fermions*, Phys. Rev. D **21** (1980) 2848, [Erratum: Phys.Rev.D 22, 1499 (1980)].

[90] S. L. Adler, *Axial vector vertex in spinor electrodynamics*, Phys. Rev. **177** (1969) 2426.

[91] J. S. Bell and R. Jackiw, *A PCAC puzzle: $\pi^0 \to \gamma\gamma$ in the σ model*, Nuovo Cim. A **60** (1969) 47.

[92] J. E. Kim and G. Carosi, *Axions and the Strong CP Problem*, Rev. Mod. Phys. **82** (2010) 557, [Erratum: Rev.Mod.Phys. 91, 049902 (2019)], arXiv: `0807.3125 [hep-ph]`.

[93] P. A. Zyla et al., *Review of Particle Physics*, PTEP **2020** (2020) 083C01.

[94] Y. Aoki et al., *FLAG Review 2021*, (2021), arXiv: `2111.09849 [hep-lat]`.

[95] A. C. Irving, C. McNeile, C. Michael, K. J. Sharkey, and H. Wittig, *Is the up quark massless?* Phys. Lett. B **518** (2001) 243, arXiv: `hep-lat/0107023`.

[96] D. R. Nelson, G. T. Fleming, and G. W. Kilcup, *Is strong CP due to a massless up quark?* Phys. Rev. Lett. **90** (2003) 021601, arXiv: `hep-lat/0112029`.

[97] C. Alexandrou et al., *Ruling Out the Massless Up-Quark Solution to the Strong **CP** Problem by Computing the Topological Mass Contribution with Lattice QCD*, Phys. Rev. Lett. **125** (2020) 232001, arXiv: `2002.07802 [hep-lat]`.

[98] V. Baluni, *CP Violating Effects in QCD*, Phys. Rev. D **19** (1979) 2227.

[99] R. J. Crewther, P. Di Vecchia, G. Veneziano, and E. Witten, *Chiral Estimate of the Electric Dipole Moment of the Neutron in Quantum Chromodynamics*, Phys. Lett. B **88** (1979) 123, [Erratum: Phys.Lett.B 91, 487 (1980)].

[100] C. Alexandrou et al., *Neutron electric dipole moment using $N_f = 2 + 1 + 1$ twisted mass fermions*, Phys. Rev. D **93** (2016) 074503, arXiv: `1510.05823 [hep-lat]`.

[101] F.-K. Guo et al., *The electric dipole moment of the neutron from 2+1 flavor lattice QCD*, Phys. Rev. Lett. **115** (2015) 062001, arXiv: `1502.02295 [hep-lat]`.

[102] F. Abusaif et al., *Storage Ring to Search for Electric Dipole Moments of Charged Particles – Feasibility Study*, Geneva: CERN, 2021, arXiv: `1912.07881 [hep-ex]`.

[103] C. Abel et al., *Measurement of the permanent electric dipole moment of the neutron*, Phys. Rev. Lett. **124** (2020) 081803, arXiv: `2001.11966 [hep-ex]`.

[104] H.-Y. Cheng, *The Strong CP Problem Revisited*, Phys. Rept. **158** (1988) 1.

[105] D. J. Gross, R. D. Pisarski, and L. G. Yaffe, *QCD and Instantons at Finite Temperature*, Rev. Mod. Phys. **53** (1981) 43.

[106] S. Weinberg, *A New Light Boson?* Phys. Rev. Lett. **40** (1978) 223.

[107] F. Wilczek, *Time's (Almost) Reversible Arrow*, Quanta Magazine (2016).

[108] C. Vafa and E. Witten, *Parity Conservation in QCD*, Phys. Rev. Lett. **53** (1984) 535.

[109] W. A. Bardeen and S.-H. Tye, *Current Algebra Applied to Properties of the Light Higgs Boson*, Phys. Lett. B **74** (1978) 229.

[110] F. Wilczek, *Problem of Strong P and T Invariance in the Presence of Instantons*, Phys. Rev. Lett. **40** (1978) 279.

[111] J. E. Kim, *Weak Interaction Singlet and Strong CP Invariance*, Phys. Rev. Lett. **43** (1979) 103.

[112] M. A. Shifman, A. I. Vainshtein, and V. I. Zakharov, *Can Confinement Ensure Natural CP Invariance of Strong Interactions?* Nucl. Phys. B **166** (1980) 493.

[113] W. A. Bardeen, R. D. Peccei, and T. Yanagida, *Constraints on variant axion models*, Nucl. Phys. B **279** (1987) 401.

[114] T. W. Donnelly, S. J. Freedman, R. S. Lytel, R. D. Peccei, and M. Schwartz, *Do Axions Exist?* Phys. Rev. D **18** (1978) 1607.

[115] F. P. Calaprice et al., *Search for axion emission in the decay of excited states of C-12*, Phys. Rev. D **20** (1979) 2708.

[116] D. J. Bechis et al., *Search for Axion Production in Low-energy Electron Bremsstrahlung*, Phys. Rev. Lett. **42** (1979) 1511, [Erratum: Phys.Rev.Lett. 43, 90 (1979)].

[117] M. Dine, W. Fischler, and M. Srednicki, *A Simple Solution to the Strong CP Problem with a Harmless Axion*, Phys. Lett. B **104** (1981) 199.

[118] A. R. Zhitnitsky, *On Possible Suppression of the Axion Hadron Interactions. (In Russian)*, Sov. J. Nucl. Phys. **31** (1980) 260.

[119] R. D. Peccei, T. T. Wu, and T. Yanagida, *A viable axion model*, Phys. Lett. B **172** (1986) 435.

[120] L. M. Krauss and F. Wilczek, *A shortlived axion variant*, Phys. Lett. B **173** (1986) 189.

[121] C. Coriano and N. Irges, *Windows over a New Low Energy Axion*, Phys. Lett. B **651** (2007) 298, arXiv: hep-ph/0612140.

[122] Y. Ema, K. Hamaguchi, T. Moroi, and K. Nakayama, *Flaxion: a minimal extension to solve puzzles in the standard model*, JHEP **01** (2017) 096, arXiv: 1612.05492 [hep-ph].

[123] S. Centelles Chuliá, C. Döring, W. Rodejohann, and U. J. Saldaña-Salazar, *Natural axion model from flavour*, JHEP **09** (2020) 137, arXiv: 2005.13541 [hep-ph].

[124] L. Di Luzio, M. Giannotti, E. Nardi, and L. Visinelli, *The landscape of QCD axion models*, Phys. Rept. **870** (2020) 1, arXiv: 2003.01100 [hep-ph].

[125] P. Sikivie, *Of Axions, Domain Walls and the Early Universe*, Phys. Rev. Lett. **48** (1982) 1156.

[126] G. Lazarides and Q. Shafi, *Axion Models with No Domain Wall Problem*, Phys. Lett. B **115** (1982) 21.

[127] M. C. Huang and P. Sikivie, *The Structure of Axionic Domain Walls*, Phys. Rev. D **32** (1985) 1560.

[128] C. Q. Geng and J. N. Ng, *The Domain Wall Number in Various Invisible Axion Models*, Phys. Rev. D **41** (1990) 3848.

[129] P. Sikivie, *Axion Cosmology*, Lect. Notes Phys. **741** (2008) 19, ed. by M. Kuster, G. Raffelt, and B. Beltran, arXiv: `astro-ph/0610440`.

[130] J. Preskill, M. B. Wise, and F. Wilczek, *Cosmology of the Invisible Axion*, Phys. Lett. B **120** (1983) 127, ed. by M. A. Srednicki.

[131] L. F. Abbott and P. Sikivie, *A Cosmological Bound on the Invisible Axion*, Phys. Lett. B **120** (1983) 133, ed. by M. A. Srednicki.

[132] M. Dine and W. Fischler, *The Not So Harmless Axion*, Phys. Lett. B **120** (1983) 137, ed. by M. A. Srednicki.

[133] J. Ipser and P. Sikivie, *Are Galactic Halos Made of Axions?* Phys. Rev. Lett. **50** (1983) 925.

[134] M. S. Turner, *Thermal production of not so invisible axions in the early Universe*, Phys. Rev. Lett. **59** (1987) 2489, [Erratum: Phys.Rev.Lett. 60, 1101 (1988)].

[135] L. D. Duffy and K. van Bibber, *Axions as Dark Matter Particles*, New J. Phys. **11** (2009) 105008, arXiv: `0904.3346 [hep-ph]`.

[136] M. S. Turner, *Windows on the Axion*, Phys. Rept. **197** (1990) 67.

[137] D. Lee, U.-G. Meißner, K. A. Olive, M. Shifman, and T. Vonk, *θ-dependence of light nuclei and nucleosynthesis*, Phys. Rev. Res. **2** (2020) 033392, arXiv: `2006.12321 [hep-ph]`.

[138] T. Vonk, *Studies on the QCD θ-vacuum in chiral perturbation theory, Vacuum structure at large-N_c, physics at $\theta \sim \pi$, and effects of θ on two-nucleon systems*, MA thesis: Rheinische Friedrich-Wilhelms-Universität Bonn, 2019.

[139] L. Ubaldi, *Effects of theta on the deuteron binding energy and the triple-alpha process*, Phys. Rev. D **81** (2010) 025011, arXiv: `0811.1599 [hep-ph]`.

[140] N. R. Acharya, F.-K. Guo, M. Mai, and U.-G. Meißner, *θ-dependence of the lightest meson resonances in QCD*, Phys. Rev. D **92** (2015) 054023, arXiv: `1507.08570 [hep-ph]`.

[141] S. Elhatisari, T. A. Lähde, D. Lee, U.-G. Meißner, and T. Vonk, *Alpha-alpha scattering in the Multiverse*, JHEP **02** (2022) 001, arXiv: `2112.09409 [hep-th]`.

[142] E. Epelbaum, H. Krebs, T. A. Lähde, D. Lee, and U.-G. Meißner, *Dependence of the triple-alpha process on the fundamental constants of nature*, Eur. Phys. J. A **49** (2013) 82, arXiv: `1303.4856 [nucl-th]`.

[143] T. A. Lähde, U.-G. Meißner, and E. Epelbaum, *An update on fine-tunings in the triple-alpha process*, Eur. Phys. J. A **56** (2020) 89, arXiv: `1906.00607 [nucl-th]`.

[144] Z.-Y. Lu, M.-L. Du, F.-K. Guo, U.-G. Meißner, and T. Vonk, *QCD θ-vacuum energy and axion properties*, JHEP **05** (2020) 001, arXiv: `2003.01625 [hep-ph]`.

[145] P. Sikivie, *Experimental Tests of the Invisible Axion*,
Phys. Rev. Lett. **51** (1983) 1415, ed. by M. A. Srednicki, [Erratum: Phys.Rev.Lett. 52, 695 (1984)].

[146] P. Sikivie, *Detection Rates for 'Invisible' Axion Searches*,
Phys. Rev. D **32** (1985) 2988, [Erratum: Phys.Rev.D 36, 974 (1987)].

[147] B. M. Brubaker et al., *First results from a microwave cavity axion search at 24 μeV*,
Phys. Rev. Lett. **118** (2017) 061302, arXiv: `1610.02580 [astro-ph.CO]`.

[148] A. Caldwell et al., *Dielectric Haloscopes: A New Way to Detect Axion Dark Matter*,
Phys. Rev. Lett. **118** (2017) 091801, arXiv: `1611.05865 [physics.ins-det]`.

[149] B. T. McAllister et al., *The ORGAN Experiment: An axion haloscope above 15 GHz*,
Phys. Dark Univ. **18** (2017) 67, arXiv: `1706.00209 [physics.ins-det]`.

[150] N. Du et al., *A Search for Invisible Axion Dark Matter with the Axion Dark Matter Experiment*,
Phys. Rev. Lett. **120** (2018) 151301, arXiv: `1804.05750 [hep-ex]`.

[151] P. Brun et al., *A new experimental approach to probe QCD axion dark matter in the mass range above 40 μeV*, Eur. Phys. J. C **79** (2019) 186,
arXiv: `1901.07401 [physics.ins-det]`.

[152] A. O. Gattone et al., *Experimental search for solar axions*,
Nucl. Phys. B Proc. Suppl. **70** (1999) 59, ed. by A. Bottino, A. Di Credico, and P. Monacelli,
arXiv: `astro-ph/9712308`.

[153] K. Zioutas et al., *A Decommissioned LHC model magnet as an axion telescope*,
Nucl. Instrum. Meth. A **425** (1999) 480, arXiv: `astro-ph/9801176`.

[154] I. G. Irastorza et al., *Towards a new generation axion helioscope*, JCAP **06** (2011) 013,
arXiv: `1103.5334 [hep-ex]`.

[155] M. Arik et al., *New solar axion search using the CERN Axion Solar Telescope with ^{4}He filling*,
Phys. Rev. D **92** (2015) 021101, arXiv: `1503.00610 [hep-ex]`.

[156] V. Anastassopoulos et al., *New CAST Limit on the Axion-Photon Interaction*,
Nature Phys. **13** (2017) 584, arXiv: `1705.02290 [hep-ex]`.

[157] K. Van Bibber, N. R. Dagdeviren, S. E. Koonin, A. Kerman, and H. N. Nelson,
Proposed experiment to produce and detect light pseudoscalars, Phys. Rev. Lett. **59** (1987) 759.

[158] P. Pugnat et al.,
First results from the OSQAR photon regeneration experiment: No light shining through a wall,
Phys. Rev. D **78** (2008) 092003, arXiv: `0712.3362 [hep-ex]`.

[159] R. Ballou et al., *New exclusion limits on scalar and pseudoscalar axionlike particles from light shining through a wall*, Phys. Rev. D **92** (2015) 092002, arXiv: `1506.08082 [hep-ex]`.

[160] D. B. Kaplan, *Opening the Axion Window*, Nucl. Phys. B **260** (1985) 215.

[161] M. Srednicki, *Axion Couplings to Matter. 1. CP Conserving Parts*,
Nucl. Phys. B **260** (1985) 689.

[162] H. Georgi, D. B. Kaplan, and L. Randall, *Manifesting the Invisible Axion at Low-energies*,
Phys. Lett. B **169** (1986) 73.

[163] S. Chang and K. Choi, *Hadronic axion window and the big bang nucleosynthesis*, Phys. Lett. B **316** (1993) 51, arXiv: hep-ph/9306216.

[164] G. Grilli di Cortona, E. Hardy, J. Pardo Vega, and G. Villadoro, *The QCD axion, precisely*, JHEP **01** (2016) 034, arXiv: 1511.02867 [hep-ph].

[165] N. Iwamoto, *Axion Emission from Neutron Stars*, Phys. Rev. Lett. **53** (1984) 1198.

[166] R. Mayle et al., *Constraints on Axions from SN 1987a*, Phys. Lett. B **203** (1988) 188.

[167] R. P. Brinkmann and M. S. Turner, *Numerical Rates for Nucleon-Nucleon Axion Bremsstrahlung*, Phys. Rev. D **38** (1988) 2338.

[168] G. Raffelt and D. Seckel, *Bounds on Exotic Particle Interactions from SN 1987a*, Phys. Rev. Lett. **60** (1988) 1793.

[169] M. S. Turner, *Axions from SN 1987a*, Phys. Rev. Lett. **60** (1988) 1797.

[170] A. Burrows, M. S. Turner, and R. P. Brinkmann, *Axions and SN 1987a*, Phys. Rev. D **39** (1989) 1020.

[171] W. Keil et al., *A Fresh look at axions and SN-1987A*, Phys. Rev. D **56** (1997) 2419, arXiv: astro-ph/9612222.

[172] G. G. Raffelt, *Astrophysical axion bounds*, Lect. Notes Phys. **741** (2008) 51, ed. by M. Kuster, G. Raffelt, and B. Beltran, arXiv: hep-ph/0611350.

[173] A. Sedrakian, *Axion cooling of neutron stars*, Phys. Rev. D **93** (2016) 065044, arXiv: 1512.07828 [astro-ph.HE].

[174] K. Hamaguchi, N. Nagata, K. Yanagi, and J. Zheng, *Limit on the Axion Decay Constant from the Cooling Neutron Star in Cassiopeia A*, Phys. Rev. D **98** (2018) 103015, arXiv: 1806.07151 [hep-ph].

[175] M. V. Beznogov, E. Rrapaj, D. Page, and S. Reddy, *Constraints on Axion-like Particles and Nucleon Pairing in Dense Matter from the Hot Neutron Star in HESS J1731-347*, Phys. Rev. C **98** (2018) 035802, arXiv: 1806.07991 [astro-ph.HE].

[176] A. Sedrakian, *Axion cooling of neutron stars. II. Beyond hadronic axions*, Phys. Rev. D **99** (2019) 043011, arXiv: 1810.00190 [astro-ph.HE].

[177] J. H. Chang, R. Essig, and S. D. McDermott, *Supernova 1987A Constraints on Sub-GeV Dark Sectors, Millicharged Particles, the QCD Axion, and an Axion-like Particle*, JHEP **09** (2018) 051, arXiv: 1803.00993 [hep-ph].

[178] P. Carenza et al., *Improved axion emissivity from a supernova via nucleon-nucleon bremsstrahlung*, JCAP **10** (2019) 016, [Erratum: JCAP 05, E01 (2020)], arXiv: 1906.11844 [hep-ph].

[179] G. G. Raffelt, *Astrophysical methods to constrain axions and other novel particle phenomena*, Phys. Rept. **198** (1990) 1.

[180] T. Vonk, F.-K. Guo, and U.-G. Meißner, *The axion-baryon coupling in SU(3) heavy baryon chiral perturbation theory*, JHEP **08** (2021) 024, arXiv: 2104.10413 [hep-ph].

[181] N. K. Glendenning, *Neutron Stars Are Giant Hypernuclei?* Astrophys. J. **293** (1985) 470.

[182] F. Weber and M. K. Weigel,
Neutron Star Properties and the Relativistic Nuclear Equation of State of Many Baryon Matter,
Nucl. Phys. A **493** (1989) 549.

[183] J. R. Ellis, J. I. Kapusta, and K. A. Olive,
Strangeness, glue and quark matter content of neutron stars, Nucl. Phys. B **348** (1991) 345.

[184] N. K. Glendenning and S. A. Moszkowski,
Reconciliation of neutron star masses and binding of the lambda in hypernuclei,
Phys. Rev. Lett. **67** (1991) 2414.

[185] R. Knorren, M. Prakash, and P. J. Ellis, *Strangeness in hadronic stellar matter*,
Phys. Rev. C **52** (1995) 3470, arXiv: `nucl-th/9506016`.

[186] J. Schaffner and I. N. Mishustin, *Hyperon rich matter in neutron stars*,
Phys. Rev. C **53** (1996) 1416, arXiv: `nucl-th/9506011`.

[187] S. Balberg, I. Lichtenstadt, and G. B. Cook, *Roles of hyperons in neutron stars*,
Astrophys. J. Suppl. **121** (1999) 515, arXiv: `astro-ph/9810361`.

[188] B. D. Lackey, M. Nayyar, and B. J. Owen,
Observational constraints on hyperons in neutron stars, Phys. Rev. D **73** (2006) 024021,
arXiv: `astro-ph/0507312`.

[189] H. Djapo, B.-J. Schaefer, and J. Wambach, *On the appearance of hyperons in neutron stars*,
Phys. Rev. C **81** (2010) 035803, arXiv: `0811.2939 [nucl-th]`.

[190] I. Bednarek, P. Haensel, J. L. Zdunik, M. Bejger, and R. Manka,
Hyperons in neutron-star cores and two-solar-mass pulsar,
Astron. Astrophys. **543** (2012) A157, arXiv: `1111.6942 [astro-ph.SR]`.

[191] S. Weissenborn, D. Chatterjee, and J. Schaffner-Bielich,
Hyperons and massive neutron stars: vector repulsion and SU(3) symmetry,
Phys. Rev. C **85** (2012) 065802, [Erratum: Phys.Rev.C 90, 019904 (2014)],
arXiv: `1112.0234 [astro-ph.HE]`.

[192] T. Miyatsu, M.-K. Cheoun, and K. Saito,
Equation of state for neutron stars in SU(3) flavor symmetry, Phys. Rev. C **88** (2013) 015802,
arXiv: `1304.2121 [nucl-th]`.

[193] M. Fortin, J. L. Zdunik, P. Haensel, and M. Bejger,
Neutron stars with hyperon cores: stellar radii and equation of state near nuclear density,
Astron. Astrophys. **576** (2015) A68, arXiv: `1408.3052 [astro-ph.SR]`.

[194] M. Oertel, C. Providência, F. Gulminelli, and A. R. Raduta,
Hyperons in neutron star matter within relativistic mean-field models,
J. Phys. G **42** (2015) 075202, arXiv: `1412.4545 [nucl-th]`.

[195] T. Katayama and K. Saito, *Hyperons in neutron stars*, Phys. Lett. B **747** (2015) 43,
arXiv: `1501.05419 [nucl-th]`.

[196] D. Chatterjee and I. Vidaña, *Do hyperons exist in the interior of neutron stars?*
Eur. Phys. J. A **52** (2016) 29, arXiv: `1510.06306 [nucl-th]`.

[197] L. Tolos, M. Centelles, and A. Ramos, *Equation of State for Nucleonic and Hyperonic Neutron Stars with Mass and Radius Constraints*, Astrophys. J. **834** (2017) 3, arXiv: 1610.00919 [astro-ph.HE].

[198] L. Tolos, M. Centelles, and A. Ramos, *The Equation of State for the Nucleonic and Hyperonic Core of Neutron Stars*, Publ. Astron. Soc. Austral. **34** (2017) e065, arXiv: 1708.08681 [astro-ph.HE].

[199] L. Tolos and L. Fabbietti, *Strangeness in Nuclei and Neutron Stars*, Prog. Part. Nucl. Phys. **112** (2020) 103770, arXiv: 2002.09223 [nucl-ex].

[200] T. Vonk, F.-K. Guo, and U.-G. Meißner, *Pion axioproduction: The Delta resonance contribution*, (2022), arXiv: 2202.00268 [hep-ph].

[201] P. Carenza, B. Fore, M. Giannotti, A. Mirizzi, and S. Reddy, *Enhanced Supernova Axion Emission and its Implications*, Phys. Rev. Lett. **126** (2021) 071102, arXiv: 2010.02943 [hep-ph].

[202] T. Fischer et al., *Observable signatures of enhanced axion emission from protoneutron stars*, Phys. Rev. D **104** (2021) 103012, arXiv: 2108.13726 [hep-ph].

θ-dependence of light nuclei and nucleosynthesis

θ-dependence of light nuclei and nucleosynthesis

Dean Lee [1,*] Ulf-G. Meißner [2,3,4,†] Keith A. Olive,[5,‡] Mikhail Shifman [5,§] and Thomas Vonk [2,∥]

[1]*Facility for Rare Isotope Beams and Department of Physics and Astronomy, Michigan State University, Michigan 48824, USA*

[2]*Helmholtz-Institut für Strahlen- und Kernphysik and Bethe Center for Theoretical Physics, Universität Bonn, D-53115 Bonn, Germany*

[3]*Institute for Advanced Simulation, Institut für Kernphysik, and Jülich Center for Hadron Physics, Forschungszentrum Jülich,*
D-52425 Jülich, Germany

[4]*Tbilisi State University, 0186 Tbilisi, Georgia*

[5]*William I. Fine Theoretical Physics Institute, School of Physics and Astronomy, University of Minnesota, Minneapolis, Minnesota 55455, USA*

We investigate the impact of the QCD vacuum at nonzero θ on the properties of light nuclei, Big Bang nucleosynthesis, and stellar nucleosynthesis. Our analysis starts with a calculation of the θ-dependence of the neutron-proton mass difference and neutron decay using chiral perturbation theory. We then discuss the θ-dependence of the nucleon-nucleon interaction using a one-boson-exchange model and compute the properties of the two-nucleon system. Using the universal properties of four-component fermions at large scattering length, we then deduce the binding energies of the three-nucleon and four-nucleon systems. Based on these results, we discuss the implications for primordial abundances of light nuclei, the production of nuclei in stellar environments, and implications for an anthropic view of the universe.

I. INTRODUCTION

One of the most outstanding questions in physics pertains to the values of the fundamental parameters in the Standard model. These include the gauge and Yukawa couplings, the latter being responsible for fermion masses and mixings. In the case of the gauge couplings, some hint is available from grand unified theories where a single unified coupling is run down from a very high energy scale to the weak scale leading to predictions for the weak scale gauge couplings in reasonable agreement with experiment. The Yukawa coupling matrices are, however, a bigger mystery which includes the generation structure of fermion masses. The answer may lie in an as yet undefined future theory (e.g., a complete string theory) in which case there is hope of a deeper understanding. It is also possible that our Universe with its observed fundamental parameters is part of a larger structure or a *Multiverse*, but we have no means to know. In this case, the observed values, may be somewhat random with no deep explanation. However, even in that case, our specific measurements of these parameters can not be completely random, as not all

*leed@frib.msu.edu

†meissner@hiskp.uni-bonn.de

‡olive@umn.edu

§shifman@umn.edu

∥vonk@hiskp.uni-bonn.de

values will permit a Universe which supports our form of life, which can carry out such measurements. This is often referred to as the anthropic principle. The anthropic principle absolves us, the Earth dwellers, from the duty of explaining the values of the governing constants, at least for the time being, until data at higher scales become available.

The term anthropic principle was coined in 1974 by Brandon Carter [1]. In the 1980s a few influential "anthropic papers" were published by Steven Weinberg, see, e.g., Ref. [2] (see also Refs. [3,4]). The anthropic principle is not a predictive theory, rather it is a philosophical idea that the governing parameters in our world should fit the intervals compatible with the existence of conscious life. The recent LHC data show no signs to support an opposite philosophical principle—that of *naturalness*.

The most remarkable and still incomprehensible example of anti-naturalness is the cosmological constant (for a different view, see e.g. [5]). Its observed value is suppressed by 124 orders of magnitude compared to the Planck scale M_P^4 (believed to be the only fundamental scale). The suppression of the electroweak scale compared to M_P is 17 orders of magnitude. The vacuum angle θ, whose natural order of magnitude ~ 1 is less than 10^{-10} in experiment [6].

It is obvious that the suppression of the cosmological constant is vital for the existence of our world. Even if it were a few orders of magnitude larger, the Universe would have entered an inflationary stage before the onset of galaxy formation. The smallness of the u, d quark masses compared to Λ_{QCD} and the fact that $m_u < m_d$ are crucial for the genesis of heavier elements in stars. However, it is widely believed that there are no anthropic limitations on θ and its suppression *must* be solved through a natural mechanism such as a symmetry including axions [7,8]. A dedicated study of this issue [9]

revealed some θ-dependence on nuclear physics but the author concludes with the statement that "these effects are not too dramatic." The authors of [7] note with regards to the vacuum angle θ that it "is hard to see an anthropic argument that θ [...] is bounded by 10^{-10}. Moreover, in the flux vacua, there is typically no light axion." For further discussions related to this issue, see Refs. [10–12]. In the present paper we revisit this issue.

While it is certainly true (and will be made clear below) that $\theta \sim 10^{-9}$ or even $\theta \sim 10^{-5}$ will not change life in our world, it seems reasonable to reconsider constraints imposed on θ from observations other than the neutron electric dipole moment (nEDM) as well as the anthropic perspective. We will see that the impact of θ on delicate aspects of nuclear physics is similar to that of the parameters $|m_u|$ or $|m_d|$. Quark mass variation of nuclear properties and reactions are considered, e.g., in Refs. [13–26]. Furthermore, if the variation of quark masses is due to an overall variation in the Yukawa couplings, it will feed into variations of a host of fundamental observables including the gauge couplings, and affect Big Bang Nucleosynthesis (BBN) [27–31], the lifetime of long-lived nuclei [32], and atomic clocks [33]. Strictly speaking, it would be more appropriate to combine the absolute values of the quark masses with their phases and analyze the limitations in the complex plane. Here, we will fix $|m_u|$ and $|m_d|$ and let θ vary. Unlike Ubaldi [9] who focused on CP-odd vertices and arrived at rather weak constrains, we will consider the θ-dependence due to CP-even vertices. For reviews on this and related issues, see, e.g., Refs. [34–38].

Our approach is limited in the sense that we do not vary all governing parameters simultaneously in a concerted way. We do not explore how variations of some of them could be masked by variation of others, for instance whether the change of θ could be compensated by that of $|m_{u,d}|$ or the impact of θ on, say, the vacuum energy density. Such a global task is a problem for the future. We will only vary θ fixing all other parameters to their observed values.

At this point, it is worth noting that the most often discussed physical effect of θ on an observable, the nEDM arising from strong CP-violation, does not impose strong anthropic constraints on θ. The nEDM stemming from the QCD θ-term is [39,40]

$$d_n(\bar{\theta}) = \mathcal{O}(10^{-16}\,\bar{\theta}\,e\,\text{cm}), \tag{1.1}$$

where $\bar{\theta} = \theta + \text{Arg}\det\mathcal{M}$ and $\mathcal{M}$ the quark mass matrix. Even if $\theta = \mathcal{O}(1)$, this is still a very small number and the physical effects of an nEDM of $\mathcal{O}(10^{-16}\,e\,\text{cm})$ on the evolution of the universe would still be negligible.

Note also that $\theta = \pi$ is a special point in which QCD has two degenerate vacua, and physics changes drastically, see, e.g., the lucid discussion in Ref. [41] (and references therein). However, here we are not interested in this special point but rather in a generic situation with $0 < \theta < \pi$.

As we discuss below, the value of θ does affect a host of hadronic properties which trigger changes in nuclear properties such as the binding energies of nuclei. Changes in θ affect the pion mass which in turn alters the neutron-proton mass difference, Δm_N which further affects the neutron decay width. We also consider the effect of θ on multi-nucleon systems and compute changes to nuclear binding energies.

The neutron-proton mass difference and the binding energy of deuteron, B_d, play a sensitive role in BBN (see Ref. [42] for the current status). As a result, changes in θ can substantially alter the abundances of the light elements produced in BBN. Thus we can set limits on θ (though they are weak) entirely independent of the nEDM. However, even with large changes in θ and large changes in the light element abundances, it is not clear that this would cause an impediment on the formation of life in the Universe. Indeed, in a related study, Steigman and Scherrer [43] addressed the question of fine-tuning in the matter-antimatter asymmetry, as measured in terms of the baryon-to-photon asymmetry η_B. While the baryon asymmetry is reliant on the existence of CP violation [44], there is no reason to suspect that the baryon asymmetry is itself related to θ. The authors of Ref. [45] found that even for $\theta \sim 1$ the observed baryon asymmetry of the universe would not be altered. Nevertheless, changes in η_B strongly affect the light element abundances, though it was concluded by Steigman and Scherrer that these could not be excluded by anthropic arguments. A similar conclusion was reached in [46] considering the effects of altered weak interactions on BBN. Here, we fix η_B and consider the changes in abundances due changes in Δm_N and B_d.

The θ induced changes will also affect stellar evolution and can lead to very different patterns of chemical evolution. In particular the changes in the nucleon-nucleon interaction, can lead to stars which yield little or no carbon or oxygen, thus potentially greatly affecting the existence of life in the Universe.

The manuscript is organized as follows: In Sec. II, we discuss the properties of various mesons and the nucleons at nonzero θ. First, we collect the knowledge about the θ-dependence of the corresponding hadron masses and coupling constants. Next, we focus on the modification of the neutron-proton mass difference and the neutron decay width. Then, we turn to the two-nucleon system in Sec. III. We first construct a simple one-boson-exchange (OBE) model to describe the two-nucleon system and then display results for the deuteron, the dineutron and the diproton with varying θ. In Sec. IV A, we combine Wigner's SU(4) symmetry with results from the literature to get a handle on the θ-dependence of the three- and four-nucleon systems. Larger nuclei are briefly discussed in Sec. IV B. Implications of these results on the nucleosynthesis in the Big Bang and in stars are discussed in Secs. V and VI, respectively. We end with a summary and a discussion of our anthropic view of the universe in Sec. VII. The Appendix contains a derivation of the neutron-proton mass difference with varying θ.

II. ONE NUCLEON

In this section, we first collect the θ-dependence of the various hadrons entering our study, i.e., of the pion, the σ, ρ and ω mesons as well as the nucleon mass. Our framework is chiral perturbation theory, in which the θ-dependence of the nucleon (and also of the light nuclei) is driven by the θ-dependence of the pion properties as well as the heavier mesons, which model the intermediate and short-range part of the nucleon-nucleon interaction. Of particular interest are the
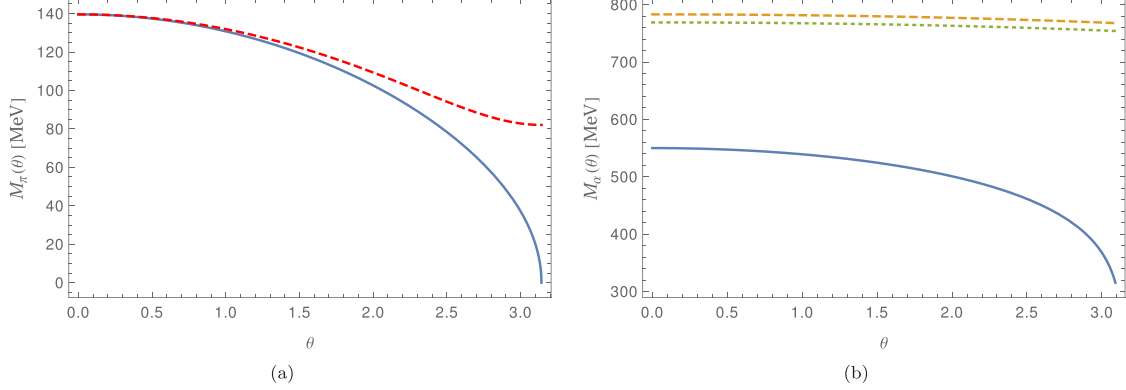
FIG. 1. The θ-dependence of the various meson masses M_α for $\alpha = \{\pi, \sigma, \rho, \omega\}$. (a) The θ-dependence of the pion in the case of two degenerate flavors (blue solid line), and in the case with $m_u \neq m_d$ (red dashed line). (b) The σ meson (blue solid line), ρ meson (green dotted line), and ω meson (orange dashed line) masses as a function of θ.

neutron-proton mass difference and the neutron decay width, which play an important role in BBN.

A. θ-dependence of hadron properties

Consider first the pion mass. We use the leading order (LO) θ-dependence for two flavors [47,48] [1],

$$M_\pi^2(\theta) = M_\pi^2 \cos\frac{\theta}{2}\sqrt{1 + \varepsilon^2 \tan^2\frac{\theta}{2}}, \qquad (2.1)$$

with $M_\pi = 139.57$ MeV, the charged pion mass, and $\varepsilon = (m_d - m_u)/(m_d + m_u)$ measures the departure from the isospin limit. For two degenerate flavors, this reduces to

$$M_\pi^2(\theta) = M_\pi^2 \cos\frac{\theta}{2}. \qquad (2.2)$$

A plot of both Eqs. (2.1) and (2.2) is shown in Fig. 1(a). Since the LO contribution gives about 95% [50] of the pion mass at $\theta = 0$, we do not need to consider higher order terms, as done e.g. in Ref. [51]. The impact of the isospin breaking term shows up mostly as $\theta \to \pi$. Note that while $\varepsilon \sim 1/3$, isospin symmetry is only broken by a few percent in nature as $(m_d - m_u)/\Lambda_{\rm QCD} \ll 1$. Here, we take $m_u = 2.27$ MeV and $m_d = 4.67$ MeV (this refers to the conventional $\overline{\rm MS}$ scheme taken at the scale $\mu = 2$ GeV).

The mass of the σ as well as the masses of the ρ and ω mesons when θ is varied are needed for the OBE model and are taken from Ref. [51], assuming $M_\omega(\theta)/M_\omega(0) = M_\rho(\theta)/M_\rho(0)$ [Fig. 1(b)].

We consider the nucleon mass in the θ vacuum to leading one-loop order (third order in the chiral expansion), which is given by [48][2]

$$m_N(\theta) = m_0 - 4c_1 M_\pi^2(\theta) - \frac{3g_A^2 M_\pi^3(\theta)}{32\pi F_\pi^2}, \qquad (2.3)$$

---

[1]An equivalent expression for the θ-dependence of the pion mass was also derived in a model of gluon dynamics in Ref. [49].

[2]Higher orders could be included, but that would go beyond the accuracy of our calculation.

where $m_0 \simeq 865$ MeV [52] is the nucleon mass in the chiral limit, $g_A = 1.27$ the axial-vector coupling constant, $F_\pi = 92.2$ MeV the pion decay constant, and $c_1 = -1.1$ GeV^{-1} [53] is a low-energy constant (LEC) from the second order chiral pion-nucleon Lagrangian, $\mathcal{L}_{\pi N}^{(2)}$, see, e.g., the review [54]. The θ-dependence of the nucleon mass is thus entirely given in terms of the pion mass, and one finds $m_N(0) = 938.92$ MeV. We show the θ dependence of the nucleon mass in Fig. 2(a).

Next, we discuss the θ-dependence of the coupling constants. The θ-dependence of the pion-nucleon coupling is related to the Goldberger-Treiman discrepancy [55]

$$g_{\pi NN}(\theta) = \frac{g_A \, m_N(\theta)}{F_\pi}\left(1 - \frac{2M_\pi^2(\theta)\bar{d}_{18}}{g_A}\right), \qquad (2.4)$$

where $\bar{d}_{18} = -0.47$ GeV^{-2} so that $g_{\pi NN}^2(0)/(4\pi) = 13.7$, which is in accordance with the most recent and precise value from Ref. [56].

As $g_{\rho\pi\pi}$ shows very little variation with θ [51], we can use universality relation $g_{\rho\pi\pi} = g_{\rho NN}$ [57] and keep $g_{\rho NN}$ as well as $g_{\omega NN}$ fixed at their values at $\theta = 0$ in what follows. Matters are different for the σ. Similar to Ubaldi [9], we employ the parametrization of Refs. [58,59]. Writing the scalar attractive piece of the nucleon-nucleon interaction as

$$H_{\rm contact} = G_S(\bar{N}N)(\bar{N}N), \qquad (2.5)$$

it is evident that

$$G_S = -\frac{g_{\sigma NN}^2}{M_\sigma^2}, \qquad (2.6)$$

when translated to an OBE model (this corresponds to resonance saturation of the corresponding LECs, see Ref. [60]). The following dependence of $G_S(\theta)$ emerges [9]:

$$G_s(\theta) = G_S(0)\left(1.4 - 0.4\frac{M_\pi^2(\theta)}{M_\pi^2}\right), \qquad (2.7)$$

where we have normalized again to the value at $\theta = 0$. Using Eq. (2.6) together with the known θ-dependence of M_σ, we

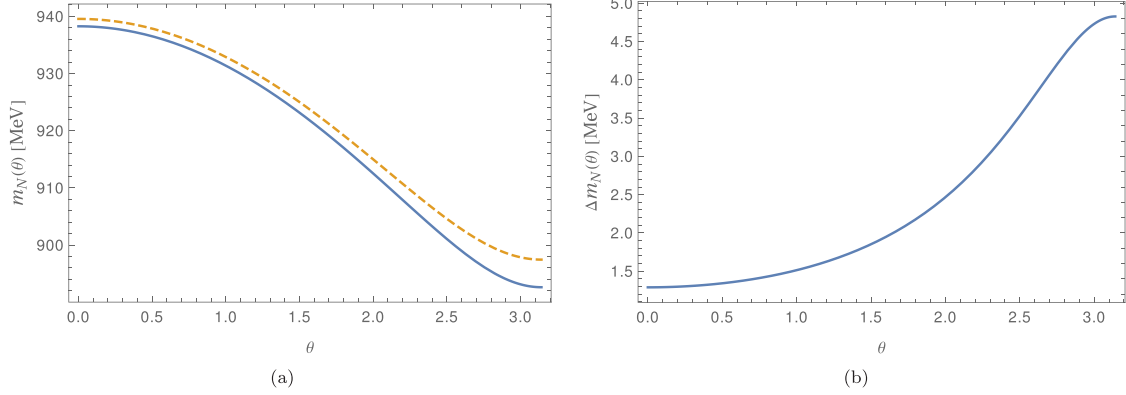FIG. 2. The θ-dependence of the nucleon masses m_N: (a) proton (blue solid line) and neutron (orange dashed line) and (b) neutron-proton mass difference.

can extract the variation of $g_{\sigma NN}$ with θ. We note that the coupling $g_{\sigma\pi\pi}$ extracted from the work of Ref. [51] also decreases with θ. We now have all of the pieces of the puzzle needed to calculate the binding energies of the various light nuclei. First, however, let us take a closer look at the neutron-proton mass difference and the neutron decay width, which also play an important role in BBN.

B. Neutron-proton mass difference

Consider the neutron-proton mass difference

$$\Delta m_N = (m_n - m_p)^{\text{QED}} + (m_n - m_p)^{\text{QCD}} \simeq 1.29 \text{ MeV}. \tag{2.8}$$

The leading contribution to the strong part to the neutron-proton mass difference arises from the second order effective pion-nucleon Lagrangian and is given by [61]

$$\begin{aligned}(m_n - m_p)^{\text{QCD}} &= 4\,c_5\,B_0\,(m_u - m_d) + \mathcal{O}\!\left(M_\pi^4\right) \\ &= -4\,c_5\,M_\pi^2\,\varepsilon + \mathcal{O}\!\left(M_\pi^4\right),\end{aligned} \tag{2.9}$$

where c_5 is a LEC. Using the most recent determination of the electromagnetic part of this mass difference, $(m_n - m_p)^{\text{QED}} = -(0.58 \pm 0.16)\,\text{MeV}$ [62], this amounts to $(m_n - m_p)^{\text{QCD}} = 1.87 \mp 0.16\,\text{MeV}$ and correspondingly, $c_5 = (-0.074 \pm 0.006)\,\text{GeV}^{-1}$. In the θ-vacuum, this term turns into [63] (for a derivation, see Appendix)

$$(m_n - m_p)^{\text{QCD}}(\theta) \simeq 4\,c_5\,B_0\,\frac{M_\pi^2}{M_\pi^2(\theta)}\,(m_u - m_d), \tag{2.10}$$

i.e the strong part of the neutron-proton mass increases (in magnitude) with θ, see Fig. 2(b). At $\theta \simeq 0.25$, $\Delta m_N(\theta)$ deviates already by about 1 % from its real world value, and for the range of $\theta = 1$–2, we find $\Delta m_N(\theta) = 1.51$–$2.47\,\text{MeV}$, using Eq. (2.1) for $M_\pi(\theta)$.

C. Neutron decay width

As we increase θ, the neutron-proton mass difference, $\Delta m_N(\theta)$, becomes larger and results in a larger three-body phase space for neutron beta decay. This increase in the phase

space integral scales roughly as the neutron-proton mass difference to the fifth power and is dominant over any expected θ-dependence in the axial vector coupling, g_A. The neutron beta decay width can be written as (for the moment, we explicitly display factors of Planck's constant $\hbar$ and the speed of light c, otherwise we work in natural units, $k_B = \hbar = c = 1$)

$$\Gamma_n = \frac{m_e^5 c^4}{2\pi^3 \hbar^6}|\mathcal{M}|^2 f, \tag{2.11}$$

where m_e is the electron mass, $\mathcal{M}$ is the weak matrix element, and f is the Fermi integral,

$$f = \int_0^{m_n - m_p - m_e} F(Z, T_e)\,p_e T_e (m_n - m_p - m_e - T_e)^2\,dT_e, \tag{2.12}$$

where $Z = 1$ is the proton charge, T_e is the electron kinetic energy, p_e is the electron momentum, and $F(Z, T_e)$ is the Fermi function that takes into account Coulomb scattering [64]. In Fig. 3, we plot $[\Gamma_n(\theta)/\Gamma_n(0)]^{1/5}$ versus $\Delta m_N(\theta) - m_e$ showing the linear behavior as expected. In Fig. 4, the neutron mean life is shown as a function of θ. We see that the lifetime drops off very quickly when θ starts to deviate from the
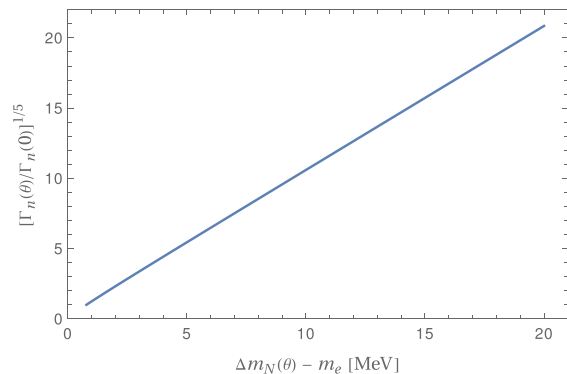

FIG. 3. Neutron decay width $\Gamma_n(\theta)$ as a function of the neutron-proton mass difference. We plot the dimensionless quantity $[\Gamma_n(\theta)/\Gamma_n(0)]^{1/5}$ vs $\Delta m_N(\theta) - m_e$.
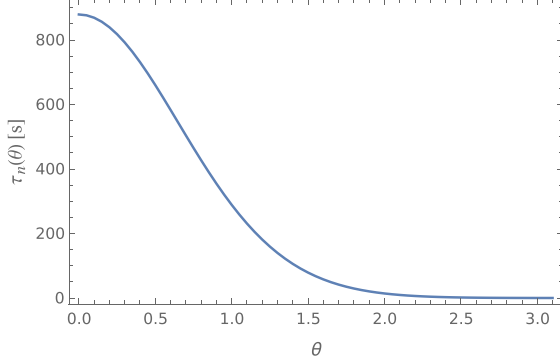
30

FIG. 4. Neutron life time $\tau_n(\theta)$ as a function of θ.

Standard model value $\theta \approx 0$. As we will see this dependence plays a big role at the start of BBN.

III. TWO NUCLEONS

Here, we outline the formalism underlying our study of the two-nucleon system. First, we construct a simple OBE model, that allows us to describe the binding energies of the deuteron and the unbound dineutron and diproton at $\theta = 0$. Then, we discuss how these two-nucleon systems change when θ varies from 0 to π.

A. OBE model

Consider first the case $\theta = 0$. We set up an OBE model inspired by Ref. [65] and work with the Schrödinger equation, as the nucleons in the deuteron move with velocities $v \ll c$. The corresponding OBE potential is given by

$$V_{\text{OBE}}(\mathbf{q}) = \sum_{\alpha=\{\pi,\sigma,\omega,\rho\}} V_{\alpha}(\mathbf{q}) \qquad (3.1)$$

where $\mathbf{q}$ denotes the momentum transfer. The static limit is applied, i.e. the four-momentum transfer squared $q^2 = (p'-p)^2 = -(\mathbf{p}'-\mathbf{p})^2 = -\mathbf{q}^2$. Setting furthermore $L = 0$, i.e. focusing on the dominant S-wave and neglecting the small D-wave contribution, the respective potentials can be reduced to

$$V_{\pi}(\mathbf{q}) = -(\boldsymbol{\tau_1} \cdot \boldsymbol{\tau_2})(\boldsymbol{\sigma_1} \cdot \boldsymbol{\sigma_2}) \frac{g_{\pi NN}^2}{\mathbf{q}^2 + M_{\pi}^2} \frac{\mathbf{q}^2}{12 m_N^2}, \qquad (3.2)$$

$$V_{\sigma}(\mathbf{q}, \mathbf{P}) = -\frac{g_{\sigma NN}^2}{\mathbf{q}^2 + M_{\sigma}^2}\left(1 + \frac{\mathbf{q}^2}{8 m_N^2} - \frac{\mathbf{P}^2}{2 m_N^2}\right), \qquad (3.3)$$

$$V_{\omega}(\mathbf{q}, \mathbf{P}) = \frac{g_{\omega NN}^2}{\mathbf{q}^2 + M_{\omega}^2}\left(1 - \frac{\mathbf{q}^2}{2 m_N^2}\left[\frac{1}{4} + \frac{1}{3}(\boldsymbol{\sigma_1} \cdot \boldsymbol{\sigma_2})\right] + \frac{3\mathbf{P}^2}{2 m_N^2}\right), \qquad (3.4)$$

$$V_{\rho}(\mathbf{q}, \mathbf{P}) = (\boldsymbol{\tau_1} \cdot \boldsymbol{\tau_2}) \frac{g_{\rho NN}^2}{\mathbf{q}^2 + M_{\rho}^2}\left(1 - \frac{\mathbf{q}^2}{2 m_N^2}\left[\frac{1}{4} + \frac{g_{\text{T}}^{\rho}}{g_{\rho NN}}\right.\right.$$
$$\left.\left. + \frac{1}{3}\left(1 + \frac{g_{\text{T}}^{\rho}}{g_{\rho NN}}\right)^2 (\boldsymbol{\sigma_1} \cdot \boldsymbol{\sigma_2})\right] + \frac{3\mathbf{P}^2}{2 m_N^2}\right), \qquad (3.5)$$

where $\mathbf{P} = (\mathbf{p}' + \mathbf{p})/2$. Terms $\propto (\mathbf{q} \times \mathbf{P})$, which in coordinate space correspond to terms $\propto \mathbf{L}$, the angular momentum operator, and terms $\propto S_{12}(\mathbf{q}) = 3(\boldsymbol{\sigma_1} \cdot \mathbf{q})(\boldsymbol{\sigma_2} \cdot \mathbf{q}) - (\boldsymbol{\sigma_1} \cdot \boldsymbol{\sigma_2})|\mathbf{q}|^2$, have been omitted. The potentials depend on the total spin S of the two-nucleon system through the factor $(\boldsymbol{\sigma_1} \cdot \boldsymbol{\sigma_2}) = 2S(S+1) - 3$ and on the total isospin I through the factor $(\boldsymbol{\tau_1} \cdot \boldsymbol{\tau_2}) = 2I(I+1) - 3$. Note also that we omit from the start the ωNN tensor coupling as the corresponding coupling constant g_{ω}^T is approximately zero, which is a good approximation, see, e.g., Refs. [65,66].

The corresponding potentials in coordinate space are of Yukawa-type and given by

$$V_{\pi}(r) = (\boldsymbol{\tau_1} \cdot \boldsymbol{\tau_2})(\boldsymbol{\sigma_1} \cdot \boldsymbol{\sigma_2})\frac{g_{\pi NN}^2}{4\pi}\frac{1}{12}\left(\frac{M_{\pi}}{m_N}\right)^2\frac{e^{-M_{\pi}r}}{r}, \qquad (3.6)$$

$$V_{\sigma}(r) = -\frac{g_{\sigma NN}^2}{4\pi}\left(1 - \frac{1}{4}\left(\frac{M_{\sigma}}{m_N}\right)^2\right)\frac{e^{-M_{\sigma}r}}{r}, \qquad (3.7)$$

$$V_{\omega}(r) = \frac{g_{\omega NN}^2}{4\pi}\left(1 + \frac{1}{2}\left(\frac{M_{\omega}}{m_N}\right)^2\left[1 + \frac{1}{3}(\boldsymbol{\sigma_1} \cdot \boldsymbol{\sigma_2})\right]\right)\frac{e^{-M_{\omega}r}}{r}, \qquad (3.8)$$

$$V_{\rho}(r) = (\boldsymbol{\tau_1} \cdot \boldsymbol{\tau_2})\frac{g_{\rho NN}^2}{4\pi}\left(1 + \frac{1}{2}\left(\frac{M_{\rho}}{m_N}\right)^2\left[1 + \frac{g_{\text{T}}^{\rho}}{g_{\rho NN}}\right.\right.$$
$$\left.\left. + \frac{1}{3}\left(1 + \frac{g_{\text{T}}^{\rho}}{g_{\rho NN}}\right)^2 (\boldsymbol{\sigma_1} \cdot \boldsymbol{\sigma_2})\right]\right)\frac{e^{-M_{\rho}r}}{r}. \qquad (3.9)$$

The OBE potential requires regularization since it is ultraviolet-divergent. This can be most easily seen from the momentum-space representation, Eqs. (3.2)–(3.5), as these potentials grow quadratically with increasing momentum transfer. A standard regularization procedure in nuclear physics is to apply either a single vertex form factor controlled by the cutoff mass Λ for the total potential, or four individual form factors controlled by the cutoff masses Λ_{α} for each meson exchange potential. Here, we are only interested in the binding energies of the nucleon-nucleon systems, therefore a single form factor is sufficient. The total OBE potential in the coordinate-space representation is then:

$$V_{\text{OBE}}(r) = \sum_{\alpha=\{\pi,\sigma,\omega,\rho\}} V_{\alpha}(r) + \frac{\Lambda}{4\pi}\frac{e^{-\Lambda r}}{r}. \qquad (3.10)$$

At $\theta = 0$, the meson masses we use are

$$M_{\pi} = 139.57 \text{ MeV}, \quad M_{\sigma} = 550 \text{ MeV},$$
$$M_{\omega} = 783 \text{ MeV}, \quad M_{\rho} = 769 \text{ MeV}. \qquad (3.11)$$

In order to assess the parameter dependence, we take two sets of parameters, cf. Ref. [65]:

$$\frac{g_{\sigma NN}^2}{4\pi} = 14.17, \quad \frac{g_{\rho NN}^2}{4\pi} = 0.80, \quad \frac{g_{\omega NN}^2}{4\pi} = 20.0,$$
$$\Lambda = 1.364 \text{ GeV}, \qquad (3.12)$$

which we call *parameter set I*, and

$$\frac{g_{\sigma NN}^2}{4\pi} = 8.06, \quad \frac{g_{\rho NN}^2}{4\pi} = 0.43, \quad \frac{g_{\omega NN}^2}{4\pi} = 10.6,$$
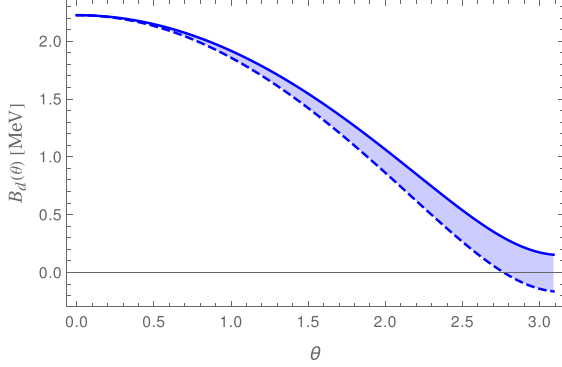$$\Lambda = 2.039 \text{ GeV}, \qquad (3.13)$$

31

FIG. 5. The binding energy of the deuteron for a θ-dependent OPE with all other meson couplings and masses are kept fixed, for parameter set I, Eq. (3.12) (solid line) and parameter set II, Eq. (3.13) (dashed line), respectively.
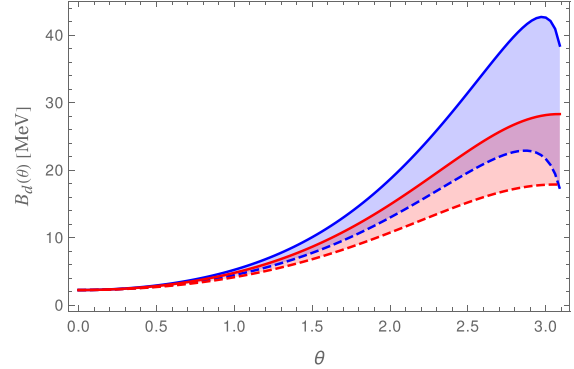

FIG. 6. The binding energy of the deuteron for the full θ-dependent OBE model in the isospin symmetric case (blue upper band) and in the case of broken isospin symmetry (red lower band) for parameter set I, Eq. (3.12) (solid lines) and parameter set II, Eq. (3.13) (dashed lines), respectively.

which we call *parameter set II*. For both sets, we take $g_{\mathrm{T}}^{\rho}/g_{\rho NN} = 6.1$ [65,66]. After solving the radial Schrödinger equation for the two nucleon system, one finds for both parameter sets a bound deuteron with binding energy $E_d = -B_d = -2.224$ MeV, and an unbound dineutron with $E_{nn} = -B_{nn} = 0.072$ MeV.

We now have all of the parts needed to investigate the θ-dependence of the binding energies of the various two-nucleon systems.

B. Spin-triplet channel

The bound state in the spin-triplet channel is the deuteron. Here, we work out the θ-dependence of its binding energy.

Consider first the case of a θ-dependent one-pion-exchange (OPE) potential, whereas all other potentials remain constant. The resulting θ-dependent deuteron binding energy is shown in Fig. 5. If all OBE exchange potentials were independent of θ except for the OPE potential, the deuteron's binding energy would slowly decrease until the deuteron would no longer be bound for $\theta \gtrsim 2.8$ for parameter set II, Eq. (3.13). This is the expected behavior of the OPE potential that led to the idea that the deuteron for $\theta \neq 0$ might not be bound anymore. This brief estimate demonstrates that the next-to-leading order contributions calculated by Ubaldi [9], which were reevaluated in Ref. [63], are (a) negligible (because they are CP-odd and only account for a shift of a few percent), but also that (b) the approach of applying first order perturbation theory is invalid, because the effects of θ on the leading order OPE potential are not small.

However, the actual contribution of the OPE potential to the total OBE potential is very small, which can be seen, e.g., by considering the individual potentials $V(r)$ of Eqs. (3.6)–(3.9). Clearly, the smallness of the OPE contribution compared to the strong repulsion of the ω exchange potential and the large attraction of the ρ and σ exchange suggests that, even if the effects of θ on the scalar and vector meson masses are not as pronounced as that for the pion, these contributions finally determine the actual θ-dependence of B_d.

Consider now the case of a full θ-dependent OBE potential. We study two cases: first, the isospin symmetric case with $m_u = m_d = (2.27 + 4.67)/2 = 3.47$ MeV, and second, the case of broken isospin symmetry with $m_u = 2.27$ MeV and $m_d = 4.67$ MeV. This gives the result shown in Fig. 6. In the isospin symmetric case, we find that after increasing and reaching a maximum at $\theta \simeq 3.0$ (parameter set I, corresponding to $B_d \simeq 42.5$ MeV) and $\theta \simeq 2.9$ (parameter set II, corresponding to $B_d \simeq 22.8$ MeV), respectively, the binding energy decreases and seems to approach to B_d in the chiral limit, $B_d^{\mathrm{c.l.}} \simeq F_{\pi}^2/m \simeq 10$ MeV [15], at least in the case of parameter set II. This behavior is expected: As we have set $m_u = m_d$, $\theta \to \pi$ effectively corresponds to $m_u = m_d \to 0$, since the charged and the neutral pion masses vanish in both cases. Because of that, all other phenomenological quantities such as the nucleon mass and the pion-nucleon coupling approach their respective values in the chiral limit.

In the case of broken isospin symmetry, the curve flattens and reaches its maximum as $\theta \to \pi$, which is given by $B_d \simeq 28.3$ MeV (parameter set I) and $B_d \simeq 17.8$ MeV (parameter set II). A useful analytic approximation for $B_d(\theta)$ is given by

$$B_d(\theta) = 2.22 + c_1(1 - \cos\theta) + c_2(1 - \cos\theta)^2 + c_3(1 - \cos\theta)^3 \tag{3.14}$$

with

unbroken isospin symmetry:

$$\begin{cases} c_1 = 9.14 & c_2 = -7.19 & c_3 = 6.30 & \text{set I} \\ c_1 = 3.25 & c_2 = 2.55 & c_3 = 0.47 & \text{set II} \end{cases}, \tag{3.15}$$

broken isospin symmetry:

$$\begin{cases} c_1 = 5.68 & c_2 = -1.02 & c_3 = 2.36 & \text{set I} \\ c_1 = 3.77 & c_2 = 0.45 & c_3 = 0.80 & \text{set II} \end{cases}. \tag{3.16}$$
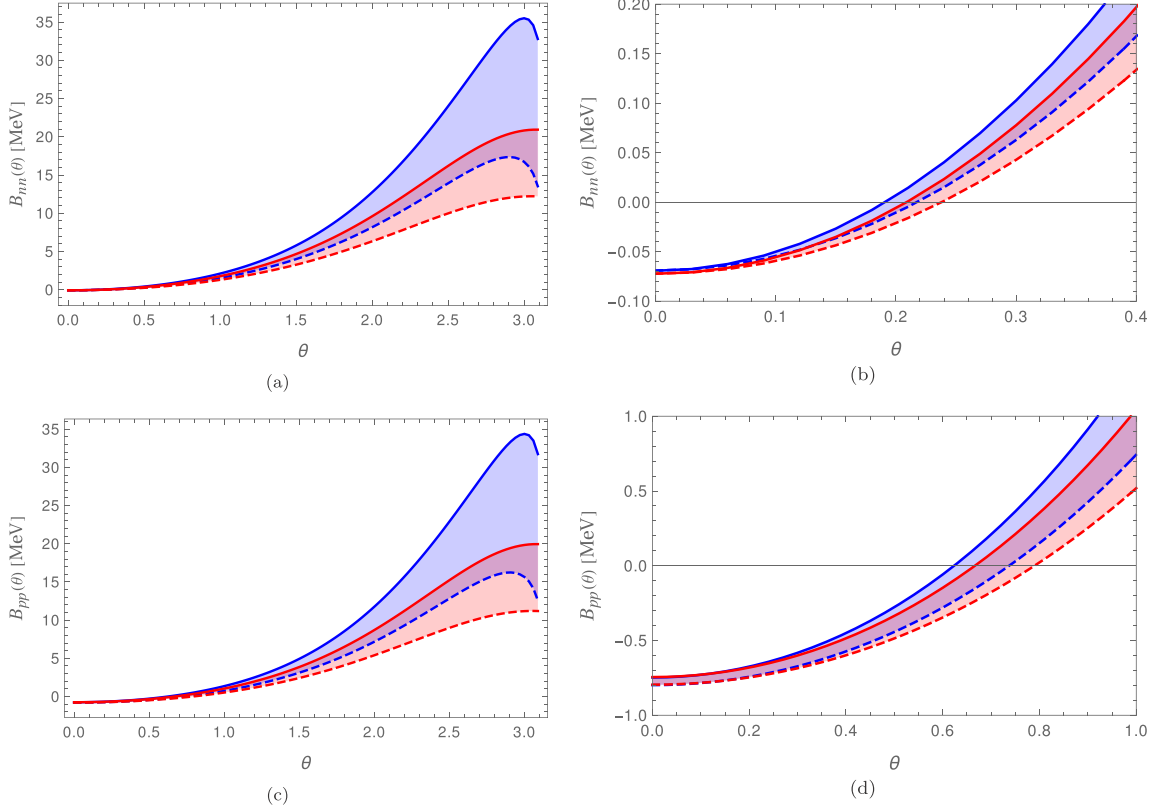
32

FIG. 7. The binding energies of the dineutron ([(a) and (b)] zoom into the region $\theta \leqslant 0.4$) and of the diproton ([(c) and (d)] zoom into the region $\theta \leqslant 1$) for the full θ-dependent OBE model. In each figure, the blue (upper) band represents the isospin symmetric case and the red (lower) band the case of broken isospin symmetry. A band is spanned by a solid line based on parameter set I, Eq. (3.12), and a dashed line based on parameter set II, Eq. (3.13).

C. Spin-singlet channel

The same analysis can be repeated for the dineutron with results shown in Figs. 7(a) and 7(b). Using Eqs. (3.6)–(3.9), one sees that the OPE and the σ exchange potentials are exactly the same for both deuteron and dineutron, i.e., with $S = 1$ and $I = 0$ (deuteron), and with $S = 0$ and $I = 1$ (dineutron). The vector exchange potentials on the other hand change in terms of the strength, but not regarding the overall sign: the ρ exchange potential is still attractive, but weakened by about 50%, whereas the ω exchange potential is still repulsive, but weakened by about 1/3. The dineutron OBE potential is thus slightly less attractive in comparison with the deuteron OBE potential, so the dineutron fails to be bound, as in the real world. However, anything that happened to the deuteron OBE potential when sending $\theta \to \pi$, this also happens to the dineutron potential, i.e., the most decisive effects come from the σ exchange potential, which is getting stronger (while the increase of the ρ exchange attraction and the increase of the ω exchange repulsion roughly neutralize), so the dineutron becomes bound. From Fig. 7(b) one sees that this happens already for $\theta \simeq 0.18$–0.24.

The overall θ-dependence of the dineutron's binding energy is the same as for the deuteron. Note that while the binding energy of the dineutron steadily increases, it remains smaller than the binding energy of the deuteron.

We note that a bound dineutron is also found in lattice QCD calculations with pion masses larger than the physical one, see Refs. [67–70], which span pion masses from 300 to 510 MeV. The central binding energies in these works span the range from 7 to 13 MeV, similar to what we find at $\theta = 1 - 2$.

We end with a short discussion of the diproton with $S = 0$ and $I = 1$. Referring to isospin symmetry, the only difference between the nn and the pp systems is the repulsive Coulomb interaction in the latter case:

$$V_C(r) = \frac{e^2}{r}, \tag{3.17}$$

with e the elementary charge. Adding this to our OBE potential Eq. (3.10), we find a constant shift of -0.67 and -0.72 MeV for sets I and II, respectively, compared to the dineutron case as shown in Figs. 7(c) and 7(d). The only visible effect of this is that the crossover point from the unbound to the bound case now happens at $\theta \simeq 0.6 - 0.8$ [Fig. 7(d)].
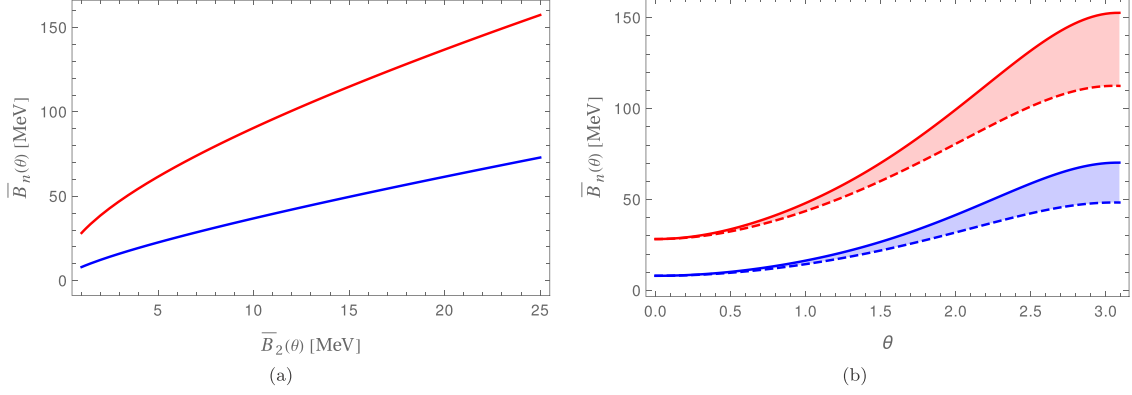
FIG. 8. (a) The SU(4)-averaged binding energy of the three- and four-nucleon systems $\bar{B}_n(\theta)$ versus the SU(4)-averaged binding energy of the two-nucleon system, $\bar{B}_2(\theta)$. Blue (lower) line: $n = 3$. Red (upper) line: $n = 4$. (b) $\bar{B}_n(\theta)$ versus θ, taking isospin breaking effects into account, for parameter set I (solid lines), and parameter set II (dashed lines). Blue (lower) band: $n = 3$. Red (upper) band: $n = 4$.

IV. MORE THAN TWO NUCLEONS

A. Three and four nucleons

We have seen that the nucleon-nucleon interaction becomes more attractive as θ increases. This is predominantly due to the decrease in the σ meson mass. Since the σ meson is a scalar particle with zero isospin, the increased attraction is approximately the same in the spin-singlet and spin-triplet channels. This is a realization of Wigner's SU(4) symmetry [71]. Wigner's SU(4) symmetry is an approximate symmetry of low-energy nuclear physics where the four spin and isospin degrees of freedom are four components of an SU(4) multiplet.

In the SU(4) limit where the spin-singlet and spin-triplet scattering lengths are large and equal, the properties of light nuclei with up to four nucleons follow the same universal behavior that describes attractive bosons at large scattering length [72–76]. We can use this information to determine the θ-dependent binding energies of ^{3}H, ^{3}He, and ^{4}He. In order to perform this analysis, we first average over nuclear states which become degenerate in the SU(4) limit. For the $A = 2$ system, we average over the physical deuteron and spin-singlet channel to arrive at an average binding energy of $\bar{B}_2 \simeq 1$ MeV. For the $A = 3$ system, we average over the physical ^{3}H and ^{3}He systems for an average binding energy of $\bar{B}_3 = 8.1$ MeV. For the $A = 4$ system, we take the physical ^{4}He binding energy, $\bar{B}_4 = 28.3$ MeV.

In order to extend these binding energies to nonzero θ, we use the numerical results from a study of bosonic clusters at large scattering length [77]. In particular, we use an empirical observation from Fig. 7 of Ref. [77] that

$$[\bar{B}_n/B]^{1/4} - [\bar{B}_2/B]^{1/4} \qquad (4.1)$$

remains approximate constant for positive scattering length $a > 0$, where B is a binding energy scale set by a combination of the range of the interaction and particle mass. Conveniently, the value of B is approximately equal to the value of $\bar{B}_4$ at infinite scattering length. We use these empirical observations to determine $\bar{B}_3(\theta)$ and $\bar{B}_4(\theta)$ in terms of $\bar{B}_2(\theta)$ using the

approximate relation

$$[\bar{B}_n(\theta)/\bar{B}_4(0)]^{1/4} - [\bar{B}_2(\theta)/\bar{B}_4(0)]^{1/4}$$
$$= [\bar{B}_n(0)/\bar{B}_4(0)]^{1/4} - [\bar{B}_2(0)/\bar{B}_4(0)]^{1/4}. \qquad (4.2)$$

In Fig. 8(a), we show the SU(4)-averaged binding energy of the three- and four-nucleon systems, $\bar{B}_3(\theta)$ and $\bar{B}_4(\theta)$, versus the SU(4)-averaged binding energy of the two-nucleon system, $\bar{B}_2(\theta)$, and in Fig. 8(b) directly as a function of θ. Our results are similar to those obtained in Ref. [78], which were computed using hyperspherical harmonics and auxiliary-field diffusion Monte Carlo. We should also mention that we find no evidence that varying theta will produce more exotic states of three or four nucleons such as a bound trineutron or tetraneutron.

B. More than four nucleons

In Ref. [79], the authors noted that the strength of the ^{4}He - ^{4}He interaction is controlled by the strength and range of the SU(4)-invariant local nucleon-nucleon interaction. By local we mean an interaction that is velocity independent. We have noted that as θ increases, the range and strength of the SU(4)-invariant local nucleon-nucleon interaction increases due to the σ exchange contribution. We have already observed the increase in the binding energies of the two-, three-, and four-nucleon systems. As discussed in Ref. [79], the increase in the range of the local interaction will also cause alpha-like nuclei to become more bound. This is discussed further in Secs. V and VI B.

Across the nuclear chart, the binding energy per nucleon will increase with θ, and the relative importance of the Coulomb interaction will decrease. As a result, the density of nucleons at nuclear saturation will also rise. Given the increase in the neutron-proton mass difference and decreased importance of the Coulomb interaction, the line of nuclear stability will shift towards nuclei with equal numbers of neutrons and protons and extend to larger nuclei.

34

V. BIG BANG NUCLEOSYNTHESIS

In the early universe the temperature, T, is high enough to keep neutrons and protons in thermal equilibrium through the weak interactions

$$n + e^+ \leftrightarrow p + \bar{\nu}_e,$$
$$n + \nu_e \leftrightarrow p + e^-,$$
$$n \leftrightarrow p + e^- + \bar{\nu}_e. \tag{5.1}$$

The weak interaction rates scale as T^5 and can be compared with the expansion rate of the Universe, given by the Hubble parameter, $H \propto T^2$ in a radiation dominated Universe. As the temperature drops, the weak rates freeze-out, i.e., they fall out of equilibrium when they drop below the Hubble rate. In standard BBN, this occurs at a temperature, $T_f \simeq 0.84$ MeV. In equilibrium, the ratio of the number densities of neutrons to protons follow the Boltzmann distribution

$$\frac{n}{p} \equiv \frac{n_n}{n_p} \simeq \exp\left[-\frac{\Delta m_N}{T}\right]. \tag{5.2}$$

At freeze-out, this ratio is about $1/4.7$. The neutron-to-proton ratio is particularly important, as it is the primary factor determining the ^{4}He abundance. The ^{4}He mass fraction, Y, can be written as

$$Y = 2X_n \equiv \frac{2(n/p)}{1 + (n/p)}, \tag{5.3}$$

and its observed value is $Y = 0.2449 \pm 0.0040$ [80]. Further, X_n is the neutron fraction. A change in θ, will therefore invariable affect the ^{4}He abundance, primarily through the change in Δm_N. While the change in θ and Δm_N does induce a change in T_f, this is minor ($<10\%$ in T_f) and we neglect it here.

The helium abundance, however, is not determined by (n/p) at freeze-out, but rather by the ratio at the time BBN begins. At the onset of BBN, deuterons are produced in the forward reaction

$$n + p \leftrightarrow d + \gamma. \tag{5.4}$$

However, initially (even though $T < B_d$), deuteron is photo-disintegrated by the backward reaction at temperatures $T_d \gtrsim 0.1$ MeV. This delay, often called the deuteron bottleneck, is caused by the large excess of photons-to-baryons (or the smallness of η_B), and allows time for some fraction of the free neutrons to decay. A rough estimate of the temperature at which deuteron starts to form is

$$T_d \sim -\frac{B_d(\theta)}{\ln \eta_B} \tag{5.5}$$

which for $\theta = 0$ yields $T_d \sim 0.1$ MeV. A more accurate evaluation would find $T_d \approx 0.064$ MeV. Below this temperature, the photo-disintegration processes become negligible and nucleosynthesis begins.

A change in the starting time of BBN changes the (n/p) at freeze-out or more accurately the neutron fraction, X_n, at freeze-out by

$$X_n(T_d) = X_n(T_f) e^{-t_d/\tau_n}, \tag{5.6}$$

where t_d is the age of the Universe corresponding to the temperature, T_d. As noted earlier, $\Gamma_n \propto (\Delta m_N)^5$, and in a
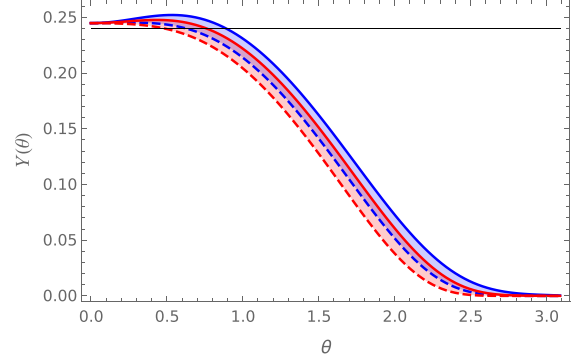

FIG. 9. The Helium mass fraction, Y, as a function of θ in the isospin symmetric case (blue upper band) and in the case of broken isospin symmetry (red lower band) for parameter set I, Eq. (3.12) (solid lines) and parameter set II, Eq. (3.13) (dashed lines).

radiation dominated Universe, $t \propto T^{-2}$, so that from (5.5), $t_d \propto B_d^{-2}$. Thus using the dependencies of Δm_N, τ_n, and B_d on θ, we can calculate $Y(\theta)$ as shown in Fig. 9. Note that to produce Fig. 9 we have used the numerical values of Γ_n and B_d as in Figs. 4 and 6, rather than the analytic approximations.

As one can see in the figure, the Helium mass fraction is relatively flat for $\theta \lesssim 1$. This is due to competing effects in determining Y. As we saw in Fig. 2(b), the neutron-proton mass difference increases with θ. This strongly suppresses the neutron-to-proton ratio, as seen in Eq. (5.2). Furthermore, because $\Gamma_n \propto (\Delta m_N)^5$, an even stronger suppression in Y occurs due to the increased neutron decay rate as seen in Eq. (5.6). However these decreases are largely canceled at low θ by the increase in B_d, which causes BBN to begin earlier, leaving less time for neutron decay. In fact, for set I parameters, at low θ this is the dominant change in Y and causes an increase in the Helium abundance. The maxima occur at $\theta = 0.42(0.54)$ and $Y = 0.248(0.252)$ for broken (unbroken) isospin symmetry. Requiring $Y > 0.24$, sets upper limits on θ of roughly 0.77 (0.50) for broken isospin, and 0.89 (0.61) for unbroken isospin for parameter sets I (II), respectively. For larger values of θ, the Helium abundance will drop below the observationally inferred limit,[3] however, as we note earlier, it is not clear that a Universe with primordial Helium and $Y < 0.05$ would prevent the formation of life and therefore can not be excluded anthropically. We also note that an increase in θ and an increased B_d will lead to an increase in the BBN value for D/H [31] which is now very tightly constrained by observation D/H $= 2.53 \pm 0.03$ [81].

An interesting subtlety occurs in the case of unbroken isospin symmetry for parameter set I. As one can see in Fig. 6, the deuteron binding energy increases above ~ 30 MeV, when $\theta \gtrsim 2.4$. In this case, there is effectively no deuteron bottleneck, as the backward reaction in (5.5) shuts off before

---

[3] While we have not run a nucleosynthetic chain in a numerical BBN analysis, the analytic approximation for Y is quite good. For $\theta = 0$, we have $Y = 0.2467$, while the current result from a full BBN analysis is $Y = 0.24696$ [42].

weak decoupling. The Helium abundance, however, is highly suppressed due to the large value of $\Delta m_N \gtrsim 3.5$ MeV and $Y \lesssim 0.05$.

As described above, the other two potentially bound dimers, the dineutron and the diproton, become bound at $\theta \simeq 0.2$ and $\theta \simeq 0.7$, respectively. Variations in the binding energy of the dineutron is expected to have little effect on the primordial abundances provided its absolute value remains smaller than the deuteron's binding energy [29,82,83]. Considering that, in this work the variations on the binding energy of the deuteron are only of a few percent, we do not expect any important role played by the binding energy of the dineutron in the calculations. For large θ, although diprotons are bound, their binding energy remains below that of deuteron and it was argued that diproton production freezes-out before the diproton bottleneck is broken [83,84].

Before concluding this section, we consider the possible impact of changes in the binding energy of unstable nuclei. In Ref. [30], changes in the nuclear part of the nucleon-nucleon potential were parameterized as

$$V_N(\mathbf{r}_{ij}) = (1 + \delta_{NN})V_N^0(\mathbf{r}_{ij}), \qquad (5.7)$$

where $V_N^0(\mathbf{r}_{ij})$ is the nucleon-nucleon potential based on the Minnesota force adapted to low mass systems [85]. The binding energy of ^{8}Be, was found to be [30]

$$B_8 = (-0.09184 + 12.208\delta_{NN}) \text{ MeV} \qquad (5.8)$$

indicating that ^{8}Be becomes bound when $\delta_{NN} \geqslant 0.00752$.[4] The binding energy of deuteron is also affected by a change in the nucleon-nucleon potential

$$B_d(\theta) = (1 + 5.716\,\delta_{NN}(\theta))B_d(0), \qquad (5.9)$$

where we have implicitly here made θ the origin of this change. From these expressions, we estimate that ^{8}Be becomes bound when $B_d(\theta) = 2.32$ MeV or when θ is 0.21 (0.23) for broken isospin, and 0.19 (0.22) for unbroken isospin for parameter sets I (II), respectively.

For stable ^{8}Be, it may be possible in principle that BBN produce elements beyond ^{7}Li. As we discuss further in the next section, changes in the nuclear potential strongly affects the triple α process and the production of carbon and oxygen in stars [30]. In the context of BBN, stable ^{8}Be increases the importance of two reactions ^{4}He$(\alpha, \gamma)^8$Be and ^{8}Be$(\alpha, \gamma)^{12}$C. Nevertheless, the detailed study in [31], found that while some ^{8}Be is produced in BBN (with a mass fraction of 10^{-16} for $\delta_{NN} = 0.0116$), no enhancement of carbon occurs as the temperature and density in the BBN environment is substantially below that in stars and the production rates are inefficient.

---

[4] ^{5}He and ^{5}Li are unbound by 0.798 and 1.69 MeV, respectively, i.e., roughly an order of magnitude more than ^{5}Be requiring a very substantial change in δ_{NN} and we do not consider this possibility here.

## VI. STELLAR NUCLEOSYNTHESIS

A. Hydrogen burning

The effects of nonzero θ will also be manifest in stellar nucleosynthesis. We first consider main sequence stars undergoing hydrogen burning. The first step of hydrogen burning is proton-proton fusion,

$$p + p \rightarrow d + e^+ + \nu_e. \qquad (6.1)$$
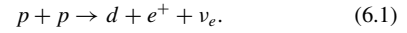
For $\theta \lesssim 0.5$, proton-proton fusion is not significantly altered from how it occurs in the physical Universe. However for $\theta \gtrsim 0.7$, the diproton becomes bound and the first step in hydrogen burning can proceed many orders of magnitude faster via radiative capture,

$$p + p \rightarrow pp + \gamma. \qquad (6.2)$$
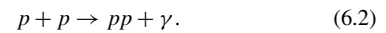
The diproton can then subsequently decay via the weak interactions to a deuteron,

$$pp \rightarrow d + e^+ + \nu_e. \qquad (6.3)$$
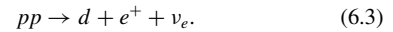
We note that while the neutron-proton mass difference grows with θ, the diproton still has a higher mass than the deuteron due to the larger binding energy of the deuteron.

Initially it was thought the rapid processing of protons to diprotons would lead to stars with extremely short lifetimes, so short so as to prevent the evolution of life on planets. However, stellar structure compensates, and burning occurs at lower temperatures and densities [84,96] and though the stars would be different, it is not clear that there is an anthropic argument against such stars.

B. Constraints on θ from the anthropic principle

The anthropic principle can constrain θ if changes in θ result in a departure of normal stellar evolution so great that planetary life would not occur. Therefore we could at minimum require that (a) enough metals (in the astronomical sense) are available, and that (b) the lifetime of stars with higher metallicity (thus allowing for rocky planets with potentially living beings) is long enough that intelligent life can evolve. Perhaps two of the most important elements for the production of life as we know it are carbon and oxygen.

There have been many studies relating the sensitivity of carbon production to fundamental physics in relation to the anthropic principle [23,24,26,86–92]. The production of ^{12}C in stars requires a triple fine tuning: (i) the decay lifetime of ^{8}Be, is relatively long, and is of order 10^{-16} s, which is four orders of magnitude longer than the scattering time for two α particles, (ii) there must exist an excited state of carbon which lies just above the energy of ^{8}Be $+ \alpha$ and (iii) the energy level of ^{16}O which sits at 7.1197 MeV must be nonresonant and below the energy of ^{12}C $+ \alpha$, at 7.1616 MeV, so that most of the produced carbon is not destroyed by further stellar processing. It is well known of course, that the existence of the excited state of ^{12}C was predicted by Hoyle [93]. Any change in fundamental physics which affects the position of the Hoyle resonance, could severely affect the production of carbon and oxygen and ultimately the existence of life.

We saw that it is perhaps not possible to place anthropic bounds on θ from BBN, as it is hard to see why a universe with

a paucity of Helium would prevent star formation or stellar processing. It is however possible to set some constraints on θ based on its effect on the triple α process leading to carbon production in stars. In addition to the change in the ^{8}Be binding energy given in Eq. (5.8), changes in θ and thus changes in the nucleon-nucleon potential, δ_{NN}, shift the energy level of the Hoyle resonance [30],

$$E_R = (0.2876 - 20.412\delta_{NN})\,\text{MeV}, \qquad (6.4)$$

where the resonant energy is given with respect to the ^{8}Be $+ \alpha$ threshold of 7.367 MeV. In standard stellar evolutionary models for massive stars, most ^{12}C is produced during the He burning phase. When the temperature becomes high enough, the ^{12}C$(\alpha, \gamma)\,^{16}$O reaction begins and ^{12}C is processed to ^{16}O. Massive stars end their He burning phases with a mixture of C and O. When $\delta_{NN} > 0$, as would be expected for $\theta \neq 0$, E_R is reduced, and the production of carbon becomes more efficient at a lower temperature. The burning of carbon to oxygen does not occur and stars end their Helium burning phases with a core of almost pure carbon.

If oxygen is not present after He burning, there is little chance to subsequently produce it. Though some oxygen is produced during carbon burning, the oxygen abundance in this phase of stellar evolution is reduced as oxygen is processed to Ne through α capture. The analysis of Ref. [30] was based on stellar evolution models [94] of 15 and 60 $M_\odot$, zero metallicity stars and found that for $\delta_{NN} \geqslant 0.3\,\%$, negligible amounts of oxygen survive the Helium burning phase. Thus an upper limit of $\delta_{NN} < 0.002$ was set which corresponds to $B_d < 2.25$ MeV. This is a rather tight bound and corresponds to upper limits on θ of 0.11 (0.11) for broken isospin, and 0.11 (0.12) for unbroken isospin for parameter sets I (II), respectively. As shown above, the dineutron and the diproton remain unbound for such values of θ, so that a universe with $0 < \theta \lesssim 0.1$ will most probably look (almost) the same as a universe with $\theta = 0$.

VII. SUMMARY AND CONCLUSIONS

Let us summarize the pertinent results of our investigation for $0 < \theta < \pi$.

(1) As θ is increased, the deuteron is more strongly bound than in our world. This means that for θ of the order one, there is much less fine-tuning than for $\theta = 0$. Also, in the case of isospin symmetry, the values for the binding energy as θ approaches π are compatible with calculations for the chiral limit.

(2) The dineutron as well as the diproton are bound for $\theta \gtrsim 0.2$ and $\theta \gtrsim 0.7$, respectively. A bound diproton has often been considered a disaster for the nucleosynthesis as we know it [95], but recent stellar calculations show that this might not be the case, see Refs. [83,84,96].

(3) Using Wigner's SU(4) symmetry and earlier results on systems with large scattering length, we have estimated the SU(4)-averaged binding energies of the three- and four-nucleon systems and found that these increase with increasing θ or with the deuteron binding energy.

(4) In general, we have found that nuclear binding energies are quite significantly altered when $\theta = \mathcal{O}(1)$. While BBN would proceed, perhaps producing far less helium and more

deuterium, changes in the deuteron binding energy would not prevent the formation of stars and eventually life. Even a stable diproton can not be excluded on this basis as stars would continue to burn Hydrogen at lower temperatures. On the other hand, changes in the binding energy of ^{8}Be and the resonant energy of the Hoyle state, would affect the triple α reaction rate and lead to a world lacking in ^{16}O.

(5) Applying the even stronger constraint not to upset the world as we enjoy it, we derived that θ must be $\lesssim 0.1$ in order to approximately recover the real nuclear reaction rates. In this case, the deviation of the neutron-proton mass difference to the real world value is less than 1% and both the diproton and the dineutron still fail to be bound.

APPENDIX: θ-DEPENDENCE OF THE NEUTRON-PROTON MASS DIFFERENCE

The strong contribution to the proton-neutron mass difference can be derived from the NLO πN Lagrangian [54]

$$\mathcal{L}_{\pi N}^{\Delta m_N} = \bar{N} c_5 \left(\chi_+ - \frac{1}{2}\langle\chi_+\rangle \right) N, \qquad (A.1)$$

where c_5 is a LEC, $N = (p, n)^T$ contains the nucleon fields, $\langle\ldots\rangle$ denotes the trace in flavor space, and

$$\chi_+ = u^\dagger \chi_\theta u^\dagger + u \chi_\theta^\dagger u. \qquad (A.2)$$

For the determination of the mass difference, $U = u^2$, which contains the pseudo-Nambu-Goldstone bosons of SU(2) chiral perturbation theory, only needs to be expanded up to its leading order constant term. In particular, in a θ-vacuum U is given by the vacuum alignment U_0. For $\chi_\theta = 2B\mathcal{M}\exp(i\theta/2)$, with $\mathcal{M} = \text{diag}\{m_u, m_d\}$ the quark mass matrix, we use the following parametrization of the vacuum alignment:

$$U_0 = \text{diag}\{e^{i\varphi}, e^{-i\varphi}\}. \qquad (A.3)$$

Minimizing the vacuum energy density in SU(2) chiral perturbation theory (or equivalently removing the tree-level tadpole term of the neutral pion), one finds [48]

$$\tan\varphi = -\varepsilon \tan\frac{\theta}{2}, \qquad (A.4)$$

or

$$\sin\varphi = \frac{-\varepsilon \tan\frac{\theta}{2}}{\sqrt{1 + \varepsilon^2 \tan^2\frac{\theta}{2}}} = \frac{-\varepsilon M_\pi^2 \sin\frac{\theta}{2}}{M_\pi^2(\theta)}, \quad \text{(A.5)}$$

$$\cos\varphi = \frac{1}{\sqrt{1 + \varepsilon^2 \tan^2\frac{\theta}{2}}} = \frac{M_\pi^2 \cos\frac{\theta}{2}}{M_\pi^2(\theta)}, \quad \text{(A.6)}$$

where we have used Eq. (2.1). With that, Eq. (A.1) becomes

$$\mathcal{L}_{\pi N}^{\Delta m_N} = \bar{N} 4 c_5 B_0 \frac{m_u \cos\left(\frac{\theta}{2} - \varphi\right) - m_d \cos\left(\frac{\theta}{2} + \varphi\right)}{2} \tau_3 N$$

$$= \bar{N} 4 c_5 B_0 \frac{M_\pi^2}{M_\pi^2(\theta)} \frac{m_u - m_d}{2} \tau_3 N, \quad \text{(A.7)}$$

which results in the strong contribution to the proton-neutron mass difference given in Eq. (2.10).

[1] B. Carter, Large number coincidences and the anthropic principle in cosmology, *IAU Symposium Confrontation of Cosmological Theories with Observational Data* (Reidel, Dordrecht, 1974), pp. 291–298.

[2] S. Weinberg, Anthropic Bound on the Cosmological Constant, Phys. Rev. Lett. **59**, 2607 (1987).

[3] For a comprehensive survey of the anthropic principle, see J. D. Barrow and F. J. Tipler, *The Anthropic Cosmological Principle* (Clarendon, Oxford, 1986).

[4] L. Susskind, The Anthropic landscape of string theory, arXiv:hep-th/0302219 [hep-th].

[5] J. Gegelia and U.-G. Meißner, Vacuum energy in the effective field theory of general relativity, Phys. Rev. D **100**, 046021 (2019).

[6] C. Abel *et al.* [nEDM], Measurement of the Permanent Electric Dipole Moment of the Neutron, Phys. Rev. Lett. **124**, 081803 (2020).

[7] T. Banks, M. Dine, and E. Gorbatov, Is there a string theory landscape? J. High Energy Phys. 08 (2004) 058.

[8] J. F. Donoghue, Dynamics of M theory vacua, Phys. Rev. D **69**, 106012 (2004).

[9] L. Ubaldi, Effects of theta on the deuteron binding energy and the triple-alpha process, Phys. Rev. D **81**, 025011 (2010).

[10] N. Kaloper and J. Terning, Landscaping the Strong CP Problem, J. High Energy Phys. 03 (2019) 032.

[11] M. Dine, L. Stephenson Haskins, L. Ubaldi, and D. Xu, Some Remarks on Anthropic Approaches to the Strong CP Problem, J. High Energy Phys. 05 (2018) 171.

[12] J. Arakawa, A. Rajaraman, and T. M. P. Tait, Emergent Solution to the Strong CP Problem, Phys. Rev. Lett. **123**, 161602 (2019).

[13] V. Flambaum and E. Shuryak, Limits on cosmological variation of strong interaction and quark masses from big bang nucleosynthesis, cosmic, laboratory and Oklo data, Phys. Rev. D **65**, 103503 (2002).

[14] S. R. Beane and M. J. Savage, The Quark mass dependence of two nucleon systems, Nucl. Phys. A **717**, 91 (2003).

[15] E. Epelbaum, U.-G. Meißner, and W. Gloeckle, Nuclear forces in the chiral limit, Nucl. Phys. A **714**, 535 (2003).

[16] V. Dmitriev and V. Flambaum, Limits on cosmological variation of quark masses and strong interaction, Phys. Rev. D **67**, 063513 (2003).

[17] V. Flambaum and E. Shuryak, Dependence of hadronic properties on quark masses and constraints on their cosmological variation, Phys. Rev. D **67**, 083507 (2003).

[18] V. F. Dmitriev, V. Flambaum, and J. Webb, Cosmological variation of deuteron binding energy, strong interaction and quark masses from big bang nucleosynthesis, Phys. Rev. D **69**, 063506 (2004).

[19] R. L. Jaffe, A. Jenkins, and I. Kimchi, Quark Masses: An Environmental Impact Statement, Phys. Rev. D **79**, 065014 (2009).

[20] J. Berengut, V. Flambaum, and V. Dmitriev, Effect of quark-mass variation on big bang nucleosynthesis, Phys. Lett. B **683**, 114 (2010).

[21] P. F. Bedaque, T. Luu, and L. Platter, Quark mass variation constraints from Big Bang nucleosynthesis, Phys. Rev. C **83**, 045803 (2011).

[22] M. K. Cheoun, T. Kajino, M. Kusakabe, and G. J. Mathews, Time Dependent Quark Masses and Big Bang Nucleosynthesis Revisited, Phys. Rev. D **84**, 043001 (2011).

[23] E. Epelbaum, H. Krebs, T. A. Lähde, D. Lee, and U.-G. Meißner, Viability of Carbon-Based Life as a Function of the Light Quark Mass, Phys. Rev. Lett. **110**, 112502 (2013).

[24] E. Epelbaum, H. Krebs, T. A. Lähde, D. Lee, and U.-G. Meißner, Dependence of the triple-alpha process on the fundamental constants of nature, Eur. Phys. J. A **49**, 82 (2013).

[25] J. Berengut, E. Epelbaum, V. Flambaum, C. Hanhart, U.-G. Meißner, J. Nebreda, and J. Pelaez, Varying the light quark mass: impact on the nuclear force and Big Bang nucleosynthesis, Phys. Rev. D **87**, 085018 (2013).

[26] T. A. Lähde, U.-G. Meißner, and E. Epelbaum, An update on fine-tunings in the triple-alpha process, Eur. Phys. J. A **56**, 89 (2020).

[27] B. A. Campbell and K. A. Olive, Nucleosynthesis and the time dependence of fundamental couplings, Phys. Lett. B **345**, 429 (1995).

[28] J. P. Kneller and G. C. McLaughlin, BBN and Lambda(QCD), Phys. Rev. D **68**, 103508 (2003).

[29] A. Coc, N. J. Nunes, K. A. Olive, J. P. Uzan, and E. Vangioni, Coupled Variations of Fundamental Couplings and Primordial Nucleosynthesis, Phys. Rev. D **76**, 023511 (2007).

[30] S. Ekstrom, A. Coc, P. Descouvemont, G. Meynet, K. A. Olive, J. P. Uzan, and E. Vangioni, Effects of the variation of fundamental constants on Pop III stellar evolution, Astron. Astrophys. **514**, A62 (2010).

[31] A. Coc, P. Descouvemont, K. A. Olive, J. P. Uzan, and E. Vangioni, The variation of fundamental constants and the role of A = 5 and A = 8 nuclei on primordial nucleosynthesis, Phys. Rev. D **86**, 043529 (2012).

[32] K. A. Olive, M. Pospelov, Y. Z. Qian, A. Coc, M. Casse, and E. Vangioni-Flam, Constraints on the variations of the fundamental couplings, Phys. Rev. D **66**, 045022 (2002).

[33] F. Luo, K. A. Olive, and J. P. Uzan, Gyromagnetic Factors and Atomic Clock Constraints on the Variation of Fundamental Constants, Phys. Rev. D **84**, 096004 (2011).

[34] C. J. Hogan, Why the universe is just so, Rev. Mod. Phys. **72**, 1149 (2000).

38

[35] L. A. Barnes, The fine-tuning of the universe for intelligent life, Publ. Astron. Soc. Aust. **29**, 529 (2012).

[36] A. Schellekens, Life at the interface of particle physics and string theory, Rev. Mod. Phys. **85**, 1491 (2013).

[37] U.-G. Meißner, Anthropic considerations in nuclear physics, Sci. Bull. **60**, 43 (2015).

[38] F. C. Adams, The degree of fine-tuning in our universe—and others, Phys. Rep. **807**, 1 (2019).

[39] V. Baluni, CP Violating Effects in QCD, Phys. Rev. D **19**, 2227 (1979).

[40] F. K. Guo, R. Horsley, U. G. Meissner, Y. Nakamura, H. Perlt, P. Rakow, G. Schierholz, A. Schiller, and J. Zanotti, The Electric Dipole Moment of the Neutron from 2+1 Flavor Lattice QCD, Phys. Rev. Lett. **115**, 062001 (2015).

[41] A. V. Smilga, QCD at theta similar to pi, Phys. Rev. D **59**, 114021 (1999).

[42] B. D. Fields, K. A. Olive, T. H. Yeh, and C. Young, Big-bang nucleosynthesis after planck, JCAP **03**, 010 (2020).

[43] G. Steigman and R. J. Scherrer, Is The Universal Matter - Antimatter Asymmetry Fine Tuned? arXiv:1801.10059 [astro-ph.CO].

[44] A. Sakharov, Violation of CP Invariance, C asymmetry, and baryon asymmetry of the universe, Sov. Phys. Usp. **34**, 392 (1991).

[45] V. Kuzmin, M. Shaposhnikov, and I. Tkachev, Strong CP violation, electroweak baryogenesis, and axionic dark matter, Phys. Rev. D **45**, 466 (1992).

[46] L. J. Hall, D. Pinner, and J. T. Ruderman, The Weak Scale from BBN, J. High Energy Phys. **12** (2014) 134.

[47] H. Leutwyler and A. V. Smilga, Spectrum of Dirac operator and role of winding number in QCD, Phys. Rev. D **46**, 5607 (1992).

[48] R. Brower, S. Chandrasekharan, J. W. Negele, and U. J. Wiese, QCD at fixed topology, Phys. Lett. B **560**, 64 (2003).

[49] T. Fugleberg, I. E. Halperin, and A. Zhitnitsky, Domain walls and theta dependence in QCD with an effective Lagrangian approach, Phys. Rev. D **59**, 074023 (1999).

[50] G. Colangelo, J. Gasser, and H. Leutwyler, The Quark Condensate from K(e4) Decays, Phys. Rev. Lett. **86**, 5008 (2001).

[51] N. R. Acharya, F. K. Guo, M. Mai, and U.-G. Meißner, θ-dependence of the lightest meson resonances in QCD, Phys. Rev. D **92**, 054023 (2015).

[52] M. Hoferichter, J. Ruiz de Elvira, B. Kubis, and U.-G. Meißner, Roy-Steiner-equation analysis of pion-nucleon scattering, Phys. Rep. **625**, 1 (2016).

[53] M. Hoferichter, J. Ruiz de Elvira, B. Kubis, and U.-G. Meißner, Matching Pion-Nucleon Roy-Steiner Equations to Chiral Perturbation Theory, Phys. Rev. Lett. **115**, 192301 (2015).

[54] V. Bernard, N. Kaiser, and U.-G. Meißner, Chiral dynamics in nucleons and nuclei, Int. J. Mod. Phys. E **4**, 193 (1995).

[55] N. Fettes, U.-G. Meißner, and S. Steininger, Pion - nucleon scattering in chiral perturbation theory. 1. Isospin symmetric case, Nucl. Phys. A **640**, 199 (1998).

[56] V. Baru, C. Hanhart, M. Hoferichter, B. Kubis, A. Nogga, and D. Phillips, Precision calculation of threshold $\pi^- d$ scattering, pi N scattering lengths, and the GMO sum rule, Nucl. Phys. A **872**, 69 (2011).

[57] J. Sakurai, Theory of strong interactions, Annals Phys. **11**, 1 (1960).

[58] J. F. Donoghue, Sigma exchange in the nuclear force and effective field theory, Phys. Lett. B **643**, 165 (2006).

[59] T. Damour and J. F. Donoghue, Constraints on the variability of quark masses from nuclear binding, Phys. Rev. D **78**, 014014 (2008).

[60] E. Epelbaum, U.-G. Meißner, W. Gloeckle, and C. Elster, Resonance saturation for four nucleon operators, Phys. Rev. C **65**, 044001 (2002).

[61] V. Bernard, N. Kaiser, and U.-G. Meißner, Aspects of chiral pion - nucleon physics, Nucl. Phys. A **615**, 483 (1997).

[62] J. Gasser, H. Leutwyler, and A. Rusetsky, On the mass difference between proton and neutron, arXiv:2003.13612 [hep-ph].

[63] T. Vonk, Studies on the QCD θ-vacuum in chiral perturbation theory, MSc. thesis, Bonn University, 2019.

[64] E. Fermi, An attempt of a theory of beta radiation. 1., Z. Phys. **88**, 161 (1934).

[65] T. E. O. Ericson and W. Weise, Pions and Nuclei, Int. Ser. Monogr. Phys. **74** (1988).

[66] P. Mergell, U.-G. Meißner, and D. Drechsel, Dispersion theoretical analysis of the nucleon electromagnetic form-factors, Nucl. Phys. A **596**, 367 (1996).

[67] S. Beane *et al.* [NPLQCD], The deuteron and exotic two-body bound states from lattice QCD, Phys. Rev. D **85**, 054511 (2012).

[68] T. Yamazaki, K. i. Ishikawa, Y. Kuramashi, and A. Ukawa, Helium nuclei, deuteron and dineutron in 2+1 flavor lattice QCD, Phys. Rev. D **86**, 074514 (2012).

[69] T. Yamazaki, K. i. Ishikawa, Y. Kuramashi, and A. Ukawa, Study of quark mass dependence of binding energy for light nuclei in 2+1 flavor lattice QCD, Phys. Rev. D **92**, 014501 (2015).

[70] K. Orginos, A. Parreno, M. J. Savage, S. R. Beane, E. Chang, and W. Detmold, Two nucleon systems at $m_\pi \sim 450$MeV from lattice QCD, Phys. Rev. D **92**, 114512 (2015).

[71] E. Wigner, On the consequences of the symmetry of the nuclear Hamiltonian on the spectroscopy of nuclei, Phys. Rev. **51**, 106 (1937).

[72] P. F. Bedaque, H. Hammer, and U. van Kolck, Renormalization of the Three-Body System with Short Range Interactions, Phys. Rev. Lett. **82**, 463 (1999).

[73] P. F. Bedaque, H. Hammer, and U. van Kolck, The Three boson system with short range interactions, Nucl. Phys. A **646**, 444 (1999).

[74] P. F. Bedaque, H. Hammer, and U. van Kolck, Effective theory of the triton, Nucl. Phys. A **676**, 357 (2000).

[75] L. Platter, H. Hammer, and U.-G. Meißner, The Four boson system with short range interactions, Phys. Rev. A **70**, 052101 (2004).

[76] L. Platter, H. W. Hammer, and U.-G. Meißner, On the correlation between the binding energies of the triton and the alpha-particle, Phys. Lett. B **607**, 254 (2005).

[77] M. Gattobigio, A. Kievsky, and M. Viviani, Energy spectra of small bosonic clusters having a large two-body scattering length, Phys. Rev. A **86**, 042513 (2012).

[78] N. Barnea, L. Contessi, D. Gazit, F. Pederiva, and U. van Kolck, Effective Field Theory for Lattice Nuclei, Phys. Rev. Lett. **114**, 052501 (2015).

[79] S. Elhatisari, N. Li, A. Rokash, J. M. Alarcon, D. Du, N. Klein, B. N. Lu, U.-G. Meißner, E. Epelbaum, H. Krebs, T. A. Lähde, D. Lee, and G. Rupak, Nuclear Binding Near a Quantum Phase Transition, Phys. Rev. Lett. **117**, 132501 (2016).

[80] E. Aver, K. A. Olive, and E. D. Skillman, The effects of He I λ10830 on helium abundance determinations, JCAP 07 (2015) 011.

[81] R. J. Cooke, M. Pettini, and C. C. Steidel, One percent determination of the primordial deuterium abundance, Astrophys. J. **855**, 102 (2018).

[82] J. P. Kneller and G. C. McLaughlin, The Effect of bound dineutrons upon BBN, Phys. Rev. D **70**, 043512 (2004).

[83] J. MacDonald and D. Mullan, Big bang nucleosynthesis: The strong force meets the weak anthropic principle, Phys. Rev. D **80**, 043507 (2009).

[84] R. A. W. Bradford, The effect of hypothetical diproton stability on the universe, J. Astrophys. Astron. **30**, 119 (2009).

[85] D. Thompson, M. Lemere, and Y. Tang, Systematic investigation of scattering problems with the resonating-group method, Nucl. Phys. A **286**, 53 (1977).

[86] M. Livio, D. Hollowell, J. W. Truran, and A. Weiss, Nature (London) **340**, 281 (1989).

[87] M. Fairbairn, carbon burning in supernovae and evolving physical constants, arXiv:astro-ph/9910328 [astro-ph].

[88] A. Csoto, H. Oberhummer, and H. Schlattl, Fine tuning the basic forces of nature through the triple alpha process in red giant stars, Nucl. Phys. A **688**, 560 (2001).

[89] H. Oberhummer, A. Csoto, and H. Schlattl, Stellar production rates of carbon and its abundance in the universe, Science **289**, 88 (2000).

[90] H. Schlattl, A. Heger, H. Oberhummer, T. Rauscher, and A. Csoto, Sensitivity of the c and o production on the 3-alpha rate, Astrophys. Space Sci. **291**, 27 (2004).

[91] C. Tur, A. Heger, and S. M. Austin, Dependence of s-process nucleosynthesis in massive stars on triple-alpha and 12C(a, g)16O reaction rate uncertainties, Astrophys. J. **702**, 1068 (2009).

[92] L. Huang, F. C. Adams, and E. Grohs, Sensitivity of carbon and oxygen yields to the triple-alpha resonance in massive stars, Astropart. Phys. **105**, 13 (2019).

[93] F. Hoyle, On nuclear reactions occuring in very hot stars. 1. the synthesis of elements from carbon to nickel, Astrophys. J. Suppl. **1**, 121 (1954).

[94] S. Ekstrom, G. Meynet, C. Chiappini, R. Hirschi, and A. Maeder, Effects of rotation on the evolution of primordial stars, Astron. Astrophys. **489**, 685 (2008).

[95] F. J. Dyson, Energy in the universe, Sci. Am. **225**, 50 (1971).

[96] L. A. Barnes, Binding the diproton in stars: Anthropic limits on the strength of gravity, JCAP 12 (2015) 050.

40

Alpha-alpha scattering in the Multiverse

Alpha-alpha scattering in the Multiverse

Serdar Elhatisari,[a] Timo A. Lähde,[b] Dean Lee,[c] Ulf-G. Meißner[d,e,f] and Thomas Vonk[d]

[a] *Faculty of Natural Sciences and Engineering, Gaziantep Islam Science and Technology University,*
Gaziantep 27010, Turkey

[b] *Institute for Advanced Simulation, Institut für Kernphysik,*
Center for Advanced Simulation and Analytics, and Jülich Center for Hadron Physics,
Forschungszentrum Jülich, D-52425 Jülich, Germany

[c] *Facility for Rare Isotope Beams and Department of Physics and Astronomy,*
Michigan State University, East Lansing, MI 48824, U.S.A.

[d] *Helmholtz-Institut für Strahlen- und Kernphysik and Bethe Center for Theoretical Physics,*
Universität Bonn, D-53115 Bonn, Germany

[e] *Institute for Advanced Simulation, Institut für Kernphysik,*
Center for Advanced Simulation and Analytics, and Jülich Center for Hadron Physics,
Forschungszentrum Jülich, D-52425 Jülich, Germany

[f] *Tbilisi State University, 0186 Tbilisi, Georgia*

E-mail: selhatisari@gmail.com, t.laehde@fz-juelich.de,
leed@frib.msu.edu, meissner@hiskp.uni-bonn.de, vonk@hiskp.uni-bonn.de

ABSTRACT: We investigate the phase shifts of low-energy α-α scattering under variations of the fundamental parameters of the Standard Model, namely the light quark mass, the electromagnetic fine-structure constant as well as the QCD θ-angle. As a first step, we recalculate α-α scattering in our Universe utilizing various improvements in the adiabatic projection method, which leads to an improved, parameter-free prediction of the S- and D-wave phase shifts for laboratory energies below 10 MeV. We find that positive shifts in the pion mass have a small effect on the S-wave phase shift, whereas lowering the pion mass adds some repulsion in the two-alpha system. The effect on the D-wave phase shift turns out to be more pronounced as signaled by the D-wave resonance parameters. Variations of the fine-structure constant have almost no effect on the low-energy α-α phase shifts. We further show that up-to-and-including next-to-leading order in the chiral expansion, variations of these phase shifts with respect to the QCD θ-angle can be expressed in terms of the θ-dependent pion mass.

https://doi.org/10.1007/JHEP02(2022)001

Contents

1 Introduction

Alpha-alpha (α-α) scattering is one of the most fundamental reactions in nuclear (astro)physics. It is the basic component of the triple-alpha (3α) reaction prevalent in hot old stars, that leads to the generation of ^{12}C and successively ^{16}O, where the ^{12}C production is enhanced through a $J^P = 0^+$ resonance at 7.65 MeV excitation energy close to the 3α-threshold, the famous Hoyle state [1]. α-α scattering itself features some fine-tuning, as the large

near-threshold S-wave results from a state with $(J^P, I) = (0^+, 0)$ at an energy $E_R \simeq 0.1\,\mathrm{MeV}$ above the threshold, see e.g. the review [2], with a tiny width of $\Gamma_R \simeq 6\,\mathrm{eV}$. It is precisely this small width (long lifetime) of the unstable $^8\mathrm{Be}$ nucleus that allows for the reaction with the third α particle in the 3α reaction at sufficiently high temperatures and densities.

The fine-tunings in these (and other) fundamental nuclear reactions together with other fine-tunings in particle physics and cosmology have led to the concept of the *Multiverse*, where our Universe with its observed values is part of a larger structure of universes featuring different sets of the fundamental constants. Related to this are anthropic considerations, which is the philosophical idea that the parameters governing our world should fit the intervals compatible with the existence of life on Earth. More details can be found in the reviews [3–7].

Coming back to nuclear physics, the closeness of the Hoyle state energy to the 3α threshold invites investigations about the stability of this resonance condition under changes of the fundamental parameters of the strong and the electromagnetic (EM) interactions, whose interplay guarantees the stability of atomic nuclei. While earlier investigations, see e.g. ref. [8], suffered from some model-dependence in the description of the nuclear forces, using the *ab initio* method of Nuclear Lattice Effective Field Theory (NLEFT) this topic was re-investigated in refs. [9–11]. More specifically, the quark mass dependence as well as the dependence on the electromagnetic fine-structure constant of the nuclear Hamiltonian was worked out, using and combining results from chiral perturbation theory (CHPT) and lattice QCD simulations for the pion decay constant, the nucleon mass and so on. Here, we will use the same chiral EFT at next-to-next-to-leading order combined with the so-called Adiabatic Projection Method (APM), that allows for *ab initio* calculations of nuclear reactions, as developed in refs. [12–14]. Using the APM, the scattering of two alpha clusters has been achieved on the lattice [15], enabled by the fact that the computational effort is approximately quadratic in the number of nucleons in the scattering clusters. The method was further refined in ref. [16]. Combining these different works, we are thus in the position to investigate the sensitivity of the low-energy α-α phase shifts on variations in the light quark mass $\hat{m}$ and the EM fine-structure constant α_{EM}. We note that α-α scattering has also recently been studied using the no-core shell model within a continuum approach [17].

While the investigation of the resonance enhancement in the 3α process due to the Hoyle state already sets rather stringent limits on the possible variations of the light quark mass and the fine-structure constant, one has to be aware that these results are afflicted with some inherent uncertainties, as in the corresponding stellar simulations only the distance of the Hoyle state to the 3α-threshold is varied. Translating this into a dependence on, say, the light quark mass assumes that only the nuclei directly involved in the 3α process are subject to these changes, but of course one should perform the complete stellar simulations (reaction networks) with appropriately modified masses and reaction rates. At present, this is only possible for Big Bang Nucleosynthesis, see e.g. refs. [18, 19], but not for the whole nuclear reaction networks in stars. Therefore, the *ab initio* computation of the dependence of α-α scattering on the fundamental parameters of the Standard Model is not subject to such uncertainties and paves the way for more elaborate network calculations in the Multiverse.

A parameter that has obtained less attention in such anthropic considerations is the QCD θ-term, as the bounds from the neutron electric dipole moment require $\theta \lesssim 10^{-10}$,

see e.g. ref. [20] for a recent lattice QCD study. Still, it is worth to reconsider bounds on the θ-angle from observations other than the neutron EDM as well as from anthropic considerations, as done e.g. in refs. [21, 22]. In particular, it was shown in [22] that nuclear binding increases with θ and that $\theta \lesssim 0.1$ would not upset the world as we know it. It is thus also of interest to study the reaction rate of the fundamental α-α scattering process as a function of θ, as will be done here.

In ref. [23], it was shown that symmetric nuclear matter without Coulomb interactions lies close to a quantum phase transition between a Bose gas of alpha clusters and a nuclear liquid. Whether one is in the Bose gas phase or the nuclear liquid phase is determined by the sign of the α-α S-wave scattering length. In turn, the α-α scattering phase shifts depend on the strength, range, and locality of the nucleon-nucleon interactions. The nucleon-nucleon interactions need enough attractive strength, range, and locality to overcome the Pauli repulsion between nucleons with the same spin and isospin [24, 25]. Locality here refers to interactions that are diagonal when written in position space. The variation of the light quark masses, electromagnetic fine-structure constant, and θ parameter will produce changes to the leading-order interactions, and we take these changes to the nucleon-nucleon interactions to be local. This choice is motivated by studies of Quantum Chromodynamics in the limit of a large number of colors showing that the nucleon-nucleon interactions reduce to local interactions with an underlying spin-isospin exchange symmetry [26–28].

The paper is organized as follows. In section 2, we introduce the dependence of the two-alpha cluster energy on the fundamental parameters of the Standard Model, the basic framework of NLEFT and give a first glimpse on some of the relevant quark (pion) mass dependences. The pion mass dependence of the nuclear Hamiltonian used here is presented in detail in section 3. Then, in section 4 we discuss the inclusion of the electromagnetic interaction and the dependence of the nuclear Hamiltonian on the fine-structure constant. Section 5 shows how the θ-dependence of α-α scattering can be inferred from the θ-dependence of the pion mass. In section 6 we collect the computational tools needed for this investigations. We give the basic APM formalism needed for our investigation and show how various quantities are obtained from Auxiliary Field Quantum Monte Carlo simulations. In section 7, we show how to extract the scattering phase shifts from the adiabatic transfer matrices. Our results are presented and discussed in section 8. We end with a summary and conclusions. Some further details of the computations are relegated to the appendices.

2 Basic concepts

We aim to compute the variation of the α-α scattering phase shifts as a function of the fundamental constants of nature following refs. [10, 11]. Since we compute the scattering phase shifts from the spectrum, we consider a linear variation in the light quark mass and the electromagnetic fine-structure constant $\alpha_{\rm EM}$ of the two-alpha cluster energy,

$$\delta E_{\alpha\alpha} \simeq \frac{\partial E_{\alpha\alpha}}{\partial M_\pi}\bigg|_{M_\pi^{\rm ph}} \delta M_\pi + \frac{\partial E_{\alpha\alpha}}{\partial \alpha_{\rm EM}}\bigg|_{\alpha_{\rm EM}^{\rm ph}} \delta\alpha_{\rm EM} \,, \tag{2.1}$$

where we have used the Gell-Mann-Oakes-Renner relation, $M_\pi^2 = 2B_0\hat{m}$, with $\hat{m} = (m_u + m_d)/2$ the light quark mass and B_0 is related to the scalar quark condensate.[1] Throughout, we work in the isospin limit as strong isospin breaking effects are expected to be very small. Further, the superscript "ph" denotes the pertinent values in Nature (the physical world). We note that this formula is applicable for changes in the modulus of the pion mass $|\delta M_\pi/M_\pi|$ and the electromagnetic fine-structure constant by $|\delta\alpha_{\rm EM}/\alpha_{\rm EM}| \lesssim 10\%$. The variation with respect to the QCD θ angle will be discussed later in a separate section.

Our computational framework is NLEFT, see refs. [29, 30] for details. In what follows, we employ a periodic cubic lattice with a spatial lattice spacing of $a = 1.97$ fm and a temporal lattice spacing $a_t = 1.32$ fm. For free nucleons we use the $\mathcal{O}(a^4)$-improved lattice Hamiltonian,

$$
\begin{aligned}
H_{\rm free} = & \frac{49}{12m_N} \sum_{\vec{n}} \sum_{i,j=0,1} a_{i,j}^\dagger(\vec{n}) a_{i,j}(\vec{n}) \\
& - \frac{3}{4m_N} \sum_{\vec{n}} \sum_{i,j=0,1} \sum_{l=1,2,3} \left[a_{i,j}^\dagger(\vec{n}) a_{i,j}(\vec{n}+\hat{l}) + a_{i,j}^\dagger(\vec{n}) a_{i,j}(\vec{n}\hat{l}) \right] \\
& - \frac{3}{40m_N} \sum_{\vec{n}} \sum_{i,j=0,1} \sum_{l=1,2,3} \left[a_{i,j}^\dagger(\vec{n}) a_{i,j}(\vec{n}+2\hat{l}) + a_{i,j}^\dagger(\vec{n}) a_{i,j}(\vec{n}-2\hat{l}) \right] \\
& - \frac{1}{180m_N} \sum_{\vec{n}} \sum_{i,j=0,1} \sum_{l=1,2,3} \left[a_{i,j}^\dagger(\vec{n}) a_{i,j}(\vec{n}+3\hat{l}) + a_{i,j}^\dagger(\vec{n}) a_{i,j}(\vec{n}-3\hat{l}) \right] , \quad (2.2)
\end{aligned}
$$

where $\vec{n}$ represents the integer-valued lattice sites, m_N is the nucleon mass, $\hat{l} = \hat{1}, \hat{2}, \hat{3}$ are unit lattice vectors in the spatial directions, $i(j)$ is a spin (isospin) index, and $a_{i,j}$ and $a_{i,j}^\dagger$ denote nucleon annihilation and creation operators.

For the leading-order (LO) nuclear interaction we use an improved action which is based on the following nucleon-nucleon (NN) scattering amplitude,

$$
\begin{aligned}
\mathcal{A}_{\rm LO} = & C_{S=0,I=1}\, f(\vec{q}) \left(\frac{1}{4} - \frac{1}{4}\vec{\sigma}_i \cdot \vec{\sigma}_j \right) \left(\frac{3}{4} + \frac{1}{4}\vec{\tau}_i \cdot \vec{\tau}_j \right) \\
& + C_{S=1,I=0}\, f(\vec{q}) \left(\frac{3}{4} + \frac{1}{4}\vec{\sigma}_i \cdot \vec{\sigma}_j \right) \left(\frac{1}{4} - \frac{1}{4}\vec{\tau}_i \cdot \vec{\tau}_j \right) \\
& + \tilde{g}_{\pi N}^2 \vec{\tau}_i \cdot \vec{\tau}_j \frac{(\vec{\sigma}_i \cdot \vec{q})(\vec{\sigma}_j \cdot \vec{q})}{\vec{q}^2 + M_\pi^2} , \quad (2.3)
\end{aligned}
$$

where $\vec{\sigma}$ and $\vec{\tau}$ denote the Pauli spin and isospin matrices, $\tilde{g}_{\pi N}$ is the strength of the one-pion-exchange (OPE) potential defined as $\tilde{g}_{\pi N} = g_A/(2\,F_\pi)$ in terms of the nucleon axial-vector coupling $g_A = 1.273(19)$ and the pion decay constant $F_\pi = 92.1$ MeV. $C_{S=0,I=1}$ and $C_{S=1,I=0}$ are the coupling constants of the short-range part of the nuclear force which are adjusted to reproduce the scattering phase shifts for the two S-wave channels, and $f(\vec{q})$ is a smearing function which is defined to reproduce the effective ranges for the two S-wave channels. We redefine the low-energy constants (LECs) of the short-range interactions in

---

[1]Because of this relation, we can equivalently use the wordings "quark mass dependence" and "pion mass dependence".

terms of linear combinations of C_0 and C_I,

$$C_0 = \frac{3}{4}C_{S=0,I=1} + \frac{1}{4}C_{S=1,I=0}, \tag{2.4}$$

$$C_I = \frac{1}{4}C_{S=0,I=1} - \frac{3}{4}C_{S=1,I=0}. \tag{2.5}$$

From eqs. (2.2) and (2.3) it is obvious that the sources of implicit M_π-dependence are the nucleon mass m_N, the coupling constant of the OPE potential $\tilde{g}_{\pi N}$, and the LECs of the short-range interactions C_0 and C_I, besides the explicit pion mass dependence in the OPE. Before discussing these in detail in section 3, let us consider the quark (pion) mass dependence of the nucleon mass and the pion decay constant to get an idea about the changes we can expect. At the leading one-loop order $\mathcal{O}(p^3)$, where p is a generic small parameter, the chiral expansion of the nucleon mass can be written as

$$m_N(M_\pi) = m_0 - 4c_1 M_\pi^2 - \frac{3g_A^2(M_\pi)M_\pi^3}{32\pi F_\pi^2(M_\pi)} + \mathcal{O}(M_\pi^4), \tag{2.6}$$

where $m_0 \simeq 865\,\text{MeV}$ [31] is the nucleon mass in the (two-flavor) chiral limit and $c_1 = -1.1\,\text{GeV}^{-1}$ is a LEC from the chiral pion-nucleon Lagrangian at next-to-leading order (NLO) [32]. Note that the leading correction of order M_π^2 is intimately linked to the pion-nucleon σ-term discussed below. At third order, the pion mass dependence of the pion decay constant and the axial-vector coupling constant is made explicit. For the pion decay constant we use the expression from the chiral expansion at NLO,

$$F_\pi(M_\pi) = F + \frac{M_\pi^2}{16\pi^2 F}\bar{l}_4 + \mathcal{O}(M_\pi^4), \tag{2.7}$$

where $F = 86.2\,\text{MeV}$ is the pion decay constant in the (two-flavor) chiral limit,[2] and $\bar{l}_4 = 4.3$ is a LEC, where we use the value from ref. [33] (which is consistent with more modern determinations). We postpone the discussion of the nucleon axial-vector coupling g_A and of the LECs C_0, C_I to the next section.

3 Pion mass dependence of the nuclear Hamiltonian

First, let us collect the knowledge about the pion mass dependence of the nuclear Hamiltonian. Specifically, the dependence of the energy $E_{\alpha\alpha}$ on the pion mass M_π can be expressed as

$$E_{\alpha\alpha} = E_{\alpha\alpha}(\tilde{M}_\pi, m_N(M_\pi), \tilde{g}_{\pi N}(M_\pi), C_0(M_\pi), C_I(M_\pi)), \tag{3.1}$$

where $\tilde{M}_\pi$ denotes the explicit M_π-dependence from the pion propagator in the OPE potential. Without going into the details of the individual terms given here, we write the variation of the two-alpha cluster energy around the physical point as

$$\left.\frac{\partial E_{\alpha\alpha}}{\partial M_\pi}\right|_{M_\pi^{\text{ph}}} = \left.\frac{\partial E_{\alpha\alpha}}{\partial \tilde{M}_\pi}\right|_{M_\pi^{\text{ph}}} + x_1 \left.\frac{\partial E_{\alpha\alpha}}{\partial m_N}\right|_{m_N^{\text{ph}}}$$
$$+ x_2 \left.\frac{\partial E_{\alpha\alpha}}{\partial \tilde{g}_{\pi N}}\right|_{\tilde{g}_{\pi N}^{\text{ph}}} + x_3 \left.\frac{\partial E_{\alpha\alpha}}{\partial C_0}\right|_{C_0^{\text{ph}}} + x_4 \left.\frac{\partial E_{\alpha\alpha}}{\partial C_I}\right|_{C_I^{\text{ph}}}, \tag{3.2}$$

---

[2]Note that throughout we do not consider variations of the strange quark mass m_s, as these are expected to be very small. Hence m_s is simply kept at its physical value.

where

$$x_1 = \left.\frac{\partial m_N}{\partial M_\pi}\right|_{M_\pi^{\mathrm{ph}}} , \; x_2 = \left.\frac{\partial \tilde{g}_{\pi N}}{\partial M_\pi}\right|_{M_\pi^{\mathrm{ph}}} , \; x_3 = \left.\frac{\partial C_0}{\partial M_\pi}\right|_{M_\pi^{\mathrm{ph}}} , \; x_4 = \left.\frac{\partial C_I}{\partial M_\pi}\right|_{M_\pi^{\mathrm{ph}}} . \tag{3.3}$$

The partial derivatives in eq. (3.2) are computed using the auxiliary field quantum Monte Carlo (AFQMC) method [29], see section 6. To obtain an accurate and model-independent description of the M_π-dependence of the LO nuclear interaction, we will use the most recent knowledge from chiral perturbation theory and lattice QCD simulations to determine the quantities in eq. (3.3).

The partial derivative $\partial E_{\alpha\alpha}/\partial \tilde{M}_\pi$ in eq. (3.2) is computed by introducing a small change in the pion mass in the OPE of the nuclear Hamiltonian, $H(\tilde{M}_\pi) \to H(\tilde{M}_\pi + \Delta \tilde{M}_\pi)$, which corresponds to a perturbative shift in the energy, $\Delta E_{\alpha\alpha}(\tilde{M}_\pi)$. In our calculations, the pion masses are shifted by $\Delta \tilde{M}_\pi = 4.59\,\mathrm{MeV}$, which equals to the empirical mass difference between the neutral and charged pions. Therefore, the partial derivative $\partial E_{\alpha\alpha}/\partial \tilde{M}_\pi$ is defined as

$$\left.\frac{\partial E_{\alpha\alpha}}{\partial \tilde{M}_\pi}\right|_{M_\pi^{\mathrm{ph}}} = \frac{\Delta E_{\alpha\alpha}(\tilde{M}_\pi)}{\Delta \tilde{M}_\pi}. \tag{3.4}$$

In what follows, we will also use the so-called K-factors. These are defined via

$$K_X^i = \left.\frac{y}{X}\frac{\partial X}{\partial y}\right|_{y^{\mathrm{ph}}} , \tag{3.5}$$

where X is an observable and the superscript $i = \{q, \pi, \alpha\}$ denotes the quantity $y = \{m_q, M_\pi, \alpha_{\mathrm{EM}}\}$, such that, e.g., K_X^q measures the sensitivity of X to changes in the light quark mass m_q. For more detailed discussion on these quantities, see, e.g., ref. [19].

The parameter x_1 can be determined from the pion-nucleon sigma term,

$$\sigma_{\pi N} = \langle N|\hat{m}(\bar{u}u + \bar{d}d)|N\rangle = M_\pi^2 \frac{\partial m_N}{\partial M_\pi^2} , \tag{3.6}$$

i.e. the quark mass dependence of the nucleon mass, via

$$x_1 = \left.\frac{\partial m_N}{\partial M_\pi}\right|_{M_\pi^{\mathrm{ph}}} = \frac{2}{M_\pi}\, \sigma_{\pi N} . \tag{3.7}$$

The most recent and precise values for $\sigma_{\pi N}$ are from the Roy-Steiner-equation analyses of pion-nucleon scattering [32, 34]. In the calculation with the inclusion of pionic hydrogen and deuterium data, the reported value is $\sigma_{\pi N} = (59.1 \pm 3.5)\,\mathrm{MeV}$, and in the calculation using only the pion-nucleon scattering data the value is $\sigma_{\pi N} = (58.1 \pm 5)\,\mathrm{MeV}$. In this study we use the value of ref. [32] and the uncertainty of ref. [34], which gives

$$x_1 = 0.84(7) . \tag{3.8}$$

The parameter x_2 in eq. (3.3) represents the dependence of the strength of the OPE potential and is given as,

$$x_2 = \left.\frac{1}{2F_\pi}\frac{\partial g_A}{\partial M_\pi}\right|_{M_\pi^{\mathrm{ph}}} - \left.\frac{g_A}{2F_\pi^2}\frac{\partial F_\pi}{\partial M_\pi}\right|_{M_\pi^{\mathrm{ph}}} . \tag{3.9}$$

For the dependence of F_π on M_π we use the results reported in ref. [19]

$$\left.\frac{\partial F_\pi}{\partial M_\pi}\right|_{M_\pi^{\mathrm{ph}}} = \frac{F_\pi}{M_\pi}\frac{K^q_{F_\pi}}{K^q_{M_\pi}} = 0.066(16)\,. \tag{3.10}$$

The M_π-dependence of the nucleon axial-vector coupling g_A is obtained from the analysis of the high-precision lattice QCD calculations [35]. We define

$$\frac{\partial g_A}{\partial M_\pi} = \frac{\partial g_A}{\partial M^*}\frac{\partial M^*}{\partial M_\pi}\,, \tag{3.11}$$

where

$$\frac{\partial M^*}{\partial M_\pi} = \frac{\partial}{\partial M_\pi}\left(\frac{M_\pi}{4\pi F_\pi}\right) = \frac{1}{4\pi F_\pi}\left(1 - \frac{M_\pi}{F_\pi}\frac{\partial F_\pi}{\partial M_\pi}\right) = 0.078(2)\ \text{l.u.}\,, \tag{3.12}$$

where l.u. stands for lattice units and $\partial g_A/\partial M^*|_{M_\pi^{\mathrm{ph}}} = -0.08(24)$. In eq. (3.12) we use the isospin-averaged pion mass $M_\pi = 138.03\,\mathrm{MeV}$. Putting pieces together, we have

$$\frac{\partial g_A}{\partial M_\pi} = -0.006(19)\ \text{l.u.}\,, \tag{3.13}$$

which gives

$$x_2 = -0.053(16)\ \text{l.u.}\,. \tag{3.14}$$

So far we have discussed the quantities x_1 and x_2 which control the M_π-dependence of the pion and nucleon properties as well as their interactions. As has been shown, we obtained a model-independent description of these quantities utilizing the results from CHPT calculations and the data from high-precision lattice QCD. Now we turn to the discussion of the quantities x_3 and x_4 which are controlling the implicit M_π-dependence of the LECs of the short-range NN interactions, $C_0(M_\pi)$ and $C_I(M_\pi)$. Since the coupling constants C_0 and C_I are adjusted to reproduce the NN scattering phase shifts in the $^1S_0$ and $^3S_1$ partial waves, it is much more convenient to express the x_3 and x_4 quantities in terms of the inverse singlet (s) and triplet (t) NN scattering lengths,

$$\bar{A}_s = \left.\frac{\partial a_s^{-1}}{\partial M_\pi}\right|_{M_\pi^{\mathrm{ph}}}\,, \quad \bar{A}_t = \left.\frac{\partial a_t^{-1}}{\partial M_\pi}\right|_{M_\pi^{\mathrm{ph}}}\,. \tag{3.15}$$

To obtain the desired expressions, we adopt the analysis of ref. [10], which employs the Lüscher finite volume formula to relate the spectrum of the NN system in a cubic periodic box to the NN scattering parameters,

$$x_3 = 0.04847 + 0.06713x_1 - 0.25101x_2 - 0.37652\bar{A}_s - 0.20467\bar{A}_t\,, \tag{3.16}$$
$$x_4 = 0.04990 - 0.00190x_1 - 0.01253x_2 - 0.12551\bar{A}_s + 0.20467\bar{A}_t\,. \tag{3.17}$$

We further use the analysis of ref. [11], which determines $\bar{A}_s$ and $\bar{A}_t$ from the most recent available lattice QCD data, see appendix A for details:

$$\bar{A}_s = 0.54(24)\,, \quad \bar{A}_t = 0.33(16)\,. \tag{3.18}$$

Finally, using the results given in eq. (3.18) with eq. (3.17), we get,

$$x_3 = -0.153(96)\,, \quad x_4 = 0.049(46)\,. \tag{3.19}$$

In what follows, we will use the values for $\bar{A}_{s,t}$ collected in eq. (3.18), noting that these are still affected by sizeable uncertainties (for a more detailed discussion, see ref. [11]). This can only be sharpened by more precise lattice QCD calculation at lower pion (quark) masses.

4 Dependence of the nuclear Hamiltonian on the fine-structure constant

First, we must briefly discuss how the electromagnetic interaction is included in our scheme. This requires a multi-step procedure. In a first step, we consider 8 nucleons (4 protons and 4 neutrons) in a box of $V \simeq (16\,\mathrm{fm})^3$, from which two α clusters are formed. Here, the EM interaction is included using the standard power counting, see e.g. [36]. In this counting, the EM interactions start to contribute at NLO. To account for the infinitely-ranged Coulomb interaction between these two clusters with charge $Z = 2$ each, we employ a second box of about $V \simeq (100\,\mathrm{fm})^3$, which is far beyond the range of the strong interactions. Within this box, a spherical wall with a radius of about 35 fm is placed subject to Coulomb boundary conditions. This allows for an exact treatment of the long-range Coulomb forces with the two α particles. For details on this procedure, we refer to refs. [15, 16].

Now, we are in the position to consider the second term on the right-hand side of eq. (2.1), which is the α_{EM}-dependence of α-α scattering. To study the α_{EM}-dependence of α-α scattering we compute the shifts $\Delta E_{\alpha\alpha}(\alpha_{\mathrm{EM}})$ and $\Delta E_{\alpha\alpha}(c_{pp})$. The former is the variation of two-alpha cluster energy due to the long-range Coulomb interaction, and the latter is the variation of two-alpha cluster energy due to a derivative-less proton-proton contact operator. This operator arises from the fact that the Coulomb interaction on the lattice becomes singular when two protons are on the same lattice site which requires a special treatment. Thus, a regularized version of the Coulomb interaction on the lattice is employed, and the coefficient of the proton-proton contact operator, c_{pp}, is determined from the proton-proton phase shifts on the lattice. The energy shift becomes,

$$Q_{\mathrm{EM}}(E_{\alpha\alpha}) = \Delta E_{\alpha\alpha}(\alpha_{\mathrm{EM}}) + x_{pp}\,\Delta E_{\alpha\alpha}(c_{pp})\,, \tag{4.1}$$

where x_{pp} is the relative strength of the proton-proton contact term caused by the regularization of the Coulomb force. The coefficient x_{pp} is computed using the data for ^{4}He [10],

$$x_{pp} = 0.39(5)\,. \tag{4.2}$$

Finally, the partial derivative in eq. (2.1) can be written as

$$\left.\frac{\partial E_{\alpha\alpha}}{\partial \alpha_{\mathrm{EM}}}\right|_{\alpha_{\mathrm{EM}}^{\mathrm{ph}}} \simeq \frac{\partial Q_{\mathrm{EM}}(E_{\alpha\alpha})}{\partial \alpha_{\mathrm{EM}}^{\mathrm{ph}}}\,. \tag{4.3}$$

5 Theta-dependence of alpha-alpha scattering

We also strive to assess the θ-dependence of α-α scattering. To that end, one might be tempted to again employ a linear variation $\propto \delta\theta$ around the physical value of θ^{ph}, similar to what we do in the case of the M_π-variation and the α_{EM}-dependence of $E_{\alpha\alpha}$, see eq. (2.1). However, it is well known that "small" variations of θ do not lead to drastic changes of nuclear physics [21, 22] and after all it is interesting in its own right to assess what is happening when θ approaches a value of, say, $\mathcal{O}(1)$. In this regime, a simple linear variation clearly would not be applicable any longer.

There is, however, a way to circumvent such a direct calculation of the θ-dependence, which is based on the observation that in a first approximation any source of θ-dependence of $E_{\alpha\alpha}$ can be traced back to the θ-dependence of M_π, which in the isospin limit is given by [37][3]

$$M_\pi^2(\theta) = 2B_0\hat{m}\cos\frac{\theta}{2}\,, \ |\theta| < \pi\,. \tag{5.1}$$

Assuming this approximation is valid, the present calculation of the M_π-dependence of $E_{\alpha\alpha}$ within a range of $|\delta M_\pi| \lesssim 0.1 M_\pi^{\text{ph}}$ can directly be translated into an assessment of the θ-dependence in a corresponding range of $|\delta\theta| \lesssim 1$.

It is not obvious that this approximation is legitimate, as M_π and θ in CHPT are in principle independent parameters, but it can be justified as follows: removing the QCD θ-term by a suitable choice of an axial U(1) transformation adds a complex phase

$$\mathcal{M} \to e^{\text{i}\frac{\theta}{2}}\mathcal{M} =: \mathcal{M}_\theta, \tag{5.2}$$

to the quark mass matrix. This θ-dependent matrix enters chiral perturbation theory via the matrix $\chi_\theta = 2B_0\mathcal{M}_\theta$, which in the isospin symmetric case is simply given by

$$\chi_\theta = \left(M_\pi^2(\theta) + \text{i}\,2B_0\hat{m}\sin\frac{\theta}{2}\right)\mathbb{1}\,. \tag{5.3}$$

Hence, inserting this expression into a given chiral Lagrangian of any order will produce terms that are either proportional to (some power of) $M_\pi(\theta)$, or proportional to (some power of) $\sin\theta/2$ (or both). While the latter are naturally absent in chiral perturbation theory at $\theta = 0$, the former simply leads to the known M_π-dependence of quantities such as m_N, $\tilde{g}_{\pi N}$, or couplings of nucleons to two or more pions.

As it turns out, at NLO, which is the maximal order we are considering here, the only term $\propto \sin\theta/2$ that might alter any of the involved quantities, in particular m_N or $\tilde{g}_{\pi N}$, comes from the NLO pion-nucleon Lagrangian [40]

$$\mathcal{L}_{\pi N}^{(2)} = c_5\bar{N}\left(\chi_+ - \frac{1}{2}\operatorname{Tr}\chi_+\right)N + \ldots\,, \tag{5.4}$$

where c_5 is another LEC, the ellipses represent other NLO terms that are of no interest here, and

$$\chi_+ = u^\dagger\chi u^\dagger + u\chi^\dagger u\,, \tag{5.5}$$

---

[3]The physics at $\theta = \pi$ is a bit more involved, see, e.g., [38, 39].

with u carrying the pion fields. This term adds a contribution to the pion-nucleon coupling that is explicitly θ-dependent, but it can be shown that its actual numerical impact is so small ($\lesssim 1$–2%) [21, 41] that it can safely be neglected. The smallness of these effects can directly be traced back to the suppression of the LEC $c_5 = (-0.09 \pm 0.01)\,\text{GeV}^{-1}$ as it parameterizes the leading isospin-breaking effects in the pion-nucleon sector [40]. This means that as long as we stick to a calculation that is of NLO at most, any non-negligible θ-dependence indeed only appears implicitly in form of $M_\pi(\theta)$ as a consequence of the first term of eq. (5.3).

Thus, our approach here is to not perform a separate calculation for assessing the θ-dependence of α-α scattering, but to simply use the results of the M_π-dependence analysis and map them onto the θ-dependence using eq. (5.1).

6 Adiabatic projection method and auxiliary field quantum Monte Carlo simulations

The adiabatic projection method is a general framework to construct a low-energy effective theory for clusters. The adiabatic projection in Euclidean time gives a systematically improvable description of the low-lying scattering cluster states and in the limit of large Euclidean projection time the description becomes exact. The details of the method can be found in refs. [12, 16]. The method starts with defining Slater-determinant of two-alpha initial cluster states $|\vec{R}\rangle$ parameterized by the relative spatial separation between the clusters on a periodic cubic lattice with a box size L,

$$|\vec{R}\rangle = \sum_{\vec{r}} |\vec{r} + \vec{R}\rangle_1 \otimes |\vec{r}\rangle_2 \;. \tag{6.1}$$

To perform the calculations efficiently, we project the initial states onto spherical harmonics with angular momentum quantum numbers ℓ and ℓ_z. To that end, we bin the cubic lattice points $\langle n_x, n_y, n_z \rangle$ with the same distance $|\vec{R}| = \sqrt{n_x^2 + n_y^2 + n_z^2}$ by weighting with spherical harmonics $Y_{\ell,\ell_z}(\hat{R})$,

$$|R\rangle^{\ell,\ell_z} = \sum_{\vec{r}} Y_{\ell,\ell_z}(\hat{R}')\delta_{\vec{R},|\vec{R}'|} |\vec{R}\rangle \;. \tag{6.2}$$

Here, ℓ and ℓ_z are not exactly good quantum numbers, see the discussion in ref. [43]. Since the initial cluster states are not necessarily orthonormal, we define the orthonormal initial cluster states

$$|\mathcal{R}\rangle^{\ell,\ell_z} = \sum_{R'} |R'\rangle^{\ell,\ell_z} [N_0^{-1/2}]_{R',R}^{\ell,\ell_z}, \tag{6.3}$$

where $[N_0^{-1}]_{R',R}^{\ell,\ell_z}$ is the norm matrix defined as

$$[N_0^{-1}]_{R',R}^{\ell,\ell_z} = {}^{\ell,\ell_z}\langle R'|R\rangle^{\ell,\ell_z} \;. \tag{6.4}$$

In the next step, the initial cluster states are evolved in Euclidean time by means of multiplying by powers of the leading order (LO) transfer matrix to form dressed cluster states,

$$|R\rangle_{n_t}^{\ell,\ell_z} = M_{\mathrm{LO}}^{n_t} |\mathcal{R}\rangle^{\ell,\ell_z} \ . \tag{6.5}$$

This procedure, by design, incorporates all the induced deformations and polarizations of the alpha clusters due to the microscopic interaction and it gives the true low-lying cluster states of the transfer matrix M_{LO}. In general the dressed cluster states are not orthonormal, thus for further calculations we use the following form of the dressed cluster states,

$$|\mathcal{R}\rangle_{n_t}^{\ell,\ell_z} = \sum_{R'} |R'\rangle_{n_t}^{\ell,\ell_z} \ [N_{L_t}^{-1/2}]_{R',R}^{\ell,\ell_z}, \tag{6.6}$$

where $[N_{L_t}^{-1/2}]_{R,R'}^{\ell,\ell_z}$ is the norm matrix at Euclidean time $L_t = 2 \times n_t$. Finally, we define the radial adiabatic transfer matrix at LO as,

$$[M_{\mathrm{LO},L_t}^a]_{R,R'}^{\ell,\ell_z} = {}_{n_t}^{\ell,\ell_z}\langle \mathcal{R}| M_{\mathrm{LO}} |\mathcal{R}'\rangle_{n_t}^{\ell,\ell_z} \ . \tag{6.7}$$

In our calculation the higher-order (HO) interactions are treated using first-order perturbation theory, thus we include the perturbative contributions from NLO, next-to-next-to-leading order (NNLO), isospin-breaking (IB), and Coulomb interactions (EM) to the leading-order radial adiabatic transfer matrix order-by-order in perturbation theory. Therefore, we define the radial adiabatic transfer matrix at a given higher order in a closed form as

$$[M_{\mathrm{HO},L_t}^a]_{R,R'}^{\ell,\ell_z} = {}_{n_t}^{\ell,\ell_z}\langle \mathcal{R}| M_{\mathrm{LO}} |\mathcal{R}'\rangle_{n_t}^{\ell,\ell_z} - \alpha_t \ {}_{n_t}^{\ell,\ell_z}\langle \mathcal{R}| : V_{\mathrm{HO}} \ M_{\mathrm{LO}} : |\mathcal{R}'\rangle_{n_t}^{\ell,\ell_z} \ , \tag{6.8}$$

where $\alpha_t = a_t/a$ is the ratio of the temporal and the spatial lattice spacings, and V_{HO} is the higher-potential at the order of interest. The colons $: \dots :$ denote normal ordering, which means that we reorder the creation and annihilation operators inside the colons and we move the creation operators to the left of the all annihilation operators with the appropriate number of anti-commutation minus signs.

So far we have discussed the adiabatic projection method for the chiral EFT Hamiltonian. Now we turn to the main interest of this paper, which is to construct the two-cluster matrix elements of the partial derivatives given in eq. (2.1). Due to the fact that we study the effects of small variations in the fundamental constants of nature on α-α scattering, the partial derivatives in eq. (2.1) are treated in a similar manner as the higher-order corrections,

$$\begin{aligned}[M_{\mathrm{HO},L_t}^{a,y}]_{R,R'}^{\ell,\ell_z} = {} & {}_{n_t}^{\ell,\ell_z}\langle \mathcal{R}| M_{\mathrm{LO}} |\mathcal{R}'\rangle_{n_t}^{\ell,\ell_z} \\ & - \alpha_t \ {}_{n_t}^{\ell,\ell_z}\langle \mathcal{R}| : V_{\mathrm{HO}} \ M_{\mathrm{LO}} : |\mathcal{R}'\rangle_{n_t}^{\ell,\ell_z} \\ & - \alpha_t \ {}_{n_t}^{\ell,\ell_z}\langle \mathcal{R}| : \left.\frac{\partial E_{\alpha\alpha}}{\partial y}\right|_{y^{\mathrm{ph}}} M_{\mathrm{LO}} : |\mathcal{R}'\rangle_{n_t}^{\ell,\ell_z} \ \delta y \,, \end{aligned} \tag{6.9}$$

we use the superscript y for the observables M_π, α_{EM} and, in principle, θ. However, as discussed in section 5, we will not perform explicit differentiations with respect to θ.

– 11 –

The two-cluster matrix elements of the LO transfer matrix, the higher order corrections, and the partial derivatives are computed by means of the auxiliary field quantum Monte Carlo (AFQMC) method. The non-perturbative quantum Monte Carlo simulations are performed using the neutral pion mass M_π and the isospin symmetry breaking effects are incorporated perturbatively. The calculation of the radial adiabatic transfer matrices in eqs. (6.7), (6.8) and (6.9) is divided into two separate parts. In the first part of the calculation, we perform the AFQMC simulation for the system of $A = 8$ nucleons (4 protons and 4 neutrons) to construct the radial adiabatic transfer matrices for two interacting α clusters. Due to the computational cost associated with such simulations, this is done on a periodic cubic lattice of length L which is not too large to prevent us from computing the matrices accurately but is not too small so that the length $L/2$ is much larger than the range of the interaction, $R \sim 1/M_\pi \simeq 1.4\,\mathrm{fm}$. In the second part of the calculation, the AFQMC simulations are performed for the system with $A = 4$ nucleons, and these simulations are done on a periodic cubic lattice of larger length due to the less computational demand. This single α cluster adiabatic matrix is used to construct the radial adiabatic transfer matrices for non-interacting two α clusters. Finally, we connect the radial adiabatic transfer matrices of interacting α clusters with the radial adiabatic transfer matrices of non-interacting α clusters in the asymptotic region to extend the radial transfer matrix of interacting α clusters to a larger volume. The aforementioned two-part approach was studied extensively for nucleon-deuteron systems in ref. [16], and it was found that the systematic errors due to extension of the radial transfer matrix are negligible.

The first *ab initio* calculation of α-α scattering was performed in ref. [15] using the same chiral Hamiltonian as adopted in this paper. However, in this paper we employ developments in the adiabatic projection method from refs. [16, 23, 42]. As discussed above, the first step of the adiabatic projection method is to define the initial cluster states, and on a periodic cubic lattice of length L the total number of initial cluster states parameterized by the relative spatial separation is $N_{\vec{R}} = 3L^2/4$. In ref. [12] it was shown that it is not required to use every possible cluster state when we are interested in only a few low-lying energies of the system of interest. Therefore, for simulating computationally demanding systems it is advantageous to construct a radial adiabatic transfer matrix defined in the subspace that is spanned by $N_{\vec{R}} < 3L^2/4$ cluster separation states. Following these findings, in ref. [15] the radial adiabatic transfer matrix for non-interacting two-alpha clusters was constructed in a smaller subspace of the two-cluster state space. In this paper, taking advantage of powerful computational resources we perform our simulations using every possible cluster state and construct the radial adiabatic transfer matrices in full space of the two-cluster state space.

7 Extracting scattering phase shifts from the adiabatic matrices

What was discussed in the previous section was the first part of the adiabatic projection method, which is constructing the adiabatic transfer matrix for the two clusters. The second part of the method is to extract the scattering or reaction parameters for the two clusters. In the previous section, by projecting the initial cluster states onto spherical harmonics

with angular momentum quantum numbers ℓ and ℓ_z, we constructed the adiabatic transfer matrix in radial coordinates, which provides a significant improvement in the computational scaling [16]. Since our adiabatic transfer matrices are defined in radial coordinates, the best approach to be used to calculate the scattering parameters is the so-called spherical wall method [43–45].

In the spherical wall method we employ a hard boundary wall condition at $r = R_{\text{wall}}$, which is the relative separation distance between two clusters in the asymptotic region. In general, the spherical wall method is used to remove the periodic boundary effects inherited from the cubic lattice and the artifacts due to the periodic boundary condition. However, in our calculations these effects are already eliminated since we construct the adiabatic transfer matrices in radial coordinates as explained in section 6. After imposing the spherical hard wall to the radial adiabatic transfer matrices, we solve the Schrödinger equation of the system and obtain the spherical scattering wave functions as well as the spectrum. In principle, due to the imposed spherical hard wall one expects that the spherical wave functions die out at R_{wall}, however, as a result of non-zero spatial lattice spacing the spherical wave functions vanish at $R'_{\text{wall}} = R_{\text{wall}} + \varepsilon_R$, where ε_R is the correction on the precise radius of the spherical wall and is defined as $|\varepsilon_R| < a/2$.

The total wave function of a two-cluster system is decomposed into the radial part $R_\ell^{(p)}(r)$ and the spherical harmonics $Y_{\ell,\ell_z}(\hat{r})$,

$$\Psi(\vec{r}) = R_\ell^{(p)}(r) \, Y_{\ell,\ell_z}(\hat{r}) \,, \tag{7.1}$$

where r is the relative spatial separation of the clusters and p is the relative momentum. The radial wave function in the asymptotic region is given by

$$R_\ell^{(p)}(r) = N_\ell(p) \left[\cos \delta_\ell(p) \, F_\ell(p\,r) + \sin \delta_\ell(p) \, G_\ell(p\,r) \right] \,, \tag{7.2}$$

where $N_\ell(p)$ is an overall normalization coefficient, and F_ℓ (G_ℓ) is the regular (irregular) Coulomb wave function.

The relative momentum p is calculated from the spectrum of the radial adiabatic transfer matrices and the dispersion relation of the two-cluster system given by,

$$E = c_0 \frac{p^2}{2\mu} + c_1 \, p^4 + c_2 \, p^6 + \dots \,, \tag{7.3}$$

where $\mu = m_\alpha/2$ is the reduced mass of the two-cluster system, m_α the mass of the α-particle, and the coefficients c_i are determined by fitting eq. (7.3) to the lattice dispersion relation. We determine the correction ε_R from the roots of the regular Coulomb wave function with the relative momentum of the non-interacting two-cluster system, p_0, around R_{wall}. Finally, we use the corrected radius of the spherical hard wall, R'_{wall}, and the relative momentum of the interacting two-cluster system, p, and solve eq. (7.2) for the scattering phase shifts,

$$\delta_\ell(p) = \tan^{-1} \left[-\frac{F_\ell(p\,R'_{\text{wall}})}{G_\ell(p\,R'_{\text{wall}})} \right] \,. \tag{7.4}$$
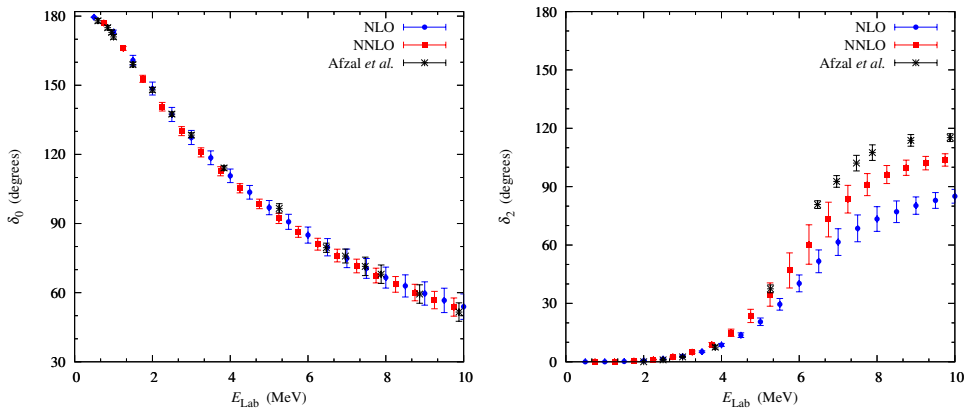
Figure 1. Left panel: S-wave α-α scattering phase shift δ_0 versus the energy in the laboratory system, E_{lab}. Right panel: D-wave α-α scattering phase shift δ_2 versus the energy in the laboratory system, E_{lab}. The blue circles and red squares represent our predictions at NLO and NNLO, respectively, while the data are given by the black crosses.

We extract the scattering phase shifts from the radial adiabatic transfer matrices with L_t time steps and perform Euclidean time extrapolating to the limit $L_t \to \infty$. Details of the extrapolation fit and all associated error estimates are discussed in appendix B.

8 Results

8.1 Our universe

Here, we discuss the results for the S- and D-wave phase shifts and the effective range parameters in the S-wave as well as the resonance parameters in the D-wave for the physical values of M_π and α_{EM} and $\theta = 0$. In figure 1, we show the S-wave phase shift δ_0 (left panel) and the D-wave phase shift δ_2 (right panel) at NLO and NNLO in comparison to the data [2]. Note that we do not show the LO result here, as the electromagnetic interaction is not yet included and therefore the predicted curve is far off the data (as discussed in more detail in ref. [15]). We find a marked improvement, both for the S-wave and the D-wave, as compared to the pioneering work in ref. [15], which is due to the improvements in the APM discussed in the earlier sections. We note that these are parameter-free predictions. Furthermore, the uncertainties are mostly stemming from the large Euclidean time extrapolation and these decrease when going from NLO to NNLO, as expected in a well-behaved expansion. Up to $E_{\text{Lab}} \simeq 3.5\,\text{MeV}$, our description of the S-wave phase shift is as good as the one obtained using halo EFT in ref. [46]. We note that the uncertainties have somewhat increased as compared to ref. [15] because, as discussed in the previous section, we use a much larger subspace of the two-cluster state space, which reduces the number of configurations used for the matrix entries, resulting in a larger statistical uncertainty. This could eventually be overcome by utilizing much more HPC resources.

– 14 –

	S-wave			D-wave	
	a_0 [10^3 fm]	r_0 [fm]	P_0 [fm^3]	E_R [MeV]	Γ_R [MeV]
NLO	$-1.80(93)$	$1.045(15)$	$-2.297(156)$	$3.05(4)$	$2.68(23)$
NNLO	$-1.55(63)$	$1.061(14)$	$-2.277(158)$	$2.93(5)$	$2.00(16)$
empirical	$-1.65(17)$	$1.084(11)$	$-1.76(22)$	$2.92(18)$	$1.35(50)$

Table 1. S-wave: the ERE parameters a_0, r_0 and P_0 at NLO and NNLO. D-wave: the resonance parameters E_R and Γ_R at NLO and NNLO. The empirical values from ref. [47] are also given.

Next, we discuss the S-wave ERE parameters a_0, r_0 and P_0 (see appendix C for definitions), collected in table 1. The fit range to determine these is from $E_{\text{Lab}} = 1.0$ to 7.7 MeV. We see that these parameters are consistent with the empirical determinations, but they are also afflicted with sizeable uncertainties. Note that there is sensitivity to the fit range as well as to the position of the 0^+ resonance, the ^{8}Be ground state, as discussed in ref. [46]. In our calculation, ^{8}Be is very weakly bound. This appears to be in contradiction to the scattering lengths given in table 1, but these values are very sensitive to the fitting range employed to extract them, see also ref. [46].

The D-wave phase shift shows a clear resonance-behaviour. Due to the large width of the resonance, the extraction of the resonance parameters (energy and width) is affected with some model-dependence. As in our earlier work, we fix the resonance energy E_R by the maximum of $d\delta/dE$ and its width Γ_R from the value of $2(d\delta/dE)^{-1}$ at E_R, see e.g. ref. [48]. The resonance parameters at NLO and NNLO are also given in table 1. We find that the resonance parameters at NNLO are much closer to the empirical ones as compared to our earlier work.

8.2 The Multiverse

8.2.1 Variations of the bound state energies

Before considering the effect of the variations of the fundamental parameters on the α-α scattering phase shifts, we discuss briefly the variation of the various bound state energies relevant to the 3α process. This provides some additional information to ref. [11] that was not explicitly displayed there. Consider first pion mass variations, keeping α_{EM} and θ at their physical values. In the left panel of figure 2, we display the variation of the energies of ^{4}He, ^{4}Be, ^{12}C and the Hoyle state ^{12}C* as a function of the varying pion mass for positive changes in M_π. These energies are denoted as E_4, E_8, E_{12} and $E_{12}^\star$, in order, see the explicit expressions in appendix D. For negative energy changes in M_π these curves only differ in the sign, that is the contribution is repulsive rather than attractive as for positive shifts in the pion mass. These different energies are obviously correlated, as shown more clearly in the right panel of figure 2, where the various K-factors for the pertinent eight and twelve particle systems are displayed as a function of the corresponding ^{4}He K-factor, $K_{E_4}^\pi$, for independent variations of $\bar{A}_s$ and $\bar{A}_t$ over the range $\{-1,\ldots,+1\}$ are shown. Of course, the actual range of these parameters as given in eq. (3.18) is smaller, but these parameters might change when better results from lattice QCD will become available.
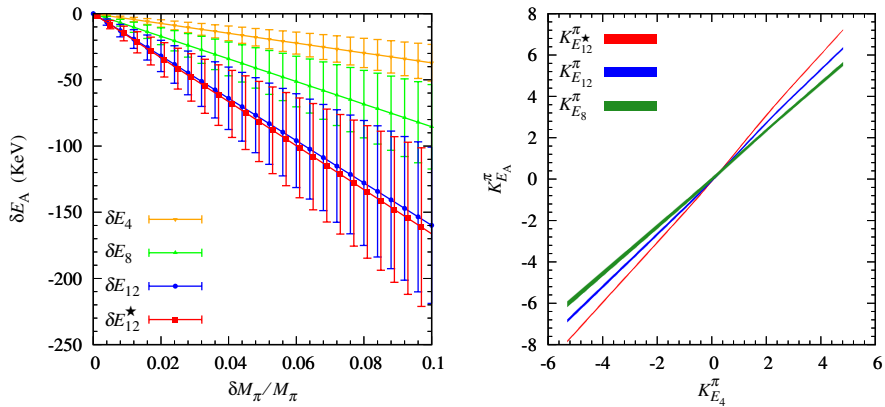
Figure 2. Left panel: variation of the ground state energy of the nuclei ^{4}He, ^{4}Be, ^{12}C and the Hoyle state ^{12}C*, respectively, under variation of the pion mass (in percent). Right panel: sensitivity of the ground state energy of the nuclei ^{8}Be, ^{12}C and the Hoyle state ^{12}C*, respectively, to changes in M_π as a function of $K_{E_4}^\pi$ under independent variations of $\bar{A}_s$ and $\bar{A}_t$ over the range $\{-1, \ldots, +1\}$.
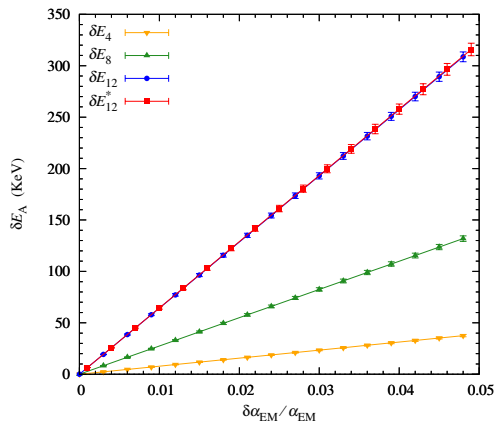

Figure 3. Variation of the ground state energy of the nuclei ^{4}He, ^{4}Be, ^{12}C and the Hoyle state ^{12}C*, respectively, under variation of the fine-structure constant (in percent).

Note that such correlations related to the production of carbon have indeed been speculated upon earlier [49, 50].

Next, we consider variations of the fine-structure constant for physical pion masses and vanishing θ angle. The variations of the energies E_4, E_8, E_{12} and $E_{12}^\star$ with varying $\alpha_{\rm EM}$ are displayed in figure 3 (for positive shifts in $\alpha_{\rm EM}$). Naively, one would expect the slopes of the different nuclei to scale as Z^2, that is in the ratio $1:4:9$ for ^{4}He, ^{8}Be and ^{12}C, in order. The observed difference from this scaling is coming from the proton-proton derivative-less contact interaction. In fact, removing the contribution from this term, one finds for $\delta\alpha_{\rm EM}/\alpha_{\rm EM} = 5\%$ the following energy shifts: $\delta E_4 = 30.65(10)\,{\rm keV}$, $\delta E_8 = 117.5(10)\,{\rm keV}$

– 16 –

and $\delta E_{12} = 283.5(10)\,\mathrm{keV}$, perfectly consistent with the Z^2 scaling. We note here that the results for negative shifts in α_{EM} are of opposite sign, that is pertinent energy shifts δE_A are negative.

8.2.2 Pion mass variations of alpha-alpha scattering

We now consider pion mass variations keeping $\alpha_{\mathrm{EM}} \simeq 1/137$ and $\theta \simeq 0$ fixed. In figure 4, we display the NLO results with variations of the pion mass up to $\pm 3\%$ (inner red bands), together with the 1σ uncertainty of the 3% variation (outer orange bands) as well as the variations up to 5% (inner dark green bands) and the 1σ uncertainty of the 5% variation (outer light green bands). As before, the left panel gives the S-wave δ_0 and the right panel the D-wave δ_2 phase shift. The pertinent 1σ uncertainties include all statistical and systematic errors properly propagated at this order. Consider now in more detail the S-wave. For positive pion mass shifts, there is very little effect on δ_0, however, this is different for negative pion mass shifts. At around $\delta M_\pi / M_\pi \simeq -5\%$, the additional repulsion unbinds the two-alpha system as seen by the phase shift starting at zero.

In the D-wave, the effects of the pion mass variation are somewhat more pronounced, as seen in the right panel of figure 4. Here, the upper (lower) part of the band refers to positive (negative) shifts in the pion mass. The pion mass variation is also reflected in the parameters of the D-wave resonance, which for a pion mass variation of $\pm 5\%$ are given by

$$
\begin{aligned}
E_R = 2.57(6)\,\mathrm{MeV}\,, &\quad \Gamma_R = 1.22(21)\,\mathrm{MeV} &\quad \delta M_\pi/M_\pi = +5\%\,, \\
E_R = 3.60(13)\,\mathrm{MeV}\,, &\quad \Gamma_R = 3.56(89)\,\mathrm{MeV} &\quad \delta M_\pi/M_\pi = -5\%\,.
\end{aligned} \tag{8.1}
$$

We now turn to the results at NNLO, showing the pertinent results for the S-wave in the left panel of figure 5 and for the D-wave in the right panel of that figure. Consider first the S-wave, where we display results for pion mass variations in the range $-7\% \leq \delta M_\pi / M_\pi \leq 10\%$. The critical value for $\delta M_\pi / M_\pi$, where the two-alpha system becomes unbound, is moved to -7%, where as positive changes of up to 10% do not lead to significant changes in the phase shift δ_0. For the D-wave, we again find a larger sensitivity (see right panel of figure 5). This is again reflected in the resonance parameters,

$$
\begin{aligned}
E_R = 2.52(15)\,\mathrm{MeV}\,, &\quad \Gamma_R = 0.92(33)\,\mathrm{MeV} &\quad \delta M_\pi/M_\pi = +5\%\,, \\
E_R = 3.22(5)\,\mathrm{MeV}\,, &\quad \Gamma_R = 2.69(26)\,\mathrm{MeV} &\quad \delta M_\pi/M_\pi = -5\%\,.
\end{aligned} \tag{8.2}
$$

We note that both at NLO and NNLO, the variations of E_R and Γ_R are almost linear in the pion mass shift.

As noted, in our calculation at NNLO, the ${}^8\mathrm{Be}$ nucleus is slightly bound, which generates some of the behaviour of the phase shifts close to zero energy. To overcome this, we also consider the pion mass dependence of the S-wave effective range function $K_0(E_{\mathrm{Lab}})$ as well as the one of the D-wave effective range function $K_2(E_{\mathrm{Lab}})$, as defined in appendix C.

Let us start with the S-wave. In figure 6, we show the pion mass variation of the S-wave effective range function with respect to the results for our Universe at NLO (left panel) and NNLO (right panel). There appears to be little effect on $K_0(E_{\mathrm{Lab}})$ at NLO, with a somewhat increased repulsion for negative pion mass shifts. More precisely, there is some
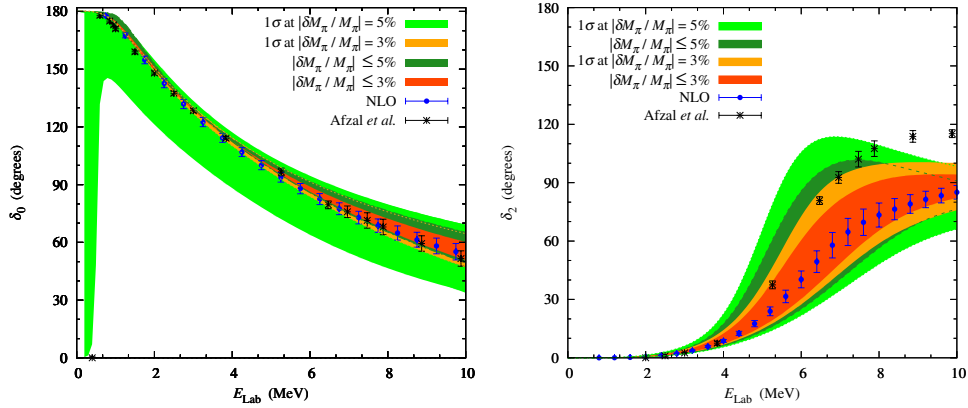
– 17 –

Figure 4. Pion mass dependence of the α-α phase shifts at NLO. Left panel: S-wave phase shift δ_0 versus the energy in the laboratory system, E_{lab}. Right panel: D-wave phase shift δ_0 versus the energy in the laboratory system, E_{lab}. The black crosses refer to the experimental data, the blue circles are the NLO results in the limit $L_t \to \infty$ at $\delta M_\pi = 0$. The red band corresponds the S-wave phase shifts with a variation in M_π within $|\delta M_\pi/M_\pi| \leq 3\%$, and the golden band refers to the errors for $|\delta M_\pi/M_\pi| = 3\%$. The dark green band corresponds to a variation in M_π within $|\delta M_\pi/M_\pi| \leq 5\%$, and the light green band refers to the errors for $|\delta M_\pi/M_\pi| = 5\%$. In the case of variation in M_π by -5% in the S-wave, due to difficulty in performing Euclidean time extrapolation at low-energies we estimate the error band from the spread in phase shifts versus the number of time steps.
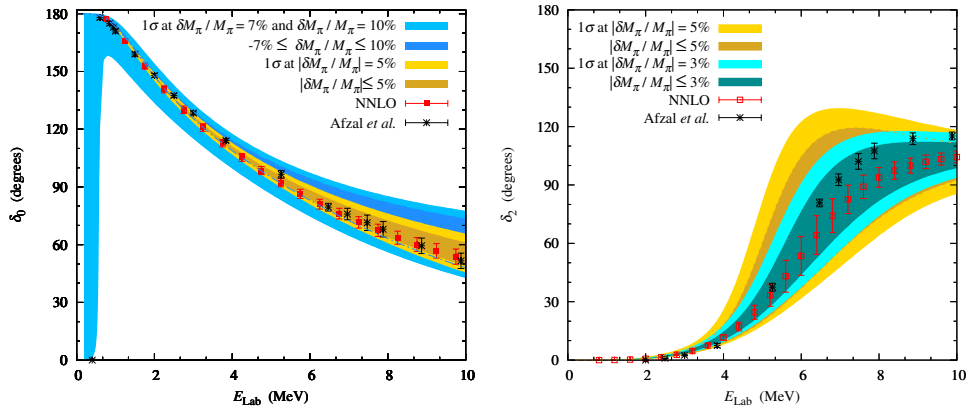
Figure 5. Pion mass dependence of the α-α phase shifts at NNLO. Left panel: S-wave phase shift δ_0 versus the energy in the laboratory system, E_{lab}. Right panel: D-wave phase shift δ_0 versus the energy in the laboratory system, E_{lab}. The black crosses refer to the experimental data, the red squares are the NNLO results in the limit $L_t \to \infty$ at $\delta M_\pi = 0$. The dark gold band corresponds to the S-wave phase shifts with a variation in M_π within $|\delta M_\pi/M_\pi| \leq 5\%$, and the light golden band refers to the errors for $|\delta M_\pi/M_\pi| = 5\%$. The dark blue band corresponds to a variation in M_π within $-7\% \leq \delta M_\pi/M_\pi \leq 10\%$, and the light blue band refers to the corresponding errors. In the case of variation in M_π by -7% in the S-wave, due to the difficulty in performing a Euclidean time extrapolation at low energies, we estimate the error band from the spread in phase shifts versus the number of time steps.
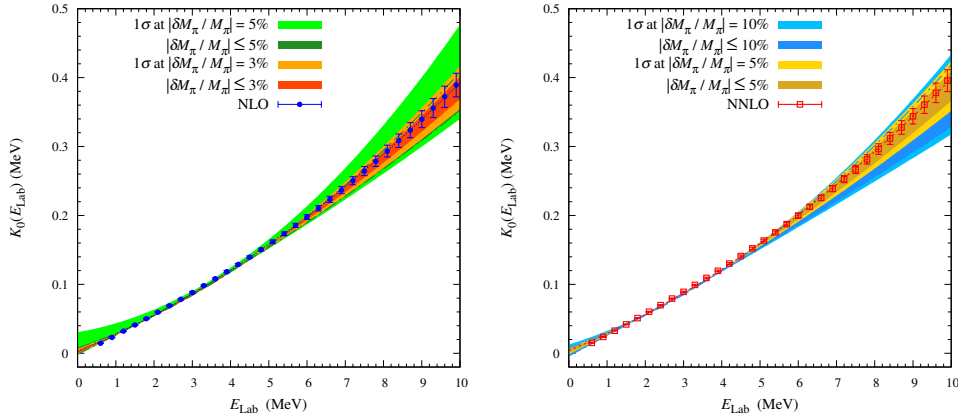
Figure 6. Pion mass dependence of the S-wave effective range function. Left panel: NLO results. The blue points refer to the results without pion mass variation, the red and dark green bands refer to changes by $\pm 5\%$ and $\pm 10\%$, in order, and the orange and light green bands are the corresponding 1σ uncertainties. Right panel: NNLO results. The red squares refer to the results without pion mass variation, the golden and dark blue bands refer to changes by $\pm 5\%$ and $\pm 10\%$, in order, and the yellow and light blue bands are the corresponding 1σ uncertainties.

added repulsion for negative mass shifts. This trend is also found at NNLO, with some increase in strength. We can quantify this by calculating the shift in the first parameter of the ERE, namely the inverse S-wave scattering length at NLO

$$
\frac{1}{a_0} = \begin{cases} -0.0017(12) & \text{for} \quad \delta M_\pi/M_\pi = -5\%, \\ -0.0025(3) & \text{for} \quad \delta M_\pi/M_\pi = -3\%, \\ -0.0019(1) & \text{for} \quad \delta M_\pi/M_\pi = 0, \\ -0.0016(1) & \text{for} \quad \delta M_\pi/M_\pi = +3\%, \\ -0.0019(1) & \text{for} \quad \delta M_\pi/M_\pi = +5\%, \end{cases} \tag{8.3}
$$

and at NNLO

$$
\frac{1}{a_0} = \begin{cases} +0.0011(6) & \text{for} \quad \delta M_\pi/M_\pi = -10\%, \\ -0.0016(1) & \text{for} \quad \delta M_\pi/M_\pi = -5\%, \\ -0.0014(1) & \text{for} \quad \delta M_\pi/M_\pi = 0, \\ -0.0013(1) & \text{for} \quad \delta M_\pi/M_\pi = +5\%, \\ -0.0021(1) & \text{for} \quad \delta M_\pi/M_\pi = +10\%, \end{cases} \tag{8.4}
$$

all in units of MeV. We note that the shifts at NNLO are a bit larger than the ones at NLO, which can be traced back to the fact that there is more short-range repulsion in the NNLO interaction and thus it is less sensitive to the pion mass dependent corrections. Clearly, the NNLO calculation should be considered more reliable.

Consider now the D-wave. In figure 7, we show the pion mass variation of the D-wave effective range function with respect to the results for our Universe at NLO (left panel) and NNLO (right panel). The effect on $K_2(E_{\text{Lab}})$ is quite pronounced, it is smallest where the
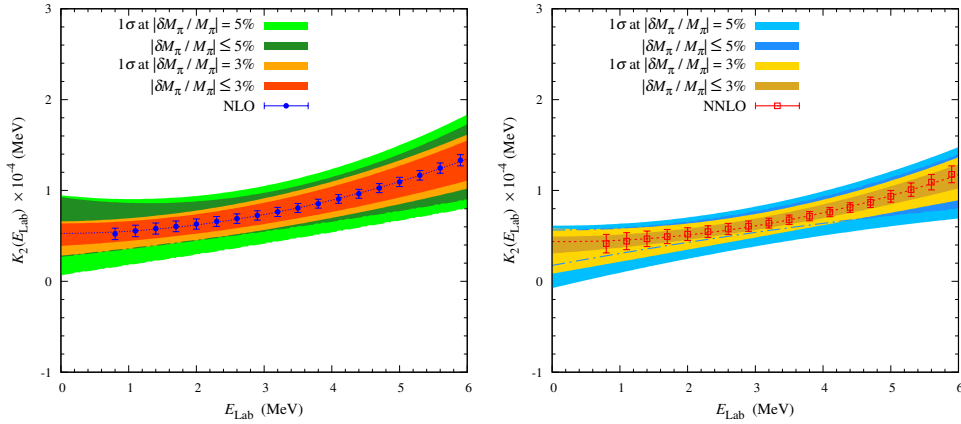
Figure 7. Pion mass dependence of the D-wave effective range function. Left panel: NLO results. The blue points refer to the results without pion mass variation, the red and dark green bands refer to changes by $\pm 5\%$ and $\pm 10\%$, in order, and the orange and light green bands are the corresponding 1σ uncertainties. Right panel: NNLO results. The red squares refer to the results without pion mass variation, the golden and dark blue bands refer to changes by $\pm 5\%$ and $\pm 10\%$, in order, and the yellow and light blue bands are the corresponding 1σ uncertainties.

phase shift passes through the resonance. We can quantify this by calculating the shifts in the inverse D-wave scattering length, at NLO first parameter of the ERE, namely the inverse D-wave scattering length at NLO

$$
\frac{1}{a_2} = \begin{cases}
9.30(2) & \text{for} \quad \delta M_\pi / M_\pi = -5\%\,, \\
6.19(5) & \text{for} \quad \delta M_\pi / M_\pi = -3\%\,, \\
5.27(5) & \text{for} \quad \delta M_\pi / M_\pi = 0\,, \\
3.79(6) & \text{for} \quad \delta M_\pi / M_\pi = +3\%\,, \\
2.42(12) & \text{for} \quad \delta M_\pi / M_\pi = +5\%\,,
\end{cases}
\tag{8.5}
$$

and at NNLO

$$
\frac{1}{a_2} = \begin{cases}
5.49(6) & \text{for} \quad \delta M_\pi / M_\pi = -5\%\,, \\
4.95(8) & \text{for} \quad \delta M_\pi / M_\pi = -3\%\,, \\
4.35(10) & \text{for} \quad \delta M_\pi / M_\pi = 0\,, \\
3.02(4) & \text{for} \quad \delta M_\pi / M_\pi = +3\%\,, \\
1.54(4) & \text{for} \quad \delta M_\pi / M_\pi = +5\%\,,
\end{cases}
\tag{8.6}
$$

all in units of $10^{-5}\,\text{MeV}^3$. Again, we find somewhat reduced changes at NNLO compared to NLO.

8.2.3 Alpha-alpha scattering with varying α_{EM}

Here, we consider the influence of variations in the fine-structure constant on the α-α phase shifts. Despite the various sources contributing to this type of modifications as discussed in
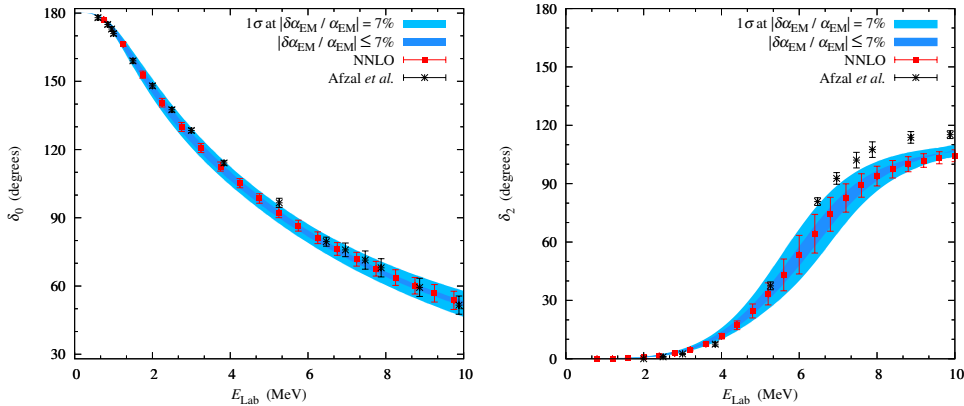
Figure 8. Dependence of the α-α phase shifts on the fine-structure constant at NNLO. Left panel: S-wave phase shift δ_0 versus the energy in the laboratory system, E_{lab}. Right panel: D-wave phase shift δ_0 versus the energy in the laboratory system, E_{lab}. The black crosses refer to the experimental data, the red squares are the results for $\delta\alpha_{\text{EM}} = 0$, the dark blue band corresponds to variations in $\alpha_{\text{EM}}/\alpha_{\text{EM}} \leq 7\%(5\%)$, for the S-(D-)wave and the light blue band represents the corresponding 1σ error.

section 4, we find that the phase shifts are little affected by variations in α_{EM}, as shown in figure 8 for the NNLO results. Here, variations of α_{EM} up to $\pm 7\%$ are displayed, where the upper (lower) part of the band refers to positive (negative) shifts in the fine-structure constant. We see that the variation in α_{EM} has essentially no effect on the phase shifts. This can be explained as follows: by far the largest EM effect is the long-range Coulomb interaction between the two clusters. Now we are measuring the phase shifts with respect to the Coulomb-modified effective range expansion (see appendix C), and thus this dominant effect is already taken care of. In contrast to the bound state energies (see section 8.2.1), the effect of the variation of the remaining, shorter-ranged EM corrections appears to be insignificant.

8.2.4   Remarks on the θ-dependence of alpha-alpha scattering

In section 5, we had shown that up to NLO, we can get the θ-dependence of the α-α scattering phase shifts directly from the θ-dependence of the pion mass. Therefore, we can directly translate the pion mass dependence of $\delta_{0,2}$ into a θ-dependence. The depicted bands of the S-wave phase shifts for $\delta M_\pi/M_\pi = -3\%$ and -5% in figure 4 correspond to a variation of $\theta = 0.7$ and 0.9, respectively. At such values of θ, the di-proton and the di-neutron are bound and element generation would proceed differently, for details see ref. [22].

We also note that a simultaneous variation of the light quark masses and θ can lead to a mutual (partial) compensation of effects, or to a mutual amplification. The latter case appears when $0 < |\theta| < \pi$ and at the same time $\delta\hat{m}/\hat{m} < 0$ as both result in a decrease of the pion mass. If one the other hand has $0 < \delta\hat{m}/\hat{m} \leq 10\%$ one can always find a value for θ such that $M_\pi(\hat{m}, \theta) = M_{\pi,\text{phys}}$ and nuclear physics would not be altered drastically (at least up to the order we are considering here).

– 21 –

9 Summary and outlook

In this work, we have considered the fundamental process of α-α scattering based on *ab initio* calculations in the framework of Nuclear Lattice Effective Field Theory, both for the physical values of the light quark mass, the fine-structure constant, and the QCD θ-angle, as well as for variations in these parameters. The main findings of this work can be summarized as follows:

- Due to improvements in the Adiabatic Projection Method compared to the pioneering study of α-α scattering in ref. [15], we obtain a very good description of the S- and D-wave phase shifts up to energies $E_{\text{lab}} \simeq 10\,\text{MeV}$ at NNLO in the chiral expansion.

- For the study of the variations under changes of the pion mass with $|\delta M_\pi/M_\pi| \le 10\%$, we rely on the pion mass dependent nuclear Hamiltonian worked out in ref. [11]. To this order, the ^{8}Be nucleus is slightly bound. In the S-wave phase shift, we find a dramatic effect (unbinding of the two-alpha system) for changes of -5% and -7% at NLO and NNLO, respectively. We have also considered the pion mass variation of the S-wave effective range function, which is less sensitive to the binding issue and shows an added repulsion for negative pion mass shifts. This additional repulsion will certainly impact the position and the lifetime of ^{8}Be. The pion mass variation on the D-wave is somewhat more pronounced, as seen by the effect on the corresponding resonance parameters and also by the D-wave effective range function.

- The dominant electromagnetic effect on the α-α scattering phase shifts is the long-ranged Coulomb potential that is included exactly by using a spherical wall with Coulomb boundary conditions. Taking this effect into account via the Coulomb-modified ERE, we find very small effects of variations of α_{EM} on the S- and D-wave phase shifts.

- We have shown that up-to-and-including NLO in the chiral expansion, the dependence of the α-α scattering phase shifts on the QCD θ-angle is entirely given by the θ-dependence of the pion mass.

In summary, we find that α-α scattering (not unexpectedly) sets weaker constraints on the variation of the light quark masses and the fine-structure constant than that given by the closeness of the 3α threshold to the Hoyle state. However, as discussed in detail e.g. in refs. [8, 11], this requires stellar modelling which introduces some model-dependence. In contrast to that, the investigation of α-α scattering discussed here is truly *ab initio* and not affected by such effects. Still, to further improve these calculations, a better determination of the pion mass dependence of the singlet and triplet NN scattering lengths from lattice QCD is mandatory.

A Details on the NN scattering parameters at varying pion mass

Here, we give some details on how we extract the values of $\bar{A}_{s,t}$ from lattice data combined with EFT methods, closely following ref. [11]. In the earlier work [10] a combination of EFT and some modelling based on resonance saturation was used to pin down the pion mass dependence of the singlet and triplet inverse scattering lengths, which unavoidably induced some uncertainty that is difficult to control. However, ref. [51] proposed to use low-energy theorems to reconstruct the energy dependence of the NN scattering amplitude in a large kinematical domain from a single observable (such as the binding energy, scattering length, effective range) at a given fixed value of the pion mass [51]. Based on this, the lattice QCD data for the deuteron, the dineutron binding energy and the ERE parameters from refs. [52–56] are used to extract the quantities $\bar{A}_s$ and $\bar{A}_t$, as these appear to be mutually consistent. To perform interpolation between these five lattice-QCD points and the experimental values of the inverse scattering lengths, a simple quadratic ansatz is used:

$$a_{s,t}^{-1}(M_\pi) = (a_{s,t}^{\mathrm{ph}})^{-1} + a(M_\pi - M_\pi^{\mathrm{ph}}) + b(M_\pi - M_\pi^{\mathrm{ph}})^2 \,. \tag{A.1}$$

The coefficients a, b are then determined from a least square fit to the available values of $a_{s,t}^{-1}$ at heavier-than-physical pion masses. This leads to the values $\bar{A}_s = 0.54$ and $\bar{A}_t = 0.33$. A cubic extrapolation yields $\bar{A}_s = 0.78$ and $\bar{A}_t = 0.49$, and we take the difference as an estimation of the uncertainty in $\bar{A}_{s,t}$. In that way, we arrive at the values given in eq. (3.18).
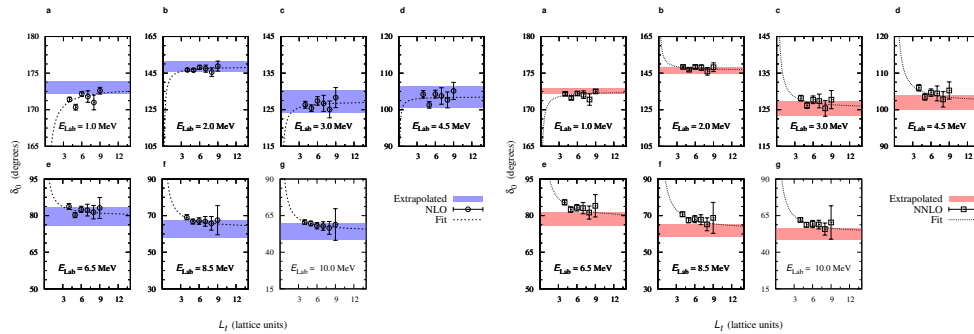
66

Figure 9. NLO (left panel) and NNLO (right panel) results for the S-wave phase shift δ_0 versus L_t for the lab energies $E_{\rm lab} = 1.0\,{\rm MeV}$, $2.0\,{\rm MeV}$, $3.0\,{\rm MeV}$, $4.5\,{\rm MeV}$, $6.5\,{\rm MeV}$, $8.5\,{\rm MeV}$ and $10.0\,{\rm MeV}$, respectively. The theoretical errors indicate the 1σ uncertainty due to the MC errors. The dotted lines are fits to the data and used to extrapolate to the $L_t \to \infty$ limit. The hatched areas represent the 1σ error of the extrapolation.
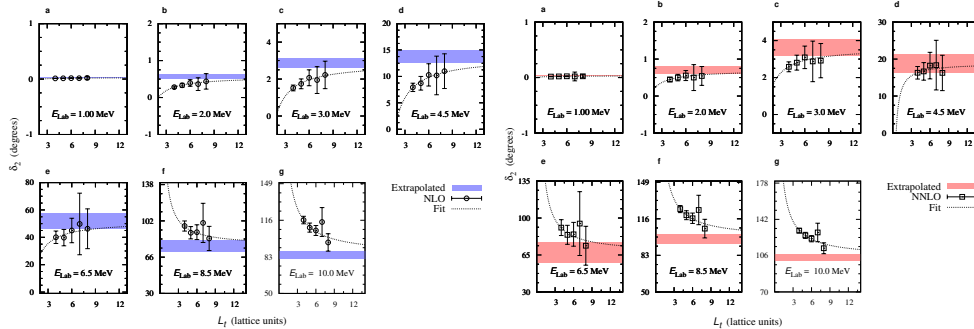

Figure 10. NLO (left panel) and NNLO (right panel) results for the D-wave phase shift δ_2 versus L_t for the lab energies $E_{\rm lab} = 1.0\,{\rm MeV}$, $2.0\,{\rm MeV}$, $3.0\,{\rm MeV}$, $4.5\,{\rm MeV}$, $6.5\,{\rm MeV}$, $8.5\,{\rm MeV}$ and $10.0\,{\rm MeV}$, respectively. The theoretical errors indicate the 1σ uncertainty due to the MC errors. The dotted lines are fits to the data and used to extrapolate to the $L_t \to \infty$ limit. The hatched areas represent the 1σ error of the extrapolation.

B   Euclidean time extrapolation

We perform the AFQMC simulations and construct the radial adiabatic transfer matrices for the S-wave and D-wave channels from $L_t = 4$ to $L_t = 10$. Based on that, we compute the pertinent phase shifts with errors calculated using a jackknife analysis of the MC data. In figures 9 and 10 we show the NLO and NNLO results for the S- and D-wave phase shifts, respectively.

The dashed lines in these figures are the exponential curves used in the extrapolation to the limit $L_t \to \infty$. This is achieved by including some residual dependence from an excited state at an energy ΔE above the ground state, utilizing the ansatz:

$$\delta_\ell(L_t, E) = \delta_\ell(E) + c_\ell(E) \exp[-\Delta E_\ell \, L_t \, a_t], \quad \ell = 0, 2, \tag{B.1}$$

where the $c_\ell(E)$ and ΔE_ℓ are fit parameters. As the gap between the α-α threshold and these excited states is rather large, one finds a fast convergence as exhibited in these figures. There, the hatched areas represent the 1σ deviation errors of the extrapolations, including the propagated MC errors of the data points.

C   The Coulomb modified ERE

Here, we collect the formulas for the Coulomb-modified ERE that was used above at NLO and NNLO. The Coulomb modified ERE takes the form [57–60]

$$K_\ell(p) = C^2_{\eta,\ell}p^{2\ell+1}\cot[\delta_\ell(p)] + \gamma h_\ell(p) = -\frac{1}{a_\ell} + \frac{1}{2}r_\ell p^2 - \frac{1}{4}P_\ell p^4 + \mathcal{O}(p^6)\,, \qquad (C.1)$$

for a partial wave with angular momentum ℓ and p is the relative momentum of the two scattering clusters. $K_\ell(p)$ is also called the effective-range function for angular momentum ℓ. The factor $C^2_{\eta,\ell}$ is defined as

$$C^2_{\eta,\ell} = \frac{2^{2\ell}}{[(2\ell+1)!]^2}C^2_{\eta,0}\prod_{s=1}^{\ell}(s^2+\eta^2)\,, \qquad (C.2)$$

where $C^2_{\eta,0}$ is the conventional Sommerfeld factor,

$$C^2_{\eta,0} = \frac{2\pi\eta}{e^{2\pi\eta}-1}\,, \qquad (C.3)$$

with $\eta = \gamma/(2p)$. Here, γ is the Coulomb parameter given by

$$\gamma = 2\mu\,\alpha_{\rm EM}\,Z_1 Z_2\,, \qquad (C.4)$$

where μ is the reduced mass of the two-alpha system and $Z_1 = Z_2 = 2$ are the charges of the two α-particles. Finally, the factor $h_\ell(p)$ in (C.1) is given by

$$h_\ell(p) = p^{2\ell}\frac{C^2_{\eta,\ell}}{C^2_{\eta,0}}\left({\rm Re}[\psi(i\eta)] - \log|\eta|\right)\,, \qquad (C.5)$$

where $\psi(z) = \Gamma'(z)/\Gamma(z)$, in which the prime denotes differentiation.

D   Bound state energies for varying pion masses

Here, we collect the derivatives of the various ground state energies and the energy of the Hoyle state with respect to the pion mass as a function of the parameters $\bar{A}_s$ and $\bar{A}_t$, using the updated values for x_1 and x_2 collected in section 3 (for details, see ref. [10]),

$$\left.\frac{\partial E_4}{\partial M_\pi}\right|_{M_\pi^{\rm ph}} = -0.339(5)\,\bar{A}_s - 0.698(4)\,\bar{A}_t + 0.042(10)\,, \qquad (D.1)$$

$$\left.\frac{\partial E_8}{\partial M_\pi}\right|_{M_\pi^{\rm ph}} = -0.796(31)\,\bar{A}_s - 1.584(22)\,\bar{A}_t + 0.098(25)\,, \qquad (D.2)$$

$$\left.\frac{\partial E_{12}}{\partial M_\pi}\right|_{M_\pi^{\rm ph}} = -1.519(27)\,\bar{A}_s - 2.884(19)\,\bar{A}_t + 0.174(46)\,, \qquad (D.3)$$

$$\left.\frac{\partial E_{12}^\star}{\partial M_\pi}\right|_{M_\pi^{\rm ph}} = -1.589(12)\,\bar{A}_s - 3.025(9)\,\bar{A}_t + 0.194(47)\,, \qquad (D.4)$$

where the error in the parenthesis is the combined statistical one from the AFQMC calculation and the systematic one due the uncertainties in x_1 and x_2.

References

[1] F. Hoyle, *On Nuclear Reactions Occuring in Very Hot Stars. 1. The Synthesis of Elements from Carbon to Nickel*, *Astrophys. J. Suppl.* **1** (1954) 121 [ɪɴSPIRE].

[2] S.A. Afzal, A.A.Z. Ahmad and S. Ali, *Systematic Survey of the α-α Interaction*, *Rev. Mod. Phys.* **41** (1969) 247 [ɪɴSPIRE].

[3] C.J. Hogan, *Why the universe is just so*, *Rev. Mod. Phys.* **72** (2000) 1149 [`astro-ph/9909295`] [ɪɴSPIRE].

[4] A.N. Schellekens, *Life at the Interface of Particle Physics and String Theory*, *Rev. Mod. Phys.* **85** (2013) 1491 [`arXiv:1306.5083`] [ɪɴSPIRE].

[5] U.-G. Meißner, *Anthropic considerations in nuclear physics*, *Sci. Bull.* **60** (2015) 43 [`arXiv:1409.2959`] [ɪɴSPIRE].

[6] J.F. Donoghue, *The Multiverse and Particle Physics*, *Ann. Rev. Nucl. Part. Sci.* **66** (2016) 1 [`arXiv:1601.05136`] [ɪɴSPIRE].

[7] F.C. Adams, *The degree of fine-tuning in our universe — and others*, *Phys. Rept.* **807** (2019) 1 [`arXiv:1902.03928`] [ɪɴSPIRE].

[8] H. Oberhummer, A. Csoto and H. Schlattl, *Stellar production rates of carbon and its abundance in the universe*, *Science* **289** (2000) 88 [`astro-ph/0007178`] [ɪɴSPIRE].

[9] E. Epelbaum, H. Krebs, T.A. Lähde, D. Lee and U.-G. Meißner, *Viability of Carbon-Based Life as a Function of the Light Quark Mass*, *Phys. Rev. Lett.* **110** (2013) 112502 [`arXiv:1212.4181`] [ɪɴSPIRE].

[10] E. Epelbaum, H. Krebs, T.A. Lähde, D. Lee and U.-G. Meißner, *Dependence of the triple-alpha process on the fundamental constants of nature*, *Eur. Phys. J. A* **49** (2013) 82 [`arXiv:1303.4856`] [ɪɴSPIRE].

[11] T.A. Lähde, U.-G. Meißner and E. Epelbaum, *An update on fine-tunings in the triple-alpha process*, *Eur. Phys. J. A* **56** (2020) 89 [`arXiv:1906.00607`] [ɪɴSPIRE].

[12] M. Pine, D. Lee and G. Rupak, *Adiabatic projection method for scattering and reactions on the lattice*, *Eur. Phys. J. A* **49** (2013) 151 [`arXiv:1309.2616`] [ɪɴSPIRE].

[13] S. Elhatisari and D. Lee, *Fermion-dimer scattering using an impurity lattice Monte Carlo approach and the adiabatic projection method*, *Phys. Rev. C* **90** (2014) 064001 [`arXiv:1407.2784`] [ɪɴSPIRE].

[14] A. Rokash, M. Pine, S. Elhatisari, D. Lee, E. Epelbaum and H. Krebs, *Scattering cluster wave functions on the lattice using the adiabatic projection method*, *Phys. Rev. C* **92** (2015) 054612 [`arXiv:1505.02967`] [ɪɴSPIRE].

[15] S. Elhatisari et al., *Ab initio alpha-alpha scattering*, *Nature* **528** (2015) 111 [`arXiv:1506.03513`] [ɪɴSPIRE].

[16] S. Elhatisari, D. Lee, U.-G. Meißner and G. Rupak, *Nucleon-deuteron scattering using the adiabatic projection method*, *Eur. Phys. J. A* **52** (2016) 174 [`arXiv:1603.02333`] [ɪɴSPIRE].

[17] K. Kravvaris, S. Quaglioni, G. Hupin and P. Navratil, *Ab initio framework for nuclear scattering and reactions induced by light projectiles*, arXiv:2012.00228 [INSPIRE].

[18] P.F. Bedaque, T. Luu and L. Platter, *Quark mass variation constraints from Big Bang nucleosynthesis*, *Phys. Rev. C* **83** (2011) 045803 [arXiv:1012.3840] [INSPIRE].

[19] J.C. Berengut et al., *Varying the light quark mass: impact on the nuclear force and Big Bang nucleosynthesis*, *Phys. Rev. D* **87** (2013) 085018 [arXiv:1301.1738] [INSPIRE].

[20] J. Dragos, T. Luu, A. Shindler, J. de Vries and A. Yousif, *Confirming the Existence of the strong CP Problem in Lattice QCD with the Gradient Flow*, *Phys. Rev. C* **103** (2021) 015202 [arXiv:1902.03254] [INSPIRE].

[21] L. Ubaldi, *Effects of theta on the deuteron binding energy and the triple-alpha process*, *Phys. Rev. D* **81** (2010) 025011 [arXiv:0811.1599] [INSPIRE].

[22] D. Lee, U.-G. Meißner, K.A. Olive, M. Shifman and T. Vonk, *θ-dependence of light nuclei and nucleosynthesis*, *Phys. Rev. Res.* **2** (2020) 033392 [arXiv:2006.12321] [INSPIRE].

[23] S. Elhatisari et al., *Nuclear binding near a quantum phase transition*, *Phys. Rev. Lett.* **117** (2016) 132501 [arXiv:1602.04539] [INSPIRE].

[24] Y. Kanada-En'yo and D. Lee, *Effective interactions between nuclear clusters*, *Phys. Rev. C* **103** (2021) 024318 [arXiv:2008.01867] [INSPIRE].

[25] A. Rokash, E. Epelbaum, H. Krebs and D. Lee, *Effective forces between quantum bound states*, *Phys. Rev. Lett.* **118** (2017) 232502 [arXiv:1612.08004] [INSPIRE].

[26] D.B. Kaplan and M.J. Savage, *The Spin flavor dependence of nuclear forces from large N QCD*, *Phys. Lett. B* **365** (1996) 244 [hep-ph/9509371] [INSPIRE].

[27] D.B. Kaplan and A.V. Manohar, *The Nucleon-nucleon potential in the $1/N_c$ expansion*, *Phys. Rev. C* **56** (1997) 76 [nucl-th/9612021] [INSPIRE].

[28] D. Lee et al., *Hidden Spin-Isospin Exchange Symmetry*, *Phys. Rev. Lett.* **127** (2021) 062501 [arXiv:2010.09420] [INSPIRE].

[29] D. Lee, *Lattice simulations for few- and many-body systems*, *Prog. Part. Nucl. Phys.* **63** (2009) 117 [arXiv:0804.3501] [INSPIRE].

[30] T.A. Lähde and U.-G. Meißner, *Nuclear Lattice Effective Field Theory: An introduction*, *Lect. Notes Phys.* **957** (2019) 1 [INSPIRE].

[31] M. Hoferichter, J. Ruiz de Elvira, B. Kubis and U.-G. Meißner, *Roy-Steiner-equation analysis of pion-nucleon scattering*, *Phys. Rept.* **625** (2016) 1 [arXiv:1510.06039] [INSPIRE].

[32] M. Hoferichter, J. Ruiz de Elvira, B. Kubis and U.-G. Meißner, *Matching pion-nucleon Roy-Steiner equations to chiral perturbation theory*, *Phys. Rev. Lett.* **115** (2015) 192301 [arXiv:1507.07552] [INSPIRE].

[33] J. Gasser and H. Leutwyler, *Chiral Perturbation Theory to One Loop*, *Annals Phys.* **158** (1984) 142 [INSPIRE].

[34] J. Ruiz de Elvira, M. Hoferichter, B. Kubis and U.-G. Meißner, *Extracting the σ-term from low-energy pion-nucleon scattering*, *J. Phys. G* **45** (2018) 024001 [arXiv:1706.01465] [INSPIRE].

[35] C.C. Chang et al., *A per-cent-level determination of the nucleon axial coupling from quantum chromodynamics*, *Nature* **558** (2018) 91 [arXiv:1805.12130] [INSPIRE].

70

[36] E. Epelbaum and U.-G. Meißner, *Isospin-violating nucleon-nucleon forces using the method of unitary transformation*, *Phys. Rev. C* **72** (2005) 044001 [`nucl-th/0502052`] [InSPIRE].

[37] R. Brower, S. Chandrasekharan, J.W. Negele and U.J. Wiese, *QCD at fixed topology*, *Phys. Lett. B* **560** (2003) 64 [`hep-lat/0302005`] [InSPIRE].

[38] A.V. Smilga, *QCD at theta similar to pi*, *Phys. Rev. D* **59** (1999) 114021 [`hep-ph/9805214`] [InSPIRE].

[39] T. Vonk, F.-K. Guo and U.-G. Meißner, *Aspects of the QCD θ-vacuum*, *JHEP* **06** (2019) 106 [*Erratum ibid.* **10** (2019) 028] [`arXiv:1905.06141`] [InSPIRE].

[40] V. Bernard, N. Kaiser and U.-G. Meißner, *Aspects of chiral pion-nucleon physics*, *Nucl. Phys. A* **615** (1997) 483 [`hep-ph/9611253`] [InSPIRE].

[41] T. Vonk, *Studies on the QCD θ-vacuum in chiral perturbation theory*, MSc Thesis, University of Bonn (2019).

[42] S. Elhatisari, *Adiabatic projection method with Euclidean time subspace projection*, *Eur. Phys. J. A* **55** (2019) 144 [`arXiv:1906.01046`] [InSPIRE].

[43] B.-N. Lu, T.A. Lähde, D. Lee and U.-G. Meißner, *Precise determination of lattice phase shifts and mixing angles*, *Phys. Lett. B* **760** (2016) 309 [`arXiv:1506.05652`] [InSPIRE].

[44] J. Carlson, V.R. Pandharipande and R.B. Wiringa, *Variational calculations of resonant states in* ^4He, *Nucl. Phys. A* **424** (1984) 47 [InSPIRE].

[45] B. Borasoy, E. Epelbaum, H. Krebs, D. Lee and U.-G. Meißner, *Two-particle scattering on the lattice: Phase shifts, spin-orbit coupling, and mixing angles*, *Eur. Phys. J. A* **34** (2007) 185 [`arXiv:0708.1780`] [InSPIRE].

[46] R. Higa, H.W. Hammer and U. van Kolck, *αα Scattering in Halo Effective Field Theory*, *Nucl. Phys. A* **809** (2008) 171 [`arXiv:0802.3426`] [InSPIRE].

[47] G. Rasche, *Effective range analysis of s- and d-wave α-α scattering*, *Nucl. Phys. A* **94** (1967) 301 [*Erratum ibid.* **119** (1968) 692] [InSPIRE].

[48] G. Hupin, S. Quaglioni and P. Navrátil, *Predictive theory for elastic scattering and recoil of protons from* ^4He, *Phys. Rev. C* **90** (2014) 061601 [`arXiv:1409.0892`] [InSPIRE].

[49] M. Livio, D. Hollowell, A. Weiss and J.W. Truran, *The anthropic significance of the existence of an excited state of* ^{12}C, *Nature* **340** (1989) 281.

[50] S. Weinberg, *Facing Up*, Harvard University Press, Cambridge, Massachusetts (2001).

[51] V. Baru, E. Epelbaum, A.A. Filin and J. Gegelia, *Low-energy theorems for nucleon-nucleon scattering at unphysical pion masses*, *Phys. Rev. C* **92** (2015) 014001 [`arXiv:1504.07852`] [InSPIRE].

[52] NPLQCD collaboration, *The Deuteron and Exotic Two-Body Bound States from Lattice QCD*, *Phys. Rev. D* **85** (2012) 054511 [`arXiv:1109.2889`] [InSPIRE].

[53] T. Yamazaki, K.-i. Ishikawa, Y. Kuramashi and A. Ukawa, *Study of quark mass dependence of binding energy for light nuclei in* $2 + 1$ *flavor lattice QCD*, *Phys. Rev. D* **92** (2015) 014501 [`arXiv:1502.04182`] [InSPIRE].

[54] K. Orginos, A. Parreno, M.J. Savage, S.R. Beane, E. Chang and W. Detmold, *Two nucleon systems at* $m_\pi \sim 450$ MeV *from lattice QCD*, *Phys. Rev. D* **92** (2015) 114512 [*Erratum ibid.* **102** (2020) 039903] [`arXiv:1508.07583`] [InSPIRE].

[55] NPLQCD collaboration, *Nucleon-Nucleon Scattering Parameters in the Limit of* SU(3) *Flavor Symmetry*, *Phys. Rev. C* **88** (2013) 024003 [`arXiv:1301.5790`] [INSPIRE].

[56] T. Yamazaki, K.-i. Ishikawa, Y. Kuramashi and A. Ukawa, *Helium nuclei, deuteron and dineutron in* $2 + 1$ *flavor lattice QCD*, *Phys. Rev. D* **86** (2012) 074514 [`arXiv:1207.4277`] [INSPIRE].

[57] H.A. Bethe, *Theory of the Effective Range in Nuclear Scattering*, *Phys. Rev.* **76** (1949) 38 [INSPIRE].

[58] J.D. Jackson and J.M. Blatt, *The Interpretation of Low Energy Proton-Proton Scattering*, *Rev. Mod. Phys.* **22** (1950) 77 [INSPIRE].

[59] H. van Haeringen and L.P. Kok, *Modified effective range function*, *Phys. Rev. A* **26** (1982) 1218 [INSPIRE].

[60] S. König, D. Lee and H.W. Hammer, *Causality constraints for charged particles*, *J. Phys. G* **40** (2013) 045106 [`arXiv:1210.8304`] [INSPIRE].

QCD θ-vacuum energy and axion properties

QCD θ-vacuum energy and axion properties

Zhen-Yan Lu,[a,b] Meng-Lin Du,[c] Feng-Kun Guo,[b,d] Ulf-G. Meißner[c,e,f]
and Thomas Vonk[c]

[a]*School of Physics and Electronic Science, Hunan University of Science and Technology,*
Xiangtan 411201, China

[b]*CAS Key Laboratory of Theoretical Physics, Institute of Theoretical Physics,*
Chinese Academy of Sciences, Beijing 100190, China

[c]*Helmholtz-Institut für Strahlen- und Kernphysik and Bethe Center for Theoretical Physics,*
Universität Bonn, D-53115 Bonn, Germany

[d]*School of Physical Sciences, University of Chinese Academy of Sciences,*
Beijing 100049, China

[e]*Institute for Advanced Simulation, Institut für Kernphysik and Jülich Center for Hadron Physics,*
Forschungszentrum Jülich, D-52425 Jülich, Germany

[f]*Tbilisi State University, 0186 Tbilisi, Georgia*

E-mail: luzhenyan@hnust.edu.cn, du@hiskp.uni-bonn.de, fkguo@itp.ac.cn,
meissner@hiskp.uni-bonn.de, vonk@hiskp.uni-bonn.de

Abstract: At low energies, the strong interaction is governed by the Goldstone bosons associated with the spontaneous chiral symmetry breaking, which can be systematically described by chiral perturbation theory. In this paper, we apply this theory to study the θ-vacuum energy density and hence the QCD axion potential up to next-to-leading order with N non-degenerate quark masses. By setting $N = 3$, we then derive the axion mass, self-coupling, topological susceptibility and the normalized fourth cumulant both analytically and numerically, taking the strong isospin breaking effects into account. In addition, the model-independent part of the axion-photon coupling, which is important for axion search experiments, is also extracted from the chiral Lagrangian supplemented with the anomalous terms up to $\mathcal{O}(p^6)$.

Contents

1 Introduction

A CP-violating topological term, i.e., the θ-term, is allowed in the Quantum Chromodynamics (QCD) Lagrangian. It can be written as

$$\mathcal{L}_\theta = \theta_0 \frac{\alpha_s}{8\pi} G^{\mu\nu,c} \tilde{G}^c_{\mu\nu}, \tag{1.1}$$

where α_s is the QCD coupling constant, $G^{\mu\nu,c}$ is the gluon field strength tensor, with c a color index, and $\tilde{G}^c_{\mu\nu} = \varepsilon_{\mu\nu\rho\sigma} G^{\rho\sigma,c}/2$ its dual. Because none of the quarks is massless, physical observables only depend on a combination of the θ_0 parameter and the phases present in the quark mass matrix $\mathcal{M}_q$, i.e., $\theta = \theta_0 + \arg \det \mathcal{M}_q$. Being a dimensionless parameter, the natural value of θ is expected to be $\mathcal{O}(1)$, which would significantly affect physical systems such as atomic nuclei, and lead to measurable effects, as nucleons, for instance, would possess a nonvanishing electric dipole moment [1]. However, the so-far negative results of experimental searches for the nucleon electric dipole moment lead to a tiny upper limit: $|\theta| \lesssim 10^{-10}$ [2–7]. To understand why the value of θ is so small is the so-called *strong CP problem*. One elegant possible solution of this problem is the Peccei-Quinn (PQ) mechanism [8, 9], which introduces a global U(1) symmetry, called PQ symmetry. This symmetry is spontaneously broken at energies much higher than the typical QCD scale of order $\mathcal{O}(1\,\text{GeV})$ and is also broken by an anomalous coupling to gluon fields. The axion appears as the corresponding Goldstone boson [10, 11] which has an anomalous coupling to $G\tilde{G}$. The parameter θ is then dynamically driven to zero at the minimum of the axion potential, giving rise to a possible solution to the strong CP problem.

In the past few decades, there have been tremendous efforts searching for the axion, denoted by a, as well as constraining to its mass m_a and decay constant f_a, see, e.g., [12–24].

Some important quantities in axion physics, such as the axion mass and self-coupling, are dictated by the axion potential. The visible axion models [10, 11] with the axion decay constant at the electroweak scale or even smaller are believed to have been ruled out by experiments. For the invisible axion [25–28], its mass window is usually assumed in the range from about 10^{-6} eV to 10^{-2} eV. According to constraints from astrophysical observations, the present bounds on the axion decay constant is 10^9 GeV $\lesssim f_a \lesssim 10^{12}$ GeV [29, 30] (we refer to refs. [24, 31–34] for several recent reviews).[1] Within the above available parameter space, the axion may be the main source of cold dark matter in the universe [36–41]. In addition, it may form a Bose-Einstein condensate [42] or even compact boson stars [43–49]. The axion can couple to the Standard Model (SM) particles like electrons, nucleons, photons and so on. However, all these couplings are suppressed by the axion decay constant f_a, which is remarkably large, resulting in the invisible axion which has very weak couplings to the SM particles [36]. Since the axion-photon coupling vertex, see eq. (4.1) below, allows for the production of an axion from the interaction of a photon with a background magnetic field, the axion-photon coupling $g_{a\gamma\gamma}$ plays a central role in axion searches in both laboratory experiments and stellar objects [24]. In this case it is very useful to study the axion properties, especially the axion-photon coupling, at a high precision from the theoretical point of view.

At low energies in QCD, all hadronic degrees of freedom are frozen and thus can be neglected except for the pseudo-Goldstone bosons of the spontaneous chiral symmetry breaking. Chiral perturbation theory (CHPT) [50–52], as the low-energy effective theory of QCD, can be used to describe the vacuum properties as well as the dynamics of QCD in the non-perturbative regime reliably. In this paper, we will calculate the θ-vacuum energy density, or equivalently the QCD axion potential, up-to-and-including next-to-leading order (NLO) in SU(N) CHPT. Setting $N = 3$, the mass and self-couplings of the axion can then be extracted from a Taylor expansion of the axion potential. In addition, we also compute the NLO corrections to the axion-photon coupling.

Before continuing, we would like to stress that a similar study was performed in ref. [53], where the QCD axion potential derived in two-flavor CHPT up to NLO (the QCD θ-vacuum energy density up to NLO was first derived in ref. [54]) is used, and a matching between two-flavor and three-flavor CHPT is performed to determine the axion-photon coupling. Here, the calculations are explicitly done in SU(N) CHPT for the θ-vacuum energy density and with $N = 3$ for the other quantities. In SU(3) CHPT, the topological susceptibility as well as the fourth cumulant of the topological distribution up to NLO have been calculated before using the Goldstone boson masses at $\theta = 0$ [55–57]. Very recently, the topological susceptibility and axion mass are calculated up to next-to-next-to-leading order and including electromagnetic corrections up to $\mathcal{O}(\alpha_{\rm em})$ in SU(2) CHPT [58]. The axion-nucleon coupling is also calculated up to the leading one-loop order in ref. [59]. Here, we derive the one-loop contribution to the SU(N) θ-vacuum energy density by a direct calculation of the logarithm of the functional determinant for the Goldstone bosons in a

---

[1]It was recently argued that there is still a possibility for a viable QCD axion model with a mass in the MeV range [35].

θ-vacuum, extending the two-flavor treatment in ref. [54] to the case of N non-degenerate flavors.[2] This study is useful when the up and down quark masses take values close to the strange quark one. This could happen in lattice QCD calculations where the quark masses are parameters that can be chosen freely.

The outline of the paper is as follows. In section 2, we generalize the calculation of the θ-vacuum energy density in the framework of SU(2) CHPT [54] to the SU(N) case with N non-degenerate quark masses. In section 3, we derive the axion properties, including the mass and self-coupling, in detail for $N = 3$. In section 4, the model-independent part of the axion-photon coupling is determined from the chiral Lagrangian supplemented with the odd-intrinsic-parity sector of the chiral effective Lagrangian. Section 5 contains a brief summary and discussion. The appendix provides a relatively detailed derivation of the recursion relation giving rise to the general solution of the vacuum angles ϕ_f.

2 θ-vacuum energy density up to NLO

The QCD axion potential as a function of a/f_a has the same form as the QCD θ-vacuum energy density as a function of θ. In this section, we compute the θ-vacuum energy density in SU(N) CHPT with N non-degenerate quark masses, which is an extension of ref. [54], where the θ-vacuum energy is computed up to NLO in the SU(2) and SU(N)-symmetric cases.

2.1 Leading order

The discovery of instantons not only solved the U(1)$_A$ problem, but also implied that there is a θ-term in the QCD Lagrangian. In order to study the physics with a θ parameter, it is common to rotate away the θ-term by performing a chiral rotation on the quark fields. At low energies, we can then match the resulting Lagrangian to the chiral Lagrangian since now the relevant degrees of freedom are the pseudo-Goldstone bosons [51, 52]. The Lagrangian density of the SU(N) CHPT at leading order (LO) in a θ-vacuum is

$$\mathcal{L}^{(2)} = \frac{F_0^2}{4} \Big[\langle D_\mu U D^\mu U^\dagger \rangle + \langle \chi_\theta U^\dagger + U \chi_\theta^\dagger \rangle \Big], \tag{2.1}$$

where $\chi_\theta = 2B_0 \mathcal{M}_q \exp[i\mathcal{X}_a \theta]$ contains the θ angle and the diagonal and real quark mass matrix is $\mathcal{M}_q = \text{diag}\{m_1, m_2, \ldots, m_N\}$, and $\langle \ldots \rangle$ denotes the trace in the flavor space. The matrix $\mathcal{X}_a$ takes the following general form:

$$\mathcal{X}_a = \text{diag}\{\mathcal{X}_1, \mathcal{X}_2, \ldots, \mathcal{X}_N\}, \quad \langle \mathcal{X}_a \rangle = 1, \tag{2.2}$$

which arises from a U(1)$_A$ chiral rotation on the quark fields eliminating the θ-term in the QCD Lagrangian. In this case, the θ-dependence is completely captured by the quark mass term. The U(1)$_A$ chiral rotation can be distributed to different quark flavors, leading to different choices of $\mathcal{X}_a$. F_0 is the pion decay constant in the three-flavor chiral limit, and $B_0 = -\langle \bar{q}q \rangle / F_0^2$ is related to the scalar quark condensate. U(x) is the field configuration for the vacuum and the Goldstone bosons of the spontaneous breaking of chiral symmetry.

---

[2]For an investigation of the axion interactions with mesons and photons using a 3-flavor chiral Lagrangian including the U(1)$_A$ anomaly, see ref. [60].

It can be written as $\mathrm{U}(x) = U_0 \tilde{U}(x)$, where $\tilde{U}(x)$ collects the Goldstone bosons, and U_0 describes the vacuum, parameterized as

$$U_0 = \mathrm{diag}\{e^{i\varphi_1}, e^{i\varphi_2}, \ldots, e^{i\varphi_N}\} \tag{2.3}$$

subject to the constraint $\sum_{i=1}^{N} \varphi_i = 0$ [55, 61]. For the SU(3) case, $\tilde{U} = e^{i\Phi/F_0}$, with Φ given by

$$\Phi = \begin{pmatrix} \pi_3 + \frac{1}{\sqrt{3}}\eta_8 & \sqrt{2}\pi^+ & \sqrt{2}K^+ \\ \sqrt{2}\pi^- & -\pi_3 + \frac{1}{\sqrt{3}}\eta_8 & \sqrt{2}K^0 \\ \sqrt{2}K^- & \sqrt{2}\bar{K}^0 & -\frac{2}{\sqrt{3}}\eta_8 \end{pmatrix}. \tag{2.4}$$

Note that the neutral flavor eigenstates in the octet of the pseudoscalar mesons as shown above, i.e. π_3 and η_8, are not mass eigenstates. Diagonalizing the mass matrix of the meson fields, one gets the physical mass eigenstates π^0 and η, which are mixtures of π_3 and η_8. By expanding the LO Lagrangian in terms of the meson fields to quadratic order, the LO θ-dependent meson masses including isospin breaking effects are obtained as

$$
\begin{aligned}
\mathring{M}^2_{\pi^\pm} &= B_0(m_1 \cos\phi_1 + m_2 \cos\phi_2), \\
\mathring{M}^2_{K^\pm} &= B_0(m_1 \cos\phi_1 + m_3 \cos\phi_3), \\
\mathring{M}^2_{K^0} &= \mathring{M}^2_{\bar{K}^0} = B_0(m_2 \cos\phi_2 + m_3 \cos\phi_3), \\
\mathring{M}^2_{\pi^0} &= B_0(m_1 \cos\phi_1 + m_2 \cos\phi_2) - \xi, \\
\mathring{M}^2_{\eta} &= \frac{1}{3}B_0\left(m_1 \cos\phi_1 + m_2 \cos\phi_2 + 4m_3 \cos\phi_3\right) + \xi,
\end{aligned} \tag{2.5}
$$

where for convenience we have defined $(m_1, m_2, m_3) \equiv (m_u, m_d, m_s)$ and

$$\phi_f \equiv \mathcal{X}_f \theta - \varphi_f. \tag{2.6}$$

The parameter ξ is given by

$$\xi = \frac{4}{3}B_0\left(m_3 \cos\phi_3 - \frac{1}{2}(m_1 \cos\phi_1 + m_2 \cos\phi_2)\right)\frac{\sin^2\epsilon_\theta}{\cos(2\epsilon_\theta)} = \mathcal{O}\left(\epsilon_\theta^2\right), \tag{2.7}$$

with ϵ_θ the π^0-η mixing angle in the θ-vacuum, which arises due to strong isospin breaking. Diagonalization of the mass matrix requires

$$\tan 2\epsilon_\theta = \frac{\sqrt{3}(m_2 \cos\phi_2 - m_1 \cos\phi_1)}{2m_3 \cos\phi_3 - m_1 \cos\phi_1 - m_2 \cos\phi_2}. \tag{2.8}$$

Obviously, the above θ-dependent Goldstone boson masses reduce to the standard SU(3) relations [52] by taking the limit $\theta = 0$ and setting $\phi_f = 0$. The dependence of ϕ_f on the θ angle needs to be determined by minimizing the vacuum energy to be discussed below.

To determine the ground state, i.e. the vacuum, we set $\tilde{U} = \mathbb{1}$. Performing the trace in eq. (2.1), one obtains the LO potential energy density

$$e^{(2)}_{\mathrm{vac}} = -F_0^2 B_0 \sum_f m_f \cos\phi_f. \tag{2.9}$$

Moreover, minimizing eq. (2.9) with respect to the parameters ϕ_f with the constraint $\sum_f \phi_f = \theta$ gives the following equations[3]

$$\begin{cases} m_1 \sin \phi_1 = m_2 \sin \phi_2 = m_3 \sin \phi_3, \\ \sum_f \phi_f = \theta, \end{cases} \tag{2.10}$$

for SU(3), and similar equations for SU(N), i.e., $m_f \sin \phi_f$ is the same for all flavors. The above equations depend only on the linear combination ϕ_f given in eq. (2.6), instead of on $\mathcal{X}_f$ and φ_f separately. This implies that ϕ_f is physical while $\mathcal{X}_f$ and φ_f are not. One can use this freedom to choose the "gauge" most convenient for the question of interest. One possible choice is to choose $\mathcal{X}_a = \mathbb{1}/N$, which is commonly used in the literature (see, e.g., refs. [54, 55, 61–63]). Noticing that the only constraint on $\mathcal{X}_a$ is $\langle \mathcal{X}_a \rangle = 1$, one may also choose the U(1)$_A$ rotations to be

$$\mathcal{X}_f = \frac{\phi_f}{\theta}, \quad \text{and} \quad \varphi_f = 0 \tag{2.11}$$

to simultaneously shift the θ angle to the quark mass matrix phase and align the vacuum properly. This is a convenient choice for the $a\gamma\gamma$ coupling (with θ changed to the dynamical axion field a/f_a) to be discussed in section 4 since this removes the leading order a-π^0 and a-η mixing.

The equations (2.10) do not admit an analytical solution in terms of elementary functions in a compact form.[4] In the isospin symmetric case, the up and down quark masses are degenerate $m_1 = m_2 \equiv m$ but $m \neq m_3$, we have $\phi_1 = \phi_2 \equiv \phi$, and then eq. (2.10) becomes [64]

$$m \sin \phi = m_3 \sin(\theta - 2\phi), \tag{2.12}$$

which allows for analytic solutions, though complicated ones.

If one focuses on the cumulants of the QCD topological distribution, which are derivatives of the vacuum energy density, $e_{\text{vac}}(\theta)$, with respect to θ,

$$c_{2n} = \frac{d^{2n} e_{\text{vac}}(\theta)}{d\theta^{2n}} \bigg|_{\theta=0}, \quad n \in \mathbb{N}, \tag{2.13}$$

one may solve eqs. (2.10) by expanding in powers of θ. Specifically, c_2 corresponds to the topological susceptibility. Up to $\mathcal{O}\left(\theta^3\right)$, one gets [55]

$$\phi_f = \frac{\bar{m}}{m_f}\theta + \left[\left(\frac{\bar{m}}{m_f}\right)^3 - \frac{\bar{m}^4}{m_f \bar{m}^{[3]}} \right] \frac{\theta^3}{6} + \mathcal{O}(\theta^5), \tag{2.14}$$

where we have introduced

$$\frac{1}{\bar{m}} = \sum_i \frac{1}{m_i}, \quad \frac{1}{\bar{m}^{[3]}} = \sum_i \frac{1}{m_i^3} \tag{2.15}$$

---

[3]For the vacuum alignment in SU(2) CHPT up to NLO, we refer to the appendix of ref. [62], which also shows that it is sufficient to consider the LO vacuum alignment for the computation of the cumulants up to $\mathcal{O}\left(p^4\right)$.

[4]In the SU(2) case, there is an analytic solution [61], which then allows to derive a closed form of the vacuum energy density up to NLO in the chiral expansion [54].

with i running over all the flavor indices considered in the theory. The solutions in eq. (2.14) are not restricted to the three-flavor case but also valid for $N > 3$. Consequently, the θ-dependence of the vacuum energy density at LO can be obtained by substituting the solution in eq. (2.14) into eq. (2.9), which gives [55]

$$e_{\mathrm{vac}}^{(2)}(\theta) = F_0^2 B_0 \left(\frac{1}{2}\bar{m}\theta^2 - \frac{\bar{m}^4}{24\bar{m}^{[3]}}\theta^4 \right) + \mathcal{O}(\theta^6). \tag{2.16}$$

In appendix A, we work out a recursion relation for ϕ_f up to an arbitrary power of θ,

$$\phi_f = \sum_{n=0}^{\infty} C_{f,2n+1}\theta^{2n+1}, \tag{2.17}$$

with $C_{f,1} = \bar{m}/m_f$ and

$$C_{f,2n+1} = \sum_{t=1}^{n} \sum_{(k_1,\ldots,k_t)} s_{K_t} \binom{K_t}{k_1,\ldots,k_t} \left[\frac{\bar{m}}{m_f} \sum_{i=1}^{N} \prod_{j=1}^{t} C_{i,2j-1}^{k_j} - \prod_{j=1}^{t} C_{f,2j-1}^{k_j} \right], \tag{2.18}$$

where k_j are non-negative integers, $K_t \equiv \sum_{j=1}^{t} k_j$, $\sum_{(k_1,\ldots,k_t)}$ means that the sum runs over all possibilities of k_j satisfying $k_1 + \cdots + (2t-1)k_t = 2n+1$, $s_{K_t} = (-1)^{(K_t-1)/2}/(K_t!)$, and $\binom{K_t}{k_1,\ldots,k_t} = K_t!/(k_1!\cdots k_t!)$ are the multinomial coefficients.

In the next subsection, we will compute the one-loop contribution of the Goldstone bosons to the energy density.

2.2 Next-to-leading order

To study the θ-vacuum energy up to the NLO, $\mathcal{O}(p^4)$, one has to include both the tree-level diagrams from $\mathcal{L}^{(4)}$ and the one-loop diagrams with innsertions from $\mathcal{L}^{(2)}$. The SU(N) chiral Lagrangian at NLO is given by

$$\mathcal{L}^{(4)} = L_6 \langle \chi_\theta U^\dagger + U\chi_\theta^\dagger \rangle^2 + L_7 \langle \chi_\theta U^\dagger - U\chi_\theta^\dagger \rangle^2 + L_8 \langle \chi_\theta^\dagger U\chi_\theta^\dagger U + U^\dagger \chi_\theta U^\dagger \chi_\theta \rangle + H_2 \langle \chi_\theta^\dagger \chi_\theta \rangle, \tag{2.19}$$

where we only display the terms relevant for the vacuum energy. The L_i and H_2 are the so-called low-energy constants (LECs) and the high-energy constant (HEC), respectively. The latter is only required for renormalization and does not appear in observables. After setting $U = U_0$ and evaluating the traces, one gets the tree-level contribution to the NLO vacuum energy density

$$e_{\mathrm{vac}}^{(4,\mathrm{tree})} = -16B_0^2 \left[L_6 \left(\sum_i m_i \cos\phi_i \right)^2 - L_7 \left(\sum_i m_i \sin\phi_i \right)^2 + \frac{L_8}{2}\sum_i m_i^2 \cos(2\phi_i) + \frac{H_2}{4}\sum_i m_i^2 \right]. \tag{2.20}$$

The LECs and HEC contain both ultraviolet (UV) finite and divergent parts. They are related to the renormalized ones, denoted by an upper index r, by [52, 65]

$$L_6 = L_6^r + \frac{N^2+2}{16N^2}\lambda, \quad L_8 = L_8^r + \frac{N^2-4}{16N}\lambda, \quad L_7 = L_7^r, \quad H_2 = H_2^r + \frac{N^2-4}{8N}\lambda, \tag{2.21}$$

with

$$\lambda = \frac{\mu^{d-4}}{16\pi^2} \left\{ \frac{1}{d-4} - \frac{1}{2} \left[\ln(4\pi) + \Gamma'(1) + 1 \right] \right\} \tag{2.22}$$

the UV divergence at the space-time dimension $d = 4$, where μ is the scale of dimensional regularization. The UV divergence in the NLO tree-level contribution exactly cancels the one arising in the one-loop contribution, as will be seen below.

Now let us calculate the one-loop contribution to the θ-vacuum energy density. In the classical CHPT papers [51, 52], the one-loop effective generating functional is expanded around the free-field configuration at $\theta = 0$. This treatment is then applied to derive the topological susceptibility and the fourth cumulant in SU(N) CHPT in refs. [55, 56, 63]. The expression for the vacuum energy density at NLO in SU(2) with non-degenerate quark masses, as well as that in SU(N) with degenerate quark masses, is derived in ref. [54], where the generating functional is expanded around the free-field configuration in the θ-vacuum. The result allows for an evaluation of any cumulant of the QCD topological charge distribution, and is the QCD axion potential at NLO [53]. Here, we generalize the result in ref. [54] to SU(N), with N non-degenerate quark masses. The effective action for the free-field configuration in the θ-vacuum is

$$Z_0(\theta) = \frac{i}{2} \ln \det D_0(\theta) = \frac{i}{2} \text{Tr} \ln D_0(\theta), \tag{2.23}$$

where "Tr" denotes traces over both the flavor (in the adjoint representation) and the coordinate spaces, and the differential operator $D_0(\theta)$ takes the following form

$$D_{0,PY}(\theta) = \delta_{PY} \left[\partial^\mu \partial_\mu + \mathring{M}_P^2(\theta) \right], \tag{2.24}$$

where $P, Y = 1, \ldots, N^2 - 1$ are the flavor indices of the Goldstone bosons, and $\mathring{M}_P(\theta)$ are θ-dependent meson masses at LO given in eq. (2.5). Within dimensional regularization, one gets the one-loop contribution to the vacuum energy density as [54]

$$\begin{aligned}
e_{\text{vac}}^{(4,\text{loop})} &= -\frac{Z_0(\theta)}{V} \\
&= -\frac{i}{2} \sum_P \int \frac{d^d p}{(2\pi)^d} \ln \left[-p^2 + \mathring{M}_P^2(\theta) \right] \\
&= \sum_P \mathring{M}_P^4(\theta) \left\{ \frac{\lambda}{2} - \frac{1}{128\pi^2} \left[1 - 2 \ln \frac{\mathring{M}_P^2(\theta)}{\mu^2} \right] \right\},
\end{aligned} \tag{2.25}$$

where V is the space-time volume, the P runs over the Goldstone boson mass eigenstates (for the SU(3) case, they are given in eq. (2.5)), and the term proportional to λ collects all the UV divergences in the one-loop contribution.

Noticing that the matrix elements of the diagonalized mass-squared matrix of the Goldstone bosons are given by

$$\delta_{PY} \mathring{M}_P^2(\theta) = \frac{1}{8} \left\langle \left\{ \lambda_P, \lambda_Y^\dagger \right\} \left(\chi_\theta^\dagger U_0 + U_0^\dagger \chi_\theta \right) \right\rangle \equiv \sigma_{PY}, \tag{2.26}$$

we obtain

$$\sum_P \mathring{M}_P^2(\theta) = \sum_P \sigma_{PP} = \frac{2(N^2-1)}{N}\sum_i m_i \cos\phi_i. \tag{2.27}$$

Similarly, we have

$$\sum_P \mathring{M}_P^4(\theta) = \sum_{P,Y}\sigma_{PY}\sigma_{YP}$$

$$= 2B_0^2\left[\frac{N^2+2}{N^2}\left(\sum_i m_i\cos\phi_i\right)^2 + \frac{N^2-4}{N}\sum_i(m_i\cos\phi_i)^2\right]. \tag{2.28}$$

With eqs. (2.20), (2.21), (2.25) and (2.28), it is straightforward to check that the UV divergence in the one-loop contribution exactly cancels that in the tree-level contribution. Finally, we obtain the θ-vacuum energy density up to NLO as

$$e_{\text{vac}} = -F_0^2 B_0\sum_i m_i\cos\phi_i - \sum_P \frac{\mathring{M}_P^4(\theta)}{128\pi^2}\left[1 - 2\ln\frac{\mathring{M}_P^2(\theta)}{\mu^2}\right]$$

$$- 16B_0^2\left[L_6^r\left(\sum_i m_i\cos\phi_i\right)^2 + N\left(NL_7^r + L_8^r\right)m_1^2\cos^2\phi_1\right], \tag{2.29}$$

where we have used the SU(N) version of eq. (2.10) to replace all $m_i\sin\phi_i$ by $m_1\sin\phi_1$, and have neglected the θ-independent terms.

From the above θ-vacuum energy density, the lowest two cumulants of the topological charge distribution up to NLO can then be easily extracted. It can be checked from eq. (2.29) that we can reproduce the expression of topological susceptibility at NLO keeping all orders in strong isospin breaking exactly given in ref. [66]. We are more interested in the axion mass and its self-coupling, and thus we will extract them from the axion potential based on the relation between the θ-vacuum energy and axion potential in the following section. Numerical values of the topological susceptibility and the normalized fourth cumulant will also be given for reference.

3 Axion mass and self-coupling

Both the axion mass and self-coupling are important quantities, since they directly affect experimental searches for the axion. For example, one tries to detect the axion in microwave cavities by stimulating their conversion to photons via the Primakoff effect within an external magnetic field [24]. The axion self-coupling plays an important role in the formation of an axion Bose-Einstein condensation [42] as well as possible boson stars [43–45, 47, 67]. This motivates the study of these two quantities in this section to high precision. Before we proceed to derive the axion mass and self-coupling up to NLO, let us discuss a little bit about the axion solution to the strong CP problem, and start with the effective Lagrangian,

$$\mathcal{L}_{G\tilde{G}} = \left(\theta + \frac{a}{f_a}\right)\frac{g_s^2}{32\pi^2}G_{\mu\nu}^c\tilde{G}^{c,\mu\nu}, \tag{3.1}$$

where in addition to the θ-term, a pseudoscalar axion field is introduced which couples to gluons. As shown by Peccei and Quinn [8, 9], the periodicity of the vacuum expectation value (VEV) $\langle G\tilde{G}\rangle$ in $\theta + a/f_a$ forces the minimum of the axion VEV to be at $\theta + \langle a\rangle/f_a = 0$, and thus the θ-dependence is eliminated. Expanding the axion field around its VEV, one sees that the θ-vacuum energy density derived in the previous section, with θ being replaced by $a_{\rm phys}/f_a$, gives the axion potential, where $a_{\rm phys} = a - \langle a\rangle$ is the physical axion field. In the following we will denote $a_{\rm phys}$ as a for simplicity, and then the axion potential is given by $V(a) = e_{\rm vac}(a/f_a)$.

Expanding $V(a)$ in powers of the axion field around the vacuum, we obtain

$$V(a) = \frac{1}{2}m_a^2 a^2 + \sum_{n=2}^{\infty} \frac{1}{(2n)!}\lambda_{2n}a^{2n}. \tag{3.2}$$

Comparing the above equation with the definition of cumulants of the QCD topological distribution in eq. (2.13), one finds the following relations for the axion mass and axion self couplings:

$$m_a^2 = \frac{c_2}{f_a^2}, \quad \lambda_{2n} = \frac{c_{2n}}{f_a^{2n}}, \tag{3.3}$$

where c_{2n} are the cumulants defined in eq. (2.13) with $n \geq 2$. Thus, the axion mass and four-axion self-coupling at LO are given by

$$m_{a,\rm LO}^2 = \frac{F_\pi^2 M_{\pi^+}^2 \bar{m}}{2f_a^2 \hat{m}}, \quad \lambda_{4,\rm LO} = -\frac{F_\pi^2 M_{\pi^+}^2 \bar{m}^4}{2f_a^4 \bar{m}^{[3]}\hat{m}}, \tag{3.4}$$

respectively, where $\hat{m} = (m_u + m_d)/2$, and we have replaced B_0 and F_0 by $M_{\pi^+}^2/(2\hat{m})$ and F_π, the physical pion mass squared and decay constant, respectively, which is legitimate at LO. One sees that at LO, the difference between the SU(3) and SU(2) expressions resides merely in the definitions of $\bar{m}$ and $\bar{m}^{[3]}$ in eq. (2.15).

In the same way we have calculated the axion mass and self-couplings at LO. Their expressions at NLO, including the higher order corrections, can be extracted from eq. (2.29). The former reads

$$m_a^2 = \frac{F_\pi^2 M_{\pi^+}^2 \bar{m}}{2f_a^2 \hat{m}}\left\{1 + \frac{16M_{\pi^+}^2}{F_\pi^2}\left[\frac{3\bar{m}}{\hat{m}}\left(3L_7^r + L_8^r\right) - L_8^r\right]\right.$$
$$\left. + \frac{\bar{m}}{m_s}\left(\mu_{\pi^0} + 2\mu_{\pi^+} - \mu_\eta\right) + \left(2\frac{\bar{m}}{m_d} - 1\right)\mu_{K^+} + \left(2\frac{\bar{m}}{m_u} - 1\right)\mu_{K^0} + \mathcal{O}\left(\frac{\delta^2}{m_s^2}\right)\right\}, \tag{3.5}$$

with $\mu_P = \frac{M_P^2}{32\pi^2 F_\pi^2}\ln\frac{M_P^2}{\mu^2}$ and $\delta = m_d - m_u$, where we have used the NLO expressions for the pion mass and decay constant [52]:

$$M_{\pi^+}^2 = B_0(m_u + m_d)\left\{1 + \mu_{\pi^0} - \frac{1}{3}\mu_\eta + \frac{16B_0}{F_0^2}\left[\hat{m}\left(2L_8^r - L_5^r\right) + \left(2\hat{m} + m_s\right)\left(2L_6^r - L_4^r\right)\right]\right\},$$
$$F_\pi = F_0\left\{1 - \mu_{\pi^+} - \mu_{\pi^0} - \frac{\mu_{K^+}}{2} - \frac{\mu_{K^0}}{2} + \frac{8B_0}{F_0^2}\left[\hat{m}L_5^r + \left(2\hat{m} + m_s\right)L_4^r\right]\right\}. \tag{3.6}$$

– 9 –

Similarly the self-coupling up to NLO can be easily obtained as

$$
\begin{aligned}
\lambda_4 = &-\frac{F_\pi^2 M_{\pi^+}^2 \bar{m}^4}{2 f_a^4 \hat{m} \bar{m}^{[3]}} \left\{ 1 + \frac{16 M_{\pi^+}^2}{F_\pi^2} \left[\frac{3 \bar{m}^{[3]}}{\hat{m} \bar{m}^2} L_6^r + 36 \frac{\bar{m}}{\hat{m}} L_7^r + \left(12 \frac{\bar{m}}{\hat{m}} - 1 \right) L_8^r \right] \right. \\
&+ \left[\frac{3 \bar{m}^{[3]}}{m_u^3} \left(1 - \frac{m_u}{m_d} \right)^2 \left(1 + \frac{m_u}{m_d} \right) + \frac{4 \bar{m}}{m_s} - 3 \right] (\mu_{\pi^0} + 2 \mu_{\pi^+}) \\
&+ \left[\frac{6 \bar{m}^{[3]}}{m_s^3} \left(1 - \frac{m_s}{m_d} \right)^2 \left(1 + \frac{m_s}{m_d} \right) + \frac{8 \bar{m}}{m_u} - 7 \right] \mu_{K^0} \\
&+ \left[\frac{6 \bar{m}^{[3]}}{m_s^3} \left(1 - \frac{m_s}{m_u} \right)^2 \left(1 + \frac{m_s}{m_u} \right) + \frac{8 \bar{m}}{m_d} - 7 \right] \mu_{K^+} \\
&+ \left. \left[\frac{3 \bar{m}^{[3]}}{m_s^3} - \frac{4 \bar{m}}{m_s} - \frac{\bar{m}^{[3]} (m_s + 3 \bar{m})^2}{m_s^2 \bar{m}^2 (m_u + m_d + 4 m_s)} \right] \mu_\eta + \mathcal{O}\left(\frac{\delta^2}{m_s^2} \right) \right\} \\
&+ \frac{3 \bar{m}^4}{32 \pi^2 f_a^4} \left[\frac{3 M_{\pi^+}^4}{m_u^2 m_d^2} + \frac{2 M_{K^+}^4}{m_u^2 m_s^2} + \frac{2 M_{K^0}^4}{m_d^2 m_s^2} + \frac{\left(2 m_u M_{K^0}^2 + 2 m_d M_{K^+}^2 - m_s M_{\pi^+}^2 \right)^2}{9 m_u^2 m_d^2 m_s^2} \right]. \quad (3.7)
\end{aligned}
$$

The numerical evaluation requires the values of the quark mass ratios and of the LECs, which have been determined by the lattice QCD calculations and experimental data. A review of the present knowledge of the LECs appearing in the chiral Lagrangian for the meson sector can be found in ref. [68]. Using the input values listed in table 1, we find the axion mass and the quartic axion self-coupling at NLO to be

$$
m_a = 5.89(10) \mu\text{eV} \cdot \frac{10^{12} \text{ GeV}}{f_a}, \quad (3.8)
$$

$$
\lambda_4 = -\left(5.86(19) \cdot \frac{10^{-2} \text{ GeV}}{f_a} \right)^4, \quad (3.9)
$$

respectively. Here we have used the charged pion mass in eq. (3.6) for eliminating the overall $B_0(m_u + m_d)$ factor in m_a^2 and λ_4. Although the difference between the charged and neutral pions from QCD is of $\mathcal{O}\left(\delta^2 \right)$, the charged pion receives an electromagnetic contribution at LO. Such an effect to the quantities of interest here can be eliminated if using the neutral pion mass instead, which amounts to replacing $M_{\pi^+}^2$ by $M_{\pi^0}^2$ in eqs. (3.5) and (3.7) and adding the following terms inside the curly brackets of these two expressions [52]:

$$
\frac{\left(M_{K^+}^2 - M_{K^0}^2 \right)_{\text{QCD}}^2}{3 M_{\pi^0}^2 \left(M_\eta^2 - M_{\pi^0}^2 \right)} \left[1 + \frac{8}{3} \Delta_{\text{GMO}} + \frac{M_{K^0}^2}{8 \pi^2 F_\pi^2} \left(1 + 6 \ln \frac{M_{K^0}^2}{M_\eta^2} \right) + \mathcal{O}\left(\hat{m}, m_s \right) \right], \quad (3.10)
$$

with

$$
\left(M_{K^+}^2 - M_{K^0}^2 \right)_{\text{QCD}} = M_{K^0}^2 - M_{K^+}^2 - M_{\pi^0}^2 + M_{\pi^+}^2,
$$

$$
\Delta_{\text{GMO}} = \frac{2 M_{K^0}^2 + 2 M_{K^+}^2 - 2 M_{\pi^+}^2 + M_{\pi^0}^2 - 3 M_\eta^2}{M_\eta^2 - M_{\pi^0}^2}, \quad (3.11)
$$

z	r	M_{π^+}	M_{π^0}	M_{K^+}	M_{K^0}	M_η
0.485(19)	27.42(12)	139.57	134.98	493.68(2)	497.61(1)	547.86(2)
F_π	L_6^r	L_7^r	L_8^r	C_7^W	C_8^W	
92.28(9)	0.0(4)	$-0.3(2)$	0.5(2)	≈ 0	0.60 ± 0.20	

Table 1. Numerical inputs used in this paper. The pion decay constant F_π, and experimental meson masses M_P are in units of MeV, and are taken from ref. [33]. The renormalized LECs L_i^r are in units of 10^{-3}; they correspond to values at scale $\mu = 770$ MeV and are taken from ref. [68]. The NNLO anomalous LECs C_7^W and C_8^W are given in units of 10^{-3} GeV^{-2}; for their determinations, see the text. For the quark mass ratios defined as $z = m_u/m_d$ and $r = m_s/\hat{m}$, we take the FLAG average of the $N_f = 2+1$ lattice results [70].

where the electromagnetic effects have been taken into account. As a result, the values in eqs. (3.8) and (3.9) become

$$m_a = 5.71(9)\mu\text{eV} \cdot \frac{10^{12} \text{ GeV}}{f_a}, \tag{3.12}$$

$$\lambda_4 = -\left(5.77(18) \cdot \frac{10^{-2} \text{ GeV}}{f_a}\right)^4, \tag{3.13}$$

which are regarded as our results for these quantities and will be used in the following.

As we mentioned earlier, both the axion mass and its self-coupling are tightly related to the cumulants of the QCD topological charge distribution through the θ-vacuum energy density, see eq. (3.3). Thus, from eq. (2.13) or (3.3) we can further extract the numerical values of the topological susceptibility χ_t and the normalized fourth cumulant $b_2 = c_4/(12\chi_t)$ [56] with the inclusion of isospin breaking effects at zero temperature, i.e.,

$$\chi_t^{1/4} = \sqrt{m_a f_a} = 75.6(6) \text{ MeV}, \tag{3.14}$$

$$b_2 = \frac{\lambda_4 f_a^2}{12 m_a^2} = -0.028(3). \tag{3.15}$$

Since the masses of the octet of pseudoscalar mesons are well-known from experiments, the uncertainties are in fact dominated by the renormalized LEC L_7^r, while the subdominant uncertainties are from the quark mass ratio $z = m_u/m_d$ and the LECs L_6^r and L_8^r. In comparison, the values of these quantities obtained here remain almost the same as the one in SU(2) case numerically, which are $\chi_t^{1/4} = 75.5(5)$ MeV and $b_2 = -0.029(2)$ [53]. And the result for the topological susceptibility is in perfect agreement with recent $N_f = 2+1+1$ lattice QCD simulation at the physical point giving $\chi_t^{1/4} = 75.6(1.8)(0.9)$ MeV [69]. This indicates that the explicit inclusion of the strange quark degree of freedom does not induce large differences on the axion properties. There are at least two compelling reasons accounting for this feature. First, the effects from the heavier quark flavors have been largely included in the corresponding SU(2) LECs. Second, in ref. [53] the authors performed their numerical calculations with a matching between two-flavor and three-flavor CHPT LECs. Thus, the inclusion of the strange-quark degree of freedom does not change the results

sizeably. Yet, the expressions given here should be useful for chiral extrapolation of lattice results performed at unphysical quark masses, in particular when the up and down quark masses are close to the strange quark one.

4 Axion-photon coupling

The axion-photon coupling is defined by the following Lagrangian (see, e.g., refs. [53,71,72]),

$$\mathcal{L}_{a\gamma\gamma} = \frac{1}{4}g_{a\gamma\gamma}aF^{\mu\nu}\tilde{F}_{\mu\nu}, \tag{4.1}$$

where $\tilde{F}_{\mu\nu} = \frac{1}{2}\varepsilon_{\mu\nu\rho\sigma}F^{\rho\sigma}$, with $F^{\mu\nu}$ the electromagnetic field tensor with the sign convention $\epsilon_{0123} = +1$. Specifically, the axion-photon coupling is given by

$$g_{a\gamma\gamma} = \frac{\alpha_{\text{em}}}{2\pi f_a}\frac{\mathcal{E}}{\mathcal{C}} + g_{a\gamma\gamma}^{\text{QCD}},$$

$$g_{a\gamma\gamma}^{\text{QCD}} = -\frac{\alpha_{\text{em}}}{2\pi f_a}6\langle\mathcal{X}_a Q^2\rangle + g_{a\gamma\gamma}^{\text{mix}} = -\frac{\alpha_{\text{em}}}{2\pi f_a}\left(\frac{2}{3} + 2\mathcal{X}_u\right) + g_{a\gamma\gamma}^{\text{mix}}, \tag{4.2}$$

where $\mathcal{E}/\mathcal{C}$ is the ratio of the electromagnetic and color anomaly coefficients, which is given by $\sum_n(Q_{\text{PQ}}Q^2)/\sum_n(Q_{\text{PQ}}T^2)$, with the sums running over all fermions with PQ charges Q_{PQ}, and T^a the QCD color generators satisfying $\langle T^a T^b\rangle = T^2\delta^{ab}/2$. The value of $\mathcal{E}/\mathcal{C}$ depends on the specific axion models. The first term in $g_{a\gamma\gamma}^{\text{QCD}}$ is the contribution from the axial rotation of the quark fields, $q \to \exp\left(i\frac{a}{2f_a}\mathcal{X}_a\gamma_5\right)q$ with $\langle\mathcal{X}_a\rangle = 1$ (here we use the convention $\gamma^5 = i\gamma^0\gamma^1\gamma^2\gamma^3$), which was introduced to eliminate the term $\frac{a}{f_a}\frac{\alpha_s}{8\pi}G_{\mu\nu}^c\tilde{G}^{c,\mu\nu}$ from the axion Lagrangian. The second term in $g_{a\gamma\gamma}^{\text{QCD}}$, $g_{a\gamma\gamma}^{\text{mix}}$, is the contribution from the a-π^0 and a-η mixings, with the π^0 and η coupled to two photons.

As discussed below eq. (2.10), there is a freedom of choosing the diagonal matrix $\mathcal{X}_a$ satisfying $\langle\mathcal{X}_a\rangle = 1$. If it is chosen as $\mathcal{X}_a = \text{diag}\{\bar{m}/m_u, \bar{m}/m_d, \bar{m}/m_s\} = \bar{m}\mathcal{M}_q^{-1}$ as in refs. [29, 73], then $U = \tilde{U} = e^{i\Phi/F_0}$, see eq. (2.11), and there is no a-π^0 or a-η mixing term in the LO chiral Lagrangian. One obtains the $\mathcal{O}\left(p^4\right)$ contribution to the model-independent $a\gamma\gamma$ coupling to be

$$g_{a\gamma\gamma}^{\text{QCD},(4)} = -\frac{\alpha_{\text{em}}}{2\pi f_a}\frac{2\left(m_u + 3\bar{m}\right)}{3m_u}. \tag{4.3}$$

This result recovers the one derived in SU(2) CHPT [53] at $\mathcal{O}(p^4)$ in the limit of $m_s \to \infty$.

The same result can also be obtained by using other choices of $\mathcal{X}_a$. In that case, one needs to consider a-meson mixing. The Wess-Zumino-Witten (WZW) Lagrangian [74, 75] with an external photon field can be used to get the mixing contribution. The Lagrangian is given by [76–78]

$$\mathcal{L}_{\text{WZW}}^{\text{em}} = -\frac{eN_c}{48\pi^2}\varepsilon^{\mu\nu\rho\sigma}A_\mu\left\langle Q\partial_\nu UU^\dagger\partial_\rho UU^\dagger\partial_\sigma UU^\dagger + QU^\dagger\partial_\nu UU^\dagger\partial_\rho UU^\dagger\partial_\sigma U\right\rangle$$
$$+i\frac{e^2N_c}{48\pi^2}\varepsilon^{\mu\nu\rho\sigma}\partial_\nu A_\rho A_\sigma\left\langle 2Q^2(U\partial_\mu U^\dagger - U^\dagger\partial_\mu U) - QU^\dagger Q\partial_\mu U + QUQ\partial_\mu U^\dagger\right\rangle, \quad (4.4)$$

where $e > 0$ is the electric charge unit, Q and N_c denote the usual diagonal quark charge matrix, $Q = \text{diag}\{2/3, -1/3, -1/3\}$ for the three-flavor case, and the number of quark

colors, respectively. Here the convention is such that U transforms under $\mathrm{SU}(3)_L \times \mathrm{SU}(3)_R$ as $U \to g_R U g_L^\dagger$ with g_L and g_R elements in $\mathrm{SU}(3)_L$ and $\mathrm{SU}(3)_R$, respectively. According to Weinberg's power counting scheme, the above WZW Lagrangian starts to contribute from $\mathcal{O}(p^4)$. The axion-meson mixing contribution can be obtained by substituting U in the above Lagrangian by $\exp\left(-i\mathcal{Y}_a \frac{a}{f_a}\right)$ with $\mathcal{Y}_a = \mathcal{X}_a - \bar{m}\mathcal{M}_q^{-1}$. One finds

$$g_{a\gamma\gamma}^{\mathrm{mix}} = \frac{\alpha_{\mathrm{em}}}{2\pi f_a}\left(2\mathcal{X}_u - 2\frac{\bar{m}}{m_u}\right). \qquad (4.5)$$

Using eq. (4.2), one again gets the expression given in eq. (4.3).

Our goal in this section is to compute the axion-photon coupling to $\mathcal{O}(p^6)$. The chiral Lagrangian with a minimal set of terms in the anomalous-parity strong sector at $\mathcal{O}(p^6)$ has been given in ref. [79], not only for SU(2) but also for SU(N) with $N \geq 3$. Based on the anomalous Lagrangians, several works have been done in the anomalous-parity sector [80, 81]. In this work, only the terms proportional to C_7^W and C_8^W are relevant to the axion-photon coupling, which read

$$\mathcal{L}_{\mathrm{ano}}^{(6)} = iC_7^W \varepsilon^{\mu\nu\rho\sigma} \langle \chi_- f_{+\mu\nu} f_{+\rho\sigma}\rangle + iC_8^W \varepsilon^{\mu\nu\rho\sigma} \langle \chi_-\rangle \langle f_{+\mu\nu} f_{+\rho\sigma}\rangle, \qquad (4.6)$$

where C_7^W and C_8^W are two LECs. We have taken the same notation as in ref. [79].

In the following, we choose $\mathcal{X}_f = \bar{m}/m_f$ and $U = \tilde{U}$ for the computation of the $a\gamma\gamma$ coupling. With this convention the diagrams relevant for the computation of the $\mathcal{O}(p^6)$ corrections to $g_{a\gamma\gamma}$ are depicted in figure 1: (a) the axion-pion and axion-eta mass mixing from the NLO tree-level Lagrangian; (b) the tree-level diagram from $\mathcal{L}_{\mathrm{ano}}^{(6)}$; (c) one-loop diagrams with one vertex taken from $\mathcal{L}_{\mathrm{WZW}}$ and the other one taken from the LO chiral Lagrangian; the contributions from diagrams (d) and (e) exactly cancel with each other with the upper photon line in diagram (d) being on shell. It is interesting to note that for the anomalous processes such as π^0, η and η' decaying into two photons, the one-loop contributions vanish when the up-down quark mass difference is neglected [82, 83]. Likewise, in the SU(2) case the sum of all one loop corrections vanishes when both photons in the final state are on-shell [53]. However, in the SU(3) case, diagram (c) does contribute to the axion-photon coupling at $\mathcal{O}(p^6)$ when taking isospin breaking effects into account. Note that the pion-eta mixing needs to be considered in order to keep $g_{a\gamma\gamma}$ scale-independent and UV finite.

Putting together all the pieces, we obtain the axion-photon coupling keeping all orders in strong isospin breaking up to $\mathcal{O}(p^6)$ as

$$\begin{aligned}
g_{a\gamma\gamma} = \frac{\alpha_{\mathrm{em}}}{2\pi f_a}\Bigg\{ &\frac{\mathcal{E}}{\mathcal{C}} - \frac{2}{3}\frac{m_u + 3\bar{m}}{m_u} \\
&- \frac{1024\pi^2}{3\hat{m}}\bar{m}M_{\pi^0}^2\left(C_7^W + 3C_8^W\right) + \frac{2\bar{m}M_{\pi^0}^2}{3\hat{m}}\left[\frac{f_+(\cos,\sin)}{\sqrt{3}M_\eta^2} + \frac{f_-(\sin,\cos)}{M_{\pi^0}^2}\right]\Bigg\}, \quad (4.7)
\end{aligned}$$
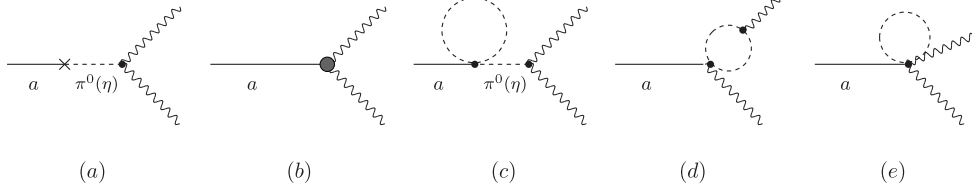
Figure 1. Feynman diagrams for the computation of the axion-photon coupling up to $\mathcal{O}\left(p^6\right)$. Here the dashed lines denote Goldstone bosons and wavy lines photons. Only pseudoscalar mesons are running in the loops.

where

$$
\begin{aligned}
f_{\pm}(\cos, \sin) = &\sqrt{3}\left(\mu_{\pi^0} - \mu_\eta\right)\cos(3\epsilon) \pm 3\left(\mu_{K^0} - \mu_{K^+}\right)\sin\epsilon - \sqrt{3}\left(\mu_{K^0} + \mu_{K^+} - 2\mu_{\pi^+}\right)\cos\epsilon \\
&- \frac{8M_{\pi^0}^2}{F_\pi^2 \hat{m}}\left(3L_7^r + L_8^r\right)\left[2\sqrt{3}(\hat{m} - m_s)\cos\epsilon \pm 3\delta\sin\epsilon\right].
\end{aligned} \tag{4.8}
$$

The functions $f_{\pm}(\sin, \cos)$ are equivalent to $f_{\pm}(\cos, \sin)$ with the sine and the cosine interchanged, i.e., $f_{\pm}(\sin, \cos) = f_{\pm}(\cos \to \sin, \sin \to \cos)$, and ϵ is the LO pion-eta mixing angle in the vacuum as can be obtained by setting $\theta = 0$ in the expression of ϵ_θ in eq. (2.8).

For the parameters C_7^W and C_8^W, it was argued in ref. [80] that C_7^W is largely suppressed compared to C_8^W as the latter receives a strong contribution from the η' while the former does not. The authors also suggested $|C_7^W| < 0.1|C_8^W|$. We use $\Gamma(\eta \to \gamma\gamma) = \frac{M_\eta^3}{64\pi}|T_\eta|^2$ with the $\eta \to \gamma\gamma$ amplitude given by [80]

$$
T_\eta = \frac{e^2}{\sqrt{3}F_\pi}\left[\frac{F_\pi}{4\pi^2 F_\eta}(1 + x_\eta) - \frac{64}{3}M_\pi^3 C_7^W + \frac{256}{3}(r - 1)M_\pi^2\left(\frac{1}{6}C_7^W + C_8^W\right) + \mathcal{O}(m_s^2)\right] \tag{4.9}
$$

to extract the value of C_8^W from the measured value of the $\eta \to \gamma\gamma$ width: $(0.516 \pm 0.020)\,\mathrm{keV}$ [33]. Following ref. [80], we take $F_\eta = (118.4 \pm 8.0)\,\mathrm{MeV}$ and assign a 30% uncertainty for the $\mathcal{O}\left(m_s^2\right)$ contribution compared to that of $\mathcal{O}\left(m_s\right)$, we get $C_8^W = (0.60 \pm 0.20) \times 10^{-3}\,\mathrm{GeV}^{-2}$, as listed in table 1. We have set C_7^W to 0 as its effect can be absorbed into the uncertainty of C_8^W.

With the input parameters presented in table 1, one gets

$$
g_{a\gamma\gamma} = \frac{\alpha_{\mathrm{em}}}{2\pi f_a}\left(\frac{\mathcal{E}}{\mathcal{C}} - 2.05(3)\right) = \left[0.197(3)\frac{\mathcal{E}}{\mathcal{C}} - 0.404(12)\right]\frac{m_a}{\mathrm{GeV}^2}. \tag{4.10}
$$

The error for the axion-photon coupling is also dominated by the uncertainties of C_8^W, r and L_7^r, which are of similar size. From eq. (4.10), we obtain $g_{a\gamma\gamma} \simeq 1.2 \times 10^{-16} \ldots 1.2 \times 10^{-13}\,\mathrm{GeV}^{-1}$ for the axion mass in the range $1 \ldots 1000\,\mu\mathrm{eV}$ with $\mathcal{E}/\mathcal{C} = 8/3$. Especially for $m_a = 6.7\,\mu\mathrm{eV}$, this equation predicts $g_{a\gamma\gamma} \simeq 8.1 \times 10^{-16}\,\mathrm{GeV}^{-1}$ for models with $\mathcal{E}/\mathcal{C} = 8/3$ like the Dine-Fischler-Srednicki-Zhitnitsky (DFSZ) model [28], which is still in the allowed region by the recent axion dark matter search, with m_a around $6.7\,\mu\mathrm{eV}$ [84].

The Primakoff effect plays a key role in axion searches. For example, the working principle for an axion helioscope [85, 86] is that axions produced in the core of the Sun are converted back into photons in a strong magnetic field. Clearly, if the ratio $\mathcal{E}/\mathcal{C} = 2$, which is

N	$m_a \left[\mu \text{eV} \cdot \frac{10^{12}\,\text{GeV}}{f_a}\right]$	$(-\lambda_4)^{1/4}\,[10^{-2}\text{GeV}/f_a]$	$g_{a\gamma\gamma}^{\text{QCD}}\ \left[\frac{\alpha_{\text{em}}}{2\pi f_a}\right]$	$\chi_t^{1/4}\,[\text{MeV}]$	b_2
2 [53]	5.70(7)	5.79(10)	$-1.92(4)$	75.5(5)	$-0.029(2)$
3	5.71(9)	5.77(18)	$-2.05(3)$	75.6(6)	$-0.028(3)$

Table 2. Summary of the main numerical results of the present work shown in the third line. For comparison we also show the results in the second line obtained in the framework of the SU(2) CHPT [53]. For the axion-photon coupling $g_{a\gamma\gamma}$, only the model-independent part, denoted by $g_{a\gamma\gamma}^{\text{QCD}}$, is shown.

quite a possibility as shown by Kaplan in ref. [71], then the $g_{a\gamma\gamma}$ would be highly suppressed. The axion detection using the Primakoff effect, such as microwave cavity experiments, or light shining through wall experiments (for a recent review, see ref. [87]) would thus be extremely difficult. Here, we present the reference values of $g_{a\gamma\gamma}$ for $\mathcal{E}/\mathcal{C} = 2$ and 8/3:

$$g_{a\gamma\gamma} = \begin{cases} -0.06(4) \times 10^{-3}/f_a, & \mathcal{E}/\mathcal{C} = 2, \\ +0.71(4) \times 10^{-3}/f_a, & \mathcal{E}/\mathcal{C} = 8/3. \end{cases} \tag{4.11}$$

With the expressions of the axion mass and the axion-photon coupling, it is straightforward to estimate the axion lifetime, namely,

$$\tau_{a\to\gamma\gamma} = \frac{64\pi}{g_{a\gamma\gamma}^2 m_a^3} = \frac{3.4 \times 10^{54}\,\text{s}}{\left[\mathcal{E}/\mathcal{C} - 2.05(3)\right]^2}\left(\frac{\mu\text{eV}}{m_a}\right)^5. \tag{4.12}$$

As the axion lifetime is inversely proportional to m_a^5, the axion is more stable when its mass is smaller. The axion lifetime is estimated as $\tau_{a\to\gamma\gamma} \gtrsim 10^{33}\,\text{s}$ if the lower limit $f_a \gtrsim 0.5 \times 10^9\,\text{GeV}$ is employed. Such a cosmologically stable particle is a well-motivated cold dark matter candidate [32, 88].

5 Summary

In this paper, we have calculated the QCD θ-vacuum energy and in turn the axion potential up-to-and-including NLO corrections in SU(N) CHPT. Unlike the SU(2) case, no analytic solutions exist for SU(N) with $N \geq 3$. We work out for the first time a recursion relation for ϕ_f, up to an arbitrary order in θ. Then, as an extension of ref. [54], by expanding the one-loop effective generating functional around the free-field configuration in a θ-vacuum, we have calculated the θ-vacuum energy density up NLO, including the one-loop contribution, in SU(N) CHPT with N non-degenerate quark flavors. With the recursion relation for the ϕ_f angles, one can compute any-order cumulants of the QCD topological charge distribution as well as the axion mass and self-couplings.

Since the QCD axion potential as a function of a/f_a takes the same form as the QCD θ-vacuum energy as a function of θ, we have also calculated the axion mass and self-coupling to NLO from the SU(3) θ-vacuum energy density taking into account the strong isospin breaking effects. With the determination of the LECs from experimental data and

lattice simulations, we have further evaluated the numerical values for axion mass and self-coupling up to NLO, which are similar to those obtained in the SU(2) case in ref. [53].

We also computed the axion-photon coupling up to $\mathcal{O}(p^6)$. Numerically, it is given by $g_{a\gamma\gamma} = \frac{\alpha_{\text{em}}}{2\pi f_a}[\mathcal{E}/\mathcal{C} - 2.05(3)]$, which implies that if $\mathcal{E}/\mathcal{C} = 2$, the axion-photon coupling would be extremely small. In this case the axion searches using $g_{a\gamma\gamma}$, such as light shining through a wall or microwave cavity experiments, would be very difficult. This might also have an important impact on the axion electrodynamics as well as the possible existence of boson stars, in which the axion-photon coupling plays a crucial role.

Acknowledgments

A   Full solution of the vacuum angles for the SU(N) case

Let us derive the expressions of the vacuum angles ϕ_f, and thus the LO vacuum energy, to all orders of θ for SU(N) here. The starting equations are the SU(N) version of eqs. (2.10)

$$\begin{cases} m_f \sin\phi_f = \text{constant}, \\ \sum_{f=1}^{N} \phi_f = \theta. \end{cases} \tag{A.1}$$

We use the following expansions,

$$\sin\phi_f = \sum_{n=0}^{\infty} s_{2n+1}\phi_f^{2n+1}, \quad \text{with } s_{2n+1} \equiv \frac{(-1)^n}{(2n+1)!},$$

$$\phi_f = \sum_{m=0}^{\infty} C_{f,2m+1}\theta^{2m+1}. \tag{A.2}$$

Once we solve all the coefficients $C_{f,2m+1}$, we then get the general solution of ϕ_f. Let

$$m_f \sin\phi_f = \sum_{n=0}^{\infty} \alpha_{2n+1}\theta^{2n+1}, \tag{A.3}$$

then eqs. (A.1) are decomposed into equations for each odd order of θ.

– 16 –

At $\mathcal{O}\left(\theta\right)$, one has

$$m_f C_{f,1} = \alpha_1, \quad \text{and} \quad \sum_{f=1}^{N} C_{f,1} = 1. \tag{A.4}$$

Thus, one gets

$$C_{f,1} = \frac{\bar{m}}{m_f} \tag{A.5}$$

with $\bar{m}$ defined in eq. (2.15).

At $\mathcal{O}\left(\theta^3\right)$, one has

$$C_{f,3} + s_3 C_{f,1}^3 = \frac{\alpha_3}{m_f}, \quad \text{and} \quad \sum_{f=1}^{N} C_{f,3} = 0, \tag{A.6}$$

the solution of which is

$$C_{f,3} = s_3 \left(\frac{\bar{m}}{m_f} \sum_{i=1}^{N} C_{i,1}^3 - C_{f,1}^3 \right). \tag{A.7}$$

Combining eqs. (A.5) and (A.7), one gets the known result in eq. (2.14).

At $\mathcal{O}\left(\theta^5\right)$, one has

$$C_{f,5} + 3s_3 C_{f,1}^2 C_{f,3} + s_5 C_{f,1}^5 = \frac{\alpha_5}{m_f}, \quad \text{and} \quad \sum_{f=1}^{N} C_{f,5} = 0, \tag{A.8}$$

the solution of which is

$$C_{f,5} = 3s_3 \left(\frac{\bar{m}}{m_f} \sum_{i=1}^{N} C_{i,1}^2 C_{i,3} - C_{f,1}^2 C_{f,3} \right) + s_5 \left(\frac{\bar{m}}{m_f} \sum_{i=1}^{N} C_{i,1}^5 - C_{f,1}^5 \right). \tag{A.9}$$

Notice that for the expansion of $\sin \phi_f$ in powers of θ in eq. (A.3), the terms at $\mathcal{O}\left(\theta^{2n+1}\right)$ are closely related to the partition of $2n+1$ into odd parts (e.g., the partitions of 5 into odd parts include 5, $3+1+1$ and $1+1+1+1+1$, see the left side of eq. (A.8)) studied in number theory.

One can go to higher orders and solve for $C_{f,2n+1}$ in the same way. Finally, one gets the recursion relation for all the coefficients as

$$C_{f,2n+1} = \sum_{t=1}^{n} \sum_{(k_1,\ldots,k_t)} s_{K_t} \binom{K_t}{k_1,\ldots,k_t} \left[\frac{\bar{m}}{m_f} \sum_{i=1}^{N} \prod_{j=1}^{t} C_{i,2j-1}^{k_j} - \prod_{j=1}^{t} C_{f,2j-1}^{k_j} \right], \tag{A.10}$$

where k_j are nonnegative integers, $K_t \equiv \sum_{j=1}^{t} k_j$, $\sum_{(k_1,\ldots,k_t)}$ means that the sum runs over all possibilities of k_j satisfying $k_1 + \cdots + (2t-1)k_t = 2n+1$, and $\binom{K_t}{k_1,\ldots,k_t} = K_t!/(k_1! \cdots k_t!)$ are the multinomial coefficients.

References

[1] R.J. Crewther, P. Di Vecchia, G. Veneziano and E. Witten, *Chiral Estimate of the Electric Dipole Moment of the Neutron in Quantum Chromodynamics*, *Phys. Lett.* **88B** (1979) 123 [*Erratum ibid.* **B 91** (1980) 487] [INSPIRE].

[2] C.A. Baker et al., *An Improved experimental limit on the electric dipole moment of the neutron*, *Phys. Rev. Lett.* **97** (2006) 131801 [hep-ex/0602020] [INSPIRE].

[3] W.C. Griffith, M.D. Swallows, T.H. Loftus, M.V. Romalis, B.R. Heckel and E.N. Fortson, *Improved Limit on the Permanent Electric Dipole Moment of* ^{199}Hg, *Phys. Rev. Lett.* **102** (2009) 101601 [arXiv:0901.2328] [INSPIRE].

[4] R.H. Parker et al., *First Measurement of the Atomic Electric Dipole Moment of* ^{225}Ra, *Phys. Rev. Lett.* **114** (2015) 233002 [arXiv:1504.07477] [INSPIRE].

[5] B. Graner, Y. Chen, E.G. Lindahl and B.R. Heckel, *Reduced Limit on the Permanent Electric Dipole Moment of* ^{199}Hg, *Phys. Rev. Lett.* **116** (2016) 161601 [*Erratum ibid.* **119** (2017) 119901] [arXiv:1601.04339] [INSPIRE].

[6] F.-K. Guo et al., *The electric dipole moment of the neutron from 2+1 flavor lattice QCD*, *Phys. Rev. Lett.* **115** (2015) 062001 [arXiv:1502.02295] [INSPIRE].

[7] NEDM collaboration, *Measurement of the permanent electric dipole moment of the neutron*, *Phys. Rev. Lett.* **124** (2020) 081803 [arXiv:2001.11966] [INSPIRE].

[8] R.D. Peccei and H.R. Quinn, *CP Conservation in the Presence of Instantons*, *Phys. Rev. Lett.* **38** (1977) 1440 [INSPIRE].

[9] R.D. Peccei and H.R. Quinn, *Constraints Imposed by CP Conservation in the Presence of Instantons*, *Phys. Rev.* **D 16** (1977) 1791 [INSPIRE].

[10] S. Weinberg, *A New Light Boson?*, *Phys. Rev. Lett.* **40** (1978) 223 [INSPIRE].

[11] F. Wilczek, *Problem of Strong P and T Invariance in the Presence of Instantons*, *Phys. Rev. Lett.* **40** (1978) 279 [INSPIRE].

[12] CAST collaboration, *Probing eV-scale axions with CAST*, *JCAP* **02** (2009) 008 [arXiv:0810.4482] [INSPIRE].

[13] Y. Inoue, Y. Akimoto, R. Ohta, T. Mizumoto, A. Yamamoto and M. Minowa, *Search for solar axions with mass around 1 eV using coherent conversion of axions into photons*, *Phys. Lett.* **B 668** (2008) 93 [arXiv:0806.2230] [INSPIRE].

[14] CAST collaboration, *New solar axion search using the CERN Axion Solar Telescope with* ^4He *filling*, *Phys. Rev.* **D 92** (2015) 021101 [arXiv:1503.00610] [INSPIRE].

[15] ADMX collaboration, *A SQUID-based microwave cavity search for dark-matter axions*, *Phys. Rev. Lett.* **104** (2010) 041301 [arXiv:0910.5914] [INSPIRE].

[16] E. Armengaud et al., *Axion searches with the EDELWEISS-II experiment*, *JCAP* **11** (2013) 067 [arXiv:1307.1488] [INSPIRE].

[17] J. Keller and A. Sedrakian, *Axions from cooling compact stars*, *Nucl. Phys.* **A 897** (2013) 62 [arXiv:1205.6940] [INSPIRE].

[18] A. Arvanitaki, M. Baryakhtar and X. Huang, *Discovering the QCD Axion with Black Holes and Gravitational Waves*, *Phys. Rev.* **D 91** (2015) 084011 [arXiv:1411.2263] [INSPIRE].

[19] B.M. Brubaker et al., *First results from a microwave cavity axion search at* $24\,\mu eV$, *Phys. Rev. Lett.* **118** (2017) 061302 [`arXiv:1610.02580`] [INSPIRE].

[20] PANDAX collaboration, *Limits on Axion Couplings from the First 80 Days of Data of the PandaX-II Experiment*, *Phys. Rev. Lett.* **119** (2017) 181806 [`arXiv:1707.07921`] [INSPIRE].

[21] CDEX collaboration, *Constraints on Axion couplings from the CDEX-1 experiment at the China Jinping Underground Laboratory*, *Phys. Rev.* **D 95** (2017) 052006 [`arXiv:1610.07521`] [INSPIRE].

[22] K. Ehret et al., *New ALPS Results on Hidden-Sector Lightweights*, *Phys. Lett.* **B 689** (2010) 149 [`arXiv:1004.1313`] [INSPIRE].

[23] OSQAR collaboration, *New exclusion limits on scalar and pseudoscalar axionlike particles from light shining through a wall*, *Phys. Rev.* **D 92** (2015) 092002 [`arXiv:1506.08082`] [INSPIRE].

[24] R. Bradley et al., *Microwave cavity searches for dark-matter axions*, *Rev. Mod. Phys.* **75** (2003) 777 [INSPIRE].

[25] M. Dine, W. Fischler and M. Srednicki, *A Simple Solution to the Strong CP Problem with a Harmless Axion*, *Phys. Lett.* **104B** (1981) 199 [INSPIRE].

[26] A.R. Zhitnitsky, *On Possible Suppression of the Axion Hadron Interactions* (in Russian), *Sov. J. Nucl. Phys.* **31** (1980) 260 [INSPIRE].

[27] J.E. Kim, *Weak Interaction Singlet and Strong CP Invariance*, *Phys. Rev. Lett.* **43** (1979) 103 [INSPIRE].

[28] M.A. Shifman, A.I. Vainshtein and V.I. Zakharov, *Can Confinement Ensure Natural CP Invariance of Strong Interactions?*, *Nucl. Phys.* **B 166** (1980) 493 [INSPIRE].

[29] J.E. Kim, *Light Pseudoscalars, Particle Physics and Cosmology*, *Phys. Rept.* **150** (1987) 1 [INSPIRE].

[30] G. Raffelt and D. Seckel, *Bounds on Exotic Particle Interactions from SN 1987a*, *Phys. Rev. Lett.* **60** (1988) 1793 [INSPIRE].

[31] J.E. Kim and G. Carosi, *Axions and the Strong CP Problem*, *Rev. Mod. Phys.* **82** (2010) 557 [*Erratum ibid.* **91** (2019) 049902] [`arXiv:0807.3125`] [INSPIRE].

[32] D.J.E. Marsh, *Axion Cosmology*, *Phys. Rept.* **643** (2016) 1 [`arXiv:1510.07633`] [INSPIRE].

[33] PARTICLE DATA GROUP collaboration, *Review of Particle Physics*, *Phys. Rev.* **D 98** (2018) 030001 [INSPIRE].

[34] L. Di Luzio, M. Giannotti, E. Nardi and L. Visinelli, *The landscape of QCD axion models*, `arXiv:2003.01100` [INSPIRE].

[35] D.S.M. Alves and N. Weiner, *A viable QCD axion in the MeV mass range*, *JHEP* **07** (2018) 092 [`arXiv:1710.03764`] [INSPIRE].

[36] J. Preskill, M.B. Wise and F. Wilczek, *Cosmology of the Invisible Axion*, *Phys. Lett.* **120B** (1983) 127 [INSPIRE].

[37] L.F. Abbott and P. Sikivie, *A Cosmological Bound on the Invisible Axion*, *Phys. Lett.* **120B** (1983) 133 [INSPIRE].

[38] M. Dine and W. Fischler, *The Not So Harmless Axion*, *Phys. Lett.* **120B** (1983) 137 [INSPIRE].

[39] L. Visinelli and P. Gondolo, *Dark Matter Axions Revisited*, *Phys. Rev.* **D 80** (2009) 035024 [arXiv:0903.4377] [INSPIRE].

[40] L. Visinelli and P. Gondolo, *Axion cold dark matter in view of BICEP2 results*, *Phys. Rev. Lett.* **113** (2014) 011802 [arXiv:1403.4594] [INSPIRE].

[41] K. Kaneta, H.-S. Lee and S. Yun, *Portal Connecting Dark Photons and Axions*, *Phys. Rev. Lett.* **118** (2017) 101802 [arXiv:1611.01466] [INSPIRE].

[42] P. Sikivie and Q. Yang, *Bose-Einstein Condensation of Dark Matter Axions*, *Phys. Rev. Lett.* **103** (2009) 111301 [arXiv:0901.1106] [INSPIRE].

[43] E.W. Kolb and I.I. Tkachev, *Axion miniclusters and Bose stars*, *Phys. Rev. Lett.* **71** (1993) 3051 [hep-ph/9303313] [INSPIRE].

[44] Y. Bai, V. Barger and J. Berger, *Hydrogen Axion Star: Metallic Hydrogen Bound to a QCD Axion BEC*, *JHEP* **12** (2016) 127 [arXiv:1612.00438] [INSPIRE].

[45] E. Braaten, A. Mohapatra and H. Zhang, *Dense Axion Stars*, *Phys. Rev. Lett.* **117** (2016) 121801 [arXiv:1512.00108] [INSPIRE].

[46] J. Eby, M. Leembruggen, P. Suranyi and L.C.R. Wijewardhana, *Collapse of Axion Stars*, *JHEP* **12** (2016) 066 [arXiv:1608.06911] [INSPIRE].

[47] D.G. Levkov, A.G. Panin and I.I. Tkachev, *Relativistic axions from collapsing Bose stars*, *Phys. Rev. Lett.* **118** (2017) 011301 [arXiv:1609.03611] [INSPIRE].

[48] L. Visinelli, S. Baum, J. Redondo, K. Freese and F. Wilczek, *Dilute and dense axion stars*, *Phys. Lett.* **B 777** (2018) 64 [arXiv:1710.08910] [INSPIRE].

[49] E. Braaten and H. Zhang, *Colloquium: The physics of axion stars*, *Rev. Mod. Phys.* **91** (2019) 041002.

[50] S. Weinberg, *Phenomenological Lagrangians*, *Physica* **A 96** (1979) 327 [INSPIRE].

[51] J. Gasser and H. Leutwyler, *Chiral Perturbation Theory to One Loop*, *Annals Phys.* **158** (1984) 142 [INSPIRE].

[52] J. Gasser and H. Leutwyler, *Chiral Perturbation Theory: Expansions in the Mass of the Strange Quark*, *Nucl. Phys.* **B 250** (1985) 465 [INSPIRE].

[53] G. Grilli di Cortona, E. Hardy, J. Pardo Vega and G. Villadoro, *The QCD axion, precisely*, *JHEP* **01** (2016) 034 [arXiv:1511.02867] [INSPIRE].

[54] F.-K. Guo and U.-G. Meißner, *Cumulants of the QCD topological charge distribution*, *Phys. Lett.* **B 749** (2015) 278 [arXiv:1506.05487] [INSPIRE].

[55] TWQCD collaboration, *Topological Susceptibility to the One-Loop Order in Chiral Perturbation Theory*, *Phys. Rev.* **D 80** (2009) 034502 [arXiv:0903.2146] [INSPIRE].

[56] V. Bernard, S. Descotes-Genon and G. Toucas, *Determining the chiral condensate from the distribution of the winding number beyond topological susceptibility*, *JHEP* **12** (2012) 080 [arXiv:1209.4367] [INSPIRE].

[57] F. Luciano and E. Meggiolaro, *Study of the theta dependence of the vacuum energy density in chiral effective Lagrangian models at zero temperature*, *Phys. Rev.* **D 98** (2018) 074001 [arXiv:1806.00835] [INSPIRE].

[58] M. Gorghetto and G. Villadoro, *Topological Susceptibility and QCD Axion Mass: QED and NNLO corrections*, *JHEP* **03** (2019) 033 [arXiv:1812.01008] [INSPIRE].

[59] T. Vonk, F.-K. Guo and U.-G. Meißner, *Precision calculation of the axion-nucleon coupling in chiral perturbation theory*, *JHEP* **03** (2020) 138 [arXiv:2001.05327] [INSPIRE].

[60] G. Landini and E. Meggiolaro, *Study of the interactions of the axion with mesons and photons using a chiral effective Lagrangian model*, *Eur. Phys. J.* **C 80** (2020) 302 [arXiv:1906.03104] [INSPIRE].

[61] R. Brower, S. Chandrasekharan, J.W. Negele and U.J. Wiese, *QCD at fixed topology*, *Phys. Lett.* **B 560** (2003) 64 [hep-lat/0302005] [INSPIRE].

[62] N.R. Acharya, F.-K. Guo, M. Mai and U.-G. Meißner, *θ-dependence of the lightest meson resonances in QCD*, *Phys. Rev.* **D 92** (2015) 054023 [arXiv:1507.08570] [INSPIRE].

[63] S. Aoki and H. Fukaya, *Chiral perturbation theory in a theta vacuum*, *Phys. Rev.* **D 81** (2010) 034022 [arXiv:0906.4852] [INSPIRE].

[64] MILC collaboration, *Effects of nonequilibrated topological charge distributions on pseudoscalar meson masses and decay constants*, *Phys. Rev.* **D 97** (2018) 074502 [arXiv:1707.05430] [INSPIRE].

[65] J. Bijnens and J. Lu, *Technicolor and other QCD-like theories at next-to-next-to-leading order*, *JHEP* **11** (2009) 116 [arXiv:0910.5424] [INSPIRE].

[66] V. Bernard, S. Descotes-Genon and G. Toucas, *Topological susceptibility on the lattice and the three-flavour quark condensate*, *JHEP* **06** (2012) 051 [arXiv:1203.0508] [INSPIRE].

[67] J. Eby, M. Leembruggen, P. Suranyi and L.C.R. Wijewardhana, *QCD Axion Star Collapse with the Chiral Potential*, *JHEP* **06** (2017) 014 [arXiv:1702.05504] [INSPIRE].

[68] J. Bijnens and G. Ecker, *Mesonic low-energy constants*, *Ann. Rev. Nucl. Part. Sci.* **64** (2014) 149 [arXiv:1405.6488] [INSPIRE].

[69] S. Borsányi et al., *Calculation of the axion mass based on high-temperature lattice quantum chromodynamics*, *Nature* **539** (2016) 69 [arXiv:1606.07494] [INSPIRE].

[70] FLAVOUR LATTICE AVERAGING GROUP collaboration, *FLAG Review 2019: Flavour Lattice Averaging Group (FLAG)*, *Eur. Phys. J.* **C 80** (2020) 113 [arXiv:1902.08191] [INSPIRE].

[71] D.B. Kaplan, *Opening the Axion Window*, *Nucl. Phys.* **B 260** (1985) 215 [INSPIRE].

[72] G. Alonso-Álvarez, M.B. Gavela and P. Quilez, *Axion couplings to electroweak gauge bosons*, *Eur. Phys. J.* **C 79** (2019) 223 [arXiv:1811.05466] [INSPIRE].

[73] H. Georgi, D.B. Kaplan and L. Randall, *Manifesting the Invisible Axion at Low-energies*, *Phys. Lett.* **169B** (1986) 73 [INSPIRE].

[74] J. Wess and B. Zumino, *Consequences of anomalous Ward identities*, *Phys. Lett.* **37B** (1971) 95 [INSPIRE].

[75] E. Witten, *Global Aspects of Current Algebra*, *Nucl. Phys.* **B 223** (1983) 422 [INSPIRE].

[76] O. Kaymakcalan, S. Rajeev and J. Schechter, *Nonabelian Anomaly and Vector Meson Decays*, *Phys. Rev.* **D 30** (1984) 594 [INSPIRE].

[77] U.-G. Meißner, *Low-Energy Hadron Physics from Effective Chiral Lagrangians with Vector Mesons*, *Phys. Rept.* **161** (1988) 213 [INSPIRE].

[78] S. Scherer and M.R. Schindler, *A Primer for Chiral Perturbation Theory*, *Lect. Notes Phys.* **830** (2012) 1.

96

[79] J. Bijnens, L. Girlanda and P. Talavera, *The Anomalous chiral Lagrangian of order p^6*, *Eur. Phys. J.* **C 23** (2002) 539 [hep-ph/0110400] [INSPIRE].

[80] K. Kampf and B. Moussallam, *Chiral expansions of the π^0 lifetime*, *Phys. Rev.* **D 79** (2009) 076005 [arXiv:0901.4688] [INSPIRE].

[81] J. Bijnens and K. Kampf, *Neutral pseudoscalar meson decays: $\pi^0 \to \gamma\gamma$ and $\eta \to \gamma\gamma$ in SU(3) limit*, *Nucl. Phys. Proc. Suppl.* **207-208** (2010) 220 [arXiv:1009.5493] [INSPIRE].

[82] J.F. Donoghue, B.R. Holstein and Y.C.R. Lin, *Chiral Loops in $\pi^0, \eta^0 \to \gamma\gamma$ and $\eta - \eta'$ Mixing*, *Phys. Rev. Lett.* **55** (1985) 2766 [*Erratum ibid.* **61** (1988) 1527] [INSPIRE].

[83] J. Bijnens, A. Bramon and F. Cornet, *Pseudoscalar Decays Into Photon-photon in Chiral Perturbation Theory*, *Phys. Rev. Lett.* **61** (1988) 1453 [INSPIRE].

[84] S. Lee, S. Ahn, J. Choi, B.R. Ko and Y.K. Semertzidis, *Axion Dark Matter Search around $6.7 \, \mu eV$*, *Phys. Rev. Lett.* **124** (2020) 101802 [arXiv:2001.05102] [INSPIRE].

[85] P. Sikivie, *Experimental Tests of the Invisible Axion*, *Phys. Rev. Lett.* **51** (1983) 1415 [*Erratum ibid.* **52** (1984) 695] [INSPIRE].

[86] CAST collaboration, *New CAST Limit on the Axion-Photon Interaction*, *Nature Phys.* **13** (2017) 584 [arXiv:1705.02290] [INSPIRE].

[87] I.G. Irastorza and J. Redondo, *New experimental approaches in the search for axion-like particles*, *Prog. Part. Nucl. Phys.* **102** (2018) 89 [arXiv:1801.08127] [INSPIRE].

[88] M. Kawasaki and K. Nakayama, *Axions: Theory and Cosmological Role*, *Ann. Rev. Nucl. Part. Sci.* **63** (2013) 69 [arXiv:1301.1123] [INSPIRE].

Precision calculation of the axion-nucleon coupling in chiral perturbation theory

Precision calculation of the axion-nucleon coupling in chiral perturbation theory

Thomas Vonk,[a] **Feng-Kun Guo**[b,c] **and Ulf-G. Meißner**[a,d,e]

[a]*Helmholtz-Institut für Strahlen- und Kernphysik and Bethe Center for Theoretical Physics, Universität Bonn, Bonn D-53115, Germany*

[b]*CAS Key Laboratory of Theoretical Physics, Institute of Theoretical Physics, Chinese Academy of Sciences, Beijing 100190, China*

[c]*School of Physical Sciences, University of Chinese Academy of Sciences, Beijing 100049, China*

[d]*Institute for Advanced Simulation, Institut für Kernphysik and Jülich Center for Hadron Physics, Forschungszentrum Jülich, Jülich D-52425, Germany*

[e]*Tbilisi State University, Tbilisi 0186, Georgia*

E-mail: vonk@hiskp.uni-bonn.de, fkguo@itp.ac.cn, meissner@hiskp.uni-bonn.de

ABSTRACT: We derive the axion-nucleon interaction Lagrangian in heavy baryon chiral perturbation theory up to next-to-next-to-leading order. The effective axion-nucleon coupling is calculated to a few percent accuracy.

Contents

1 Introduction

More than forty years after the proposal to add another symmetry in QCD, viz. the Peccei-Quinn (PQ) symmetry $\mathrm{U}(1)_{\mathrm{PQ}}$ [1, 2], the pseudo-Nambu-Goldstone boson resulting from the spontaneous breakdown of this symmetry, the QCD axion, remains one of the most favored candidates for a Beyond the Standard Model (BSM) particle. The reasons are manifold: originally introduced as a resolution of the so-called strong-CP problem, i.e. the question why the observable QCD vacuum angle $\bar{\theta} = \theta_{\mathrm{QCD}} + \arg \det \mathcal{M}_q$ (with $\mathcal{M}_q$ the quark mass matrix) is such a small quantity (current measurements of the neutron electric dipole moment imply $|\bar{\theta}| \lesssim 10^{-11}$ [3–5]), its experimental detection would not only unequivocally solve the strong-CP problem, but potentially also provide an answer (or complement the answer) on the question of the nature of the cosmological dark matter, another pressing issue in contemporary physics research. At the same time a model with PQ symmetry breaking can lead to massive Majorana or Dirac neutrinos depending on the choice of assigning PQ charges to the SM particles and Higgses [6–15]. Moreover, the fact that axions and PQ symmetries arise quite naturally in superstring theory [16] increases their popularity further.

If the QCD axion indeed exists, its couplings to Standard Model particles, i.e. matter particles and gauge bosons, and hence to composite particles as nucleons, must be very weak, because these are controlled by the very large axion decay constant f_a. Currently only lower and upper bounds on these couplings can be given. If these bounds are determined from nuclear processes, the exactness of the determination of f_a then strongly depends on the accuracy of our knowledge on the effective axion-nucleon coupling strength.

– 1 –

The leading order axion-nucleon coupling has been derived long ago in ref. [17] for the Peccei-Quinn-Weinberg-Wilczek (PQWW) axion [1, 2, 18, 19] based on current algebra techniques, and — building upon the same work — in refs. [20–23] in a more general manner. Here, we strive for deriving the axion-nucleon interaction in heavy baryon chiral perturbation theory (HBCHPT) for an arbitrary axion model coupling to hadrons as well as, in particular, for the Kim-Shifman-Vainstein-Zakharov (KSVZ) axion [24, 25] and the Dine-Fischler-Srednicki-Zhitnitskii (DFSZ) axion [26, 27]. To leading order, this has been done in ref. [28], so we extend their analysis to sub-leading orders, because more precise estimations of the axion-nucleon coupling allow for improved determinations of astrophysical constraints on the axion mass, or, equivalently, the axion decay constant, e.g. from the axion bremsstrahlung processes [29–36]. Of course, for improved calculations of such type of processes one also has to analyze corrections to multi-nucleon axion couplings, which goes beyond the scope of this work.

Our work is organized as follows: in section 2, we recapitulate the interaction Lagrangian between quarks and the axion. Then, in section 3, we derive the axion-nucleon interaction to the third order, that is including all terms up to next-to-next-to-leading order and pion loop contributions. We also give the numerical values of the axion coupling to neutrons and protons. We end with a short summary in section 4.

2 Axion-quark interaction Lagrangian

Consider the QCD Lagrangian including the axion field $a(x)$ at energies below the PQ scale [1, 2] with $q = (u, d, s, c, b, t)^{\mathrm{T}}$,

$$\mathcal{L}_{\mathrm{QCD}} = \mathcal{L}_{\mathrm{QCD},0} - \bar{q}\mathcal{M}_q q + \frac{a}{f_a}\frac{g^2}{16\pi^2}\mathrm{Tr}\left[G_{\mu\nu}\tilde{G}^{\mu\nu}\right] + \frac{\partial^\mu a}{2f_a}J_\mu^{\mathrm{PQ}}, \qquad (2.1)$$

where $\mathcal{L}_{\mathrm{QCD},0}$ contains all terms that are not of interest in what follows, including the axion-photon interaction term [28, 37, 38]. Furthermore, $\mathcal{M}_q = \mathrm{diag}\,(m_u, m_d, m_s, m_c, m_b, m_t)$ is the quark mass matrix, f_a is the axion decay constant, g the strong interaction coupling constant, $G_{\mu\nu} = G_{\mu\nu}^a\lambda^a/2$ is the conventional gluon field strength tensor with λ^a the Gell-Mann matrices, and $\tilde{G}_{\mu\nu} = \frac{1}{2}\epsilon_{\mu\nu\alpha\beta}G^{\alpha\beta}$ its dual, where the trace hence acts in the color space. The PQ current is given by

$$J_\mu^{\mathrm{PQ}} = f_a\partial_\mu a + \bar{q}\gamma_\mu\gamma_5\mathcal{X}_q q, \qquad (2.2)$$

from which the first term gives rise to the kinetic term of the axion, whereas the second term describes the axion-quark interactions proportional to the model-dependent coupling constants combined in the matrix $\mathcal{X}_q = \mathrm{diag}(X_q)$ acting in the flavor space. These are given by

$$\begin{aligned}
X_q^{\mathrm{KSVZ}} &= 0\,, \\
X_{u,c,t}^{\mathrm{DFSZ}} &= \frac{1}{3}\frac{x^{-1}}{x + x^{-1}} = \frac{1}{3}\sin^2\beta\,, \\
X_{d,s,b}^{\mathrm{DFSZ}} &= \frac{1}{3}\frac{x}{x + x^{-1}} = \frac{1}{3}\cos^2\beta = \frac{1}{3} - X_{u,c,t}^{\mathrm{DFSZ}}\,,
\end{aligned} \qquad (2.3)$$

for the KSVZ axion and the DFSZ axion, respectively, and $x = \cot\beta$ is the ratio of the vacuum expectation values (VEVs) of the two Higgs doublets. We exclude the PQWW axion from the analysis since it has been ruled out experimentally [17, 38].

Note that we do not integrate out the heavy quarks from the beginning. As, depending on the model, the axion couplings to heavy quarks are quite a possibility, they might contribute to the axion-nucleon interactions due to sea quark effects. Additionally, as the couplings X_q are scale-dependent quantities [28], running effects enter the couplings to nucleons, which can only be recovered if the axion interactions with heavy quarks are taken along within the calculations, to wit in the form of isoscalar currents.

It is advisable to perform an axial rotation on the quark fields in order to remove the term $\propto a \, \mathrm{Tr}\left[G_{\mu\nu}\tilde{G}^{\mu\nu}\right]$ in eq. (2.1) by transforming

$$q \to \exp\left(i\gamma_5 \frac{a}{2f_a}\mathcal{Q}_a\right) q \tag{2.4}$$

with

$$\mathcal{Q}_a = \frac{\mathcal{M}_q^{-1}}{\mathrm{Tr}\,\mathcal{M}_q^{-1}} \approx \frac{1}{1+z+w}\,\mathrm{diag}\left(1, z, w, 0, 0, 0\right), \tag{2.5}$$

where $z = m_u/m_d$ and $w = m_u/m_s$. The particular form of $\mathcal{Q}_a$ has been chosen in order to avoid the leading order π^0–a mass mixing [22]. This is equivalent to the vacuum alignment for the θ-vacuum case.

With that transformation, the Lagrangian can be written as

$$\mathcal{L}'_{\mathrm{QCD}} = \mathcal{L}'_{\mathrm{QCD},0} - (\bar{q}_L \mathcal{M}_a q_R + \mathrm{h.c.}) + \frac{\partial^\mu a}{2f_a} J_\mu^a, \tag{2.6}$$

where now the non-derivative axion-quark interactions are entirely shifted into the phase of the mass matrix,

$$\mathcal{M}_a = \exp\left(i\frac{a}{f_a}\mathcal{Q}_a\right)\mathcal{M}_q, \tag{2.7}$$

whereas the derivative axion-quark interactions are present in the coupling to the axion current

$$J_\mu^a = J_\mu^{\mathrm{PQ}} - \bar{q}\gamma_\mu\gamma_5\mathcal{Q}_a q, \tag{2.8}$$

which is now anomaly-free [17, 39]. The terms in J_μ^a must be split into isoscalar and isovector pieces in order to translate it later into an effective field theory (EFT) language. Consider the two-dimensional subspace of eq. (2.8) with $q = (u,d)^{\mathrm{T}}$:

$$\begin{aligned} J_\mu^{a,ud} &= f_a\partial_\mu a + \bar{q}\gamma_\mu\gamma_5\left(\mathcal{X}_q - \mathcal{Q}_a\right)q \\ &= f_a\partial_\mu a + c_{u-d}\bar{q}\gamma_\mu\gamma_5\tau_3 q + c_{u+d}\bar{q}\gamma_\mu\gamma_5 q, \end{aligned} \tag{2.9}$$

where τ_3 is the conventional third Pauli matrix and we have introduced the abbreviations

$$\begin{aligned} c_{u-d} &= \frac{1}{2}\left(X_u - X_d - \frac{1-z}{1+z+w}\right), \\ c_{u+d} &= \frac{1}{2}\left(X_u + X_d - \frac{1+z}{1+z+w}\right). \end{aligned} \tag{2.10}$$

– 3 –

Setting furthermore

$$c_s = X_s - \frac{w}{1+z+w}, \qquad c_{c,b,t} = X_{c,b,t} \tag{2.11}$$

and inserting eq. (2.9) into eq. (2.6), one finds the general axion-quark interaction Lagrangian

$$\begin{aligned}
\mathcal{L}_{a-q} = & - \bar{q}_L \mathcal{M}_a q_R + \text{h.c.} \\
& + \left(\bar{q} \gamma^\mu \frac{\partial_\mu a}{2f_a} \left(c_{u-d} \tau_3 + c_{u+d} \mathbf{1} \right) \gamma_5 q \right)_{q=(u,d)^{\mathrm{T}}} + \left(c_q \bar{q} \gamma^\mu \frac{\partial_\mu a}{2f_a} \gamma_5 q \right)_{q=(s,c,b,t)^{\mathrm{T}}}, \tag{2.12}
\end{aligned}$$

which is now expressed in a suitable basis so that the isovector and isoscalar parts of the axion-nucleon interaction can easily be extracted.

3 Axion-nucleon interaction in heavy baryon chiral perturbation theory

3.1 The Lagrangian

We construct the HBCHPT Lagrangian with the additional axion field and its interactions by adapting the one developed in ref. [40] (including the notation) and adding additional terms allowed from symmetries containing the isoscalar axial currents. Usually, the axial currents entering the HBCHPT Lagrangian as external sources are taken to be traceless in order to avoid subtleties arising from the $\mathrm{U}(1)_A$ anomaly. However, here our model is anomaly-free by construction and we now have to add the isoscalar axial currents appearing separately in the Lagrangian in eq. (2.12) that are not traceless. This is done in complete analogy to the traceless axial currents.

We introduce

$$u = \sqrt{U} = \exp\left(i \frac{\pi^a \tau_a}{2F_\pi} \right) \tag{3.1}$$

which contains the three pseudo-Nambu-Goldstone bosons of the spontaneously broken chiral symmetry, with the index $a = 1, 2, 3$ and summation implied. Furthermore, F_π is the pion decay constant in the chiral limit, for which we will take the physical value $92.1\,\mathrm{MeV}$ for the difference to the chiral limit value only amounts to effects of higher orders than those considered here. The isovector axial current a_μ enters the theory by means of the chiral connection Γ_μ of the covariant derivative,

$$D_\mu = \partial_\mu + \Gamma_\mu = \partial_\mu + \frac{1}{2} \left[u^\dagger \partial_\mu u + u \partial_\mu u^\dagger - i u^\dagger a_\mu u + i u a_\mu u^\dagger \right], \tag{3.2}$$

the so-called vielbein,

$$u_\mu = i \left[u^\dagger \partial_\mu u - u \partial_\mu u^\dagger - i u^\dagger a_\mu u - i u a_\mu u^\dagger \right], \tag{3.3}$$

and the field-strength tensor,

$$F_{\mu\nu}^{\mathrm{L,R}} = \mp \partial_\mu a_\nu \pm \partial_\nu a_\mu - i \left[a_\mu, a_\nu \right], \tag{3.4}$$

where we have set $v_\mu = 0$ for the external vector field. Note that the field-strength tensor vanishes in the present model because $a_\mu \propto \partial_\mu a\, \tau_3$ as can be read off from the

Lagrangian (2.12). Introducing thus the isoscalar axial current $a^s_{\mu,i} \propto c_i \partial_\mu a \, \mathbb{1}$, we can construct similar objects: a connection

$$\tilde{\Gamma}_\mu = \frac{1}{2} \left[-iu^\dagger a^s_{\mu,i} u + iu a^s_{\mu,i} u^\dagger \right] = 0, \qquad (3.5)$$

which vanishes due to $a^s_{\mu,i} u = u a^s_{\mu,i}$, and a vielbein equivalent

$$\tilde{u}_{\mu,i} = i \left[-iu^\dagger a^s_{\mu,i} u - iu a^s_{\mu,i} u^\dagger \right] = 2a^s_{\mu,i}. \qquad (3.6)$$

The corresponding field strength tensors, of course, vanish as in the case of the isovector axial current. The index $i = (u + d, s, c, b, t)$ runs over all isoscalar quark combinations, cf. eq. (2.12). Furthermore, we need as the last building block,

$$\chi_\pm = u^\dagger \chi u^\dagger \pm u \chi^\dagger u, \qquad (3.7)$$

where $\chi = 2B(s - ip)$ includes the external scalar and pseudoscalar fields $s(x)$ and $p(x)$, and B is a constant related to quark condensate $\Sigma = -\langle \bar{u}u \rangle$ via $B = \lim_{m_u,m_d \to 0}(\Sigma/F^2)$. Collecting the proton and neutron fields in the isodoublet $N(x) = (p, n)^{\mathrm{T}}$, the most general HBCHPT Lagrangian up to order $\mathcal{O}(p^3)$ in the low-energy expansion,

$$\mathcal{L}_{\pi N} = \mathcal{L}^{(1)}_{\pi N} + \mathcal{L}^{(2)}_{\pi N} + \mathcal{L}^{(3)}_{\pi N} + \ldots, \qquad (3.8)$$

reads

$$
\begin{aligned}
\mathcal{L}_{\pi N} = \bar{N} \bigg\{ & iv \cdot D + g_A S \cdot u + g_0^i S \cdot \tilde{u}_i - \frac{ig_A}{2m} \{S \cdot D, v \cdot u\} - \frac{ig_0^i}{2m} \{S \cdot D, v \cdot \tilde{u}_i\} \\
& + \frac{g_A}{8m^2} [D^\mu, [D_\mu, S \cdot u]] + \frac{g_0^i}{8m^2} [D^\mu, [D_\mu, S \cdot \tilde{u}_i]] \\
& - \frac{g_A}{4m^2} v \cdot \overleftarrow{D} S \cdot u \, v \cdot D - \frac{g_0^i}{4m^2} v \cdot \overleftarrow{D} S \cdot \tilde{u}_i \, v \cdot D \\
& - \frac{g_A}{4m^2} (\{S \cdot D, v \cdot u\} v \cdot D + \text{h.c.}) - \frac{g_0^i}{4m^2} (\{S \cdot D, v \cdot \tilde{u}_i\} v \cdot D + \text{h.c.}) \\
& - \frac{g_A}{8m^2} (S \cdot u \, D^2 + \text{h.c.}) - \frac{g_0^i}{8m^2} (S \cdot \tilde{u}_i \, D^2 + \text{h.c.}) \qquad (3.9) \\
& - \frac{g_A}{4m^2} \left(S \cdot \overleftarrow{D} u \cdot D + \text{h.c.} \right) - \frac{g_0^i}{4m^2} \left(S \cdot \overleftarrow{D} \tilde{u}_i \cdot D + \text{h.c.} \right) \\
& + d_{16}(\lambda) S \cdot u \, \text{Tr}\,[\chi_+] + d_{16}^i(\lambda) S \cdot \tilde{u}_i \, \text{Tr}\,[\chi_+] + d_{17} S^\mu \, \text{Tr}\,[u_\mu \chi_+] \\
& + id_{18} S^\mu [D_\mu, \chi_-] + id_{19} S^\mu [D_\mu, \text{Tr}[\chi_-]] \\
& + \tilde{d}_{25}(\lambda) v \cdot \overleftarrow{D} S \cdot u \, v \cdot D + \tilde{d}_{25}^i(\lambda) v \cdot \overleftarrow{D} S \cdot \tilde{u}_i \, v \cdot D \\
& + \tilde{d}_{29}(\lambda) (S^\mu [v \cdot D, u_\mu] v \cdot D + \text{h.c.}) + \tilde{d}_{29}^i(\lambda) (S^\mu [v \cdot D, \tilde{u}_{\mu,i}] v \cdot D + \text{h.c.}) \bigg\} N,
\end{aligned}
$$

where we only show terms that are relevant for the subsequent calculations, i.e. we consider only terms that produce either $a^n NN$ tree-level interactions with $n = 1$ up to next-to-next-to-leading order (terms with $n > 1$ are suppressed by factors f_a^{-n}), or leading order interactions involving pions that contribute to the leading one-loop order. For instance, because $\mathcal{Q}_a$ commutes with the quark mass matrix, the c_5 term containing χ_+ in the next-to-leading order pion-nucleon Lagrangian, which contributes to the CP-odd πNN coupling in the θ-vacuum, does not lead to a tree-level aNN vertex, and is only relevant to the aNN coupling for $\mathcal{O}(p^4)$ calculations. Note that there is no isoscalar counterpart to the d_{17} term proportional to a low-energy constant (LEC) d_{17}^i, since such a term would have the same structure as the d_{16}^i term, because $\tilde{u}_i \propto \mathbb{1}$, and thus not independent. The terms in the first line are the leading order and next-to-leading order terms, while all the other terms are the next-to-next-to-leading order terms.

In the Lagrangian (3.9), v_μ is the nucleon four-velocity and $N = N_v$ are velocity-dependent nucleon fields with mass m. Strictly speaking, m is the nucleon mass in the two-flavor chiral limit, often denoted as $\mathring{m}_N$. We will suppress the index v in what follows. The axial couplings g_A and g_0^i should also be taken in the chiral limit, but we will later match them with the nucleon matrix elements Δq, which refer to the physical values of the quark masses, see below. S_μ is the covariant spin-operator,

$$S_\mu = \frac{i}{2}\gamma_5 \sigma_{\mu\nu} v^\nu\,, \tag{3.10}$$

which has the following properties in d dimensions needed later, employing dimensional regularization to deal with the appearing divergences:

$$S \cdot v = 0\,, \quad S^2 = \frac{1-d}{4}\,, \quad \{S_\mu, S_\nu\} = \frac{1}{2}\left(v_\mu v_\nu - g_{\mu\nu}\right). \tag{3.11}$$

Besides the parameters already mentioned, a number of new LECs $d_n^{(i)}$ and $\tilde{d}_n^{(i)}$ appear, of which some depend on the scale λ and are divergent in order to absorb the one-loop ultraviolet divergences in dimensional regularization. Of these, only the LECs d_{16} and d_{16}^i have finite pieces,

$$d_{16}^{(i)}(\lambda) = d_{16}^{(i),r}(\lambda) + \frac{\beta_{16}^{(i)}}{F_\pi^2}L(\lambda) = \bar{d}_{16}^{(i)} + \frac{\beta_{16}^{(i)}}{F_\pi^2}\left(L(\lambda) + \frac{1}{(4\pi)^2}\ln\frac{M_\pi}{\lambda}\right), \tag{3.12}$$

where $d_{16}^{(i),r}(\lambda)$ denote the renormalized, scale-dependent LECs, whereas $\bar{d}_{16}^{(i)}$ denote the scale-independent counterparts. The terms $\propto \tilde{d}_{25,29}^{(i)}$ are only needed for the absorption of divergences of the one-loop functional, so the corresponding LECs have no finite part,

$$\tilde{d}_{25,29}^{(i)}(\lambda) = \frac{\beta_{25,29}^{(i)}}{F_\pi^2}\left(L(\lambda) + \frac{1}{(4\pi)^2}\ln\frac{M_\pi}{\lambda}\right). \tag{3.13}$$

In these equations, $L(\lambda)$ contains the divergence at space-time dimension $d = 4$,

$$L(\lambda) = \frac{\lambda^{d-4}}{(4\pi)^2}\left(\frac{1}{d-4} - \frac{1}{2}\left[\ln(4\pi) + \Gamma'(1) + 1\right]\right), \tag{3.14}$$

and the β-functions are set to cancel the divergences of the one-loop functional, as discussed below.

In order to derive the full axion-nucleon coupling at $\mathcal{O}(p^3)$, the Lagrangian (3.9) has to be expressed in terms of the axion field a and the matrix-valued field u has to be expanded to the required order. For the $\mathcal{O}(p^3)$ tree-level contribution, we hence can set $u = \mathbb{1}$, whereas for the $\mathcal{O}(p^3)$ pion-loop contributions, we have to expand u to $\mathcal{O}(\pi^2)$. Both calculations are done in the subsequent sections.

3.2 Tree-level contributions at $\mathcal{O}(p^3)$

All interaction terms of the Lagrangian (3.9) contribute. The expressions for the external sources can be read off from the axion-quark interaction Lagrangian (2.12):

$$
\begin{aligned}
s &= \mathcal{M}_a\,, \\
p &= v_\mu = 0\,, \\
a_\mu &= c_{u-d}\frac{\partial_\mu a}{2f_a}\tau_3\,, \\
a^s_{\mu,i} &= c_i\frac{\partial_\mu a}{2f_a}\mathbb{1}\,.
\end{aligned}
\tag{3.15}
$$

Setting hence $u = \mathbb{1}$ and expanding the exponential in $\mathcal{M}_a$, cf. eq. (2.7), up to $\mathcal{O}(a^1)$, we find

$$
\begin{aligned}
D_\mu &= \partial_\mu\,, \\
u_\mu &= c_{u-d}\frac{\partial_\mu a}{f_a}\tau_3\,, \\
\tilde{u}_{\mu,i} &= c_i\frac{\partial_\mu a}{f_a}\tau_3\,, \\
\chi_+ &= 4B\mathcal{M}_q\,, \\
\chi_- &= \frac{4iM_\pi^2}{f_a}\frac{m_u m_d}{(m_u + m_d)^2}a\,,
\end{aligned}
\tag{3.16}
$$

where we have inserted the leading order pion mass $M_\pi^2 = B(m_u + m_d)$. Introducing the abbreviation

$$
g_a = g_A c_{u-d}\tau_3 + g_0^i c_i \mathbb{1}\,,
\tag{3.17}
$$

the single axion-nucleon interaction Lagrangian reads

$$
\begin{aligned}
\mathcal{L}_{aN}^{\text{int.}} = \frac{1}{f_a}\bar{N}\Bigg\{\ & g_a S \cdot (\partial a) - \frac{ig_a}{2m}\{S\cdot\partial, v\cdot(\partial a)\} \\
& + \frac{g_a}{4m^2}\bigg(\overset{\leftarrow}{\partial}_\mu S\cdot(\partial a)\,\partial^\mu - v\cdot\overset{\leftarrow}{\partial}S\cdot(\partial a)\,v\cdot\partial \\
& \qquad\quad - (\{S\cdot\partial, v\cdot(\partial a)\}\,v\cdot\partial + \text{h.c.}) - \bigg(S\cdot\overset{\leftarrow}{\partial}(\partial a)\cdot\partial + \text{h.c.}\bigg)\bigg)
\end{aligned}
$$

$$+4M_\pi^2\Bigg(\left[d_{16}(\lambda)\tau_3+d_{17}\frac{m_u-m_d}{m_u+m_d}\right]c_{u-d}+d_{16}^i(\lambda)c_i$$

$$-\left[d_{18}+2d_{19}\right]\frac{m_u m_d}{(m_u+m_d)^2}\Bigg)S\cdot(\partial a)$$

$$+\left(\tilde{d}_{25}(\lambda)c_{u-d}\tau_3+\tilde{d}_{25}^i(\lambda)c_i\right)v\cdot\overleftarrow{\partial}\,S\cdot(\partial a)\,v\cdot\partial$$

$$+\left(\tilde{d}_{29}(\lambda)c_{u-d}\tau_3+\tilde{d}_{29}^i(\lambda)c_i\right)\left(S^\mu\left[v\cdot\partial,(\partial a)\right]v\cdot\partial+\text{h.c.}\right)\Bigg\}N\,. \qquad (3.18)$$

From that, we can derive the corresponding tree-level NNa-vertex Feynman rule,

$$=-\frac{1}{f_a}\Bigg(g_a\left[1+\frac{1}{2m}\left(\omega-\omega'\right)-\frac{1}{4m^2}\left(\omega^2+\omega'\left(\omega-\omega'\right)-p^2\right)\right]$$

$$+4M_\pi^2\left[\left(d_{16}(\lambda)\tau_3+d_{17}\frac{m_u-m_d}{m_u+m_d}\right)c_{u-d}+d_{16}^i(\lambda)c_i-(d_{18}+2d_{19})\frac{m_u m_d}{(m_u+m_d)^2}\right]$$

$$+\left[\tilde{d}_{25}(\lambda)c_{u-d}\tau_3+\tilde{d}_{25}^i(\lambda)c_i\right]\omega\omega'+\left[\tilde{d}_{29}(\lambda)c_{u-d}\tau_3+\tilde{d}_{29}^i(\lambda)c_i\right]\left(\omega-\omega'\right)^2\Bigg)S\cdot q$$

$$+\frac{g_a}{mf_a}\left[\left(\omega-\omega'\right)-\frac{1}{2m}(\omega^2-\omega'^2)+\frac{1}{4m}(p^2-p'^2)\right]S\cdot p\,, \qquad (3.19)$$

where q is the momentum of the outgoing axion, p the momentum of the incoming nucleon, and $p'=p-q$ the momentum of the outgoing nucleon. Furthermore, we have set $\omega^{(\prime)}=v\cdot p^{(\prime)}$. Note that this expression (3.19) contains divergences due to the terms $\propto d_{16}^{(i)}(\lambda)$ and $\propto\tilde{d}_{25,29}^{(i)}(\lambda)$.

3.3 Pion-loop contributions

According to the usual power counting scheme, see, e.g., ref. [41], one-loop diagrams start contributing at $\mathcal{O}(p^3)$. The relevant diagrams are shown in figure 1. Note that axion loop contributions are negligibly small due to the $1/f_a$ suppressions. We thus have to determine the $NN\pi$-, $NN\pi a$-, and $NN\pi\pi a$-vertex Feynman rules from the leading order terms of the Lagrangian (3.9). Expanding hence

$$u=\exp\left(i\frac{\pi^a\tau_a}{2F_\pi}\right)=\mathbb{1}+i\frac{\pi^a\tau_a}{2F_\pi}-\frac{\pi^a\tau_a\pi^b\tau_b}{8F_\pi^2}+\mathcal{O}(\pi^3)\,, \qquad (3.20)$$

we find

$$D_\mu=\partial_\mu+i\frac{c_{u-d}}{2f_aF_\pi}\partial_\mu a\,\epsilon_{3ab}\pi^a\tau^b\,,$$

$$u_\mu=-\frac{\partial_\mu\pi^a}{F_\pi}\tau_a+c_{u-d}\frac{\partial_\mu a}{f_a}\tau_3+c_{u-d}\frac{\partial_\mu a\,\pi^a\pi^b}{2f_aF_\pi^2}\left(\tau_a\delta_{3b}-\tau_3\delta_{ab}\right)\,, \qquad (3.21)$$

$$\tilde{u}_{\mu,i}=c_i\frac{\partial_\mu a}{f_a}\tau_3\,,$$

and thus

$$\mathcal{L}_{N\pi}^{\text{int.}} = \bar{N}\Bigg\{ -\frac{1}{F_\pi}S\cdot(\partial\pi^a)\tau_a + \frac{1}{f_a}(g_A c_{u-d}\tau_3 + g_0^i c_i)S\cdot(\partial a) - \frac{c_{u-d}}{2f_a F_\pi}v\cdot(\partial a)\epsilon_{3ab}\pi^a\tau^b$$
$$+ \frac{g_A c_{u-d}}{2f_a F_\pi^2}S\cdot(\partial a)\pi^a\pi^b\left(\tau_a\delta_{3b} - \tau_3\delta_{ab}\right)\Bigg\}N\,. \tag{3.22}$$

This yields the following Feynman rules with k the outgoing pion momentum, and q the outgoing axion momentum:

$$\text{pion propagator:} \quad \frac{i\delta_{ab}}{k^2 - M_\pi^2 + i\eta}\,,$$

$$\text{nucleon propagator:} \quad \frac{i}{v\cdot p + i\eta}\,,$$

$$NN\pi\text{-vertex:} \quad \frac{g_A}{F_\pi}S\cdot k\,\tau_a\,,$$

$$NNa\text{-vertex:} \quad -\frac{1}{f_a}(g_A c_{u-d}\tau_3 + g_0^i c_i)S\cdot q\,,$$

$$NN\pi a\text{-vertex:} \quad \frac{c_{u-d}}{2f_a F_\pi}v\cdot q\,\epsilon_{3ab}\tau_b\,,$$

$$NN\pi\pi a\text{-vertex:} \quad -\frac{g_A c_{u-d}}{2f_a F_\pi^2}S\cdot q\,(\tau_a\delta_{3b} - \tau_3\delta_{ab})\,.$$

In what follows, we will make use of the loop functions given in the appendix of ref. [41]:

$$\Delta_\pi = -\frac{1}{i}\int\frac{\mathrm{d}^d k}{(2\pi)^d}\frac{1}{k^2 - M_\pi^2 + i\eta} = 2M_\pi^2\left(L(\lambda) + \frac{1}{(4\pi)^2}\ln\frac{M_\pi}{\lambda}\right) + \mathcal{O}(d-4)\,, \tag{3.23}$$

$$\frac{1}{i}\int\frac{\mathrm{d}^d k}{(2\pi)^d}\frac{\{1, k_\mu, k_\mu k_\nu\}}{(k^2 - M_\pi^2 + i\eta)(\omega - v\cdot k + i\eta)} = \{J_0(\omega), v_\mu J_1(\omega), g_{\mu\nu}J_2(\omega) + v_\mu v_\nu J_3(\omega)\}\,, \tag{3.24}$$

where $L(\lambda)$ is given in eq. (3.14), and

$$J_0(\omega) = -4\omega L + \frac{2\omega}{(4\pi)^2}\left(1 - 2\ln\frac{M_\pi}{\lambda}\right) - \frac{1}{4\pi^2}\sqrt{M_\pi^2 - \omega^2}\arccos\frac{-\omega}{M_\pi} + \mathcal{O}(d-4)\,, \quad (3.25)$$

$$J_1(\omega) = wJ_0(\omega) + \Delta_\pi\,, \tag{3.26}$$

$$J_2(\omega) = \frac{1}{d-1}\left[(M_\pi^2 - \omega^2)J_0(\omega) - \omega\Delta_\pi\right]\,, \tag{3.27}$$

$$J_3(\omega) = wJ_1(\omega) - J_2(\omega)\,, \tag{3.28}$$

where in particular the expression of $J_0(\omega)$ is valid for $\omega < M_\pi$, which is the region we are interested in.
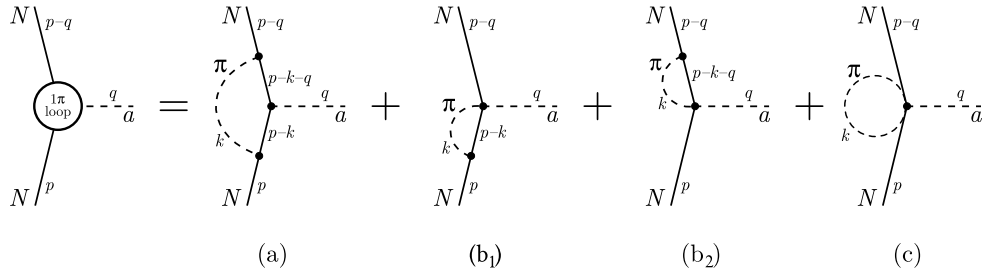
Figure 1. Pion loop contributions to $N \to N + a$.

3.3.1 Diagram (a)

Using the Feynman rules given above, the first loop diagram is calculated as

$$(\text{a}) = \frac{\hat{g}_a g_A^2}{f_a F_\pi^2} S^\mu \, S \cdot q \, S^\nu \frac{1}{i} \int \frac{\mathrm{d}^d k}{(2\pi)^d} \frac{k_\mu k_\nu}{(k^2 - M_\pi^2 + i\eta)} \frac{1}{(\omega' - v \cdot k + i\eta)(\omega - v \cdot k + i\eta)} \,, \quad (3.29)$$

where we have set (summation over i, j implied)

$$\hat{g}_a = \tau_i g_a \tau_j \delta_{ij} = -g_A c_{u-d} \tau_3 + 3 g_0^i c_i \mathbb{1} \,. \quad (3.30)$$

Using the identity

$$\frac{1}{(\omega' - v \cdot k + i\eta)(\omega - v \cdot k + i\eta)} = \frac{1}{\omega' - \omega} \left[\frac{1}{\omega - v \cdot k + i\eta} - \frac{1}{\omega' - v \cdot k + i\eta} \right], \quad (3.31)$$

the equation (3.29) can be written as

$$(\text{a}) = \frac{\hat{g}_a g_A^2}{f_a F_\pi^2} S^\mu \, S \cdot q \, S^\nu \frac{1}{\omega' - \omega} \left(\frac{1}{i} \int \frac{\mathrm{d}^d k}{(2\pi)^d} \frac{k_\mu k_\nu}{(k^2 - M_\pi^2 + i\eta)(\omega - v \cdot k + i\eta)} - \omega \to \omega' \right)$$

$$= \frac{\hat{g}_a g_A^2}{f_a F_\pi^2} S^\mu \, S \cdot q \, S^\nu \frac{1}{\omega' - \omega} \left(g_{\mu\nu} \left[J_2(\omega) - J_2(\omega') \right] + v_\mu v_\nu \left[J_3(\omega) - J_3(\omega') \right] \right). \quad (3.32)$$

The terms $\propto J_3(\omega^{(\prime)})$ vanish because of eq. (3.11). The final result is found using the anticommutator (3.11) and inserting the loop function (3.27),

$$(\text{a}) = \frac{\hat{g}_a}{6 f_a} \left(\frac{g_A}{4\pi F_\pi} \right)^2 \left\{ -M_\pi^2 + \frac{1}{\omega - \omega'} \left(\omega^3 - \omega'^3 \right. \right.$$

$$\left. + 2 \left[\left(M_\pi^2 - \omega^2 \right)^{\frac{3}{2}} \arccos \frac{-\omega}{M_\pi} - \left(M_\pi^2 - \omega'^2 \right)^{\frac{3}{2}} \arccos \frac{-\omega'}{M_\pi} \right] \right) \right\} S \cdot q$$

$$+ \frac{\hat{g}_a g_A^2}{6 f_a F_\pi^2} \left(3 M_\pi^2 - 2 \left(\omega - \omega' \right)^2 - 6 \omega \omega' \right) \left(L(\lambda) + \frac{1}{(4\pi)^2} \ln \frac{M_\pi}{\lambda} \right) S \cdot q \,, \quad (3.33)$$

where we have separated the finite, scale-independent terms (the first and second lines) from the divergent or scale-dependent ones (the third line).

3.3.2 Diagrams (b_1) and (b_2)

Diagrams (b$_1$) and (b$_2$) have the same structure:

$$(\text{b}_1) \propto S^\mu \frac{1}{i} \int \frac{\mathrm{d}^d k}{(2\pi)^d} \frac{k_\mu}{(M_\pi^2 - k^2 + i\eta)(\omega - v \cdot k + i\eta)} = S \cdot v \, J_1(\omega) = 0 \,, \qquad (3.34)$$

where we once again made use of $S \cdot v = 0$, see (3.11). For diagram (b$_2$) one just needs to replace $\omega \to \omega'$.

3.3.3 Diagram (c)

The last diagram is divergent:

$$(\text{c}) = -\frac{g_A c_{u-d}}{f_a F_\pi^2} S \cdot q \, \frac{1}{i} \int \frac{\mathrm{d}^d k}{(2\pi)^d} \frac{1}{k^2 - M_\pi^2 + i\eta} = \frac{2 g_A c_{u-d} M_\pi^2}{f_a F_\pi^2} \left(L(\lambda) + \frac{1}{(4\pi)^2} \ln \frac{M_\pi}{\lambda} \right) .$$
$$(3.35)$$

3.4 Axion-nucleon coupling at $\mathcal{O}(p^3)$

In order to remove the divergences appearing in the coupling (3.19) and diagrams (a) and (c), we utilize the following set of β-functions:

$$\beta_{16} = \frac{g_A}{8}(4 - g_A^2) \,, \quad \beta_{25} = g_A^3 \,, \qquad \beta_{29} = \frac{g_A^3}{3} \,,$$
$$\beta_{16}^i = \frac{3}{8} g_A^2 g_0^i \,, \qquad \beta_{25}^i = -3 g_A^2 g_0^i \,, \quad \beta_{29}^i = -g_A^2 g_0^i \,, \qquad (3.36)$$

where β_{16}, β_{25}, and β_{29} have been calculated already before within the theory without axions [42]. The remaining β-functions β_{16}^i, β_{25}^i, and β_{29}^i are new in the theory with axions and have been worked out here for the first time. We thus have a finite NNa-vertex with the Feynman rule:

$$
\begin{aligned}
&= -\frac{1}{f_a} \Bigg(g_a \left[1 + \frac{1}{2m} (\omega - \omega') - \frac{1}{4m^2} (\omega^2 + \omega'(\omega - \omega') - p^2) \right] - \frac{\hat{g}_a}{6} \left(\frac{g_A}{4\pi F_\pi} \right)^2 \\
&\quad \times \left[M_\pi^2 - \frac{1}{\omega - \omega'} \left(\omega^3 - \omega'^3 + 2 \left[(M_\pi^2 - \omega^2)^{\frac{3}{2}} \arccos \frac{-\omega}{M_\pi} - (M_\pi^2 - \omega'^2)^{\frac{3}{2}} \arccos \frac{-\omega'}{M_\pi} \right] \right) \right] \\
&\quad + 4 M_\pi^2 \left[\left(\bar{d}_{16} \tau_3 + d_{17} \frac{m_u - m_d}{m_u + m_d} \right) c_{u-d} + \bar{d}_{16}^i c_i - (d_{18} + 2 d_{19}) \frac{m_u m_d}{(m_u + m_d)^2} \right] \Bigg) S \cdot q \\
&\quad + \frac{g_a}{m f_a} \left[(\omega - \omega') - \frac{1}{2m} (\omega^2 - \omega'^2) + \frac{1}{4m} (p^2 - p'^2) \right] S \cdot p \,, \qquad (3.37)
\end{aligned}
$$

For the following estimation of the coupling strengths of the axion-proton and the axion-neutron vertex, we assume the rest frame of the incoming nucleon, i.e. $v = (1,0,0,0)^{\mathrm{T}}$, so

that $\omega = p = 0$ and $\omega' = -v \cdot q \ll m$. In the rest frame, eq. (3.37) becomes

$$\begin{aligned}
\text{(diagram)} = &-\frac{1}{f_a}\left(g_a\left[1-\frac{\omega'}{2m}+\left(\frac{\omega'}{2m}\right)^2\right]\right.\\
&\left.+\frac{\hat{g}_a}{6}\left(\frac{g_A M_\pi}{4\pi F_\pi}\right)^2\left[-1+\left(\frac{\omega'}{M_\pi}\right)^2-\frac{2}{\omega' M_\pi^2}\left(\frac{\pi M_\pi^3}{2}-\left(M_\pi^2-\omega'^2\right)^{\frac{3}{2}}\arccos\frac{-\omega'}{M_\pi}\right)\right]\right.\\
&\left.+4M_\pi^2\left[\left(\bar{d}_{16}\tau_3+d_{17}\frac{m_u-m_d}{m_u+m_d}\right)c_{u-d}+\bar{d}_{16}^i c_i-(d_{18}+2d_{19})\frac{m_u m_d}{(m_u+m_d)^2}\right]\right)S\cdot q\\
= &-\frac{1}{f_a}\left(g_a f_1(w')+\frac{\hat{g}_a}{6}\left(\frac{g_A M_\pi}{4\pi F_\pi}\right)^2 f_2(w')+g_a^{\mathrm{N^2LO}}\right)S\cdot q\,,
\end{aligned}\tag{3.38}$$

where

$$f_1(\omega') = 1-\frac{\omega'}{2m}+\left(\frac{\omega'}{2m}\right)^2\,,\tag{3.39}$$

$$f_2(\omega') = -1+\left(\frac{\omega'}{M_\pi}\right)^2-\frac{2}{\omega' M_\pi^2}\left(\frac{\pi M_\pi^3}{2}-\left(M_\pi^2-\omega'^2\right)^{\frac{3}{2}}\arccos\frac{-\omega'}{M_\pi}\right)\,,\tag{3.40}$$

$$g_a^{\mathrm{N^2LO}} = 4M_\pi^2\left[\left(\bar{d}_{16}\tau_3+d_{17}\frac{m_u-m_d}{m_u+m_d}\right)c_{u-d}+\bar{d}_{16}^i c_i-(d_{18}+2d_{19})\frac{m_u m_d}{(m_u+m_d)^2}\right]\,.\tag{3.41}$$

Since we are working in the very-low-energy regime, the function $f_2(w')$ may be approximated for $\omega' \ll M_\pi$. A series expansion around $\omega' = 0$ yields

$$f_2(\omega') = 1-\frac{3\pi}{2}\frac{\omega'}{M_\pi}-\frac{5}{3}\left(\frac{\omega'}{M_\pi}\right)^2+\mathcal{O}\left(\left(\frac{\omega'}{M_\pi}\right)^3\right)\,,\tag{3.42}$$

so that we find the axion-nucleon coupling at zero momentum transfer

$$G_{\mathrm{aNN}} = -\frac{1}{f_a}g_{\mathrm{aNN}} = -\frac{1}{f_a}\left(g_a+g_a^{\mathrm{loop}}+g_a^{\mathrm{N^2LO}}\right)\,,\tag{3.43}$$

with

$$g_a^{\mathrm{loop}} = \frac{\hat{g}_a}{6}\left(\frac{g_A M_\pi}{4\pi F_\pi}\right)^2\,.\tag{3.44}$$

The respective axion-proton and axion-neutron vertices can be determined by inserting the expressions for c_{u-d} and the c_i's from eq. (2.10) and eq. (2.11) and by matching g_A and the g_0^i's to the nucleon matrix elements, i.e.

$$\begin{aligned}
g_A &= \Delta u - \Delta d\,,\\
g_0^{u+d} &= \Delta u + \Delta d\,,\\
g_0^q &= \Delta q\,, \text{ for } q=s,c,b,t\,,
\end{aligned}\tag{3.45}$$

where $s^\mu \Delta q = \langle p|\bar{q}\gamma^\mu\gamma_5 q|p\rangle$, with s^μ the spin of the proton. The proton and neutron matrix elements are related by isospin symmetry, i.e. $\langle p|\bar{u}\gamma^\mu\gamma_5 u|p\rangle = \langle n|\bar{d}\gamma^\mu\gamma_5 d|n\rangle$, $\langle p|\bar{d}\gamma^\mu\gamma_5 d|p\rangle = \langle n|\bar{u}\gamma^\mu\gamma_5 u|n\rangle$, and $\langle p|\bar{q}\gamma^\mu\gamma_5 q|p\rangle = \langle n|\bar{q}\gamma^\mu\gamma_5 q|n\rangle$ for $q = s, c, b, t$. In particular we find

$$g_a^p = -\frac{\Delta u + z\Delta d + w\Delta s}{1 + z + w} + \Delta u X_u + \Delta d X_d + \sum_{q=\{s,c,b,t\}} \Delta q X_q \,, \tag{3.46}$$

$$\hat{g}_a^p = -\frac{(1+2z)\Delta u + (2+z)\Delta d + 3w\Delta s}{1+z+w}$$
$$+ (\Delta u + 2\Delta d)X_u + (2\Delta u + \Delta d)X_d + 3\sum_{q=\{s,c,b,t\}} \Delta q X_q \,, \tag{3.47}$$

for the case of axion-proton interaction, and

$$g_a^n = -\frac{z\Delta u + \Delta d + w\Delta s}{1 + z + w} + \Delta d X_u + \Delta u X_d + \sum_{q=\{s,c,b,t\}} \Delta q X_q \,, \tag{3.48}$$

$$\hat{g}_a^n = -\frac{(2+z)\Delta u + (1+2z)\Delta d + 3w\Delta s}{1+z+w}$$
$$+ (2\Delta u + \Delta d)X_u + (\Delta u + 2\Delta d)X_d + 3\sum_{q=\{s,c,b,t\}} \Delta q X_q \,, \tag{3.49}$$

for the case of axion-neutron coupling.

We extract the respective quantities from the recent FLAG review [43], which are here given in the $\overline{\text{MS}}$ scheme at the scale $\mu = 2\,\text{GeV}$ (we utilize the nucleon matrix elements calculated on the lattice with $N_f = 2 + 1$ excluding isospin breaking effects). The LEC d_{18} is taken from ref. [44] (fixed by the Goldberger-Treiman discrepancy), whereas $\bar{d}_{16}$ has been adopted from ref. [45]:

$$
\begin{array}{lll}
\Delta u = 0.847(50), & \Delta d = -0.407(34), & \Delta s = -0.035(13), \\
m_u = 2.27(9)\,\text{MeV}, & m_d = 4.67(9)\,\text{MeV}, & M_\pi = 136.10(1.82)\,\text{MeV}, \\
z = 0.485(19), & w = 0.025(1), & \mathring{m}_N = 0.8726(31)\,\text{GeV}, \\
\bar{d}_{16} = 0.4(1.3)\,\text{GeV}^{-2}, & d_{18} = -0.44(24)\,\text{GeV}^{-2}, &
\end{array} \tag{3.50}
$$

where the nucleon mass in the chiral limit $m = \mathring{m}_N$ has been estimated via the third order relation (which is the accuracy to which we are working)

$$m_{N,\text{phys}} = \mathring{m}_N - 4c_1 M_\pi^2 - \frac{3g_A^2 M_\pi^3}{32\pi F_\pi^2} + \mathcal{O}(M_\pi^4) \,, \tag{3.51}$$

with $c_1 = -1.07(2)\,\text{GeV}^{-1}$ at $\mathcal{O}(p^3)$ from ref. [44]. Note that the pion mass is taken to be the leading order pion mass $M_\pi = \sqrt{B(m_u + m_d)}$. The $\bar{d}_{16}^i$'s are of course hitherto undetermined since they are new LECs in the theory with axions.

Inserting these values, one finds

$$g_a^p = -0.430(36) + 0.847(50)X_u - 0.407(34)X_d - 0.035(13)X_s \,, \tag{3.52}$$

$$\hat{g}_a^p = -0.433(36) + 0.033(84)X_u + 1.287(106)X_d - 0.105(39)X_s \,, \tag{3.53}$$

$$g_a^{p,\text{loop}} = -0.002(1) + 0.0001(3)X_u + 0.005(2)X_d - 0.0004(2)X_s \,, \tag{3.54}$$

for the case of axion-proton interaction, and

$$g_a^n = -0.002(30) - 0.407(34)X_u + 0.847(50)X_d - 0.035(13)X_s \,, \tag{3.55}$$

$$\hat{g}_a^n = -0.861(30) + 1.287(106)X_u + 0.033(84)X_d - 0.105(39)X_s \,, \tag{3.56}$$

$$g_a^{n,\text{loop}} = -0.003(1) + 0.005(2)X_u + 0.0001(3)X_d - 0.0004(2)X_s \,, \tag{3.57}$$

for the interaction of axions with neutrons. Note that g_a^p and g_a^n are nothing but the pure leading order coupling strengths, which were reported already in ref. [28] (eq. (2.49) in their paper). Here we have used the most recent values for the involved quantities and neglected terms $\propto \Delta c, \Delta b, \Delta t$, because these contributions are well beyond the accuracy of the present N^{2}LO estimations of the coupling strengths.

The corrections to the leading order couplings (3.52) and (3.55) stemming from the chiral expansion to N^{2}LO is given by

$$\begin{aligned}
g_a^{p,\text{N}^2\text{LO}} = {}& 0.002(7) \\
& + \left(-0.036(1)\bar{d}_{16}^{u+d} - 0.001(0)\bar{d}_{16}^s + 0.004(0)d_{17} + 0.033(1)d_{19} \right) \text{GeV}^2 \\
& + \left(0.015(48) + \left[0.037(1)\bar{d}_{16}^{u+d} - 0.013(1)d_{17} \right] \text{GeV}^2 \right) X_u \\
& + \left(-0.015(48) + \left[0.037(1)\bar{d}_{16}^{u+d} + 0.013(1)d_{17} \right] \text{GeV}^2 \right) X_d \\
& + 0.074(2)\,\text{GeV}^2\, \bar{d}_{16}^s X_s \,, \tag{3.58}
\end{aligned}$$

$$\begin{aligned}
g_a^{n,\text{N}^2\text{LO}} = {}& 0.012(7) \\
& + \left(-0.036(1)\bar{d}_{16}^{u+d} - 0.001(0)\bar{d}_{16}^s + 0.004(0)d_{17} + 0.033(1)d_{19} \right) \text{GeV}^2 \\
& + \left(-0.015(48) + \left[0.037(1)\bar{d}_{16}^{u+d} - 0.013(1)d_{17} \right] \text{GeV}^2 \right) X_u \\
& + \left(0.015(48) + \left[0.037(1)\bar{d}_{16}^{u+d} + 0.013(1)d_{17} \right] \text{GeV}^2 \right) X_d \\
& + 0.074(2)\,\text{GeV}^2\, \bar{d}_{16}^s X_s \,. \tag{3.59}
\end{aligned}$$

Since the values of the remaining LECs appearing in this expression are unknown, we estimate the strength of the contribution of $g_a^{\text{N}^2\text{LO}}$ by assuming that the undetermined LECs are of $\mathcal{O}(\text{GeV}^{-2})$ following the conventional naturalness arguments, see e.g. [45, 46]. We expect the values of these LECs to be comparable to the ones known from $\bar{d}_{16}$ and d_{18}, so we make the *ansatz* $|\bar{d}_{16}^i| = 0.5(5)\,\text{GeV}^{-2}$ and likewise $|d_{17,19}| = 0.5(5)\,\text{GeV}^{-2}$, and perform a Monte Carlo simulation assuming a normal distribution for each undetermined LEC. This yields

$$g_a^{p,\text{N}^2\text{LO}} = 0.002(35) + 0.015(56)X_u - 0.015(56)X_d + 0.000(52)X_s \,, \tag{3.60}$$

$$g_a^{n,\text{N}^2\text{LO}} = 0.012(35) - 0.015(56)X_u + 0.015(56)X_d + 0.000(52)X_s \,, \tag{3.61}$$

so that our final result for the axion-nucleon coupling (3.43) reads

$$g_{\text{app}} = -0.430(50) + 0.862(75)X_u - 0.417(66)X_d - 0.035(54)X_s \,, \tag{3.62}$$

$$g_{\text{ann}} = 0.007(46) - 0.417(66)X_u + 0.862(75)X_d - 0.035(54)X_s \,. \tag{3.63}$$

Note that we are still working at the matching scale $\mu = 2\,\text{GeV}$ (in contrast to [28]).

Collecting all contributions, one gets for the KSVZ model with $X_q = 0$,

$$g_{\text{app}}^{\text{KSVZ}} = -0.430(50) \,, \tag{3.64}$$

$$g_{\text{ann}}^{\text{KSVZ}} = 0.007(46) \,, \tag{3.65}$$

while for the DFSZ axion,

$$g_{\text{app}}^{\text{DFSZ}} = -0.581(58) + 0.438(38)\sin^2\beta \,, \tag{3.66}$$

$$g_{\text{ann}}^{\text{DFSZ}} = 0.283(55) - 0.415(38)\sin^2\beta \,. \tag{3.67}$$

The coupling of axions to nucleons hence is always non-zero in both models, even though $g_{\text{ann}}^{\text{KSVZ}} = 0$ is possibile within the error range. In the DFSZ model, the strength of the coupling to protons g_{app} can range from $-0.581(58)$ at $\sin^2\beta = 0$ to $-0.143(69)$ at $\sin^2\beta = 1$. The coupling to neutrons may take on values from $+0.283(55)$ at $\sin^2\beta = 0$ to $-0.132(67)$ at $\sin^2\beta = 1$, which means that in the DSFZ model g_{ann} might still vanish depending on the value of β.

4   Summary

In this work, we have calculated the axion-nucleon couplings at the next-to-next-to-leading order in two-flavor non-relativistic baryon chiral perturbation theory. Including all phenomenological knowledge from a variety of sources, we find the N^{2}LO corrections of a few percent only. These couplings are therefore pinned down to a high precision.

Although we have reached a higher accuracy in the framework of chiral perturbation theory, the errors are still relatively large for two reasons. Firstly, there are still sizeable uncertainties stemming from the LO nucleon matrix elements calculated on the lattice, and secondly there are considerable uncertainties from the undetermined LECs. In fact, a possible future detection of the axion could be used to determine these LECs by applying the method of Bayesian inference. This is, however, not expected to be the case in the near future, because one would need more precise determinations of all other involved quantities such as the nucleon matrix elements Δq or the quark masses (which might be achieved in a few years in lattice QCD), and at the same time very precise measurements of the axion-nucleon coupling would be necessary. The formula in eq. (3.37) is hence primarily of relevance particularly for any future study on the axion-nucleon interaction, since the numerical values for the respective couplings can always be brought up to date by using the presented formulas and inserting the most recent estimations for the involved quantities.

In the future, it would be interesting to work out explicitly the chiral corrections to the axion-photon interaction and the influence of the strange quark.

Acknowledgments

References

[1] R.D. Peccei and H.R. Quinn, *CP Conservation in the Presence of Instantons*, *Phys. Rev. Lett.* **38** (1977) 1440 [INSPIRE].

[2] R.D. Peccei and H.R. Quinn, *Constraints Imposed by CP Conservation in the Presence of Instantons*, *Phys. Rev.* **D 16** (1977) 1791 [INSPIRE].

[3] V. Baluni, *CP Violating Effects in QCD*, *Phys. Rev.* **D 19** (1979) 2227 [INSPIRE].

[4] F.-K. Guo et al., *The electric dipole moment of the neutron from 2 + 1 flavor lattice QCD*, *Phys. Rev. Lett.* **115** (2015) 062001 [arXiv:1502.02295] [INSPIRE].

[5] J. Dragos, T. Luu, A. Shindler, J. de Vries and A. Yousif, *Confirming the Existence of the strong CP Problem in Lattice QCD with the Gradient Flow*, arXiv:1902.03254 [INSPIRE].

[6] R.N. Mohapatra and G. Senjanović, *The Superlight Axion and Neutrino Masses*, *Z. Phys.* **C 17** (1983) 53 [INSPIRE].

[7] P. Langacker, R.D. Peccei and T. Yanagida, *Invisible Axions and Light Neutrinos: Are They Connected?*, *Mod. Phys. Lett.* **A 1** (1986) 541 [INSPIRE].

[8] X.-G. He and R.R. Volkas, *Models Featuring Spontaneous CP Violation: An Invisible Axion and Light Neutrino Masses*, *Phys. Lett.* **B 208** (1988) 261 [*Erratum ibid.* **B 218** (1989) 508] [INSPIRE].

[9] M. Shin, *Light Neutrino Masses and Strong CP Problem*, *Phys. Rev. Lett.* **59** (1987) 2515 [*Erratum ibid.* **60** (1988) 383] [INSPIRE].

[10] C.-S. Chen and L.-H. Tsai, *Peccei-Quinn symmetry as the origin of Dirac Neutrino Masses*, *Phys. Rev.* **D 88** (2013) 055015 [arXiv:1210.6264] [INSPIRE].

[11] S. Bertolini, L. Di Luzio, H. Kolešová and M. Malinský, *Massive neutrinos and invisible axion minimally connected*, *Phys. Rev.* **D 91** (2015) 055014 [arXiv:1412.7105] [INSPIRE].

[12] P.-H. Gu, *Peccei-Quinn symmetry for Dirac seesaw and leptogenesis*, *JCAP* **07** (2016) 004 [arXiv:1603.05070] [INSPIRE].

[13] D. Suematsu, *Dark matter stability and one-loop neutrino mass generation based on Peccei-Quinn symmetry*, *Eur. Phys. J.* **C 78** (2018) 33 [arXiv:1709.02886] [INSPIRE].

[14] M. Reig and R. Srivastava, *Spontaneous proton decay and the origin of Peccei-Quinn symmetry*, *Phys. Lett.* **B 790** (2019) 134 [arXiv:1809.02093] [INSPIRE].

[15] E. Peinado, M. Reig, R. Srivastava and J.W.F. Valle, *Dirac neutrinos from Peccei-Quinn symmetry: a fresh look at the axion*, arXiv:1910.02961 [INSPIRE].

[16] P. Svrček and E. Witten, *Axions In String Theory*, *JHEP* **06** (2006) 051 [hep-th/0605206] [INSPIRE].

[17] T.W. Donnelly, S.J. Freedman, R.S. Lytel, R.D. Peccei and M. Schwartz, *Do Axions Exist?*, *Phys. Rev.* **D 18** (1978) 1607 [INSPIRE].

[18] S. Weinberg, *A New Light Boson?*, *Phys. Rev. Lett.* **40** (1978) 223 [INSPIRE].

[19] F. Wilczek, *Problem of Strong P and T Invariance in the Presence of Instantons*, *Phys. Rev. Lett.* **40** (1978) 279 [INSPIRE].

[20] D.B. Kaplan, *Opening the Axion Window*, *Nucl. Phys.* **B 260** (1985) 215 [INSPIRE].

[21] M. Srednicki, *Axion Couplings to Matter. 1. CP Conserving Parts*, *Nucl. Phys.* **B 260** (1985) 689 [INSPIRE].

[22] H. Georgi, D.B. Kaplan and L. Randall, *Manifesting the Invisible Axion at Low-energies*, *Phys. Lett.* **B 169** (1986) 73 [INSPIRE].

[23] S. Chang and K. Choi, *Hadronic axion window and the big bang nucleosynthesis*, *Phys. Lett.* **B 316** (1993) 51 [hep-ph/9306216] [INSPIRE].

[24] J.E. Kim, *Weak Interaction Singlet and Strong CP Invariance*, *Phys. Rev. Lett.* **43** (1979) 103 [INSPIRE].

[25] M.A. Shifman, A.I. Vainshtein and V.I. Zakharov, *Can Confinement Ensure Natural CP Invariance of Strong Interactions?*, *Nucl. Phys.* **B 166** (1980) 493 [INSPIRE].

[26] M. Dine, W. Fischler and M. Srednicki, *A Simple Solution to the Strong CP Problem with a Harmless Axion*, *Phys. Lett.* **B 104** (1981) 199 [INSPIRE].

[27] A.R. Zhitnitsky, *On Possible Suppression of the Axion Hadron Interactions* (in Russian), *Sov. J. Nucl. Phys.* **31** (1980) 260 [INSPIRE].

[28] G. Grilli di Cortona, E. Hardy, J. Pardo Vega and G. Villadoro, *The QCD axion, precisely*, *JHEP* **01** (2016) 034 [arXiv:1511.02867] [INSPIRE].

[29] N. Iwamoto, *Axion Emission from Neutron Stars*, *Phys. Rev. Lett.* **53** (1984) 1198 [INSPIRE].

[30] R. Mayle, J.R. Wilson, J.R. Ellis, K.A. Olive, D.N. Schramm and G. Steigman, *Constraints on Axions from SN 1987a*, *Phys. Lett.* **B 203** (1988) 188 [INSPIRE].

[31] R.P. Brinkmann and M.S. Turner, *Numerical Rates for Nucleon-Nucleon Axion Bremsstrahlung*, *Phys. Rev.* **D 38** (1988) 2338 [INSPIRE].

[32] G. Raffelt and D. Seckel, *Bounds on Exotic Particle Interactions from SN 1987a*, *Phys. Rev. Lett.* **60** (1988) 1793 [INSPIRE].

[33] W. Keil, H.-T. Janka, D.N. Schramm, G. Sigl, M.S. Turner and J.R. Ellis, *A Fresh look at axions and SN-1987A*, *Phys. Rev.* **D 56** (1997) 2419 [astro-ph/9612222] [INSPIRE].

[34] C. Hanhart, D.R. Phillips and S. Reddy, *Neutrino and axion emissivities of neutron stars from nucleon-nucleon scattering data*, *Phys. Lett.* **B 499** (2001) 9 [astro-ph/0003445] [INSPIRE].

[35] J.H. Chang, R. Essig and S.D. McDermott, *Supernova 1987A Constraints on Sub-GeV Dark Sectors, Millicharged Particles, the QCD Axion and an Axion-like Particle*, *JHEP* **09** (2018) 051 [arXiv:1803.00993] [INSPIRE].

[36] P. Carenza, T. Fischer, M. Giannotti, G. Guo, G. Martínez-Pinedo and A. Mirizzi, *Improved axion emissivity from a supernova via nucleon-nucleon bremsstrahlung*, *JCAP* **10** (2019) 016 [arXiv:1906.11844] [InSPIRE].

[37] J.E. Kim, *Light Pseudoscalars, Particle Physics and Cosmology*, *Phys. Rept.* **150** (1987) 1 [InSPIRE].

[38] J.E. Kim and G. Carosi, *Axions and the Strong CP Problem*, *Rev. Mod. Phys.* **82** (2010) 557 [*Erratum ibid.* **91** (2019) 049902] [arXiv:0807.3125] [InSPIRE].

[39] W.A. Bardeen and S.H.H. Tye, *Current Algebra Applied to Properties of the Light Higgs Boson*, *Phys. Lett.* **B 74** (1978) 229 [InSPIRE].

[40] N. Fettes, U.-G. Meißner and S. Steininger, *Pion-nucleon scattering in chiral perturbation theory. 1. Isospin symmetric case*, *Nucl. Phys.* **A 640** (1998) 199 [hep-ph/9803266] [InSPIRE].

[41] V. Bernard, N. Kaiser and U.-G. Meißner, *Chiral dynamics in nucleons and nuclei*, *Int. J. Mod. Phys.* **E 4** (1995) 193 [hep-ph/9501384] [InSPIRE].

[42] G. Ecker, *Chiral invariant renormalization of the pion-nucleon interaction*, *Phys. Lett.* **B 336** (1994) 508 [hep-ph/9402337] [InSPIRE].

[43] FLAVOUR LATTICE AVERAGING Group, *FLAG Review 2019*, *Eur. Phys. J.* **C 80** (2020) 113 [arXiv:1902.08191] [InSPIRE].

[44] M. Hoferichter, J. Ruiz de Elvira, B. Kubis and U.-G. Meißner, *Matching pion-nucleon Roy-Steiner equations to chiral perturbation theory*, *Phys. Rev. Lett.* **115** (2015) 192301 [arXiv:1507.07552] [InSPIRE].

[45] D. Siemens, V. Bernard, E. Epelbaum, A.M. Gasparyan, H. Krebs and U.-G. Meißner, *Elastic and inelastic pion-nucleon scattering to fourth order in chiral perturbation theory*, *Phys. Rev.* **C 96** (2017) 055205 [arXiv:1704.08988] [InSPIRE].

[46] V. Bernard, *Chiral Perturbation Theory and Baryon Properties*, *Prog. Part. Nucl. Phys.* **60** (2008) 82 [arXiv:0706.0312] [InSPIRE].

The axion-baryon coupling in SU(3) heavy baryon chiral perturbation theory

The axion-baryon coupling in SU(3) heavy baryon chiral perturbation theory

Thomas Vonk,[a] **Feng-Kun Guo**[b,c] **and Ulf-G. Meißner**[a,d,e]

[a]*Helmholtz-Institut für Strahlen- und Kernphysik and Bethe Center for Theoretical Physics,*
Universität Bonn, Bonn D-53115, Germany

[b]*CAS Key Laboratory of Theoretical Physics, Institute of Theoretical Physics,*
Chinese Academy of Sciences, Beijing 100190, China

[c]*School of Physical Sciences, University of Chinese Academy of Sciences,*
Beijing 100049, China

[d]*Institute for Advanced Simulation, Institut für Kernphysik and Jülich Center for Hadron Physics,*
Forschungszentrum Jülich, Jülich D-52425, Germany

[e]*Tbilisi State University, Tbilisi 0186, Georgia*

E-mail: vonk@hiskp.uni-bonn.de, fkguo@itp.ac.cn,
meissner@hiskp.uni-bonn.de

ABSTRACT: In the past, the axion-nucleon coupling has been calculated in the framework of SU(2) heavy baryon chiral perturbation theory up to third order in the chiral power counting. Here, we extend these earlier studies to the case of heavy baryon chiral perturbation theory with SU(3) flavor symmetry and derive the axion coupling to the full SU(3) baryon octet, showing that the axion also significantly couples to hyperons. As studies on dense nuclear matter suggest the possible existence of hyperons in stellar objects such as neutron stars, our results should have phenomenological implications related to the so-called axion window.

https://doi.org/10.1007/JHEP08(2021)024

Contents

1 Introduction

Soon after the discovery of the instanton solution of euclidean Yang-Mills gauge field theories [1], it has been realized that the vacuum structure of theories such as quantum chromodynamics (QCD) is highly non-trivial and that a so-called θ-term appears [2]

$$\mathcal{L}_{\mathrm{QCD}} = \mathcal{L}_{\mathrm{QCD},0} + \theta \left(\frac{g}{4\pi} \right)^2 \mathrm{Tr} \left[G_{\mu\nu} \tilde{G}^{\mu\nu} \right], \tag{1.1}$$

which is CP non-invariant as long as no quark is massless and as long as the effective angle $\bar{\theta} = \theta + \mathrm{Arg} \det \mathcal{M}$ is non-zero, where $\mathcal{M}$ refers to the quark mass matrix. In eq. (1.1), $\mathcal{L}_{\mathrm{QCD},0}$ denotes the usual QCD Lagrangian without the θ-term, g is the QCD coupling

constant, $G_{\mu\nu}$ the gluon field strength tensor, $\tilde{G}^{\mu\nu} = \epsilon^{\mu\nu\alpha\beta}G_{\alpha\beta}/2$ its dual, and Tr denotes the trace in color space. As a consequence, the neutron acquires an electric dipole moment $\propto \bar{\theta}$ [3]. Theoretical estimations of the $\bar{\theta}$-induced neutron electric dipole moment (nEDM) roughly vary between $|d_n| \approx 10^{-16}\bar{\theta}\, e\, \text{cm}$ and $|d_n| \approx 10^{-15}\bar{\theta}\, e\, \text{cm}$; see refs. [4–7]. The extreme small upper limit for the physical value of the nEDM determined in experiments (the most recent result is $|d_n| < 1.8 \times 10^{-26}\, e\, \text{cm}$ (90% C.L.) [8]) implies

$$\bar{\theta} \lesssim 10^{-11}\,, \tag{1.2}$$

which is a rather unnatural value for a quantity that in principle might take on values between 0 and 2π (where $\theta = \pi$ is a special point [9]). Even though $\bar{\theta}$ of $\mathcal{O}(1)$ would alter nuclear physics and big bang and stellar nucleosynthesis considerably [10], such anthropic considerations do not constrain $\bar{\theta}$ to such a tiny value. One possible way to explain why $\bar{\theta} \approx 0$ (in other words, to resolve the so-called "strong CP-problem") is the Peccei-Quinn mechanism [11, 12], which features a new global chiral symmetry, now usually labeled $\text{U}(1)_{\text{PQ}}$, and which automatically leads to $\bar{\theta} = 0$. The physical relic of this mechanism is not only a CP-conserving QCD Lagrangian, but also a new, very light pseudoscalar pseudo-Nambu-Goldstone boson with zero bare mass called axion [13, 14], which soon after its theoretical description also became a serious dark matter candidate [15–21], possibly forming Bose-Einstein condensates [22]. Both, the fact that the Peccei-Quinn mechanism provides an elegant solution to the strong CP-problem, and that it at the same time might provide a solution to the missing matter problem of the universe, accounts for the unwavering interest in the axion, even though it has not been detected yet and its existence hence remains hypothetical.

The original ("visible") Peccei-Quinn-Weinberg-Wilczek (PQWW) axion with a decay constant at the electroweak scale and a mass in the keV/MeV region seems to be ruled out experimentally [4, 23–25], although there are still attempts to make the experimental data compatible with the original model [26, 27]. However, these models require a lot of additional assumptions including that these axions restrictively couple to the first generation fermions (up and down quark, electron) and are accidentally pion-phobic. The clearly preferred models are the so-called "invisible" axion models such as the Kim-Shifman-Vainstein-Zakharov (KSVZ) axion model [28, 29] (which sometimes is called "hadronic" as it does not couple to leptons) or the Dine-Fischler-Srednicki-Zhitnitsky (DFSZ) axion model [30, 31]. Phenomenologically, the physical properties of such an (almost) invisible axion such as its mass and the couplings to standard model particles (quarks, leptons, gauge bosons) are governed by its expectedly large decay constant, which is traditionally estimated as being [4, 15, 16, 32]

$$10^9\, \text{GeV} \lesssim f_a \lesssim 10^{12}\, \text{GeV}\,, \tag{1.3}$$

such that the axion mass [33, 34]

$$m_a \approx 5.7 \left(\frac{10^{12}\, \text{GeV}}{f_a} \right) \times 10^{-6}\, \text{eV} \tag{1.4}$$

presumably would be somewhere between a few μeV and 0.1 eV. The lifetime of the QCD axion, which may decay into two photons, is incredibly large [33]

$$\tau_a \approx \left(\frac{1\,\text{eV}}{m_a}\right)^5 \times 10^{24}\,\text{s}\,. \tag{1.5}$$

Note that the traditional axion window, eq. (1.3), is set in order to match cold dark matter requirements of the canonical invisible axion models that solve the strong CP-problem. However, axions and axion-like particles have been considered also in the context of several other models with decay constants considerably smaller or larger than the window of eq. (1.3). For example, in the case of hadronic axions a decay constant as small as $f_a \approx 10^6$ GeV has been proposed [35], while in string theories axions and axion-like particles might appear at the GUT or even the Planck scale, i.e. $10^{15}\,\text{GeV} \lesssim f_a \lesssim 10^{18}\,\text{GeV}$ [36].

As a consequence of its (model-dependent) coupling to standard model particles, the axion of course also couples to composite particles such as mesons or baryons. One possible method of estimating constraints on the axion decay constant (or equivalently its mass) rests upon this coupling to baryons, in particular to nucleons, namely through nuclear bremsstrahlung processes in stellar objects [37–51] (see also the overviews [4, 33, 52, 53]). The leading order aN coupling has been derived several times since the early days [23, 35, 54–56]. More recently, this leading order coupling has been reexamined in ref. [57]. Moreover, such an analysis has been carried out up-to-and-including $\mathcal{O}(p^3)$ in SU(2) heavy baryon chiral perturbation theory (HBCHPT) in our previous work [58], where p denotes a small parameter (see below in section 2.2).

In this paper, we extend these previous studies using SU(3) HBCHPT in two regards: (i) we extend the calculations of the axion-nucleon couplings to the SU(3) case, up-to-and-including $\mathcal{O}(p^3)$, and (ii) we derive the couplings of the axion to the full ground state baryon octet (section 4). At this point one might wonder whether this extension is indeed useful given the fact that the most relevant coupling of the axion to baryons, i.e. the coupling to nucleons, is already known to good precision in the literature cited above, certainly precise enough for any phenomenological purpose. In this sense, the present study on the one hand is of rather theoretical interest, unraveling the explicit NNLO structure of the axion-nucleon coupling explicitly respecting the strange quark mass dependence. On the other hand, however, extending the analysis to the SU(3) case, we show that the traditional "invisible" axion also significantly couples to hyperons which has further phenomenological implications, since it has been suggested that hyperons might exist in the cores of neutron stars [59–86]. While it is a matter of ongoing research whether the seemingly energetically inevitable existence of hyperons in dense cores are compatible with the observed maximum masses of neutron stars (this question is related to the expected softening of the equation of state and known in the literature as "hyperon puzzle"), it is clear that approaches to constrain axion properties from cooling of neutron stars based on axion-nucleon bremsstrahlung alone might turn out to be insufficient. Depending on the underlying model and parameter sets, particularly the Λ and the Σ^- might appear in significant fractions of the total baryon number. As will be shown in this study, the axion coupling to these particular hyperons is of a similar order as that to the nucleons (in fact,

it could even be much larger than that to the neutron depending on the axion models), suggesting a revision of axion parameter constraints from stellar cooling.

Before performing the calculations of the axion-baryon couplings, we start with the explicit implementation of our framework and work out its ingredients and building blocks, which are the main topics of the following section 2. This section ends with some remarks of the general form of the axion-baryon coupling (section 2.3). The actual calculations of the axion-baryon couplings up to the leading one-loop level are performed in section 3, and the results are discussed in section 4.

2 SU(3) chiral perturbation theory with axions: general remarks

2.1 Ingredients from the axion-quark interaction Lagrangian

Consider the general QCD Lagrangian with axions below the electroweak symmetry breaking scale [32]

$$\mathcal{L}_{\mathrm{QCD}} = \mathcal{L}_{\mathrm{QCD},0} + \frac{a}{f_a}\left(\frac{g}{4\pi}\right)^2 \mathrm{Tr}\left[G_{\mu\nu}\tilde{G}^{\mu\nu}\right] + \bar{q}\gamma^\mu\gamma_5\frac{\partial_\mu a}{2f_a}\mathcal{X}_q q\,, \tag{2.1}$$

where $q = (u,d,s,c,b,t)^{\mathrm{T}}$ collects the quark fields and a refers to the axion field with decay constant f_a. The second term is a remnant of the θ-term of eq. (1.1) after the spontaneous breakdown of the Peccei-Quinn symmetry. Depending on the underlying axion model, axions might additionally couple directly to the quark fields, which is here present in the form of the last term. Here, we assume the canonical scenario that the couplings are flavor conserving at tree-level, i.e. $\mathcal{X}_q = \mathrm{diag}\{X_q\}$ is a diagonal 6×6 matrix acting in flavor space, where the X_q's, $q = \{u,d,s,c,b,t\}$, are the coupling constants of the respective axion-quark interactions. These are given, for instance, by

$$\begin{aligned} X_q^{\mathrm{KSVZ}} &= 0\,, \\ X_{u,c,t}^{\mathrm{DFSZ}} &= \frac{1}{3}\frac{x^{-1}}{x+x^{-1}} = \frac{1}{3}\sin^2\beta\,, \\ X_{d,s,b}^{\mathrm{DFSZ}} &= \frac{1}{3}\frac{x}{x+x^{-1}} = \frac{1}{3}\cos^2\beta = \frac{1}{3} - X_{u,c,t}^{\mathrm{DFSZ}}\,, \end{aligned} \tag{2.2}$$

for the KSVZ-type axions and DFSZ-type axions, respectively, where $x = \cot\beta$ is the ratio of the vacuum expectation values (VEVs) of the two Higgs doublets within the latter models. Note that $\mathcal{L}_{\mathrm{QCD},0}$ in eq. (2.1) also contains a quark mass term $\bar{q}\mathcal{M}_q q$, with $\mathcal{M}_q = \mathrm{diag}\{m_q\}$ being the real, diagonal and γ_5-free quark mass matrix.

As usual, it is advisable to perform a transformation on the quark fields,

$$q \to \exp\left(i\gamma_5\frac{a}{2f_a}\mathcal{Q}_a\right)q\,, \tag{2.3}$$

in order to remove the second term of eq. (2.1). Choosing

$$\mathcal{Q}_a = \frac{\mathcal{M}_q^{-1}}{\left\langle \mathcal{M}_q^{-1}\right\rangle} \approx \frac{1}{1+z+w}\,\mathrm{diag}\left(1,z,w,0,0,0\right)\,, \tag{2.4}$$

which corresponds to vacuum alignment in the θ-vacuum case, we can avoid the leading order mass mixing between the axion and the neutral pseudo-Nambu-Goldstone bosons of the spontaneous breaking of SU(3) chiral symmetry, the π^0 and the η, from the beginning. Here, $\langle\ldots\rangle$ denotes the trace in flavor space, $z = m_u/m_d$ and $w = m_u/m_s$. Now the axion-quark interaction Lagrangian is given by

$$\mathcal{L}_{a-q} = -\left(\bar{q}_L\mathcal{M}_a q_R + \text{h.c.}\right) + \bar{q}\gamma^\mu\gamma_5\frac{\partial_\mu a}{2f_a}\left(\mathcal{X}_q - \mathcal{Q}_a\right)q\,, \tag{2.5}$$

where q_L and q_R are the left- and right-handed projections of the quark fields, and

$$\mathcal{M}_a = \exp\left(i\frac{a}{f_a}\mathcal{Q}_a\right)\mathcal{M}_q\,. \tag{2.6}$$

Considering only the three-dimensional subspace of flavor space, i.e. $q = (u,d,s)^\text{T}$, and introducing

$$\begin{aligned}
c^{(1)} &= \frac{1}{3}\left(X_u + X_d + X_s - 1\right),\\
c^{(3)} &= \frac{1}{2}\left(X_u - X_d - \frac{1-z}{1+z+w}\right),\\
c^{(8)} &= \frac{1}{2\sqrt{3}}\left(X_u + X_d - 2X_s - \frac{1+z-2w}{1+z+w}\right),
\end{aligned} \tag{2.7}$$

we can decompose the matrix $\mathcal{X}_q - \mathcal{Q}_a$ into traceless parts and parts with non-vanishing trace, so that

$$\begin{aligned}
\mathcal{L}_{a-q} = &-\left(\bar{q}_L\mathcal{M}_a q_R + \text{h.c.}\right)\\
&+\left(\bar{q}\gamma^\mu\gamma_5\frac{\partial_\mu a}{2f_a}\left(c^{(1)}\mathbb{1} + c^{(3)}\lambda_3 + c^{(8)}\lambda_8\right)q\right)_{q=(u,d,s)^\text{T}}\\
&+\sum_{q=\{c,b,t\}}\left(\bar{q}\gamma^\mu\gamma_5\frac{\partial_\mu a}{2f_a}X_q q\right),
\end{aligned} \tag{2.8}$$

where λ_3 and λ_8 refer to the third and eighth Gell-Mann matrices, respectively. From this form of the axion-quark interaction Lagrangian, we can directly read off the required ingredients for the axionic SU(3) heavy baryon chiral Lagrangian, i.e. the external currents

$$\begin{aligned}
s &= \mathcal{M}_a\,,\\
a_\mu &= \frac{\partial_\mu a}{2f_a}\left(c^{(3)}\lambda_3 + c^{(8)}\lambda_8\right),\\
a_{\mu,i}^{(s)} &= c_i\frac{\partial_\mu a}{2f_a}\mathbb{1}\,, \qquad\qquad i = 1,\ldots,4\,.
\end{aligned} \tag{2.9}$$

Here we have set

$$c_1 = c^{(1)}\,, \qquad c_2 = X_c\,, \qquad c_3 = X_b\,, \qquad c_4 = X_t\,. \tag{2.10}$$

Note that in contrast to usual chiral perturbation theory, it is also necessary to add isosinglet axial-vector currents $a^{(s)}_{\mu,i}$ in order to preserve the full QCD axion interaction. This is possible here, as the subtleties that usually arise due to the $U(1)_A$ anomaly are absent, because the model is now anomaly-free.

If one considers also flavor-changing axion-quark couplings at tree-level, $\mathcal{X}_q$ would be non-diagonal. In this case, it is likewise appropriate to decompose $\mathcal{X}_q - \mathcal{Q}_a$ into traceless parts and parts with non-vanishing trace, such that

$$a_\mu = \frac{\partial_\mu a}{2f_a} \sum_{i=1}^{8} C^{(i)} \lambda_i \,, \tag{2.11}$$

with $C^{(i)}$ depending on the allowed flavor-changing processes and λ_i the eight Gell-Mann matrices. This then would cause baryon conversion processes. At this point we note that depending on the underlying model Higgs loops may induce off-diagonal couplings, which would be loop-suppressed but might be relevant due to unsuppressed top Yukawa couplings [87]. As stated above, we here stick to the most prevalent models excluding such flavor-changing axion-quark couplings at tree-level.

2.2 Building blocks of the chiral Lagrangian

The framework we use in this paper is chiral perturbation theory (CHPT) including baryons, meaning the effective field theory of QCD in the low-energy sector. CHPT is used to explore meson-baryon systems based on a systematic expansion in small momenta and quark masses below the scale of the spontaneous breakdown of chiral symmetry, $\Lambda_\chi \sim 1\,\text{GeV}$, as first developed by Gasser, Sainio, and Švarc for the two-flavor case [88] and by Krause for the three-flavor case [89]. However, while baryons can easily be incorporated into CHPT in a consistent manner respecting all symmetries, the power-counting scheme engineered to systematically arrange the infinitely many terms allowed by the fundamental symmetries is spoiled by the fact that the baryon masses m_B, which do not vanish in the chiral limit, are roughly of the same order as Λ_χ. One way to overcome this problem is to realize that all mass scales need to be assigned to a scaling in the power counting and thus to treat the baryons as extremely heavy, static fermions, which is the idea behind HBCHPT [90–93]. In this scheme, the four momentum of a baryon field is decomposed as

$$k_\mu = m_B v_\mu + p_\mu \tag{2.12}$$

with the four-velocity v_μ subject to the constraint $v^2 = 1$, and p_μ a small residual momentum satisfying $(v \cdot p) \ll m_B$. After integrating out the heavy degrees of freedom, the resulting Lagrangian is expressed in terms of the heavy baryon field B, which is now characterized by a fixed velocity v_μ (for convenience, we refrain from writing B_v to explicitly mark the v dependence). Additionally, it is possible to simplify the Dirac algebra by expressing any Dirac bilinear by means of v_μ and the Pauli-Lubanski spin operator

$$S_\mu = \frac{i}{2}\gamma_5 \sigma_{\mu\nu} v^\nu \,, \tag{2.13}$$

which satisfies the relations

$$\{S_\mu, S_\nu\} = \frac{1}{2}(v_\mu v_\nu - g_{\mu\nu}), \quad [S_\mu, S_\nu] = i\epsilon_{\mu\nu\rho\sigma}v^\rho S^\sigma, \quad (v \cdot S) = 0, \quad S^2 = \frac{1-d}{4}, \quad (2.14)$$

where the last one is valid in d spacetime dimensions. In eq. (2.14) and in what follows, [,] refers to the commutator and { , } to the anticommutator.

Any term in the effective Lagrangian consists of a number of elements from a small set of basic building blocks, from which we will present those that are relevant for axionic SU(3) HBCHPT. In this three-flavor case, the ground state baryon octet consisting of the nucleons p and n and the hyperons Σ, Λ, and Ξ are collected in a single 3×3 matrix

$$B = \begin{pmatrix} \frac{1}{\sqrt{2}}\Sigma_3 + \frac{1}{\sqrt{6}}\Lambda_8 & \Sigma^+ & p \\ \Sigma^- & -\frac{1}{\sqrt{2}}\Sigma_3 + \frac{1}{\sqrt{6}}\Lambda_8 & n \\ \Xi^- & \Xi^0 & -\frac{2}{\sqrt{6}}\Lambda_8 \end{pmatrix}, \quad (2.15)$$

where

$$\begin{aligned} \Sigma_3 &= \cos\epsilon\ \Sigma^0 - \sin\epsilon\ \Lambda, \\ \Lambda_8 &= \sin\epsilon\ \Sigma^0 + \cos\epsilon\ \Lambda. \end{aligned} \quad (2.16)$$

Equation (2.15) corresponds to the adjoint representation of SU(3). Due to isospin breaking, the physical Σ^0 and Λ are mixed states made of the Σ_3 and Λ_8. This mixing is usually parameterized by the mixing angle ϵ and one has

$$\tan 2\epsilon = \frac{\langle \lambda_3 \mathcal{M}_q \rangle}{\langle \lambda_8 \mathcal{M}_q \rangle}. \quad (2.17)$$

The pseudoscalar mesons, the pseudo-Nambu-Goldstone bosons of the spontaneous breakdown of chiral symmetry, appear in the Lagrangian in form of a unitary matrix

$$u = \sqrt{U} = \exp\left(i\frac{\Phi}{2F_p}\right), \quad (2.18)$$

where F_p is the pseudoscalar decay constant in the chiral limit and Φ is a Hermitian 3×3 matrix given by

$$\Phi = \sqrt{2} \begin{pmatrix} \frac{1}{\sqrt{2}}\pi_3 + \frac{1}{\sqrt{6}}\eta_8 & \pi^+ & K^+ \\ \pi^- & -\frac{1}{\sqrt{2}}\pi_3 + \frac{1}{\sqrt{6}}\eta_8 & K^0 \\ K^- & \bar{K}^0 & -\frac{2}{\sqrt{6}}\eta_8 \end{pmatrix}. \quad (2.19)$$

Again, the physical mass eigenstates of the neutral particles of the diagonal are mixed states as a consequence of isospin breaking effects and one has

$$\begin{aligned} \pi_3 &= \cos\epsilon\ \pi^0 - \sin\epsilon\ \eta, \\ \eta_8 &= \sin\epsilon\ \pi^0 + \cos\epsilon\ \eta. \end{aligned} \quad (2.20)$$

Using the leading order meson masses,

$$M_{\pi^\pm}^2 = B_0(m_u + m_d)\,,$$

$$M_{\pi^0}^2 = B_0(m_u + m_d) + \frac{2}{3}B_0(m_u + m_d - 2m_s)\frac{\sin^2\epsilon}{\cos 2\epsilon}\,,$$

$$M_{K^\pm}^2 = B_0(m_u + m_s)\,,$$

$$M_{K^0}^2 = B_0(m_d + m_s)\,,$$

$$M_\eta^2 = \frac{1}{3}B_0(m_u + m_d + 4m_s) - \frac{2}{3}B_0(m_u + m_d - 2m_s)\frac{\sin^2\epsilon}{\cos 2\epsilon}\,,$$

(2.21)

where B_0 is a parameter from the $\mathcal{O}(p^2)$ meson Lagrangian related to the scalar quark condensate. One can further derive

$$\sin 2\epsilon = \frac{2}{\sqrt{3}}\frac{M_{K^\pm}^2 - M_{K^0}^2}{M_{\pi^0}^2 - M_\eta^2}\,,$$

$$\cos 2\epsilon = \frac{2}{3}\frac{2M_{\pi^\pm}^2 - M_{K^\pm}^2 - M_{K^0}^2}{M_{\pi^0}^2 - M_\eta^2}\,,$$

(2.22)

using eq. (2.17), which is valid at leading order.

Any other particle such as the axion enters the theory in form of an external current. In the present case, we need five axial-vector currents a_μ and $a_{\mu,i}^{(s)}$, $i = 1, \dots, 4$, corresponding to the isovector and isoscalar parts of the axion-matter interaction; compare eq. (2.9). Furthermore, a scalar external field s is needed to account for the explicit chiral symmetry breaking due to the light quark masses. Setting $\chi = 2B_0 s$, it is then convenient to define

$$u_\mu = i\left[u^\dagger \partial_\mu u - u\partial_\mu u^\dagger - iu^\dagger a_\mu u - iua_\mu u^\dagger\right]\,,$$

$$u_{\mu,i} = i\left[-iu^\dagger a_{\mu,i}^{(s)} u - iua_{\mu,i}^{(s)} u^\dagger\right] = 2a_{\mu,i}^{(s)}\,,$$

$$\chi_\pm = u^\dagger \chi u^\dagger \pm u\chi^\dagger u\,,$$

(2.23)

which all transform in the same way under chiral transformations. Additionally, one defines the chiral covariant derivative

$$[\mathcal{D}_\mu, B] = \partial_\mu B + [\Gamma_\mu, B]\,,$$

(2.24)

where

$$\Gamma_\mu = \frac{1}{2}\left[u^\dagger \partial_\mu u + u\partial_\mu u^\dagger - iu^\dagger a_\mu u + iua_\mu u^\dagger\right]$$

(2.25)

is the chiral connection. Assigning systematically a chiral dimension p to these building blocks in order to establish the power-counting method mentioned above, the effective Lagrangian is constructed by considering all combinations allowed by the underlying symmetries. The terms of the meson-baryon Lagrangian then can be arranged according to the chiral dimension,

$$\mathcal{L}_{\Phi B} = \mathcal{L}_{\Phi B}^{(1)} + \mathcal{L}_{\Phi B}^{(2)} + \mathcal{L}_{\Phi B}^{(3)} + \cdots + \mathcal{L}_\Phi^{(2)} + \mathcal{L}_\Phi^{(4)} + \dots\,,$$
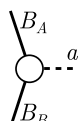
(2.26)

where the superscript "(i)" denotes the Lagrangian containing all terms of $\mathcal{O}(p^i)$. In the case of the purely mesonic Lagrangians $\mathcal{L}_\Phi^{(i)}$, i is restricted to even numbers. Chiral loops start contributing at $\mathcal{O}(p^3)$ (see section 3.6), which means that $\mathcal{L}_{\Phi B}^{(3)}$ contains a number of low-energy constants and counter-terms needed for the renormalization (ch. 3.4 and 3.5). Note that in non-relativistic HBCHPT the Lagrangian (2.26) contains an inverse power series in m_B, the average octet mass in the chiral limit, which starts contributing at $\mathcal{O}(p^2)$ (see section 3.2). The leading order meson-baryon Lagrangian is given by

$$\mathcal{L}_{\Phi B}^{(1)} = \left\langle i \bar{B} v^\mu \left[\mathcal{D}_\mu, B \right] \right\rangle + D \left\langle \bar{B} S^\mu \left\{ u_\mu, B \right\} \right\rangle + F \left\langle \bar{B} S^\mu \left[u_\mu, B \right] \right\rangle + D^i \left\langle \bar{B} S^\mu u_{\mu,i} B \right\rangle, \quad (2.27)$$

which in contrast to the two-flavor case contains two isovector axial-vector coupling constants D and F, and in the present case of axionic HBCHPT the coupling constants D^i to account for the isoscalar interactions.

2.3 General form of the axion-baryon coupling

For any process $B_B \to B_A + a$, where B_A and B_B denote arbitrary baryons and a an axion, the general Feynman rule for the vertex in the baryon rest frame has the form

$$\begin{array}{c} B_A \\ \diagup \\ \bigcirc \cdots a \\ \diagup \\ B_B \end{array} = G_{aAB} \left(S \cdot q \right), \quad (2.28)$$

where q_μ is the four-momentum of the outgoing axion. The coupling constant G_{aAB} consists of a power series in $1/f_a$

$$G_{aAB} = -\frac{1}{f_a} g_{aAB} + \mathcal{O}\left(\frac{1}{f_a^2} \right). \quad (2.29)$$

Due to the expected huge value of f_a, it is sufficient to determine the leading order term $\propto g_{aAB}/f_a$, where

$$g_{aAB} = g_{aAB}^{(1)} + g_{aAB}^{(2)} + g_{aAB}^{(3)} + \ldots \quad (2.30)$$

can be expanded according to the power counting rules of HBCHPT. Here in particular

$$\begin{aligned} g_{aAB}^{(1)} &= g_{aAB}^{\text{LO, tree}}, \\ g_{aAB}^{(2)} &= g_{aAB}^{1/m_B}, \\ g_{aAB}^{(3)} &= g_{aAB}^{\text{N}^2\text{LO, tree}} + g_{aAB}^{1/m_B^2} + g_{aAB}^{\text{LO, loop}}, \end{aligned} \quad (2.31)$$

where g_{aAB}^{LO} and $g_{aAB}^{\text{N}^2\text{LO}}$ refer to the contributions from the leading and next-to-next-to-leading order chiral Lagrangian, i.e. from $\mathcal{L}_{\Phi B}^{(1)}$ and $\mathcal{L}_{\Phi B}^{(3)}$ of eq. (2.26), respectively. Furthermore, g_{aAB}^{1/m_B} and g_{aAB}^{1/m_B^2} refer to the $\mathcal{O}(m_B^{-1})$ and $\mathcal{O}(m_B^{-2})$ contributions from the expansion in the average baryon mass in the chiral limit m_B, which additionally appear in HBCHPT (see section 3.2). In this paper, we will determine each of these contributions to g_{aAB} up to $\mathcal{O}\left(p^3 \right)$.

As we work in the physical basis, A and B in G_{aAB} and g_{aAB} can be understood as SU(3) indices running from 1 to 8 that directly relate to the physical baryon fields. G_{a44}, for

instance, thus gives the axion-proton coupling G_{app}, whereas G_{a66} gives the axion-neutron coupling G_{ann} (see appendix A). In this basis, the matrix of G_{aAB} is mostly diagonal as we exclude flavor-changing axion-quark couplings, i.e. $G_{aAB} = 0$ for $A \neq B$, with the only exception of $G_{a38} = G_{a83}$, i.e. $G_{a\Sigma^0\Lambda}$, which is related to the Σ^0–Λ mixing.

3 Determining the axion-baryon coupling

3.1 Leading order: tree level contributions

From the Lagrangian eq. (2.27), we can determine the leading order axion-baryon coupling by inserting[1]

$$\Gamma_\mu = 0 \,,$$

$$u_\mu = \frac{\partial_\mu a}{f_a} \left(c^{(3)} \lambda_3 + c^{(8)} \lambda_8 \right) ,$$

$$u_{\mu,i} = c_i \frac{\partial_\mu a}{f_a} \mathbb{1} \,,$$

(3.1)

which gives

$$\mathcal{L}_{\Phi B}^{(1),\text{int}} = \frac{g_{AB}}{f_a} \bar{B}_A \left(S \cdot \partial a \right) B_B \,,$$

(3.2)

where A and B are SU(3) indices in the physical basis (see appendix A). Here we have defined

$$g_{AB} = \frac{1}{2} \left\{ D \left(c^{(3)} \left\langle \tilde{\lambda}_A^\dagger \left\{ \lambda_3, \tilde{\lambda}_B \right\} \right\rangle + c^{(8)} \left\langle \tilde{\lambda}_A^\dagger \left\{ \lambda_8, \tilde{\lambda}_B \right\} \right\rangle \right) \right.$$
$$\left. + F \left(c^{(3)} \left\langle \tilde{\lambda}_A^\dagger \left[\lambda_3, \tilde{\lambda}_B \right] \right\rangle + c^{(8)} \left\langle \tilde{\lambda}_A^\dagger \left[\lambda_8, \tilde{\lambda}_B \right] \right\rangle \right) + 2 c_i D^i \delta_{AB} \right\} .$$

(3.3)

The matrix elements of g_{AB} are given in table 4 in appendix B. As we are working in the physical basis including the Σ^0–Λ mixing, g_{AB} actually includes effects of $\mathcal{O}(p^2)$. The pure leading order axion-baryon coupling is found by setting $\epsilon = 0$, i.e. by replacing $\tilde{\lambda}_{A/B} \rightarrow \hat{\lambda}_{A/B}$, see eq. (A.14) of appendix A. In this case, λ_3 and λ_8 can be replaced by $\hat{\lambda}_3$ and $\hat{\lambda}_8$ so that the coupling can be expressed by means of the structure constants $\hat{f}_{ABC}$ and $\hat{d}_{ABC}$:

$$g_{AB}^0 = g_{AB}|_{\epsilon=0} = c^{(3)} \left(D\hat{d}_{AB3} - F\hat{f}_{AB3} \right) + c^{(8)} \left(D\hat{d}_{AB8} - F\hat{f}_{AB8} \right) + c_i D^i \delta_{AB} . \quad (3.4)$$

It is hence clear that $g_{aAB}^{(1)}$ in eq. (2.30) is simply given by

$$g_{aAB}^{(1)} = g_{AB}^0. \tag{3.5}$$

---

[1]Note that in our previous work [58], there is a typo in the corresponding SU(2) equations, i.e. eqs. (3.16) and (3.21): $\tilde{u}_{\mu,i}$ is not given by $\tilde{u}_{\mu,i} = c_i \frac{\partial_\mu a}{f_a} \tau_3$. The correct expression is $\tilde{u}_{\mu,i} = c_i \frac{\partial_\mu a}{f_a} \mathbb{1}$.

3.2 Expansion in the baryon mass

The Lagrangian containing the corrections due to the finite baryon masses m_B in the heavy-baryon expansion up to $\mathcal{O}\left(p^3\right)$ corresponding to terms proportional to $1/m_B$ and $1/m_B^2$ is given by [93]

$$\mathcal{L}^{1/m_B} = \bar{B}_A \left\{ \frac{1}{2m_B}\gamma_0 \left[\mathcal{B}_{(1)}^{AC}\right]^\dagger \gamma_0 \mathcal{B}_{(1)}^{CB} - \frac{1}{4m_B^2}\gamma_0 \left[\mathcal{B}_{(1)}^{AC}\right]^\dagger \gamma_0 \mathcal{A}_{(1)}^{CD}\mathcal{B}_{(1)}^{DB} \right\} B_B \,. \tag{3.6}$$

Here

$$\mathcal{A}_{(1)}^{AB} = \frac{1}{2}\Big(\left\langle \tilde{\lambda}_A^\dagger \left[i\left(v\cdot\mathcal{D}\right),\tilde{\lambda}_B\right]\right\rangle + D \left\langle \tilde{\lambda}_A^\dagger \left\{\left(S\cdot u\right),\tilde{\lambda}_B\right\}\right\rangle$$

$$+ F \left\langle \tilde{\lambda}_A^\dagger \left[\left(S\cdot u\right),\tilde{\lambda}_B\right]\right\rangle + D^i \left\langle \tilde{\lambda}_A^\dagger \left(S\cdot u_i\right)\tilde{\lambda}_B\right\rangle\Big), \tag{3.7}$$

and

$$\mathcal{B}_{(1)}^{AB} = \frac{1}{2}\Big(\left\langle \tilde{\lambda}_A^\dagger \left[i\gamma^\mu\mathcal{D}_\mu^\perp,\tilde{\lambda}_B\right]\right\rangle - \frac{D}{2} \left\langle \tilde{\lambda}_A^\dagger \left\{\left(v\cdot u\right)\gamma_5,\tilde{\lambda}_B\right\}\right\rangle$$

$$- \frac{F}{2} \left\langle \tilde{\lambda}_A^\dagger \left[\left(v\cdot u\right)\gamma_5,\tilde{\lambda}_B\right]\right\rangle - \frac{D^i}{2} \left\langle \tilde{\lambda}_A^\dagger \left(v\cdot u_i\right)\gamma_5\tilde{\lambda}_B\right\rangle\Big), \tag{3.8}$$

where for any four-vector x_μ

$$x_\mu^\perp = v_\mu\left(v\cdot x\right) - x_\mu \,. \tag{3.9}$$

In the present case of axionic HBCHPT, we find

$$\mathcal{A}_{(1)}^{AB} = i\left(v\cdot\partial\right)\delta_{AB} + \frac{1}{f_a}g_{AB}\left(S\cdot\partial a\right), \tag{3.10}$$

$$\mathcal{B}_{(1)}^{AB} = i\gamma^\mu\partial_\mu^\perp\delta_{AB} - \frac{1}{2f_a}g_{AB}\left(v\cdot\partial a\right)\gamma_5 \,, \tag{3.11}$$

with g_{AB} as defined in eq. (3.3), so that

$$\mathcal{L}^{1/m_B} = \frac{1}{f_a}\bar{B}_A \bigg\{ \frac{ig_{AB}}{2m_B}\left\{\left(S\cdot\partial\right),\left(v\cdot\partial a\right)\right\} + \frac{g_{AB}}{4m_B^2}\Big[-\partial^\mu\left(S\cdot\partial a\right)\partial_\mu + \left(v\cdot\partial\right)\left(S\cdot\partial a\right)\left(v\cdot\partial\right)$$

$$- \left(\left\{\left(S\cdot\partial\right),\left(v\cdot\partial a\right)\right\}\left(v\cdot\partial\right)+\text{h.c.}\right)$$

$$+ \left(\left(S\cdot\partial\right)\left(\partial a\cdot\partial\right)+\text{h.c.}\right)\Big] \bigg\} B_B \,. \tag{3.12}$$

Let p be the momentum of the incoming baryon, p' the momentum of the outgoing baryon, and $\omega^{(\prime)} = \left(v\cdot p^{(\prime)}\right)$, then the resulting vertex Feynman rule reads

$$= -\frac{g_{AB}}{f_a}\left\{ \frac{1}{2m_B}\left(\omega - \omega'\right) - \frac{1}{4m_B^2}\left(\omega^2 - \omega'^2 + \omega\omega' - p^2\right)\right\}\left(S\cdot q\right)$$

$$+ \frac{g_{AB}}{f_a}\left\{ \frac{1}{m_B}\left(\omega - \omega'\right) - \frac{1}{2m_B^2}\left(\omega^2 - \omega'^2 - \frac{1}{2}\left(p^2 - p'^2\right)\right)\right\}\left(S\cdot p\right), \tag{3.13}$$

– 11 –

134

which is in complete analogy to the SU(2) case [58]. In the baryon rest frame with $p = 0$, $\omega = 0$, $v = (1, 0, 0, 0)^{\mathrm{T}}$, and $\omega' = (v \cdot p') = -(v \cdot q) = -q_0 \ll m_B$, where q_0 is the relativistic energy of the outgoing axion, we finally find (see eqs. (2.30) and (2.31))

$$g_{aAB}^{\mathrm{LO,\ tree}} + g_{aAB}^{1/m_B} + g_{aAB}^{1/m_B^2} = g_{AB} \left\{ 1 + \frac{q_0}{2 m_B} + \frac{q_0^2}{4 m_B^2} \right\}. \tag{3.14}$$

3.3 Next-to-next-to-leading order: contributions from χ_-

At next-to-next-to-leading order, there are several contributions that have to be considered. We can differentiate terms with finite low-energy constants (LECs) that are $\propto \chi_-$, terms with LECs having finite and ultraviolet (UV) divergent pieces $\propto \chi_+$, and terms proportional some LECs that have no finite pieces serving as counter-terms to cancel UV divergences from the loop contributions. We start with the former.

Up to $\mathcal{O}(1/f_a)$, χ_-, see eqs. (2.6) and (2.23), can be written as

$$\chi_- = \frac{4 i M_{\pi^\pm}^2}{f_a} \frac{z}{(1+z)^2} \left(1 + \frac{w}{1+z} \right)^{-1} a \mathbb{1}, \tag{3.15}$$

where $M_{\pi^\pm}^2$ is the leading order mass of the charged pions given in eq. (2.21). The contributing terms of $\mathcal{L}_{\Phi B}^{(3)}$ are (here and in the following section, we enumerate the LECs according to the list of terms in ref. [95])

$$\mathcal{L}^{\chi_-} = -i d_2 \left(\left\langle \left(\partial \bar{B} \cdot S \right) \chi_- B \right\rangle + \left\langle \bar{B} \chi_- (S \cdot \partial B) \right\rangle \right)$$
$$- i d_3 \left(\left\langle \left(\partial \bar{B} \cdot S \right) \langle \chi_- \rangle B \right\rangle + \left\langle \bar{B} \langle \chi_- \rangle (S \cdot \partial B) \right\rangle \right). \tag{3.16}$$

Inserting eq. (3.15) yields

$$\begin{array}{l} \text{(diagram: vertex with } B_A,\ B_B,\ a) \end{array} = \frac{4 M_{\pi^\pm}^2}{f_a} \frac{z}{(1+z)^2} \left(1 + \frac{w}{1+z} \right)^{-1} (d_2 + 3 d_3)\, \delta_{AB}\, (S \cdot q). \tag{3.17}$$

The reason for writing the coupling in this way is to match it to the corresponding terms in the SU(2) case, which are given by [58]

$$\begin{array}{l} \text{(diagram: vertex with } N,\ N,\ a) \end{array} = \frac{4 M_{\pi^\pm}^2}{f_a} \frac{z}{(1+z)^2} (d_{18} + 2 d_{19}) (S \cdot q), \tag{3.18}$$

where N is the nucleon field, and d_{18} and d_{19} are LECs from the next-to-next-to-leading order SU(2) πN Lagrangian [96]. Apart from a substitution of the LECs, the main difference between the SU(3) case, eq. (3.17), and the SU(2) case, eq. (3.18), is the explicit effect of the strange quark mass m_s in the factor $(1 + w/(1+z))^{-1}$, which reduces to unity at $m_s \to \infty$, i.e. $w \to 0$. In the SU(3) case, the finite value of w accounts for a correction of about two percent.

3.4 Next-to-next-to-leading order: contributions from χ_+

From eqs. (2.6) and (2.23), one can readily determine that

$$\chi_+ = 4B_0\mathcal{M}_q + \mathcal{O}\left(f_a^{-2}\right). \tag{3.19}$$

The relevant terms from $\mathcal{L}_{\Phi B}^{(3)}$ are [95]

$$
\begin{aligned}
\mathcal{L}^{\chi_+} = {} & d_{41}(\lambda)\left(\left\langle \bar{B}S^\mu\left[u_\mu,[\chi_+,B]\right]\right\rangle + \left\langle \bar{B}S^\mu\left[\chi_+,[u_\mu,B]\right]\right\rangle\right) \\
& + d_{42}(\lambda)\left(\left\langle \bar{B}S^\mu\left[u_\mu,\{\chi_+,B\}\right]\right\rangle + \left\langle \bar{B}S^\mu\left\{\chi_+,[u_\mu,B]\right\}\right\rangle\right) \\
& + d_{43}(\lambda)\left(\left\langle \bar{B}S^\mu\left\{u_\mu,[\chi_+,B]\right\}\right\rangle + \left\langle \bar{B}S^\mu\left[\chi_+,\{u_\mu,B\}\right]\right\rangle\right) \\
& + d_{44}(\lambda)\left(\left\langle \bar{B}S^\mu\left\{u_\mu,\{\chi_+,B\}\right\}\right\rangle + \left\langle \bar{B}S^\mu\left\{\chi_+,\{u_\mu,B\}\right\}\right\rangle\right) \\
& + d_{45}(\lambda)\left\langle \bar{B}S^\mu\left[u_\mu,B\right]\right\rangle\langle\chi_+\rangle + d_{46}(\lambda)\left\langle \bar{B}S^\mu\left\{u_\mu,B\right\}\right\rangle\langle\chi_+\rangle \\
& + d_{47}(\lambda)\left\langle \bar{B}S^\mu B\right\rangle\langle u_\mu\chi_+\rangle + d_{43}^i(\lambda)\left\langle \bar{B}\left(S\cdot u_i\right)\left[\chi_+,B\right]\right\rangle \\
& + d_{44}^i(\lambda)\left\langle \bar{B}\left(S\cdot u_i\right)\left\{\chi_+,B\right\}\right\rangle + d_{46}^i(\lambda)\left\langle \bar{B}\left(S\cdot u_i\right)B\right\rangle\langle\chi_+\rangle.
\end{aligned} \tag{3.20}
$$

The LECs depend on the scale λ and are given by

$$d_k^{(i)}(\lambda) = d_k^{(i),r}(\lambda) + \frac{\beta_k^{(i)}}{F_p^2}L(\lambda), \qquad k = \{41,\dots,47\}. \tag{3.21}$$

In this equation, $d_k^{(i),r}(\lambda)$ refer to the renormalized LECs, and $L(\lambda)$ contains the pole for spacetime dimension $d = 4$,

$$L(\lambda) = \frac{\lambda^{d-4}}{(4\pi)^2}\left(\frac{1}{d-4} - \frac{1}{2}\left[\ln(4\pi) - \gamma + 1\right]\right), \tag{3.22}$$

where γ is the Euler-Mascheroni constant. The β-functions are set to cancel the divergences of the one-loop functional, as discussed below. We write the resulting tree-level vertex as

$$= -\frac{4M_{\pi^\pm}^2}{f_a}\frac{z}{1+z}\hat{d}_{AB}(\lambda)\left(S\cdot q\right), \tag{3.23}$$

where we have set

$$
\begin{aligned}
\hat{d}_{AB}(\lambda) = {} & \frac{1}{2m_u}\Bigg(c^{(3)}\Big\{ d_{41}(\lambda)\left(\left\langle \hat{\lambda}_A^\dagger\left[\lambda_3,\left[\mathcal{M}_q,\hat{\lambda}_B\right]\right]\right\rangle + \left\langle \hat{\lambda}_A^\dagger\left[\mathcal{M}_q,\left[\lambda_3,\hat{\lambda}_B\right]\right]\right\rangle\right) \\
& + d_{42}(\lambda)\left(\left\langle \hat{\lambda}_A^\dagger\left[\lambda_3,\left\{\mathcal{M}_q,\hat{\lambda}_B\right\}\right]\right\rangle + \left\langle \hat{\lambda}_A^\dagger\left\{\mathcal{M}_q,\left[\lambda_3,\hat{\lambda}_B\right]\right\}\right\rangle\right) \\
& + d_{43}(\lambda)\left(\left\langle \hat{\lambda}_A^\dagger\left\{\lambda_3,\left[\mathcal{M}_q,\hat{\lambda}_B\right]\right\}\right\rangle + \left\langle \hat{\lambda}_A^\dagger\left[\mathcal{M}_q,\left\{\lambda_3,\hat{\lambda}_B\right\}\right]\right\rangle\right) \\
& + d_{44}(\lambda)\left(\left\langle \hat{\lambda}_A^\dagger\left\{\lambda_3,\left\{\mathcal{M}_q,\hat{\lambda}_B\right\}\right\}\right\rangle + \left\langle \hat{\lambda}_A^\dagger\left\{\mathcal{M}_q,\left\{\lambda_3,\hat{\lambda}_B\right\}\right\}\right\rangle\right)
\end{aligned}
$$

$$+ d_{45}(\lambda) \left\langle \hat{\lambda}_A^\dagger \left[\lambda_3, \hat{\lambda}_B \right] \right\rangle \langle \mathcal{M}_q \rangle + d_{46}(\lambda) \left\langle \hat{\lambda}_A^\dagger \left\{ \lambda_3, \hat{\lambda}_B \right\} \right\rangle \langle \mathcal{M}_q \rangle$$

$$+ 2d_{47}(\lambda) \delta_{AB} \left\langle \lambda_3 \mathcal{M}_q \right\rangle \Big\}$$

$$+ c^{(8)} \Big\{ d_{41}(\lambda) \left(\left\langle \hat{\lambda}_A^\dagger \left[\lambda_8, \left[\mathcal{M}_q, \hat{\lambda}_B \right] \right] \right\rangle + \left\langle \hat{\lambda}_A^\dagger \left[\mathcal{M}_q, \left[\lambda_8, \hat{\lambda}_B \right] \right] \right\rangle \right)$$

$$+ d_{42}(\lambda) \left(\left\langle \hat{\lambda}_A^\dagger \left[\lambda_8, \left\{ \mathcal{M}_q, \hat{\lambda}_B \right\} \right] \right\rangle + \left\langle \hat{\lambda}_A^\dagger \left\{ \mathcal{M}_q, \left[\lambda_8, \hat{\lambda}_B \right] \right\} \right\rangle \right)$$

$$+ d_{43}(\lambda) \left(\left\langle \hat{\lambda}_A^\dagger \left\{ \lambda_8, \left[\mathcal{M}_q, \hat{\lambda}_B \right] \right\} \right\rangle + \left\langle \hat{\lambda}_A^\dagger \left[\mathcal{M}_q, \left\{ \lambda_8, \hat{\lambda}_B \right\} \right] \right\rangle \right)$$

$$+ d_{44}(\lambda) \left(\left\langle \hat{\lambda}_A^\dagger \left\{ \lambda_8, \left\{ \mathcal{M}_q, \hat{\lambda}_B \right\} \right\} \right\rangle + \left\langle \hat{\lambda}_A^\dagger \left\{ \mathcal{M}_q, \left\{ \lambda_8, \hat{\lambda}_B \right\} \right\} \right\rangle \right)$$

$$+ d_{45}(\lambda) \left\langle \hat{\lambda}_A^\dagger \left[\lambda_8, \hat{\lambda}_B \right] \right\rangle \langle \mathcal{M}_q \rangle + d_{46}(\lambda) \left\langle \hat{\lambda}_A^\dagger \left\{ \lambda_8, \hat{\lambda}_B \right\} \right\rangle \langle \mathcal{M}_q \rangle$$

$$+ 2d_{47}(\lambda) \delta_{AB} \left\langle \lambda_8 \mathcal{M}_q \right\rangle \Big\}$$

$$+ c_i \Big\{ d_{43}^i(\lambda) \left\langle \hat{\lambda}_A \left[\mathcal{M}_q, \hat{\lambda}_B \right] \right\rangle + d_{44}^i(\lambda) \left\langle \hat{\lambda}_A \left\{ \mathcal{M}_q, \hat{\lambda}_B \right\} \right\rangle$$

$$+ 2d_{46}^i(\lambda) \delta_{AB} \left\langle \mathcal{M}_q \right\rangle \Big\} \bigg). \tag{3.24}$$

The matrix elements of $\hat{d}_{AB}$ are given in eqs. (B.1)–(B.9) of appendix B.

3.5 Next-to-next-to-leading order: counter-terms

The counter-terms needed for the renormalization have been worked out in ref. [93]. For the present case, we need the terms $i = \{36, 37, 38, 39\}$ from this paper, which are given by

$$\begin{aligned} \mathcal{L}^{\text{c.t.}} &= d_{36}(\lambda) \left\langle \left(v \cdot \partial \bar{B} \right) \left\{ (S \cdot u), (v \cdot \partial B) \right\} \right\rangle \\ &+ d_{37}(\lambda) \left\langle \left(v \cdot \partial \bar{B} \right) \left[(S \cdot u), (v \cdot \partial B) \right] \right\rangle \\ &+ d_{38}(\lambda) \left\langle \bar{B} \left\{ \left[(v \cdot \partial), \left[(v \cdot \partial), (S \cdot u) \right] \right], B \right\} \right\rangle \\ &+ d_{39}(\lambda) \left\langle \bar{B} \left[\left[(v \cdot \partial), \left[(v \cdot \partial), (S \cdot u) \right] \right], B \right] \right\rangle \\ &+ d_{36}^i(\lambda) \left\langle \left(v \cdot \partial \bar{B} \right) (S \cdot u_i) (v \cdot \partial B) \right\rangle \\ &+ d_{38}^i(\lambda) \left\langle \bar{B} \left[(v \cdot \partial), \left[(v \cdot \partial), (S \cdot u_i) \right] \right] B \right\rangle, \end{aligned} \tag{3.25}$$

where we have added two terms in order to account for the isoscalar interactions. The LECs have no finite part, i.e.

$$d_k^{(i)}(\lambda) = \frac{\beta_k^{(i)}}{F_p^2} L(\lambda), \qquad k = \{36, \dots, 39\}. \tag{3.26}$$

Their contribution to the tree-level vertex is given by

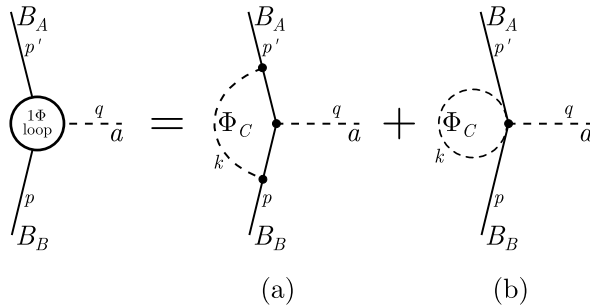$$= -\frac{1}{f_a} \hat{d}_{AB}^{\text{c.t.}}(\lambda) (S \cdot q), \tag{3.27}$$

– 14 –

Figure 1. Non-vanishing meson loop contributions to $B_B \to B_A + a$.

with

$$
\begin{aligned}
\hat{d}_{AB}^{c.t.}(\lambda) = & \left(d_{36}(\lambda)\omega\omega' - d_{38}(\lambda)\left(\omega - \omega'\right)^2 \right) \left(c^{(3)}\hat{d}_{AB3} + c^{(8)}\hat{d}_{AB8} \right) \\
& - \left(d_{37}(\lambda)\omega\omega' - d_{39}(\lambda)\left(\omega - \omega'\right)^2 \right) \left(c^{(3)}\hat{f}_{AB3} + c^{(8)}\hat{f}_{AB8} \right) \\
& + \left(d_{36}^i(\lambda)\omega\omega' - d_{38}^i(\lambda)\left(\omega - \omega'\right)^2 \right) c_i \delta_{AB} \, .
\end{aligned}
\tag{3.28}
$$

3.6 Loops

There are only two non-vanishing single meson loops that contribute to the $\mathcal{O}(p^3)$ axion-baryon vertex at $\mathcal{O}(1/f_a)$, which are shown in figure 1. In this figure, mesons are identified by means of the SU(3) index C in the physical basis including the π^0–η mixing, cf. eqs. (2.19) and (A.3). Note that the potential diagrams with a $a\Phi BB$ vertex and a meson line connected to one baryon leg vanish because $(v \cdot S) = 0$, see eq. (2.14), as has been shown in ref. [58] for the corresponding diagrams in the SU(2) case, which have the same topology.

3.6.1 Diagram (a)

Using the leading order meson-baryon vertex rule, one finds

$$
\begin{aligned}
\text{(a)} = & \frac{1}{f_a F_p^2} \sum_C g_{ABC}^{(a)} S^\mu \left(S \cdot q \right) S^\nu \frac{1}{i} \int \frac{\mathrm{d}^d k}{(2\pi)^d} \frac{k_\mu k_\nu}{(k^2 - M_{\Phi_C}^2 + i\eta)(\omega' - v \cdot k + i\eta)(\omega - v \cdot k + i\eta)} \\
= & \frac{1}{6 f_a} \frac{1}{(4\pi F_p)^2} \sum_C g_{ABC}^{(a)} \Bigg\{ - M_{\Phi_C}^2 \\
& + \frac{1}{\omega - \omega'} \left(\omega^3 - \omega'^3 + 2 \left[\left(M_{\Phi_C}^2 - \omega^2 \right)^{\frac{3}{2}} \arccos \frac{-\omega}{M_{\Phi_C}} - \left(M_{\Phi_C}^2 - \omega'^2 \right)^{\frac{3}{2}} \arccos \frac{-\omega'}{M_{\Phi_C}} \right] \right) \\
& + \left(3 M_{\Phi_C}^2 - 2 \left(\omega - \omega' \right)^2 - 6\omega\omega' \right) \left((4\pi)^2 L(\lambda) + \ln \frac{M_{\Phi_C}}{\lambda} \right) \Bigg\} \left(S \cdot q \right) ,
\end{aligned}
\tag{3.29}
$$

– 15 –

where we have applied dimensional regularization and used the properties in eq. (2.14). Moreover, we have defined

$$
\begin{aligned}
g_{ABC}^{(a)} = \frac{1}{4} \sum_{D,E} &\left(D \left\langle \hat{\lambda}_A^\dagger \left\{ \tilde{\lambda}_C, \hat{\lambda}_E \right\} \right\rangle + F \left\langle \hat{\lambda}_A^\dagger \left[\tilde{\lambda}_C, \hat{\lambda}_E \right] \right\rangle \right) g_{ED}^0 \\
&\times \left(D \left\langle \hat{\lambda}_D^\dagger \left\{ \tilde{\lambda}_C^\dagger, \hat{\lambda}_B \right\} \right\rangle + F \left\langle \hat{\lambda}_D^\dagger \left[\tilde{\lambda}_C^\dagger, \hat{\lambda}_B \right] \right\rangle \right),
\end{aligned}
\tag{3.30}
$$

in order to handle all meson loops for all baryons B_A and B_B at the same time. Here g_{ED}^0 refers to eq. (3.4), the leading order axion-baryon coupling. Equation (3.29) contains UV divergences, which will be treated below in section 3.6.3. The expression for diagram (a) can be simplified by considering the baryon rest frame and expanding around $q_0 \ll M_{\Phi_C}$ for all mesons Φ_C, which yields

$$
\begin{aligned}
\text{(a)} = \frac{1}{6 f_a} \sum_C g_{ABC}^{(a)} \left(\frac{M_{\Phi_C}}{4\pi F_p} \right)^2 &\left\{ 1 + \frac{3\pi}{2} \frac{q_0}{M_{\Phi_C}} - \frac{5}{3} \left(\frac{q_0}{M_{\Phi_C}} \right)^2 \right. \\
&\left. + \left(3 - 2 \left(\frac{q_0}{M_{\Phi_C}} \right)^2 \right) \left((4\pi)^2 L(\lambda) + \ln \frac{M_{\Phi_C}}{\lambda} \right) \right\} (S \cdot q).
\end{aligned}
\tag{3.31}
$$

3.6.2 Diagram (b)

Expanding u up to order Φ^2 yields

$$
u_\mu = -\frac{\partial_\mu a}{8 f_a F_p^2} \left(c^{(3)} \left[\Phi, [\Phi, \lambda_3] \right] + c^{(8)} \left[\Phi, [\Phi, \lambda_8] \right] \right),
\tag{3.32}
$$

so the vertex rule for the $a B_A B_B \Phi_C \Phi_C$-vertex in the physical basis derived from $\mathcal{L}_{\Phi B}^{(1)}$ can be written as

$$
\frac{1}{f_a F_p^2} g_{ABC}^{(b)} (S \cdot q),
\tag{3.33}
$$

where we have defined the coupling constant

$$
\begin{aligned}
g_{ABC}^{(b)} = \frac{1}{8} \left\{ c^{(3)} \left(D \left\langle \hat{\lambda}_A^\dagger \left\{ \left[\tilde{\lambda}_C, \left[\tilde{\lambda}_C^\dagger, \lambda_3 \right] \right], \hat{\lambda}_B \right\} \right\rangle + F \left\langle \hat{\lambda}_A^\dagger \left[\left[\tilde{\lambda}_C, \left[\tilde{\lambda}_C^\dagger, \lambda_3 \right] \right], \hat{\lambda}_B \right] \right\rangle \right) \right. \\
\left. + c^{(8)} \left(D \left\langle \hat{\lambda}_A^\dagger \left\{ \left[\tilde{\lambda}_C, \left[\tilde{\lambda}_C^\dagger, \lambda_8 \right] \right], \hat{\lambda}_B \right\} \right\rangle + F \left\langle \hat{\lambda}_A^\dagger \left[\left[\tilde{\lambda}_C, \left[\tilde{\lambda}_C^\dagger, \lambda_8 \right] \right], \hat{\lambda}_B \right] \right\rangle \right) \right\}.
\end{aligned}
\tag{3.34}
$$

In fact, this vertex and thus diagram (b) is independent of the mixing angle ϵ so one might as well substitute $\tilde{\lambda}_C \to \hat{\lambda}_C$ in eq. (3.34). Therefore, one can also express the coupling constant by means of the structure constants defined in eqs. (A.9) and (A.14),

$$
g_{ABC}^{(b)} = \frac{1}{4} \sum_{D,E} \hat{f}_{ECD} \left(c^{(3)} \hat{f}_{3CD} \left[D \hat{d}_{AEB} + F \hat{f}_{AEB} \right] + c^{(8)} \hat{f}_{8CD} \left[D \hat{d}_{AEB} + F \hat{f}_{AEB} \right] \right).
\tag{3.35}
$$

The loops of diagram (b) for all mesons Φ_C can then be calculated as

$$
\begin{aligned}
\text{(b)} &= \frac{1}{2f_a F_p^2} \left(S \cdot q\right) \sum_C g_{ABC}^{(b)} \frac{1}{i} \int \frac{\mathrm{d}^d k}{(2\pi)^d} \frac{1}{k^2 - M_{\Phi_C}^2 + i\eta} \\
&= -\frac{1}{f_a F_p^2} \left(S \cdot q\right) \sum_C g_{ABC}^{(b)} M_{\Phi_C}^2 \left(L(\lambda) + \frac{1}{(4\pi)^2} \ln \frac{M_{\Phi_c}}{\lambda} \right).
\end{aligned}
\tag{3.36}
$$

3.6.3 Renormalization

The divergences appearing in the meson loop calculations in dimensional regularization are canceled by setting appropriate β functions for the LECs appearing in $\hat{d}_{AB}(\lambda)$, eq. (3.24), and $\hat{d}_{AB}^{c.t.}(\lambda)$, eq. (3.27),

$$
\begin{aligned}
\beta_{36} &= 2D\left(D^2 + 3F^2\right), & \beta_{36}^i &= -\frac{4}{3}D^i\left(13D^2 + 9F^2\right), \\
\beta_{37} &= \frac{2}{3}F\left(5D^2 - 9F^2\right), & \beta_{38} &= -\frac{2}{3}D\left(D^2 + 3F^2\right), \\
\beta_{38}^i &= \frac{4}{9}D^i\left(13D^2 + 9F^2\right), & \beta_{39} &= -\frac{2}{9}F\left(5D^2 - 9F^2\right), \\
\beta_{41} &= -\frac{1}{48}D\left(9D^2 + 7F^2 - 9\right), & \beta_{42} &= -\frac{3}{16}F\left(D^2 - F^2 - 1\right), \\
\beta_{43} &= -\frac{1}{48}F\left(7D^2 + 9F^2 - 9\right), & \beta_{43}^i &= -\frac{5}{6}DFD^i, \\
\beta_{44} &= -\frac{1}{48}D\left(23D^2 + 9F^2 - 9\right), & \beta_{44}^i &= -\frac{1}{4}D^i\left(D^2 - 3F^2\right), \\
\beta_{45} &= -\frac{1}{36}F\left(D^2 - 9F^2 - 9\right), & \beta_{46} &= \frac{1}{36}D\left(17D^2 - 9F^2 + 9\right), \\
\beta_{46}^i &= \frac{1}{18}D^i\left(13D^2 + 9F^2\right) & \beta_{47} &= \frac{1}{2}D\left(D^2 + 3F^2 - 1\right),
\end{aligned}
\tag{3.37}
$$

of which the β_k's are in accordance with the ones given in ref. [93], and the β_k^i's have been worked out here for the first time. With that, the full renormalized $\mathcal{O}(p^3)$ contribution reads

$$
g_{aAB}^{\text{N}^2\text{LO, tree}} + g_{aAB}^{\text{LO, loop}} = \frac{4M_{\pi^\pm}^2 z}{1+z} \left(\hat{d}_{AB}^r(\lambda) - \frac{d_2 + 3d_3}{1+z+w}\delta_{AB} \right) - \frac{1}{27}g_{AB}^{\text{loop},r} + g_{AB}^{\text{loop,sc}}(\lambda), \tag{3.38}
$$

where we have neglected terms of $\mathcal{O}\left(q_0/M_{\Phi_C}\right)$. Moreover, $\hat{d}_{AB}^r$ refers to eq. (3.24) with renormalized LECs, and

$$
g_{AB}^{\text{loop},r} = \frac{9}{2} \sum_C g_{ABC}^{(a)} \left(\frac{M_{\Phi_C}}{4\pi F_p} \right)^2, \tag{3.39}
$$

$$
g_{AB}^{\text{loop,sc}}(\lambda) = \sum_C \left(-\frac{1}{2}g_{ABC}^{(a)} + g_{ABC}^{(b)} \right) \left(\frac{M_{\Phi_C}}{4\pi F_p} \right)^2 \ln \frac{M_{\Phi_C}}{\lambda}. \tag{3.40}
$$

The matrix elements of $g_{AB}^{\text{loop},r}$ are given in eqs. (B.10)–(B.18) of appendix B.

4 Results

4.1 Leading order axion-baryon coupling

Using the nucleon matrix elements Δq defined by $s^\mu \Delta q = \langle p|\bar{q}\gamma^\mu \gamma_5 q|p\rangle$, s^μ being the spin of the proton, we set

$$(D+F) = g_A = \Delta u - \Delta d, \quad -(D-3F) = \Delta u + \Delta d - 2\Delta s, \tag{4.1}$$
$$D^1 = \Delta u + \Delta d + \Delta s, \qquad D^i = \Delta q_i, \text{ for } i = \{2,3,4\}, \ \Delta q_i = \{\Delta c, \Delta b, \Delta t\},$$

where the respective baryon matrix elements are related to the ones from the nucleons by flavor symmetry. From now on, we neglect terms $\propto \{\Delta c, \Delta b, \Delta t\}$, which basically represent sea quark effects beyond the numerical uncertainties of the dominant contributions of the up, down, and strange quarks (at least in the standard DFSZ scenario, where the couplings to heavy quarks are of the same order as the couplings to the light quarks; if alternatively the couplings X_c, X_b, and X_t or only one or two of them were much stronger than X_u, X_d, and X_s, these sea quark terms could not be ignored any longer). Inserting this into the result for the leading order axion-baryon coupling constant $g_{aAB}^{(1)}$, eq. (3.4) (see also table 4 in appendix B), we find

$$g_{a\Sigma^+\Sigma^+}^{(1)} = -\frac{\Delta u + z\Delta s + w\Delta d}{1+z+w} + \Delta u X_u + \Delta s X_d + \Delta d X_s,$$

$$g_{a\Sigma^-\Sigma^-}^{(1)} = -\frac{\Delta s + z\Delta u + w\Delta d}{1+z+w} + \Delta s X_u + \Delta u X_d + \Delta d X_s,$$

$$g_{a\Sigma^0\Sigma^0}^{(1)} = -\frac{\frac{\Delta u + \Delta s}{2}(1+z) + w\Delta d}{1+z+w} + \frac{\Delta u + \Delta s}{2}(X_u + X_d) + \Delta d X_s,$$

$$g_{app}^{(1)} = -\frac{\Delta u + z\Delta d + w\Delta s}{1+z+w} + \Delta u X_u + \Delta d X_d + \Delta s X_s,$$

$$g_{a\Xi^-\Xi^-}^{(1)} = -\frac{\Delta s + z\Delta d + w\Delta u}{1+z+w} + \Delta s X_u + \Delta d X_d + \Delta u X_s,$$

$$g_{ann}^{(1)} = -\frac{\Delta d + z\Delta u + w\Delta s}{1+z+w} + \Delta d X_u + \Delta u X_d + \Delta s X_s, \tag{4.2}$$

$$g_{a\Xi^0\Xi^0}^{(1)} = -\frac{\Delta d + z\Delta s + w\Delta u}{1+z+w} + \Delta d X_u + \Delta s X_d + \Delta u X_s,$$

$$g_{a\Lambda\Lambda}^{(1)} = -\frac{\frac{\Delta u + 4\Delta d + \Delta s}{6}(1+z) + \frac{2\Delta u - \Delta d + 2\Delta s}{3}w}{1+z+w}$$
$$\qquad\qquad + \frac{\Delta u + 4\Delta d + \Delta s}{6}(X_u + X_d) + \frac{2\Delta u - \Delta d + 2\Delta s}{3}X_s,$$

$$g_{a\Sigma^0\Lambda}^{(1)} = -\frac{\frac{\Delta u - 2\Delta d + \Delta s}{2\sqrt{3}}(1-z)}{1+z+w} + \frac{\Delta u - 2\Delta d + \Delta s}{2\sqrt{3}}(X_u - X_d).$$

In particular, $g_{app}^{(1)}$ and $g_{ann}^{(1)}$ are exactly the same as in the SU(2) case. Using [97]

$$\Delta u = 0.847(50), \qquad \Delta d = -0.407(34), \qquad \Delta s = -0.035(13), \tag{4.3}$$

– 18 –

which correspond to

$$D = \frac{1}{2}\Delta u - \Delta d + \frac{1}{2}\Delta s = 0.813(43)\,,$$

$$F = \frac{1}{2}\Delta u - \frac{1}{2}\Delta s = 0.441(26)\,,$$

$$D^1 = 0.405(62)\,,$$

(4.4)

and [97]

$$z = 0.485(19)\,, \qquad w = 0.025(1)\,,$$

(4.5)

we obtain

$$g_{a\Sigma^+\Sigma^+}^{(1)} = -0.543(34) + 0.847(50)X_u - 0.035(13)X_d - 0.407(34)X_s\,,$$

$$g_{a\Sigma^-\Sigma^-}^{(1)} = -0.242(21) - 0.035(13)X_u + 0.847(50)X_d - 0.407(34)X_s\,,$$

$$g_{a\Sigma^0\Sigma^0}^{(1)} = -0.396(25) + 0.417(25)X_u + 0.395(25)X_d - 0.407(35)X_s\,,$$

$$g_{app}^{(1)} = -0.430(36) + 0.847(50)X_u - 0.407(34)X_d - 0.035(13)X_s\,,$$

$$g_{a\Xi^-\Xi^-}^{(1)} = 0.140(15) - 0.035(13)X_u - 0.407(34)X_d + 0.847(50)X_s\,,$$

(4.6)

$$g_{ann}^{(1)} = -0.002(30) - 0.407(34)X_u + 0.847(50)X_d - 0.035(13)X_s\,,$$

$$g_{a\Xi^0\Xi^0}^{(1)} = 0.267(23) - 0.407(34)X_u - 0.035(13)X_d + 0.847(50)X_s\,,$$

$$g_{a\Lambda\Lambda}^{(1)} = 0.126(25) - 0.147(25)X_u - 0.125(25)X_d + 0.677(35)X_s\,,$$

$$g_{a\Sigma^0\Lambda}^{(1)} = -0.153(10) + 0.463(25)X_u - 0.476(25)X_d + 0.013(1)X_s\,,$$

where we also considered corrections from the non-vanishing mixing angle ϵ related to isospin breaking in the cases of the Σ^0 and the Λ (which is why there also appears a term $\propto X_s$ in $g_{a\Sigma^0\Lambda}^{(1)}$). In table 1, we list the results for the KSVZ axion, where $X_q = 0$, and the DFSZ axion, where the axion-quark couplings X_q depend on the angle β related to the VEVs of the involved Higgs doublets (see above, eq. (2.2)). In the KSVZ model, the strongest couplings are hence to be expected for the Σ^+ and the proton, which is also true for the DFSZ model at small values of $\sin^2\beta$ (in this region, also the Ξ^0 shows a considerably large coupling with an opposite sign). As noted already in many previous works, the axion-neutron coupling in some scenarios is strongly suppressed and might even vanish in the KSVZ model and the DFSZ model at $\sin^2\beta \approx 2/3$ (corresponding to $x = 1/\sqrt{2}$, where x is the ratio of the VEVs of the two Higgs doublets). The axion-neutron coupling is also the only baryon conserving coupling that might vanish in the DFSZ model, as it is the only one that changes its sign when varying $\sin^2\beta$ from zero to unity. At $\sin^2\beta = 1$, also the Σ^0–Λ mixing vertex disappears. At the same value of $\sin^2\beta$, the couplings are somehow "harmonized", i.e. the couplings of the axion to particles of the same strangeness S are approximately the same, which is due to flavor symmetry. In case of the neutron and the proton with $S = 0$ one then has $g_{aAB}^{(1),\sin^2\beta=1} \approx -0.14$, in case of the Σ particles with $S = 1$, one has $g_{aAB}^{(1),\sin^2\beta=1} \approx -0.26$, and in case of the two Ξ baryons with $S = 2$, one has $g_{aAB}^{(1),\sin^2\beta=1} \approx 0.13$. The difference among the particles with the same S can be determined

Process	$g_{aAB}^{(1)}$				
	KSVZ	DFSZ			
		general	$\sin^2 \beta = 0$	$\sin^2 \beta = \frac{2}{3}$	$\sin^2 \beta = 1$
$\Sigma^+ \to \Sigma^+ + a$	$-0.543(34)$	$-0.690(36) + 0.430(21)\sin^2\beta$	$-0.690(36)$	$-0.404(36)$	$-0.261(38)$
$\Sigma^- \to \Sigma^- + a$	$-0.242(21)$	$-0.095(29) - 0.158(21)\sin^2\beta$	$-0.095(29)$	$-0.201(23)$	$-0.254(22)$
$\Sigma^0 \to \Sigma^0 + a$	$-0.396(25)$	$-0.400(29) + 0.143(12)\sin^2\beta$	$-0.400(29)$	$-0.305(27)$	$-0.257(27)$
$p \to p + a$	$-0.430(36)$	$-0.577(38) + 0.430(21)\sin^2\beta$	$-0.577(38)$	$-0.291(38)$	$-0.147(39)$
$\Xi^- \to \Xi^- + a$	$0.140(15)$	$0.287(25) - 0.158(21)\sin^2\beta$	$0.287(25)$	$0.181(17)$	$0.128(16)$
$n \to n + a$	$-0.002(30)$	$0.269(34) - 0.406(21)\sin^2\beta$	$0.269(34)$	$-0.002(31)$	$-0.138(22)$
$\Xi^0 \to \Xi^0 + a$	$0.267(23)$	$0.531(29) - 0.406(21)\sin^2\beta$	$0.531(29)$	$0.267(25)$	$0.131(26)$
$\Lambda \to \Lambda + a$	$0.126(25)$	$0.310(29) - 0.233(12)\sin^2\beta$	$0.310(29)$	$0.155(27)$	$0.077(26)$
$\Sigma^0 \to \Lambda + a$ $\Lambda \to \Sigma^0 + a$	$-0.153(10)$	$-0.308(13) + 0.309(16)\sin^2\beta$	$-0.308(13)$	$-0.102(11)$	$0.000(13)$

Table 1. Leading order axion-baryon couplings $g_{aAB}^{(1)}$ for the KSVZ axion and the DFSZ axion.

as being always

$$\Delta g_{aAB}^{(1),\sin^2\beta=1} = \frac{2 - 4z - w}{3(1 + z + w)}\left(\Delta q_1 - \Delta q_2\right) \approx 0.008\left(\Delta q_1 - \Delta q_2\right), \qquad (4.7)$$

where AB here denotes particles of the same strangeness, and Δq_1 and Δq_2 depends on the quark content of these particles, i.e. $(\Delta q_1 - \Delta q_2) = (\Delta s - \Delta u)$ in the case of the Σ baryons, $(\Delta q_1 - \Delta q_2) = (\Delta d - \Delta u)$ in the case of the nucleons, and $(\Delta q_1 - \Delta q_2) = (\Delta d - \Delta s)$ in the case of the Ξ particles (note that in cases with Σ^0 an additional factor $1/2$ and corrections from $\epsilon \neq 0$ appear in eq. (4.7)).

4.2 Loop corrections and estimation of the NNLO LECs

As stated already, the results for the leading order axion-nucleon coupling in the $N_f = 3$ case are entirely in line with the results of the $N_f = 2$ case, which is also true for the $\mathcal{O}\left(p^2\right)$ and $\mathcal{O}\left(p^3\right)$ corrections stemming from the expansion in $1/m_B$ that appear in the non-relativistic heavy baryon limit, with the only exception that the nucleon mass in the chiral limit m_0 appearing in the SU(2) case is substituted by the average baryon mass in the chiral limit m_B. In the limit of soft axions, i.e. $q_0 \to 0$, these terms, see eq. (3.14), rapidly vanish.

The more significant corrections stem from the one-meson loop contributions, eq. (3.38). For the calculation of the corresponding matrix elements, we use the physical meson masses and decay constants [98, 99], $M_{\pi^\pm} = 139.57\,\mathrm{MeV}$, $M_{\pi^0} = 134.98\,\mathrm{MeV}$, $M_{K^\pm} = 493.68\,\mathrm{MeV}$, $M_{K^0} = 497.61\,\mathrm{MeV}$, $M_\eta = 547.86\,\mathrm{MeV}$, $F_\pi = 92.1(6)\,\mathrm{MeV}$, $F_K = 110.3(5)\,\mathrm{MeV}$, and $F_\eta = 118(9)\,\mathrm{MeV}$. Inserting this numerical input, yields

$$g_{a\Sigma^+\Sigma^+}^{\text{loop}} = 0.096(7) - 0.148(10)X_u - 0.003(5)X_d + 0.202(16)X_s\,,$$
$$g_{a\Sigma^-\Sigma^-}^{\text{loop}} = 0.046(6) - 0.003(5)X_u - 0.148(10)X_d + 0.202(16)X_s\,,$$
$$g_{a\Sigma^0\Sigma^0}^{\text{loop}} = 0.072(7) - 0.076(8)X_u - 0.076(8)X_d + 0.202(16)X_s\,,$$

Process	g_{AB}^{loop}				
	KSVZ	DFSZ			
		general	$\sin^2\beta = 0$	$\sin^2\beta = \frac{2}{3}$	$\sin^2\beta = 1$
$\Sigma^+ \to \Sigma^+ + a$	$0.096(7)$	$0.162(9) - 0.116(7)\sin^2\beta$	$0.162(9)$	$0.085(8)$	$0.046(8)$
$\Sigma^- \to \Sigma^- + a$	$0.046(6)$	$0.064(9) - 0.019(7)\sin^2\beta$	$0.064(9)$	$0.051(6)$	$0.045(8)$
$\Sigma^0 \to \Sigma^0 + a$	$0.072(7)$	$0.114(9) - 0.068(7)\sin^2\beta$	$0.114(9)$	$0.069(8)$	$0.046(8)$
$p \to p + a$	$0.046(5)$	$0.100(6) - 0.094(5)\sin^2\beta$	$0.100(6)$	$0.038(6)$	$0.007(6)$
$\Xi^- \to \Xi^- + a$	$-0.112(8)$	$-0.122(11) + 0.038(8)\sin^2\beta$	$-0.122(11)$	$-0.096(8)$	$-0.083(8)$
$n \to n + a$	$-0.028(5)$	$-0.046(7) + 0.051(5)\sin^2\beta$	$-0.046(7)$	$-0.012(6)$	$0.05(6)$
$\Xi^0 \to \Xi^0 + a$	$-0.145(11)$	$-0.186(13) + 0.102(8)\sin^2\beta$	$-0.186(13)$	$-0.118(12)$	$-0.084(12)$
$\Lambda \to \Lambda + a$	$-0.095(7)$	$-0.112(8) + 0.050(5)\sin^2\beta$	$-0.112(8)$	$-0.079(7)$	$-0.062(8)$
$\Sigma^0 \to \Lambda + a$ $\Lambda \to \Sigma^0 + a$	$0.030(3)$	$0.060(4) - 0.059(3)\sin^2\beta$	$0.060(4)$	$0.020(3)$	$0.001(4)$

Table 2. One-meson loop contributions to the axion-baryon couplings g_{AB}^{loop}, eq. (3.38), for the KSVZ axion and the DFSZ axion calculated at the scale $\lambda = 1\,\mathrm{GeV}$.

$$g_{app}^{\mathrm{loop}} = 0.046(5) - 0.119(11)X_u + 0.098(7)X_d + 0.064(8)X_s\,,$$
$$g_{a\Xi^-\Xi^-}^{\mathrm{loop}} = -0.112(8) + 0.086(8)X_u + 0.182(16)X_d - 0.211(16)X_s\,,$$
$$g_{ann}^{\mathrm{loop}} = -0.028(5) + 0.098(7)X_u - 0.119(11)X_d + 0.064(8)X_s\,,$$
$$g_{a\Xi^0\Xi^0}^{\mathrm{loop}} = -0.145(11) + 0.182(16)X_u + 0.086(8)X_d - 0.211(16)X_s\,,$$
$$g_{a\Lambda\Lambda}^{\mathrm{loop}} = -0.095(7) + 0.099(9)X_u + 0.099(9)X_d - 0.149(9)X_s\,,$$
$$g_{a\Sigma^0\Lambda}^{\mathrm{loop}} = 0.030(3) - 0.089(7)X_u + 0.089(7)X_d + 0.000(1)X_s\,, \tag{4.8}$$

where we have set the scale at $\lambda = 1\,\mathrm{GeV}$. The corresponding results for the KSVZ and DFSZ models are displayed in table 2. As expected, the loop contributions are indeed subleading, where the orders of magnitude of the individual terms range between low $\mathcal{O}\left(10^{-1}\right)$ and $\mathcal{O}\left(10^{-2}\right)$. Note that just using F_π or F_p for all the decay constants does not lead to any notable change in these results since the formal difference is of higher order, $\mathcal{O}(p^5)$, in the chiral expansion.

It is remarkable that the loop corrections to the axion-proton vertex are about one tenth of the full SU(2) result [58], which shows that in this particular case the three-flavor expansion works similar to the case of the magnetic moments [100], but different to the baryon masses [101] or weak hyperon decays [102]. Consequently, the largest uncertainty in these calculations is related to the values of the LECs, as discussed next.

As for the tree-level contributions from the NNLO Lagrangian (see section 3.4), we stated already that the values of the involved LECs are undetermined hitherto. The scale-dependent parts $\propto d_k^r(\lambda)$ are expected to compensate the scale-dependence of the loop contributions, such that the actual observable, g_{aAB}, remains scale-independent at $\mathcal{O}(p^3)$. For the following estimation of these hitherto unknown LECs, we therefore only consider the scale-independent part such that we can leave aside the scale-dependent loop contributions in our final estimation of the axion-baryon coupling at $\mathcal{O}(p^3)$. Our understanding of the problem is a Bayesian one: while formally each LEC may take on any arbitrary value, we

nevertheless expect that with sufficient probability the LECs are restricted to values that lead to NNLO contributions to g_{aAB} of roughly the same order as the loop contributions discussed above. In other words: we assume that these contributions are indeed *sub-*leading in comparison to the leading order contributions, which is basically a naturalness argument [103, 104]. That this assumption is justified in the present case directly follows from the numerical results of the loop corrections discussed before. This argument is of course not universally valid, but it is nevertheless appropriate in a Bayesian sense, meaning that our results from this ansatz can be used as priors in future determinations of the LECs once suitable experimental or lattice QCD data is available for fitting procedures. Although it is not expected that the axion-nucleon coupling will be measured experimentally with sufficient accuracy in the near future, one may use lattice QCD to compute the relevant couplings by introducing an external isoscalar axial source into the QCD action to mimic the axion, and compute the corresponding form factors.

In practice, we performed a Monte Carlo sampling of the ten involved LECs d_{41}^r, ..., d_{47}^r and d_{43}^i, d_{44}^i, and d_{46}^i within a reasonable range of $\mathcal{O}\left(1\,\mathrm{GeV}^{-2}\right)$ and extracted those sets of LECs that lead to NNLO corrections to g_{aAB} of low $\mathcal{O}\left(10^{-1}\right)$. In particular, we set 0.15 as a numerical constraint, which is rather conservative (in view of the loop contributions given above). The allowed regions for the values of the respective LECs are then given by probability distributions of Gaußian type centered around zero (as the overall sign of the NNLO corrections is in principle undetermined from this method). With this approach, one obtains

$$
\begin{aligned}
d_{41}^r &= 0.00(4)\,\mathrm{GeV}^{-2}, & d_{42}^r &= 0.00(4)\,\mathrm{GeV}^{-2}, \\
d_{43}^r &= 0.00(4)\,\mathrm{GeV}^{-2}, & d_{43}^{i,r} &= 0.00(11)\,\mathrm{GeV}^{-2}, \\
d_{44}^r &= 0.00(6)\,\mathrm{GeV}^{-2}, & d_{44}^{i,r} &= 0.00(17)\,\mathrm{GeV}^{-2}, \\
d_{45}^r &= 0.00(6)\,\mathrm{GeV}^{-2}, & d_{46}^r &= 0.00(11)\,\mathrm{GeV}^{-2}, \\
d_{46}^{i,r} &= 0.00(14)\,\mathrm{GeV}^{-2}, & d_{47}^r &= 0.00(14)\,\mathrm{GeV}^{-2}.
\end{aligned}
\tag{4.9}
$$

Moreover, one finds that some of the extrapolated probability distributions of the LECs are correlated. The most important correlation coefficients are given by

$$
\begin{aligned}
\mathrm{corr}(d_{41}^r, d_{44}^r) &= 0.72, & \mathrm{corr}(d_{41}^r, d_{46}^r) &= -0.59, \\
\mathrm{corr}(d_{41}^r, d_{47}^r) &= -0.84, & \mathrm{corr}(d_{44}^r, d_{46}^r) &= -0.89, \\
\mathrm{corr}(d_{44}^r, d_{47}^r) &= -0.85, & \mathrm{corr}(d_{46}^r, d_{47}^r) &= 0.70, \\
\mathrm{corr}(d_{42}^r, d_{45}^r) &= -0.85, & \mathrm{corr}(d_{44}^{i,r}, d_{46}^{i,r}) &= -0.84,
\end{aligned}
$$

while all other correlation coefficients are negligibly small.

If one additionally considers the large-N_c approach, where N_c is the number of colors, it is to be expected that the LECs for the terms with two flavor traces ($d_{45,46,47}^r$ and $d_{46}^{i,r}$) are suppressed relative to those with only one flavor trace ($d_{41,42,43,44}^r$ and $d_{43,44}^{i,r}$) by $\mathcal{O}\left(1/N_c\right)$; see, e.g., refs. [105, 106]. Therefore, we performed another Monte Carlo sampling for the LECs, where this expectation is taken into account, namely by assigning a larger

probability to such sets obeying this expected rule in comparison to sets of LECs deviating from it, which are considered less probable. The result is

$$d_{41}^r = 0.00(3)\,\mathrm{GeV}^{-2}, \qquad\qquad d_{42}^r = 0.00(2)\,\mathrm{GeV}^{-2},$$
$$d_{43}^r = 0.00(4)\,\mathrm{GeV}^{-2}, \qquad\qquad d_{43}^{i,r} = 0.00(10)\,\mathrm{GeV}^{-2},$$
$$d_{44}^r = 0.00(3)\,\mathrm{GeV}^{-2}, \qquad\qquad d_{44}^{i,r} = 0.00(13)\,\mathrm{GeV}^{-2},$$
$$d_{45}^r = 0.00(1)\,\mathrm{GeV}^{-2}, \qquad\qquad d_{46}^r = 0.00(1)\,\mathrm{GeV}^{-2},$$
$$d_{46}^{i,r} = 0.00(7)\,\mathrm{GeV}^{-2}, \qquad\qquad d_{47}^r = 0.00(1)\,\mathrm{GeV}^{-2}.$$

As expected, the probability distributions of the rather suppressed LECs become considerably thinner, even though it is not excluded that they in reality may achieve higher values. For the following estimation of the axion-baryon coupling at NNLO, however, we stick to the less rigid estimation of the LECs given in eq. (4.9).

The last contribution to the $\mathcal{O}\left(q^3\right)$ axion-baryon coupling stem from terms $\propto \chi_-$ discussed in section 3.3. From the matching with SU(2), eq. (3.18), we deduce that

$$(d_{18} + 2d_{19})_{\mathrm{SU}(2)} = (d_2 + 3d_3)\left(1 + \frac{w}{1+z}\right)^{-1}, \tag{4.10}$$

where neither the value of the LEC d_{19} from the SU(2) case, nor the values of d_2 and d_3 from the SU(3) case are known. The LEC d_{18} is fixed by the Goldberger-Treiman discrepancy and given by [107]

$$d_{18} = -0.44(24)\,\mathrm{GeV}^{-2}. \tag{4.11}$$

Using this matching with SU(2) and applying the same Bayesian approach as described above, we extrapolate

$$d_2 = -0.45(24)\,\mathrm{GeV}^{-2}, \qquad d_3 = 0.15(92)\,\mathrm{GeV}^{-2}. \tag{4.12}$$

Finally, we can collect all contributions to estimate the full $\mathcal{O}\left(p^3\right)$ axion-baryon couplings given by

$$g_{aAB} = g_{AB} + \frac{4M_{\pi^\pm}^2 z}{1+z}\left(\hat{d}_{AB}^r - \frac{d_2 + 3d_3}{1+z+w}\delta_{AB}\right) - \frac{1}{27}g_{AB}^{\mathrm{loop},r}, \tag{4.13}$$

which results in

$$g_{a\Sigma^+\Sigma^+} = -0.547(84) + 0.850(98)X_u - 0.032(88)X_d - 0.455(93)X_s,$$
$$g_{a\Sigma^-\Sigma^-} = -0.245(80) - 0.030(88)X_u + 0.852(99)X_d - 0.456(93)X_s,$$
$$g_{a\Sigma^0\Sigma^0} = -0.399(78) + 0.420(63)X_u + 0.397(63)X_d - 0.456(93)X_s,$$
$$g_{app} = -0.432(86) + 0.836(99)X_u - 0.418(91)X_d - 0.053(84)X_s,$$
$$g_{a\Xi^-\Xi^-} = 0.166(79) - 0.083(84)X_u - 0.455(91)X_d + 0.854(97)X_s, \tag{4.14}$$
$$g_{ann} = 0.003(83) - 0.398(90)X_u + 0.856(99)X_d - 0.053(84)X_s,$$
$$g_{a\Xi^0\Xi^0} = 0.303(81) - 0.424(91)X_u - 0.052(84)X_d + 0.854(96)X_s,$$
$$g_{a\Lambda\Lambda} = 0.138(87) - 0.159(74)X_u - 0.137(74)X_d + 0.663(92)X_s,$$
$$g_{a\Sigma^0\Lambda} = -0.161(24) + 0.441(68)X_u - 0.497(68)X_d + 0.012(24)X_s.$$

The corresponding results for the KSVZ and the DFSZ axion are collected in table 3. Note that while in the leading order case the uncertainties arise from the errors of the

Process	g_{aAB}				
	KSVZ	DFSZ			
		general	$\sin^2\beta = 0$	$\sin^2\beta = \frac{2}{3}$	$\sin^2\beta = 1$
$\Sigma^+ \to \Sigma^+ + a$	$-0.547(84)$	$-0.709(94) + 0.446(54)\sin^2\beta$	$-0.709(94)$	$-0.412(88)$	$-0.263(91)$
$\Sigma^- \to \Sigma^- + a$	$-0.245(80)$	$-0.113(92) - 0.142(54)\sin^2\beta$	$-0.113(92)$	$-0.208(84)$	$-0.255(85)$
$\Sigma^0 \to \Sigma^0 + a$	$-0.399(78)$	$-0.417(87) + 0.158(43)\sin^2\beta$	$-0.417(87)$	$-0.311(80)$	$-0.259(81)$
$p \to p + a$	$-0.432(86)$	$-0.589(96) + 0.436(53)\sin^2\beta$	$-0.589(96)$	$-0.298(90)$	$-0.153(92)$
$\Xi^- \to \Xi^- + a$	$0.166(79)$	$0.299(91) - 0.161(52)\sin^2\beta$	$0.299(91)$	$0.192(83)$	$0.138(84)$
$n \to n + a$	$0.003(83)$	$0.271(94) - 0.400(53)\sin^2\beta$	$0.271(94)$	$0.004(87)$	$-0.130(88)$
$\Xi^0 \to \Xi^0 + a$	$0.303(81)$	$0.570(92) - 0.409(52)\sin^2\beta$	$0.570(92)$	$0.298(85)$	$0.162(87)$
$\Lambda \to \Lambda + a$	$0.138(87)$	$0.314(96) - 0.228(47)\sin^2\beta$	$0.314(96)$	$0.161(90)$	$0.085(90)$
$\Sigma^0 \to \Lambda + a$ $\Lambda \to \Sigma^0 + a$	$-0.161(24)$	$-0.323(33) + 0.309(32)\sin^2\beta$	$-0.323(33)$	$-0.117(30)$	$-0.014(33)$

Table 3. Axion-baryon couplings g_{aAB}, eq. (4.13), for the KSVZ axion and the DFSZ axion at $\mathcal{O}\left(p^3\right)$.

quark ratios z and w, and the nucleon matrix elements Δu, Δd, and Δs, the uncertainties in the next-to-next-to-leading order case are dominated by the lack of knowledge of the involved LECs.

5 Summary

In this paper, we have worked out the axion-baryon coupling in SU(3) HBCHPT up to $\mathcal{O}\left(q^3\right)$ in the chiral power counting and found — in the case of the axion-nucleon coupling constants — good agreement with the already known results obtained in the SU(2) chiral approach. One of the most important outcomes of this study is that the axion-baryon coupling strengths are all of roughly the same order for all members of the baryon octet with only a few exceptions. The most prominent and well-known example is the axion-neutron coupling that might vanish in the KSVZ and the DSFZ model for particular values of $\sin^2\beta$. Given the fact that the axion couples to hyperons with similar strength as it couples to nucleons (or even stronger, especially if the coupling to neutrons is suppressed), our results suggest a revision of axion emissivity of dense stellar objects such as neutron stars, where the cores might contain strange matter in large amounts, as have been proposed in the literature (see the References given in the introduction).

In this study, we considered rather "traditional" models. Tree-level axion-quark interactions, if any, are of the same order for all flavors, and there are no flavor-changing processes. Our calculations, however, can in principle be extended to flavor non-conserving processes by adjusting the matrix $\mathcal{X}_q$ accordingly and follow the strategy described in eq. (2.11). This then would lead to new terms in the axion-baryon interaction Lagrangian including baryon-changing processes.

The other modification of our calculations would be to consider models in which the couplings of the axion to the charm, bottom, and top quark are much stronger than the couplings to the up, down, and strange quarks. Such a model can easily lead to very strong

axion-nucleon couplings driven by sea-quark effects (thus avoiding the problem of vanishing axion-neutron coupling), which in the end are balanced by correspondingly larger values of f_a, as has bee shown recently in ref. [108]. Such ideas are entirely compatible with our calculations: while the formulae derived in section 3 would be unaffected, the only difference would be that the numerical calculations of section 4 have to be adjusted as the terms $\propto \Delta q_i$ of (4.1) can not be neglected any more.

Our studies using both SU(2) and SU(3) symmetry have shown that the axion-baryon couplings for rather standard axion models are now known to good precision, but also that in the next-to-next-to-leading order case a higher precision is currently unattainable due to the lack of knowledge of some LECs. In this study, we used a Monte Carlo sampling procedure to extrapolate the most probable values of these unknown LECs, where "probable" here has to be understood in a Bayesian sense. It should thus be clear that our numerical leading order results, eq. (4.6), are more solid than the numerical estimations of the NNLO results.

Once the knowledge of the parameters in questions is enhanced, the numerical results of this work can easily be updated. However, the current uncertainties of g_{aAB} are not the major concern considering the fact that the axion window in terms of f_a is still very large. The largest uncertainties regarding the existence of axions is hence strongly linked to the uncertainty of f_a and in the end it is not g_{aAB} that counts, but $G_{aAB} = -g_{aAB}/f_a$, see eqs. (2.28) and (2.29). At last, we suggest that G_{aAB} may be computed using lattice QCD by introducing an external isoscalar axial source to mimic the axion.

Acknowledgments

A SU(3) generators in the physical basis and structure constants

In the present work, we mainly make use of the physical basis [89], based on a set of traceless, non-Hermitian matrices $\tilde{\lambda}_A$, $A = \{1, \ldots, 8\}$, such that the baryon octet matrix B, eq. (2.15), and the pseudoscalar meson octet matrix Φ, eq. (2.19), can be decomposed as

$$
\begin{aligned}
B &= \frac{1}{\sqrt{2}} \sum_A \tilde{\lambda}_A B_A \,, \\
\bar{B} &= \frac{1}{\sqrt{2}} \sum_A \bar{B}_A \tilde{\lambda}_A^\dagger \,, \\
\Phi &= \sum_A \tilde{\lambda}_A \Phi_A \,,
\end{aligned}
\tag{A.1}
$$

where the baryon fields B_A and the meson fields Φ_A can directly be equated with the physical particles, i.e.

$$B_1 = \Sigma^+\,, \qquad B_2 = \Sigma^-\,, \qquad B_3 = \Sigma^0\,, \qquad B_4 = p\,,$$
$$B_5 = \Xi^-\,, \qquad B_6 = n\,, \qquad B_7 = \Xi^0\,, \qquad B_8 = \Lambda\,, \tag{A.2}$$

and

$$\Phi_1 = \pi^+\,, \qquad \Phi_2 = \pi^-\,, \qquad \Phi_3 = \pi^0\,, \qquad \Phi_4 = K^+\,,$$
$$\Phi_5 = K^-\,, \qquad \Phi_6 = K^0\,, \qquad \Phi_7 = \bar{K}^0\,, \qquad \Phi_8 = \eta\,. \tag{A.3}$$

The explicit form of the generators $\tilde{\lambda}_A$ is

$$\tilde{\lambda}_1 = \tilde{\lambda}_2^\dagger = \begin{pmatrix} 0 & \sqrt{2} & 0 \\ 0 & 0 & 0 \\ 0 & 0 & 0 \end{pmatrix}\,, \quad \tilde{\lambda}_4 = \tilde{\lambda}_5^\dagger = \begin{pmatrix} 0 & 0 & \sqrt{2} \\ 0 & 0 & 0 \\ 0 & 0 & 0 \end{pmatrix}\,, \quad \tilde{\lambda}_6 = \tilde{\lambda}_7^\dagger = \begin{pmatrix} 0 & 0 & 0 \\ 0 & 0 & \sqrt{2} \\ 0 & 0 & 0 \end{pmatrix}\,,$$

$$\tilde{\lambda}_3 = \begin{pmatrix} \cos\epsilon + \frac{1}{\sqrt{3}}\sin\epsilon & 0 & 0 \\ 0 & -\cos\epsilon + \frac{1}{\sqrt{3}}\sin\epsilon & 0 \\ 0 & 0 & -\frac{2}{\sqrt{3}}\sin\epsilon \end{pmatrix}\,, \tag{A.4}$$

$$\tilde{\lambda}_8 = \begin{pmatrix} -\sin\epsilon + \frac{1}{\sqrt{3}}\cos\epsilon & 0 & 0 \\ 0 & \sin\epsilon + \frac{1}{\sqrt{3}}\cos\epsilon & 0 \\ 0 & 0 & -\frac{2}{\sqrt{3}}\cos\epsilon \end{pmatrix}\,,$$

where ϵ is the mixing angle given in eq. (2.17). These matrices are related to the common Gell-Mann matrices λ_a by a unitary 8×8 transformation matrix N via

$$\tilde{\lambda}_a = \sum_a N_{Aa}\lambda_a\,, \qquad \lambda_a = \sum_A N_{Aa}^* \tilde{\lambda}_A = \sum_A N_{Aa}\tilde{\lambda}_A^\dagger\,. \tag{A.5}$$

The non-zero matrix elements of N are (note the sign convention that deviates from the one in [89])

$$N_{11} = N_{44} = N_{66} = \frac{1}{\sqrt{2}}\,, \qquad\qquad N_{21} = N_{54} = N_{76} = \frac{1}{\sqrt{2}}\,,$$
$$N_{22} = N_{55} = N_{77} = -\frac{i}{\sqrt{2}}\,, \qquad\qquad N_{12} = N_{45} = N_{67} = \frac{i}{\sqrt{2}}\,, \tag{A.6}$$
$$N_{33} = N_{88} = \cos\epsilon\,, \qquad\qquad N_{38} = -N_{83} = \sin\epsilon$$

and obey

$$\sum_a N_{Aa}^* N_{Ba} = \delta_{AB}, \qquad \sum_A N_{Aa}^* N_{Ab} = \delta_{ab}\,. \tag{A.7}$$

As the Gell-Mann matrices, the $\tilde{\lambda}_A$'s are ortho-normalized to a value of 2,

$$\left\langle \tilde{\lambda}_A^\dagger \tilde{\lambda}_B \right\rangle = 2\delta_{AB}\,. \tag{A.8}$$

Moreover, they satisfy the commutator and anticommutator relations

$$\left[\tilde{\lambda}_A^\dagger, \tilde{\lambda}_B\right] = \sum_C \tilde{f}_{ABC}\tilde{\lambda}_C^\dagger = \sum_C \tilde{f}_{BAC}\tilde{\lambda}_C \,,$$

$$\left[\tilde{\lambda}_A, \tilde{\lambda}_B\right] = \sum_C \tilde{f}_{CAB}\tilde{\lambda}_C \,,$$

$$\left[\tilde{\lambda}_A^\dagger, \tilde{\lambda}_B^\dagger\right] = \sum_C \tilde{f}_{CBA}\tilde{\lambda}_C^\dagger \,,$$
$$\tag{A.9}$$

$$\left\{\tilde{\lambda}_A^\dagger, \tilde{\lambda}_B\right\} = \frac{4}{3}\delta_{AB}\mathbb{1} + \sum_C \tilde{d}_{ABC}\tilde{\lambda}_C^\dagger = \frac{4}{3}\delta_{AB}\mathbb{1} + \sum_C \tilde{d}_{BAC}\tilde{\lambda}_C \,,$$

which gives the product rule

$$\tilde{\lambda}_A^\dagger \tilde{\lambda}_B = \frac{2}{3}\delta_{AB}\mathbb{1} + \frac{1}{2}\sum_C \left(\tilde{d}_{ABC} + \tilde{f}_{ABC}\right)\tilde{\lambda}_C^\dagger$$

$$= \frac{2}{3}\delta_{AB}\mathbb{1} + \frac{1}{2}\sum_C \left(\tilde{d}_{BAC} + \tilde{f}_{BAC}\right)\tilde{\lambda}_C \,.$$
$$\tag{A.10}$$

The structure constants defined in eq. (A.9) can be evaluated using

$$\tilde{f}_{ABC} = \frac{1}{2}\left\langle \tilde{\lambda}_A^\dagger \left[\tilde{\lambda}_B, \tilde{\lambda}_C\right]\right\rangle \,,$$

$$\tilde{d}_{ABC} = \frac{1}{2}\left\langle \tilde{\lambda}_A^\dagger \left\{\tilde{\lambda}_B, \tilde{\lambda}_C\right\}\right\rangle \,,$$
$$\tag{A.11}$$

and are related to the corresponding structure constants of the Gell-Mann representation via

$$\tilde{f}_{ABC} = 2i \sum_{a,b,c} N_{Aa}^* N_{Bb} N_{Cc} f^{abc} \,,$$

$$\tilde{d}_{ABC} = 2 \sum_{a,b,c} N_{Aa}^* N_{Bb} N_{Cc} d^{abc} \,.$$
$$\tag{A.12}$$

In contrast to the structure constants f^{abc} (d^{abc}) of the Gell-Mann representation, which are totally anti-symmetric (symmetric), the structure constants $\tilde{f}_{ABC}$ ($\tilde{d}_{ABC}$) of the physical basis are anti-symmetric (symmetric) in the last two indices only. Finally, there are sum rules for the structure constants:

$$\sum_{C,D} \tilde{f}_{ACD}\tilde{f}_{BCD} = \sum_{C,D} \tilde{f}_{CAD}\tilde{f}_{CBD} = 12\delta_{AB} \,,$$

$$\sum_{C,D} \tilde{d}_{ACD}\tilde{d}_{BCD} = \sum_{C,D} \tilde{d}_{CAD}\tilde{d}_{CBD} = \frac{20}{3}\delta_{AB} \,.$$
$$\tag{A.13}$$

Often, we also need the generators at $\epsilon = 0$, and therefore it is convenient to set

$$\hat{\lambda}_A = \tilde{\lambda}_A\Big|_{\epsilon=0} \,,$$

$$\hat{f}_{ABC} = \tilde{f}_{ABC}\Big|_{\epsilon=0} \,,$$
$$\tag{A.14}$$

$$\hat{d}_{ABC} = \tilde{d}_{ABC}\Big|_{\epsilon=0} \,.$$

The properties eqs. (A.8)–(A.13) are then of course also valid for the $\hat{\lambda}_A$'s with $\tilde{f}_{ABC}$ and $\tilde{d}_{ABC}$ replaced by $\hat{f}_{ABC}$ and $\hat{d}_{ABC}$, respectively. Note that now one has

$$\hat{\lambda}_3 = \lambda_3 , \qquad \hat{\lambda}_8 = \lambda_8 . \tag{A.15}$$

The non-zero elements of the structure constants in this representation are

$$
\begin{aligned}
\hat{f}_{147} &= -\hat{f}_{256} = \hat{f}_{416} = -\hat{f}_{527} = \hat{f}_{624} = -\hat{f}_{715} = \sqrt{2} , \\
\hat{f}_{443} &= -\hat{f}_{553} = -\hat{f}_{663} = \hat{f}_{773} = -\hat{f}_{345} = \hat{f}_{367} = -1 , \\
\hat{f}_{448} &= -\hat{f}_{558} = \hat{f}_{668} = -\hat{f}_{778} = -\hat{f}_{845} = -\hat{f}_{867} = -\sqrt{3} , \\
\hat{f}_{113} &= -\hat{f}_{223} = -\hat{f}_{312} = -2 .
\end{aligned}
\tag{A.16}
$$

Similarly,

$$
\begin{aligned}
\hat{d}_{147} &= \hat{d}_{256} = \hat{d}_{416} = \hat{d}_{527} = \hat{d}_{624} = \hat{d}_{715} = \sqrt{2} , \\
\hat{d}_{443} &= \hat{d}_{553} = -\hat{d}_{663} = -\hat{d}_{773} = \hat{d}_{345} = -\hat{d}_{367} = 1 , \\
\hat{d}_{118} &= \hat{d}_{228} = \hat{d}_{338} = \hat{d}_{812} = \hat{d}_{833} = -\hat{d}_{888} = \frac{2}{\sqrt{3}} , \\
\hat{d}_{448} &= \hat{d}_{558} = \hat{d}_{668} = \hat{d}_{778} = \hat{d}_{845} = \hat{d}_{867} = -\frac{1}{\sqrt{3}} .
\end{aligned}
\tag{A.17}
$$

B   Matrix elements of g_{AB}, $\hat{d}_{AB}$, and g_{AB}^{loop}

Here we collect the matrix elements of the several contributions to the axion-baryon coupling. Table 4 shows the matrix elements of g_{AB} as defined in eq. (3.3) in the physical basis at $\epsilon \neq 0$, see eq. (2.17).

In eqs. (B.1)–(B.9), we list the non-zero matrix elements of the next-to-next-to-leading order contributions to the axion-baryon coupling as defined in eqs. (3.23) and (3.24). Here we refrain from explicitly marking the scale dependence of the LECs $d_k^{(i)}(\lambda)$.

$$
\begin{aligned}
\hat{d}_{11} = {}& c^{(3)} \left\{ (4d_{41} + d_{47}) \left(1 - \frac{1}{z}\right) + 4d_{42} \left(1 + \frac{1}{z}\right) + 2d_{45} \left(1 + \frac{1}{z} + \frac{1}{w}\right) \right\} \\
&+ \frac{c^{(8)}}{\sqrt{3}} \left\{ 4d_{43} \left(1 - \frac{1}{z}\right) + 4d_{44} \left(1 + \frac{1}{z}\right) + 2d_{46} \left(1 + \frac{1}{z} + \frac{1}{w}\right) \right. \\
&\qquad\qquad \left. + d_{47} \left(1 + \frac{1}{z} - \frac{2}{w}\right) \right\} \\
&+ c_i \left\{ d_{43}^i \left(1 - \frac{1}{z}\right) + d_{44}^i \left(1 + \frac{1}{z}\right) + d_{46}^i \left(1 + \frac{1}{z} + \frac{1}{w}\right) \right\} ,
\end{aligned}
\tag{B.1}
$$

$$\hat{d}_{22} = c^{(3)}\left\{(4d_{41}+d_{47})\left(1-\frac{1}{z}\right)-4d_{42}\left(1+\frac{1}{z}\right)-2d_{45}\left(1+\frac{1}{z}+\frac{1}{w}\right)\right\}$$
$$+\frac{c^{(8)}}{\sqrt{3}}\left\{-4d_{43}\left(1-\frac{1}{z}\right)+4d_{44}\left(1+\frac{1}{z}\right)+2d_{46}\left(1+\frac{1}{z}+\frac{1}{w}\right)\right.$$
$$\left.+d_{47}\left(1+\frac{1}{z}-\frac{2}{w}\right)\right\}$$
$$+c_i\left\{-d^i_{43}\left(1-\frac{1}{z}\right)+d^i_{44}\left(1+\frac{1}{z}\right)+d^i_{46}\left(1+\frac{1}{z}+\frac{1}{w}\right)\right\}, \tag{B.2}$$

$$\hat{d}_{33} = c^{(3)}\left(4d_{44}+d_{47}\right)\left(1-\frac{1}{z}\right)$$
$$+\frac{c^{(8)}}{\sqrt{3}}\left\{4d_{44}\left(1+\frac{1}{z}\right)+2d_{46}\left(1+\frac{1}{z}+\frac{1}{w}\right)+d_{47}\left(1+\frac{1}{z}-\frac{2}{w}\right)\right\}$$
$$+c_i\left\{d^i_{44}\left(1+\frac{1}{z}\right)+d^i_{46}\left(1+\frac{1}{z}+\frac{1}{w}\right)\right\}, \tag{B.3}$$

$$\hat{d}_{44} = c^{(3)}\left\{2\left(d_{41}+d_{43}\right)\left(1-\frac{1}{w}\right)+2\left(d_{42}+d_{44}\right)\left(1+\frac{1}{w}\right)\right.$$
$$\left.+\left(d_{45}+d_{46}\right)\left(1+\frac{1}{z}+\frac{1}{w}\right)+d_{47}\left(1-\frac{1}{z}\right)\right\}$$
$$+\frac{c^{(8)}}{\sqrt{3}}\left\{2\left(3d_{41}-d_{43}\right)\left(1-\frac{1}{w}\right)+2\left(3d_{42}-d_{44}\right)\left(1+\frac{1}{w}\right)\right.$$
$$\left.+\left(3d_{45}-d_{46}\right)\left(1+\frac{1}{z}+\frac{1}{w}\right)+d_{47}\left(1+\frac{1}{z}-\frac{2}{w}\right)\right\}$$
$$+c_i\left\{d^i_{43}\left(1-\frac{1}{w}\right)+d^i_{44}\left(1+\frac{1}{w}\right)+d^i_{46}\left(1+\frac{1}{z}+\frac{1}{w}\right)\right\}, \tag{B.4}$$

$$\hat{d}_{55} = c^{(3)}\left\{2\left(d_{41}-d_{43}\right)\left(1-\frac{1}{w}\right)-2\left(d_{42}-d_{44}\right)\left(1+\frac{1}{w}\right)\right.$$
$$\left.-\left(d_{45}-d_{46}\right)\left(1+\frac{1}{z}+\frac{1}{w}\right)+d_{47}\left(1-\frac{1}{z}\right)\right\}$$
$$+\frac{c^{(8)}}{\sqrt{3}}\left\{2\left(3d_{41}+d_{43}\right)\left(1-\frac{1}{w}\right)-2\left(3d_{42}+d_{44}\right)\left(1+\frac{1}{w}\right)\right.$$
$$\left.-\left(3d_{45}+d_{46}\right)\left(1+\frac{1}{z}+\frac{1}{w}\right)+d_{47}\left(1+\frac{1}{z}-\frac{2}{w}\right)\right\}$$
$$+c_i\left\{-d^i_{43}\left(1-\frac{1}{w}\right)+d^i_{44}\left(1+\frac{1}{w}\right)+d^i_{46}\left(1+\frac{1}{z}+\frac{1}{w}\right)\right\}, \tag{B.5}$$

152

Process	$A = B$	g_{AB}
$\Sigma^+ \to \Sigma^+ + a$	1	$2\left(\frac{c^{(8)}}{\sqrt{3}}D + c^{(3)}F\right) + c_i D^i$
$\Sigma^- \to \Sigma^- + a$	2	$2\left(\frac{c^{(8)}}{\sqrt{3}}D - c^{(3)}F\right) + c_i D^i$
$\Sigma^0 \to \Sigma^0 + a$	3	$\frac{2}{\sqrt{3}}\left(c^{(3)}\sin 2\epsilon + c^{(8)}\cos 2\epsilon\right)D + c_i D^i$
$p \to p + a$	4	$c^{(3)}(D+F) - \frac{c^{(8)}}{\sqrt{3}}(D-3F) + c_i D^i$
$\Xi^- \to \Xi^- + a$	5	$c^{(3)}(D-F) - \frac{c^{(8)}}{\sqrt{3}}(D+3F) + c_i D^i$
$n \to n + a$	6	$-c^{(3)}(D+F) - \frac{c^{(8)}}{\sqrt{3}}(D-3F) + c_i D^i$
$\Xi^0 \to \Xi^0 + a$	7	$-c^{(3)}(D-F) - \frac{c^{(8)}}{\sqrt{3}}(D+3F) + c_i D^i$
$\Lambda \to \Lambda + a$	8	$-\frac{2}{\sqrt{3}}\left(c^{(3)}\sin 2\epsilon + c^{(8)}\cos 2\epsilon\right)D + c_i D^i$
Process	$A \neq B$	g_{AB}
$\Sigma^0 \to \Lambda + a$	$A=8,\ B=3$	$\frac{2}{\sqrt{3}}\left(c^{(3)}\cos 2\epsilon + c^{(8)}\sin 2\epsilon\right)D$
$\Lambda \to \Sigma^0 + a$	$A=3,\ B=8$	

Table 4. Non-zero matrix elements of g_{AB}, eq. (3.3).

$$
\begin{aligned}
\hat{d}_{66} = c^{(3)}&\Big\{-2\,(d_{41}+d_{43})\left(\frac{1}{z}-\frac{1}{w}\right) - 2\,(d_{42}+d_{44})\left(\frac{1}{z}+\frac{1}{w}\right) \\
&- (d_{45}+d_{46})\left(1+\frac{1}{z}+\frac{1}{w}\right) + d_{47}\left(1-\frac{1}{z}\right)\Big\} \\
+ \frac{c^{(8)}}{\sqrt{3}}&\Big\{2\,(3d_{41}-d_{43})\left(\frac{1}{z}-\frac{1}{w}\right) + 2\,(3d_{42}-d_{44})\left(\frac{1}{z}+\frac{1}{w}\right) \\
&+ (3d_{45}-d_{46})\left(1+\frac{1}{z}+\frac{1}{w}\right) + d_{47}\left(1+\frac{1}{z}-\frac{2}{w}\right)\Big\} \\
+ c_i&\Big\{d^i_{43}\left(\frac{1}{z}-\frac{1}{w}\right) + d^i_{44}\left(\frac{1}{z}+\frac{1}{w}\right) + d^i_{46}\left(1+\frac{1}{z}+\frac{1}{w}\right)\Big\},
\end{aligned}
\tag{B.6}
$$

$$
\begin{aligned}
\hat{d}_{77} = c^{(3)}&\Big\{-2\,(d_{41}-d_{43})\left(\frac{1}{z}-\frac{1}{w}\right) + 2\,(d_{42}-d_{44})\left(\frac{1}{z}+\frac{1}{w}\right) \\
&+ (d_{45}-d_{46})\left(1+\frac{1}{z}+\frac{1}{w}\right) + d_{47}\left(1-\frac{1}{z}\right)\Big\} \\
+ \frac{c^{(8)}}{\sqrt{3}}&\Big\{-2\,(3d_{41}+d_{43})\left(\frac{1}{z}-\frac{1}{w}\right) - 2\,(3d_{42}+d_{44})\left(\frac{1}{z}+\frac{1}{w}\right) \\
&- (3d_{45}+d_{46})\left(1+\frac{1}{z}+\frac{1}{w}\right) + d_{47}\left(1+\frac{1}{z}-\frac{2}{w}\right)\Big\} \\
+ c_i&\Big\{-d^i_{43}\left(\frac{1}{z}-\frac{1}{w}\right) + d^i_{44}\left(\frac{1}{z}+\frac{1}{w}\right) + d^i_{46}\left(1+\frac{1}{z}+\frac{1}{w}\right)\Big\},
\end{aligned}
\tag{B.7}
$$

$$\hat{d}_{88} = c^{(3)} \left(\frac{4}{3} d_{44} + d_{47} \right) \left(1 - \frac{1}{z} \right)$$

$$+ \frac{c^{(8)}}{\sqrt{3}} \left\{ \frac{4}{3} d_{44} \left(1 + \frac{1}{z} - \frac{8}{w} \right) - 2 d_{46} \left(1 + \frac{1}{z} + \frac{1}{w} \right) + d_{47} \left(1 + \frac{1}{z} - \frac{2}{w} \right) \right\} \qquad \text{(B.8)}$$

$$+ c_i \left\{ \frac{1}{3} d_{44}^i \left(1 + \frac{1}{z} + \frac{4}{w} \right) + d_{46}^i \left(1 + \frac{1}{z} + \frac{1}{w} \right) \right\}.$$

For the only non-diagonal matrix elements, one has $\hat{d}_{38} = \hat{d}_{83}$, which is given by

$$\hat{d}_{38} = \frac{c^{(3)}}{\sqrt{3}} \left\{ 4 d_{44} \left(1 + \frac{1}{z} \right) + d_{46} \left(1 + \frac{1}{z} + \frac{1}{w} \right) \right\} + \left(\frac{4 c^{(8)}}{3} d_{44} + \frac{c_i}{\sqrt{3}} d_{44}^i \right) \left(1 - \frac{1}{z} \right). \quad \text{(B.9)}$$

Eqs. (B.10)–(B.18) show the matrix elements of the finite one meson loop contributions $g_{AB}^{\text{loop},r}$, cf. eq. (3.39), of diagram (a) (figure 1). The expressions have been simplified using the leading order relations (2.21) and (2.22). Moreover, we have set $\mu_{\Phi_C} = M_{\Phi_C}/(4\pi F_p)$ for any meson Φ_C.

$$g_{11}^{\text{loop},r} = c^{(3)} \left\{ -3D \left(3D^2 - 11F^2 \right) \left(\mu_{K^\pm}^2 - \mu_{K^0}^2 \right) \right.$$

$$\left. - F \left(D^2 - 9F^2 \right) \left(4\mu_{\pi^\pm}^2 + \mu_{K^\pm}^2 + \mu_{K^0}^2 \right) - 24 D^2 F \mu_{\pi^\pm}^2 \right\}$$

$$+ \frac{c^{(8)}}{\sqrt{3}} \left\{ -D \left(D^2 + 9F^2 \right) \left(16\mu_{\pi^\pm}^2 + \mu_{K^\pm}^2 + \mu_{K^0}^2 \right) \right.$$

$$\left. + 54 D F^2 \left(4\mu_{\pi^\pm}^2 - \mu_{K^\pm}^2 - \mu_{K^0}^2 \right) - 3F \left(7D^2 + 9F^2 \right) \left(\mu_{K^\pm}^2 - \mu_{K^0}^2 \right) \right\} \qquad \text{(B.10)}$$

$$+ c_i D^i \left\{ 30 D F \left(\mu_{K^\pm}^2 - \mu_{K^0}^2 \right) + \left(D^2 + 9F^2 \right) \left(4\mu_{\pi^\pm}^2 + \mu_{K^\pm}^2 + \mu_{K^0}^2 \right) \right.$$

$$\left. + 12 D^2 \left(\mu_{K^\pm}^2 + \mu_{K^0}^2 \right) \right\},$$

$$g_{22}^{\text{loop},r} = c^{(3)} \left\{ -3D \left(3D^2 - 11F^2 \right) \left(\mu_{K^\pm}^2 - \mu_{K^0}^2 \right) \right.$$

$$\left. + F \left(D^2 - 9F^2 \right) \left(4\mu_{\pi^\pm}^2 + \mu_{K^\pm}^2 + \mu_{K^0}^2 \right) + 24 D^2 F \mu_{\pi^\pm}^2 \right\}$$

$$+ \frac{c^{(8)}}{\sqrt{3}} \left\{ -D \left(D^2 + 9F^2 \right) \left(16\mu_{\pi^\pm}^2 + \mu_{K^\pm}^2 + \mu_{K^0}^2 \right) \right.$$

$$\left. + 54 D F^2 \left(4\mu_{\pi^\pm}^2 - \mu_{K^\pm}^2 - \mu_{K^0}^2 \right) + 3F \left(7D^2 + 9F^2 \right) \left(\mu_{K^\pm}^2 - \mu_{K^0}^2 \right) \right\} \qquad \text{(B.11)}$$

$$+ c_i D^i \left\{ -30 D F \left(\mu_{K^\pm}^2 - \mu_{K^0}^2 \right) + \left(D^2 + 9F^2 \right) \left(4\mu_{\pi^\pm}^2 + \mu_{K^\pm}^2 + \mu_{K^0}^2 \right) \right.$$

$$\left. + 12 D^2 \left(\mu_{K^\pm}^2 + \mu_{K^0}^2 \right) \right\},$$

$$g_{33}^{\mathrm{loop},r} = c^{(3)} D \left(17D^2 - 9F^2\right) \left(\mu_{K^\pm}^2 - \mu_{K^0}^2\right)$$

$$+ \frac{c^{(8)}}{\sqrt{3}} \Big\{ -D \left(D^2 + 9F^2\right) \left(16\mu_{\pi^\pm}^2 + \mu_{K^\pm}^2 + \mu_{K^0}^2\right)$$

$$+ 54DF^2 \left(4\mu_{\pi^\pm}^2 - \mu_{K^\pm}^2 - \mu_{K^0}^2\right) \Big\} \tag{B.12}$$

$$+ c_i D^i \Big\{ \left(D^2 + 9F^2\right) \left(4\mu_{\pi^\pm}^2 + \mu_{K^\pm}^2 + \mu_{K^0}^2\right) + 12D^2 \left(\mu_{K^\pm}^2 + \mu_{K^0}^2\right) \Big\},$$

$$g_{44}^{\mathrm{loop},r} = c^{(3)} \Big\{ -D \left(D^2 + 3F^2\right) \left(5\mu_{\pi^\pm}^2 + 8\mu_{K^\pm}^2 - 4\mu_{K^0}^2\right) + 60DF^2 \left(\mu_{K^\pm}^2 - \mu_{K^0}^2\right)$$

$$- D^2 F \left(11\mu_{\pi^\pm}^2 + 14\mu_{K^\pm}^2 - 10\mu_{K^0}^2\right) - 9F^3 \left(\mu_{\pi^\pm}^2 - 2\mu_{K^\pm}^2 - 2\mu_{K^0}^2\right) \Big\}$$

$$+ \frac{c^{(8)}}{\sqrt{3}} \Big\{ -D^3 \left(13\mu_{\pi^\pm}^2 - 8\mu_{K^\pm}^2 - 14\mu_{K^0}^2\right) + 9DF^2 \left(9\mu_{\pi^\pm}^2 - 4\mu_{K^\pm}^2 - 2\mu_{K^0}^2\right)$$

$$+ 3D^2 F \left(3\mu_{\pi^\pm}^2 - 14\mu_{K^\pm}^2 - 4\mu_{K^0}^2\right) + 27F^3 \left(\mu_{\pi^\pm}^2 + 2\mu_{K^\pm}^2\right) \Big\} \tag{B.13}$$

$$+ c_i D^i \Big\{ 30DF \left(\mu_{\pi^\pm}^2 - \mu_{K^0}^2\right) + \left(D^2 + 9F^2\right) \left(\mu_{\pi^\pm}^2 + 4\mu_{K^\pm}^2 + \mu_{K^0}^2\right)$$

$$+ 12D^2 \left(\mu_{\pi^\pm}^2 + \mu_{K^0}^2\right) \Big\},$$

$$g_{55}^{\mathrm{loop},r} = c^{(3)} \Big\{ -D \left(D^2 + 3F^2\right) \left(5\mu_{\pi^\pm}^2 + 8\mu_{K^\pm}^2 - 4\mu_{K^0}^2\right) + 60DF^2 \left(\mu_{K^\pm}^2 - \mu_{K^0}^2\right)$$

$$+ D^2 F \left(11\mu_{\pi^\pm}^2 + 14\mu_{K^\pm}^2 - 10\mu_{K^0}^2\right) + 9F^3 \left(\mu_{\pi^\pm}^2 - 2\mu_{K^\pm}^2 - 2\mu_{K^0}^2\right) \Big\}$$

$$+ \frac{c^{(8)}}{\sqrt{3}} \Big\{ -D^3 \left(13\mu_{\pi^\pm}^2 - 8\mu_{K^\pm}^2 - 14\mu_{K^0}^2\right) + 9DF^2 \left(9\mu_{\pi^\pm}^2 - 4\mu_{K^\pm}^2 - 2\mu_{K^0}^2\right)$$

$$- 3D^2 F \left(3\mu_{\pi^\pm}^2 - 14\mu_{K^\pm}^2 - 4\mu_{K^0}^2\right) - 27F^3 \left(\mu_{\pi^\pm}^2 + 2\mu_{K^\pm}^2\right) \Big\} \tag{B.14}$$

$$+ c_i D^i \Big\{ -30DF \left(\mu_{\pi^\pm}^2 - \mu_{K^0}^2\right) + \left(D^2 + 9F^2\right) \left(\mu_{\pi^\pm}^2 + 4\mu_{K^\pm}^2 + \mu_{K^0}^2\right)$$

$$+ 12D^2 \left(\mu_{\pi^\pm}^2 + \mu_{K^0}^2\right) \Big\},$$

155

$$g_{66}^{\text{loop},r} = c^{(3)}\Big\{ D\left(D^2 + 3F^2\right)\left(5\mu_{\pi^\pm}^2 - 4\mu_{K^\pm}^2 + 8\mu_{K^0}^2\right) + 60DF^2\left(\mu_{K^\pm}^2 - \mu_{K^0}^2\right)$$
$$+ D^2F\left(11\mu_{\pi^\pm}^2 - 10\mu_{K^\pm}^2 + 14\mu_{K^0}^2\right) + 9F^3\left(\mu_{\pi^\pm}^2 - 2\mu_{K^\pm}^2 - 2\mu_{K^0}^2\right)\Big\}$$
$$+ \frac{c^{(8)}}{\sqrt{3}}\Big\{ -D^3\left(13\mu_{\pi^\pm}^2 - 14\mu_{K^\pm}^2 - 8\mu_{K^0}^2\right) + 9DF^2\left(9\mu_{\pi^\pm}^2 - 2\mu_{K^\pm}^2 - 4\mu_{K^0}^2\right)$$
$$+ 3D^2F\left(3\mu_{\pi^\pm}^2 - 4\mu_{K^\pm}^2 - 14\mu_{K^0}^2\right) + 27F^3\left(\mu_{\pi^\pm}^2 + 2\mu_{K^0}^2\right)\Big\} \tag{B.15}$$
$$+ c_i D^i\Big\{ 30DF\left(\mu_{\pi^\pm}^2 - \mu_{K^\pm}^2\right) + \left(D^2 + 9F^2\right)\left(\mu_{\pi^\pm}^2 + \mu_{K^\pm}^2 + 4\mu_{K^0}^2\right)$$
$$+ 12D^2\left(\mu_{\pi^\pm}^2 + \mu_{K^\pm}^2\right)\Big\},$$

$$g_{77}^{\text{loop},r} = c^{(3)}\Big\{ D\left(D^2 + 3F^2\right)\left(5\mu_{\pi^\pm}^2 - 4\mu_{K^\pm}^2 + 8\mu_{K^0}^2\right) + 60DF^2\left(\mu_{K^\pm}^2 - \mu_{K^0}^2\right)$$
$$- D^2F\left(11\mu_{\pi^\pm}^2 - 10\mu_{K^\pm}^2 + 14\mu_{K^0}^2\right) - 9F^3\left(\mu_{\pi^\pm}^2 - 2\mu_{K^\pm}^2 - 2\mu_{K^0}^2\right)\Big\}$$
$$+ \frac{c^{(8)}}{\sqrt{3}}\Big\{ -D^3\left(13\mu_{\pi^\pm}^2 - 14\mu_{K^\pm}^2 - 8\mu_{K^0}^2\right) + 9DF^2\left(9\mu_{\pi^\pm}^2 - 2\mu_{K^\pm}^2 - 4\mu_{K^0}^2\right)$$
$$- 3D^2F\left(3\mu_{\pi^\pm}^2 - 4\mu_{K^\pm}^2 - 14\mu_{K^0}^2\right) - 27F^3\left(\mu_{\pi^\pm}^2 + 2\mu_{K^0}^2\right)\Big\} \tag{B.16}$$
$$+ c_i D^i\Big\{ -30DF\left(\mu_{\pi^\pm}^2 - \mu_{K^\pm}^2\right) + \left(D^2 + 9F^2\right)\left(\mu_{\pi^\pm}^2 + \mu_{K^\pm}^2 + 4\mu_{K^0}^2\right)$$
$$+ 12D^2\left(\mu_{\pi^\pm}^2 + \mu_{K^\pm}^2\right)\Big\},$$

$$g_{88}^{\text{loop},r} = -5c^{(3)}D\left(D^2 - 9F^2\right)\left(\mu_{K^\pm}^2 - \mu_{K^0}^2\right)$$
$$+ \frac{c^{(8)}}{\sqrt{3}}\Big\{ D\left(D^2 + 27F^2\right)\left(\mu_{K^\pm}^2 + \mu_{K^0}^2\right) + 4D^3\left(10\mu_{\pi^\pm}^2 - 3\mu_{K^\pm}^2 - 3\mu_{K^0}^2\right)\Big\} \tag{B.17}$$
$$+ c_i D^i\Big\{ 3\left(D^2 + 9F^2\right)\left(\mu_{K^\pm}^2 + \mu_{K^0}^2\right) - 4D^2\left(4\mu_{\pi^\pm}^2 + \mu_{K^\pm}^2 + \mu_{K^0}^2\right)\Big\}.$$

The only non-diagonal matrix elements are given by

$$g_{38}^{\text{loop},r} = \frac{c^{(3)}}{\sqrt{3}}D\Big\{ \left(D^2 - 9F^2\right)\left(8\mu_{\pi^\pm}^2 - \mu_{K^\pm}^2 - \mu_{K^0}^2\right) + 8D^2\left(\mu_{\pi^\pm}^2 - 2\mu_{K^\pm}^2 - 2\mu_{K^0}^2\right)\Big\}$$
$$+ \Big\{ c^{(8)}D\left(11D^2 - 27F^2\right) - 3\sqrt{3}c_i D^i\left(D^2 - 3F^2\right)\Big\}\left(\mu_{K^\pm}^2 - \mu_{K^0}^2\right) \tag{B.18}$$

and $g_{83}^{\text{loop},r} = g_{38}^{\text{loop},r}$.

References

[1] A.A. Belavin, A.M. Polyakov, A.S. Schwartz and Y.S. Tyupkin, *Pseudoparticle Solutions of the Yang-Mills Equations*, *[Phys. Lett. B](#)* **59** (1975) 85 [[INSPIRE](#)].

[2] C.G. Callan Jr., R.F. Dashen and D.J. Gross, *The Structure of the Gauge Theory Vacuum*, *[Phys. Lett. B](#)* **63** (1976) 334 [[INSPIRE](#)].

[3] V. Baluni, *CP Violating Effects in QCD*, *[Phys. Rev. D](#)* **19** (1979) 2227 [[INSPIRE](#)].

[4] J.E. Kim and G. Carosi, *Axions and the Strong CP Problem*, *[Rev. Mod. Phys.](#)* **82** (2010) 557 [*Erratum ibid.* **91** (2019) 049902] [[arXiv:0807.3125](#)] [[INSPIRE](#)].

[5] C. Alexandrou et al., *Neutron electric dipole moment using $N_f = 2 + 1 + 1$ twisted mass fermions*, *[Phys. Rev. D](#)* **93** (2016) 074503 [[arXiv:1510.05823](#)] [[INSPIRE](#)].

[6] F.-K. Guo et al., *The electric dipole moment of the neutron from $2 + 1$ flavor lattice QCD*, *[Phys. Rev. Lett.](#)* **115** (2015) 062001 [[arXiv:1502.02295](#)] [[INSPIRE](#)].

[7] CPEDM collaboration, *Storage Ring to Search for Electric Dipole Moments of Charged Particles — Feasibility Study*, in *[CERN Yellow Reports: Monographs](#)* **3**, CERN, Geneva Switzerland, [arXiv:1912.07881](#) [[INSPIRE](#)].

[8] NEDM collaboration, *Measurement of the permanent electric dipole moment of the neutron*, *[Phys. Rev. Lett.](#)* **124** (2020) 081803 [[arXiv:2001.11966](#)] [[INSPIRE](#)].

[9] A.V. Smilga, *QCD at $\theta \sim \pi$*, *[Phys. Rev. D](#)* **59** (1999) 114021 [[hep-ph/9805214](#)] [[INSPIRE](#)].

[10] D. Lee, U.-G. Meißner, K.A. Olive, M. Shifman and T. Vonk, *θ-dependence of light nuclei and nucleosynthesis*, *[Phys. Rev. Res.](#)* **2** (2020) 033392 [[arXiv:2006.12321](#)] [[INSPIRE](#)].

[11] R.D. Peccei and H.R. Quinn, *CP Conservation in the Presence of Instantons*, *[Phys. Rev. Lett.](#)* **38** (1977) 1440 [[INSPIRE](#)].

[12] R.D. Peccei and H.R. Quinn, *Constraints Imposed by CP Conservation in the Presence of Instantons*, *[Phys. Rev. D](#)* **16** (1977) 1791 [[INSPIRE](#)].

[13] S. Weinberg, *A New Light Boson?*, *[Phys. Rev. Lett.](#)* **40** (1978) 223 [[INSPIRE](#)].

[14] F. Wilczek, *Problem of Strong P and T Invariance in the Presence of Instantons*, *[Phys. Rev. Lett.](#)* **40** (1978) 279 [[INSPIRE](#)].

[15] J. Preskill, M.B. Wise and F. Wilczek, *Cosmology of the Invisible Axion*, *[Phys. Lett. B](#)* **120** (1983) 127 [[INSPIRE](#)].

[16] L.F. Abbott and P. Sikivie, *A Cosmological Bound on the Invisible Axion*, *[Phys. Lett. B](#)* **120** (1983) 133 [[INSPIRE](#)].

[17] M. Dine and W. Fischler, *The Not So Harmless Axion*, *[Phys. Lett. B](#)* **120** (1983) 137 [[INSPIRE](#)].

[18] J. Ipser and P. Sikivie, *Are Galactic Halos Made of Axions?*, *[Phys. Rev. Lett.](#)* **50** (1983) 925 [[INSPIRE](#)].

[19] M.S. Turner, *Thermal Production of Not SO Invisible Axions in the Early Universe*, *Phys. Rev. Lett.* **59** (1987) 2489 [*Erratum ibid.* **60** (1988) 1101] [INSPIRE].

[20] L.D. Duffy and K. van Bibber, *Axions as Dark Matter Particles*, *New J. Phys.* **11** (2009) 105008 [arXiv:0904.3346] [INSPIRE].

[21] D.J.E. Marsh, *Axion Cosmology*, *Phys. Rept.* **643** (2016) 1 [arXiv:1510.07633] [INSPIRE].

[22] P. Sikivie and Q. Yang, *Bose-Einstein Condensation of Dark Matter Axions*, *Phys. Rev. Lett.* **103** (2009) 111301 [arXiv:0901.1106] [INSPIRE].

[23] T.W. Donnelly, S.J. Freedman, R.S. Lytel, R.D. Peccei and M. Schwartz, *Do Axions Exist?*, *Phys. Rev. D* **18** (1978) 1607 [INSPIRE].

[24] F.P. Calaprice et al., *Search for axion emission in the decay of excited states of ^{12}C*, *Phys. Rev. D* **20** (1979) 2708 [INSPIRE].

[25] D.J. Bechis et al., *Search for Axion Production in Low-energy Electron Bremsstrahlung*, *Phys. Rev. Lett.* **42** (1979) 1511 [*Erratum ibid.* **43** (1979) 90] [INSPIRE].

[26] D.S.M. Alves and N. Weiner, *A viable QCD axion in the MeV mass range*, *JHEP* **07** (2018) 092 [arXiv:1710.03764] [INSPIRE].

[27] J. Liu, N. McGinnis, C.E.M. Wagner and X.-P. Wang, *Challenges for a QCD Axion at the 10 MeV Scale*, *JHEP* **05** (2021) 138 [arXiv:2102.10118] [INSPIRE].

[28] J.E. Kim, *Weak Interaction Singlet and Strong CP Invariance*, *Phys. Rev. Lett.* **43** (1979) 103 [INSPIRE].

[29] M.A. Shifman, A.I. Vainshtein and V.I. Zakharov, *Can Confinement Ensure Natural CP Invariance of Strong Interactions?*, *Nucl. Phys. B* **166** (1980) 493 [INSPIRE].

[30] M. Dine, W. Fischler and M. Srednicki, *A Simple Solution to the Strong CP Problem with a Harmless Axion*, *Phys. Lett. B* **104** (1981) 199 [INSPIRE].

[31] A.R. Zhitnitsky, *On Possible Suppression of the Axion Hadron Interactions* (in Russian), *Sov. J. Nucl. Phys.* **31** (1980) 260 [INSPIRE].

[32] J.E. Kim, *Light Pseudoscalars, Particle Physics and Cosmology*, *Phys. Rept.* **150** (1987) 1 [INSPIRE].

[33] L. Di Luzio, M. Giannotti, E. Nardi and L. Visinelli, *The landscape of QCD axion models*, *Phys. Rept.* **870** (2020) 1 [arXiv:2003.01100] [INSPIRE].

[34] Z.-Y. Lu, M.-L. Du, F.-K. Guo, U.-G. Meißner and T. Vonk, *QCD θ-vacuum energy and axion properties*, *JHEP* **05** (2020) 001 [arXiv:2003.01625] [INSPIRE].

[35] S. Chang and K. Choi, *Hadronic axion window and the big bang nucleosynthesis*, *Phys. Lett. B* **316** (1993) 51 [hep-ph/9306216] [INSPIRE].

[36] P. Svrček and E. Witten, *Axions In String Theory*, *JHEP* **06** (2006) 051 [hep-th/0605206] [INSPIRE].

[37] N. Iwamoto, *Axion Emission from Neutron Stars*, *Phys. Rev. Lett.* **53** (1984) 1198 [INSPIRE].

[38] R. Mayle, J.R. Wilson, J.R. Ellis, K.A. Olive, D.N. Schramm and G. Steigman, *Constraints on Axions from SN 1987a*, *Phys. Lett. B* **203** (1988) 188 [INSPIRE].

[39] R.P. Brinkmann and M.S. Turner, *Numerical Rates for Nucleon-Nucleon Axion Bremsstrahlung*, *Phys. Rev. D* **38** (1988) 2338 [INSPIRE].

[40] G. Raffelt and D. Seckel, *Bounds on Exotic Particle Interactions from SN 1987a*, *Phys. Rev. Lett.* **60** (1988) 1793 [INSPIRE].

[41] M.S. Turner, *Axions from SN 1987a*, *Phys. Rev. Lett.* **60** (1988) 1797 [INSPIRE].

[42] A. Burrows, M.S. Turner and R.P. Brinkmann, *Axions and SN 1987a*, *Phys. Rev. D* **39** (1989) 1020 [INSPIRE].

[43] W. Keil, H.-T. Janka, D.N. Schramm, G. Sigl, M.S. Turner and J.R. Ellis, *A Fresh look at axions and SN-1987A*, *Phys. Rev. D* **56** (1997) 2419 [astro-ph/9612222] [INSPIRE].

[44] G.G. Raffelt, *Astrophysical axion bounds*, in *Lecture Notes in Physics* **741**, Springer (2008), pp. 51–71 [hep-ph/0611350] [INSPIRE].

[45] J. Keller and A. Sedrakian, *Axions from cooling compact stars*, *Nucl. Phys. A* **897** (2013) 62 [arXiv:1205.6940] [INSPIRE].

[46] A. Sedrakian, *Axion cooling of neutron stars*, *Phys. Rev. D* **93** (2016) 065044 [arXiv:1512.07828] [INSPIRE].

[47] K. Hamaguchi, N. Nagata, K. Yanagi and J. Zheng, *Limit on the Axion Decay Constant from the Cooling Neutron Star in Cassiopeia A*, *Phys. Rev. D* **98** (2018) 103015 [arXiv:1806.07151] [INSPIRE].

[48] M.V. Beznogov, E. Rrapaj, D. Page and S. Reddy, *Constraints on Axion-like Particles and Nucleon Pairing in Dense Matter from the Hot Neutron Star in HESS J1731-347*, *Phys. Rev. C* **98** (2018) 035802 [arXiv:1806.07991] [INSPIRE].

[49] A. Sedrakian, *Axion cooling of neutron stars. II. Beyond hadronic axions*, *Phys. Rev. D* **99** (2019) 043011 [arXiv:1810.00190] [INSPIRE].

[50] J.H. Chang, R. Essig and S.D. McDermott, *Supernova 1987A Constraints on Sub-GeV Dark Sectors, Millicharged Particles, the QCD Axion, and an Axion-like Particle*, *JHEP* **09** (2018) 051 [arXiv:1803.00993] [INSPIRE].

[51] P. Carenza, T. Fischer, M. Giannotti, G. Guo, G. Martínez-Pinedo and A. Mirizzi, *Improved axion emissivity from a supernova via nucleon-nucleon bremsstrahlung*, *JCAP* **10** (2019) 016 [*Erratum JCAP* **05** (2020) E01] [arXiv:1906.11844] [INSPIRE].

[52] G.G. Raffelt, *Astrophysical methods to constrain axions and other novel particle phenomena*, *Phys. Rept.* **198** (1990) 1 [INSPIRE].

[53] M.S. Turner, *Windows on the Axion*, *Phys. Rept.* **197** (1990) 67 [INSPIRE].

[54] D.B. Kaplan, *Opening the Axion Window*, *Nucl. Phys. B* **260** (1985) 215 [INSPIRE].

[55] M. Srednicki, *Axion Couplings to Matter. 1. CP Conserving Parts*, *Nucl. Phys. B* **260** (1985) 689 [INSPIRE].

[56] H. Georgi, D.B. Kaplan and L. Randall, *Manifesting the Invisible Axion at Low-energies*, *Phys. Lett. B* **169** (1986) 73 [INSPIRE].

[57] G. Grilli di Cortona, E. Hardy, J. Pardo Vega and G. Villadoro, *The QCD axion, precisely*, *JHEP* **01** (2016) 034 [arXiv:1511.02867] [INSPIRE].

[58] T. Vonk, F.-K. Guo and U.-G. Meißner, *Precision calculation of the axion-nucleon coupling in chiral perturbation theory*, *JHEP* **03** (2020) 138 [arXiv:2001.05327] [INSPIRE].

[59] N.K. Glendenning, *The hyperon composition of neutron stars*, *Phys. Lett. B* **114** (1982) 392 [INSPIRE].

[60] N.K. Glendenning, *Neutron Stars Are Giant Hypernuclei?*, *Astrophys. J.* **293** (1985) 470 [INSPIRE].

[61] O.V. Maxwell, *Neutrino Emission Processes in Hyperon Populated Neutron Stars*, *Astrophys. J.* **316** (1987) 691 [INSPIRE].

[62] F. Weber and M.K. Weigel, *Neutron Star Properties and the Relativistic Nuclear Equation of State of Many Baryon Matter*, *Nucl. Phys. A* **493** (1989) 549 [INSPIRE].

[63] J.R. Ellis, J.I. Kapusta and K.A. Olive, *Strangeness, glue and quark matter content of neutron stars*, *Nucl. Phys. B* **348** (1991) 345 [INSPIRE].

[64] N.K. Glendenning and S.A. Moszkowski, *Reconciliation of neutron star masses and binding of the Λ in hypernuclei*, *Phys. Rev. Lett.* **67** (1991) 2414 [INSPIRE].

[65] R. Knorren, M. Prakash and P.J. Ellis, *Strangeness in hadronic stellar matter*, *Phys. Rev. C* **52** (1995) 3470 [nucl-th/9506016] [INSPIRE].

[66] J. Schaffner and I.N. Mishustin, *Hyperon rich matter in neutron stars*, *Phys. Rev. C* **53** (1996) 1416 [nucl-th/9506011] [INSPIRE].

[67] S. Balberg, I. Lichtenstadt and G.B. Cook, *Roles of hyperons in neutron stars*, *Astrophys. J. Suppl.* **121** (1999) 515 [astro-ph/9810361] [INSPIRE].

[68] M. Baldo, G.F. Burgio and H.J. Schulze, *Hyperon stars in the Brueckner-Bethe-Goldstone theory*, *Phys. Rev. C* **61** (2000) 055801 [nucl-th/9912066] [INSPIRE].

[69] H. Shen, *Complete relativistic equation of state for neutron stars*, *Phys. Rev. C* **65** (2002) 035802 [nucl-th/0202030] [INSPIRE].

[70] B.D. Lackey, M. Nayyar and B.J. Owen, *Observational constraints on hyperons in neutron stars*, *Phys. Rev. D* **73** (2006) 024021 [astro-ph/0507312] [INSPIRE].

[71] H. Djapo, B.-J. Schaefer and J. Wambach, *On the appearance of hyperons in neutron stars*, *Phys. Rev. C* **81** (2010) 035803 [arXiv:0811.2939] [INSPIRE].

[72] I. Bednarek, P. Haensel, J.L. Zdunik, M. Bejger and R. Manka, *Hyperons in neutron-star cores and two-solar-mass pulsar*, *Astron. Astrophys.* **543** (2012) A157 [arXiv:1111.6942] [INSPIRE].

[73] S. Weissenborn, D. Chatterjee and J. Schaffner-Bielich, *Hyperons and massive neutron stars: vector repulsion and* SU(3) *symmetry*, *Phys. Rev. C* **85** (2012) 065802 [*Erratum ibid.* **90** (2014) 019904] [arXiv:1112.0234] [INSPIRE].

[74] T. Miyatsu, M.-K. Cheoun and K. Saito, *Equation of state for neutron stars in* SU(3) *flavor symmetry*, *Phys. Rev. C* **88** (2013) 015802 [arXiv:1304.2121] [INSPIRE].

[75] L.L. Lopes and D.P. Menezes, *Hypernuclear matter in a complete* SU(3) *symmetry group*, *Phys. Rev. C* **89** (2014) 025805 [arXiv:1309.4173] [INSPIRE].

[76] M. Fortin, J.L. Zdunik, P. Haensel and M. Bejger, *Neutron stars with hyperon cores: stellar radii and equation of state near nuclear density*, *Astron. Astrophys.* **576** (2015) A68 [arXiv:1408.3052] [INSPIRE].

[77] M. Oertel, C. Providência, F. Gulminelli and A.R. Raduta, *Hyperons in neutron star matter within relativistic mean-field models*, *J. Phys. G* **42** (2015) 075202 [arXiv:1412.4545] [INSPIRE].

[78] T. Katayama and K. Saito, *Hyperons in neutron stars*, *Phys. Lett. B* **747** (2015) 43 [arXiv:1501.05419] [INSPIRE].

160

[79] D. Chatterjee and I. Vidaña, *Do hyperons exist in the interior of neutron stars?*, *Eur. Phys. J. A* **52** (2016) 29 [arXiv:1510.06306] [ɪɴSPIRE].

[80] L. Tolos, M. Centelles and A. Ramos, *Equation of State for Nucleonic and Hyperonic Neutron Stars with Mass and Radius Constraints*, *Astrophys. J.* **834** (2017) 3 [arXiv:1610.00919] [ɪɴSPIRE].

[81] L. Tolos, M. Centelles and A. Ramos, *The Equation of State for the Nucleonic and Hyperonic Core of Neutron Stars*, *Publ. Astron. Soc. Austral.* **34** (2017) e065 [arXiv:1708.08681] [ɪɴSPIRE].

[82] R. Negreiros, L. Tolos, M. Centelles, A. Ramos and V. Dexheimer, *Cooling of Small and Massive Hyperonic Stars*, *Astrophys. J.* **863** (2018) 104 [arXiv:1804.00334] [ɪɴSPIRE].

[83] T.-T. Sun, S.-S. Zhang, Q.-L. Zhang and C.-J. Xia, *Strangeness and Δ resonance in compact stars with relativistic-mean-field models*, *Phys. Rev. D* **99** (2019) 023004 [arXiv:1808.02207] [ɪɴSPIRE].

[84] D.D. Ofengeim, M.E. Gusakov, P. Haensel and M. Fortin, *Bulk viscosity in neutron stars with hyperon cores*, *Phys. Rev. D* **100** (2019) 103017 [arXiv:1911.08407] [ɪɴSPIRE].

[85] M. Fortin, A.R. Raduta, S. Avancini and C. Providência, *Relativistic hypernuclear compact stars with calibrated equations of state*, *Phys. Rev. D* **101** (2020) 034017 [arXiv:2001.08036] [ɪɴSPIRE].

[86] L. Tolos and L. Fabbietti, *Strangeness in Nuclei and Neutron Stars*, *Prog. Part. Nucl. Phys.* **112** (2020) 103770 [arXiv:2002.09223] [ɪɴSPIRE].

[87] K. Choi, S.H. Im, H.J. Kim and H. Seong, *Precision axion physics with running axion couplings*, arXiv:2106.05816 [ɪɴSPIRE].

[88] J. Gasser, M.E. Sainio and A. Švarc, *Nucleons with Chiral Loops*, *Nucl. Phys. B* **307** (1988) 779 [ɪɴSPIRE].

[89] A. Krause, *Baryon Matrix Elements of the Vector Current in Chiral Perturbation Theory*, *Helv. Phys. Acta* **63** (1990) 3 [ɪɴSPIRE].

[90] E.E. Jenkins and A.V. Manohar, *Baryon chiral perturbation theory using a heavy fermion Lagrangian*, *Phys. Lett. B* **255** (1991) 558 [ɪɴSPIRE].

[91] V. Bernard, N. Kaiser, J. Kambor and U.-G. Meißner, *Chiral structure of the nucleon*, *Nucl. Phys. B* **388** (1992) 315 [ɪɴSPIRE].

[92] V. Bernard, N. Kaiser and U.-G. Meißner, *Chiral dynamics in nucleons and nuclei*, *Int. J. Mod. Phys. E* **4** (1995) 193 [hep-ph/9501384] [ɪɴSPIRE].

[93] G. Müller and U.-G. Meißner, *Renormalization of the three flavor Lagrangian in heavy baryon chiral perturbation theory*, *Nucl. Phys. B* **492** (1997) 379 [hep-ph/9610275] [ɪɴSPIRE].

[94] J.A. Oller, M. Verbeni and J. Prades, *Meson-baryon effective chiral lagrangians to $\mathcal{O}(q^3)$*, *JHEP* **09** (2006) 079 [hep-ph/0608204] [ɪɴSPIRE].

[95] M. Frink and U.-G. Meißner, *On the chiral effective meson-baryon Lagrangian at third order*, *Eur. Phys. J. A* **29** (2006) 255 [hep-ph/0609256] [ɪɴSPIRE].

[96] N. Fettes, U.-G. Meißner and S. Steininger, *Pion-nucleon scattering in chiral perturbation theory. 1. Isospin symmetric case*, *Nucl. Phys. A* **640** (1998) 199 [hep-ph/9803266] [ɪɴSPIRE].

[97] Flavour Lattice Averaging Group, *FLAG Review 2019: Flavour Lattice Averaging Group (FLAG)*, *Eur. Phys. J. C* **80** (2020) 113 [`arXiv:1902.08191`] [InSPIRE].

[98] Particle Data collaboration, *Review of Particle Physics*, *Prog. Theor. Exp. Phys.* **2020** (2020) 083C01 [InSPIRE].

[99] M. Kolesár and J. Říha, *Application of Bayesian statistics to η-meson decay constant in χPT*, *Nucl. Part. Phys. Proc.* **309–311** (2020) 103 [`arXiv:1912.09164`] [InSPIRE].

[100] U.-G. Meißner and S. Steininger, *Baryon magnetic moments in chiral perturbation theory*, *Nucl. Phys. B* **499** (1997) 349 [`hep-ph/9701260`] [InSPIRE].

[101] B. Borasoy and U.-G. Meißner, *Chiral Expansion of Baryon Masses and σ-Terms*, *Annals Phys.* **254** (1997) 192 [`hep-ph/9607432`] [InSPIRE].

[102] J. Bijnens, H. Sonoda and M.B. Wise, *On the Validity of Chiral Perturbation Theory for Weak Hyperon Decays*, *Nucl. Phys. B* **261** (1985) 185 [InSPIRE].

[103] A. Manohar and H. Georgi, *Chiral Quarks and the Nonrelativistic Quark Model*, *Nucl. Phys. B* **234** (1984) 189 [InSPIRE].

[104] M.R. Schindler and D.R. Phillips, *A Bayesian approach to chiral extrapolations*, *PoS* **CD09** (2009) 019 [`arXiv:0909.3865`] [InSPIRE].

[105] J. Gasser and H. Leutwyler, *Chiral Perturbation Theory: Expansions in the Mass of the Strange Quark*, *Nucl. Phys. B* **250** (1985) 465 [InSPIRE].

[106] A.V. Manohar, *Large N QCD*, in proceedings of *Les Houches Summer School in Theoretical Physics, Session 68: Probing the Standard Model of Particle Interactions*, Les Houches, France, 28 July–5 September 1997, `hep-ph/9802419` [InSPIRE].

[107] M. Hoferichter, J. Ruiz de Elvira, B. Kubis and U.-G. Meißner, *Matching pion-nucleon Roy-Steiner equations to chiral perturbation theory*, *Phys. Rev. Lett.* **115** (2015) 192301 [`arXiv:1507.07552`] [InSPIRE].

[108] L. Darmé, L. Di Luzio, M. Giannotti and E. Nardi, *Selective enhancement of the QCD axion couplings*, *Phys. Rev. D* **103** (2021) 015034 [`arXiv:2010.15846`] [InSPIRE].

Pion axioproduction: The Delta resonance contribution

Pion axioproduction: The Δ resonance contribution

Thomas Vonk[*]

Helmholtz-Institut für Strahlen- und Kernphysik and Bethe Center for Theoretical Physics,
Universität Bonn, D-53115 Bonn, Germany

Feng-Kun Guo[†]

CAS Key Laboratory of Theoretical Physics, Institute of Theoretical Physics,
Chinese Academy of Sciences, Beijing 100190, China
and School of Physical Sciences, University of Chinese Academy of Sciences, Beijing 100049, China

Ulf-G. Meißner[‡]

Helmholtz-Institut für Strahlen- und Kernphysik and Bethe Center for Theoretical Physics,
Universität Bonn, D-53115 Bonn, Germany,
Institute for Advanced Simulation, Institut für Kernphysik and Jülich Center for Hadron Physics,
Forschungszentrum Jülich, D-52425 Jülich, Germany and Tbilisi State University, 0186 Tbilisi, Georgia

The process of pion axioproduction, $aN \to \pi N$, with an intermediate Δ resonance is analyzed using baryon chiral parturbation theory. The Δ resonance is included in two ways: First, deriving the $a\Delta N$-vertices, the axion is brought into contact with the resonance, and, second, taking the results of πN elastic scattering including the Δ, it is implicitly included in the form of a pion rescattering diagram. As a result, the partial wave cross section of axion-nucleon scattering shows an enhancement in the energy region around the Δ resonance. Because of the isospin breaking, the enhancement is not as pronounced as previously anticipated. However, since the isospin breaking here is much milder than that for usual hadronic processes, novel axion-search experiments might still exploit this effect.

I. INTRODUCTION

A model that might resolve two of the known problems of two different (but related) physical fields—in the present case the strong-CP problem of quantum chromodynamics (QCD) and the dark matter issue of astrophysics and cosmology [1–7]—is clearly worth investigating. Such a model is the Peccei-Quinn model [8,9] and the theory of the axion [10,11], especially the "invisble" axion models such as the Kim-Shifman-Vainstein-Zakharov (KSVZ) axion model [12,13] and the Dine-Fischler-Srednicki-Zhitnitsky (DFSZ) axion model [14,15]. However, the time theorists and experimentalists effortfully spent on the search for signals that might verify this model now comprises more than four decades, and still there is no axion in sight.

Because of that it is important to study all kinds of related processes hoping to figure out some underlying phenomenon that might enhance the chance of its detection, if only for a few percent.

Recently, Carenza *et al.* [16] have proposed that the pion axioproduction [17] $aN \to \pi N$ is such a process, because at certain axion energies, around 200 MeV–300 MeV, an enhanced axion-nucleon cross section due to the Δ resonance can be expected. This in turn would possibly make axion detections accessible for underground water Cherenkov detectors. Such axions might be produced in protosupernova cores in the presence of pions, where besides the axion production via axion-nucleon bremsstrahlung $NN \to aNN$, the pion-induced process $\pi N \to aN$ might play a more important role than previously thought [16,18], leading to a possible enhancement of the number spectrum of axions with energies around 200 MeV–300 MeV.

In this study, we take a closer look at exactly this process, namely $aN \to \pi N$ with the Δ resonance, showing that there is indeed a region of enhancement. This enhancement is, however, at least an order of magnitude less pronounced than that anticipated by Carenza *et al.* [16], which we will discuss in more detail below in Sec. IV.

[*]vonk@hiskp.uni-bonn.de
[†]fkguo@itp.ac.cn
[‡]meissner@hiskp.uni-bonn.de

Having said that, it is important to remind the reader that the traditional window for the QCD axion as a dark matter candidate dictates [1,2,19,20]

$$10^9 \text{ GeV} \lesssim f_a \lesssim 10^{12} \text{ GeV}, \tag{1}$$

where f_a is the axion decay constant which eventually controls and suppresses the axion mass [21,22]

$$m_a \approx 5.7 \left(\frac{10^{12} \text{ GeV}}{f_a} \right) \times 10^{-6} \text{ eV}, \tag{2}$$

and the axion-nucleon coupling $G_{aN} \propto 1/f_a$. This means that despite the possible enhancement due to the presence of baryon resonances, the reaction cross section still remains tiny.

A very suitable framework for studying the process at hand is chiral perturbation theory (CHPT), which has been successfully extended to the meson-nucleon and Δ-meson-nucleon sectors, and which in the past also has been applied to the study of the axion-nucleon interaction [23,24], after the leading order axion-nucleon interaction had been studied for years in the context of current algebra, which is equivalent to a leading-order calculation in CHPT [25–29]. In this paper we use these results including the thereby accrued knowledge of the underlying structure of the axion-nucleon coupling. Moreover, we show how to include the Δ baryon into the model.

In Sec. II we first give a short discussion of the kinematics and the general isospin structure of the $aN \to \pi N$ scattering amplitude, as well as a brief presentation of baryon CHPT with axions and the Δ resonance. Then we work out the amplitudes of the individual Feynman diagrams contributing to the pion axioproduction in Sec. III. Putting the pieces together, we finally discuss the results in Sec. IV.

II. THEORETICAL FOUNDATION

A. Kinematics

The process under consideration is

$$a(q) + N(p) \to \pi^b(q') + N(p'), \tag{3}$$

where a denotes the axion, N is a nucleon (either the proton or the neutron), and π^b is a pion with the isospin index b. As usual, we define the Lorentz-invariant Mandelstam variables

$$s = (p+q)^2, \quad t = (p-p')^2, \quad u = (p-q')^2, \tag{4}$$

for the four-momenta q, p of the incoming particles and q', p' of the outgoing particles. The invariants of Eq. (4) fulfill the on shell relation

$$s + t + u = 2m_N^2 + m_a^2 + M_\pi^2, \tag{5}$$

which can be used to eliminate one of the three variables, which we choose to be u. Throughout this paper we use the center-of-mass system (c.m.), where for the three-momenta $\mathbf{p} + \mathbf{q} = \mathbf{p}' + \mathbf{q}' = 0$. Using the well-known Källén function

$$\lambda(a, b, c) = a^2 + b^2 + c^2 - 2ab - 2ac - 2bc, \tag{6}$$

the c.m. energies of the incoming and outgoing nucleons can be written as

$$E_\mathbf{p} = \frac{s + m_N^2 - m_a^2}{2\sqrt{s}}, \qquad E_{\mathbf{p}'} = \frac{s + m_N^2 - M_\pi^2}{2\sqrt{s}}, \tag{7}$$

and one has

$$|\mathbf{p}| = |\mathbf{q}| = \frac{\sqrt{\lambda(s, m_N^2, m_a^2)}}{2\sqrt{s}},$$

$$|\mathbf{p}'| = |\mathbf{q}'| = \frac{\sqrt{\lambda(s, m_N^2, M_\pi^2)}}{2\sqrt{s}}. \tag{8}$$

Moreover, setting $z = \cos\theta$, where θ is the c.m. scattering angle, we have

$$(\mathbf{p} \cdot \mathbf{p}') = |\mathbf{p}||\mathbf{p}'|z, \tag{9}$$

so we can reexpress the second Mandelstam t variable as

$$t = 2(m_N^2 - E_\mathbf{p}E_{\mathbf{p}'} + |\mathbf{p}||\mathbf{p}'|z). \tag{10}$$

Before discussing how these kinematic quantities enter the scattering amplitudes, we briefly take a look at the isospin structure of the process.

B. Isospin structure

For the πN elastic scattering, it is common to decompose the scattering amplitude $T_{\pi N \to \pi N}^{ab}$, where a is the isospin index of the incoming pion and b for the outgoing one, according to the isospin structure. In the isospin limit, the decomposition reads

$$T_{\pi N \to \pi N}^{ab} = T^+ \delta_{ab} + T^- \frac{1}{2}[\tau_a, \tau_b], \tag{11}$$

where τ_a and τ_b are the Pauli matrices and $[,]$ denotes the commutator. However, for the present process $aN \to \pi^b N$ we are particularly interested in transitions including the Δ resonance, as suggested in Ref. [16], which is an isospin-$\frac{3}{2}$ particle. As the axion is an isoscalar, no isospin symmetric aN interaction can lead to the appearance of the Δ resonance, so we are especially interested in isospin-breaking interactions. Indeed, the isovector axial-vector current a_μ (see below) introduces such isospin breaking pieces into the axion-baryon interaction, which can be seen, for instance, below in Eqs. (27) and (33).

As it turns out, it is possible to decompose the scattering amplitude $T_{aN \to \pi N}^b$ into

166

$$T^b_{aN \to \pi N} = T^+ \delta_{3b} + T^{3+} \tau_3 + T^- \frac{1}{2}[\tau_b, \tau_3], \quad (12)$$

which is comparable to the case of πN scattering with isospin violation, see, e.g., Refs. [30,31]. Any of the four possible amplitudes can be expressed by means of the three objects $T^+, T^{3+},$ and T^-,

$$\begin{aligned} T_{ap \to \pi^0 p} &= T^+ + T^{3+}, \\ T_{an \to \pi^0 n} &= T^+ - T^{3+}, \\ T_{ap \to \pi^+ n} &= \sqrt{2}(T^{3+} + T^-), \\ T_{an \to \pi^- p} &= \sqrt{2}(T^{3+} - T^-). \end{aligned} \quad (13)$$

The part of the amplitude that leads to isospin violation and thus to possible enhancement due to the Δ resonances, which we denote by $T^{3/2}$, is found by taking the difference

$$T^{3/2} = T^+ - T^-, \quad (14)$$

or alternatively,

$$\begin{aligned} T^{3/2} &= T_{ap \to \pi^0 p} - \frac{1}{\sqrt{2}} T_{ap \to \pi^+ n} \\ &= T_{an \to \pi^0 n} + \frac{1}{\sqrt{2}} T_{an \to \pi^- p}, \end{aligned} \quad (15)$$

where the latter expressions have the advantage that one can also easily account for differences in the charged and neutral pion masses, which improves the accuracy of the calculation.

C. Partial wave decomposition

It is known from πN scattering that the Δ resonance chiefly affects the P_{33} partial wave (where we, as usual, make use of the spectroscopic notation $l_{2I,2j}$, $l = S, P, D, \ldots$ being the orbital angular momentum, I being the isospin, and $j = l + s$ the total angular momentum). Therefore, it is expedient to also focus on the P_{33} partial wave in the present study of the $aN \to \pi N$ reaction.

To this end, we decompose any of the amplitudes given above as

$$T = \bar{u}(p') \left\{ A(s,t) + B(s,t) \frac{1}{2}(\not{q} + \not{q}') \right\} u(p), \quad (16)$$

where we make use of the well-known notation, $\not{q} = \gamma^\mu q_\mu$. One then can project out any partial wave of definite total angular momentum $j = l \pm 1/2$, abbreviated as $l\pm$, by

$$T_{l\pm}(s) = \frac{\sqrt{E_{\mathbf{p}} + m_N} \sqrt{E_{\mathbf{p}'} + m_N}}{2} \{A_l(s) + (\sqrt{s} - m_N)B_l(s)\} + \frac{\sqrt{E_{\mathbf{p}} - m_N} \sqrt{E_{\mathbf{p}'} - m_N}}{2} \{-A_{l\pm 1}(s) + (\sqrt{s} + m_N)B_{l\pm 1}(s)\}, \quad (17)$$

where

$$\begin{aligned} A_l(s) &= \int_{-1}^{+1} A(s, t(s,z)) P_l(z) \mathrm{d}z, \\ B_l(s) &= \int_{-1}^{+1} B(s, t(s,z)) P_l(z) \mathrm{d}z, \end{aligned} \quad (18)$$

using the well-known Legendre polynomials $P_l(z)$.

D. Partial wave cross section

For experiments, the most useful quantity is the cross section

$$\mathrm{d}\sigma = \frac{1}{\mathcal{F}} |\mathcal{M}|^2 \mathrm{d}\Pi_2, \quad (19)$$

with the flux factor

$$\mathcal{F} = 4\sqrt{(p \cdot q) - m_N m_a} = 4|\mathbf{p}|\sqrt{s}, \quad (20)$$

and the two-body phase space

$$\begin{aligned} \int \mathrm{d}\Pi_2 &= \int \frac{\mathrm{d}^3 p'}{(2\pi)^3} \frac{\mathrm{d}^3 q'}{(2\pi)^3} \frac{1}{2E_{\mathbf{p}'} 2E_{\mathbf{q}'}} (2\pi)^4 \delta^4(p + q - p' - q') \\ &= \int \mathrm{d}\Omega \frac{1}{16\pi^2} \frac{|\mathbf{p}'|}{\sqrt{s}}, \end{aligned} \quad (21)$$

where in both cases the right-most expressions are valid in the c.m. frame. The total cross section is hence given by

$$\sigma = \frac{1}{64\pi^2 s} \frac{|\mathbf{p}'|}{|\mathbf{p}|} \int \mathrm{d}\Omega |\mathcal{M}|^2, \quad (22)$$

which can be expanded in terms of partial wave cross sections as

$$\sigma = \sum_l \sigma_{l\pm}. \qquad (23)$$

The inverse of Eq. (17) is given by

$$T = 2m_N \chi_f^\dagger \sum_l \left\{ [(l+1)T_{l+} + lT_{l-}]P_l(z) \right.$$
$$\left. - i\boldsymbol{\sigma} \cdot (\hat{\mathbf{q}}' \times \hat{\mathbf{q}})(T_{l+} - T_{l-}) \frac{\mathrm{d}P_l}{\mathrm{d}z} \right\} \chi_i, \qquad (24)$$

where χ_i and χ_f are the Pauli spinors of the incoming and outgoing nucleons, respectively, and $\hat{\mathbf{q}}^{(\prime)} = \mathbf{q}^{(\prime)}/|\mathbf{q}^{(\prime)}|$. For the $j = \frac{3}{2}$ case, one finds

$$\sigma_{1+} = \frac{1}{8\pi s} \frac{|\mathbf{p}'|}{|\mathbf{p}|} |T_{1+}|^2. \qquad (25)$$

The bottom line of the previous elaborations then is that we will derive the amplitudes $A^{\pm,3+}(s,t)$ and $B^{\pm,3+}(s,t)$ for any Feynman diagram of interest and use Eqs. (12) and (17) in order to determine the P_{33} partial wave amplitude $T^{33}_{aN\to\pi N}$ for the pertinent processes. This amplitude in turn is used to ascertain the corresponding cross section via Eq. (25). The theoretical framework of determining $A^{\pm,3+}(s,t)$ and $B^{\pm,3+}(s,t)$ is CHPT.

E. Baryon chiral perturbation theory with axions

The way of incorporating the axion into CHPT is discussed in detail in Ref. [24]. Here, we will only outline the major steps. First, recall that in the standard QCD axion models, the KSVZ and DFSZ ones, the axion-quark couplings X_q appearing in the QCD Lagrangian after the spontaneous breakdown of Peccei-Quinn symmetry are flavor diagonal and given by

$$X_q^{\mathrm{KSVZ}} = 0,$$
$$X_{u,c,t}^{\mathrm{DFSZ}} = \frac{1}{3}\frac{x^{-1}}{x + x^{-1}} = \frac{1}{3}\sin^2\beta,$$
$$X_{d,s,b}^{\mathrm{DFSZ}} = \frac{1}{3}\frac{x}{x + x^{-1}} = \frac{1}{3}\cos^2\beta = \frac{1}{3} - X_{u,c,t}^{\mathrm{DFSZ}}, \qquad (26)$$

where $x = \cot\beta$ is the ratio of the vacuum expectation values of the two Higgs doublets in the DFSZ model. After a chiral rotation removing the axion-gluon coupling terms in the Lagrangian, the whole axion-quark interaction can be decomposed into isovector and isoscalar parts with the couplings

$$c_{u-d} = \frac{1}{2}\left(X_u - X_d - \frac{1-z}{1+z+w}\right),$$
$$c_{u+d} = \frac{1}{2}\left(X_u + X_d - \frac{1+z}{1+z+w}\right),$$
$$c_s = X_s - \frac{w}{1+z+w},$$
$$c_{c,b,t} = X_{c,b,t}, \qquad (27)$$

where $z = m_u/m_d$ and $w = m_u/m_s$ are the quark mass ratios of the three light quarks. In what follows, the c_i, $(i = \{1, ..., 5\})$, refer to the isoscalar couplings $\{u + d, s, c, b, t\}$ and in any equation a summation over repeated i is implied. It is these couplings that enter the Lagrangian of CHPT in the form of external currents [32]

$$a_\mu = c_{u-d}\frac{\partial_\mu a}{2f_a}\tau_3, \qquad a_{\mu,i}^{(s)} = c_i\frac{\partial_\mu a}{2f_a}\mathbb{1}. \qquad (28)$$

The transition to CHPT is phenomenologically related to the confinement of quarks and gluons into mesons and baryons at low energies and the observation that the QCD Lagrangian is approximately invariant under the chiral symmetry $\mathrm{SU}(N_f)_L \times \mathrm{SU}(N_f)_R$, with N_f the number of light quark flavors, which is spontaneously broken into the vector subgroup. Hence, in SU(2) baryon CHPT nucleons and pions are the relevant degrees of freedom rather than the more fundamental quarks and gluons. The application of power counting rules then leads to a systematic perturbative description of any low-energy strong interaction process, as long as the applied Lagrangian respects all pertinent symmetries, as first worked out by Weinberg [33].

For the meson-nucleon sector that we are interested in, we follow the description of baryon CHPT given in Ref. [34]. The pions enter the theory in the form of a unitary 2×2 matrix

$$u = \sqrt{U} = \exp\left(i\frac{\pi^a\tau_a}{2F_\pi}\right), \qquad (29)$$

where F_π is the pion decay constant. Strictly speaking, this should be the pion decay constant in the chiral limit, F, but to the order we are working on we can use the physical value. With this unitary matrix and the external currents a_μ and $a_\mu^{(s)}$, see Eq. (28), one forms the following basic building blocks

$$u_\mu = i[u^\dagger\partial_\mu u - u\partial_\mu u^\dagger - iu^\dagger a_\mu u - iua_\mu u^\dagger],$$
$$u_{\mu,i} = i[-iu^\dagger a_{\mu,i}^{(s)}u - iua_{\mu,i}^{(s)}u^\dagger] = 2a_{\mu,i}^{(s)},$$
$$D_\mu = \partial_\mu + \Gamma_\mu$$
$$= \partial_\mu + \frac{1}{2}[u^\dagger\partial_\mu u + u\partial_\mu u^\dagger - iu^\dagger a_\mu u + iua_\mu u^\dagger]. \qquad (30)$$

Note that we only introduce and show the axial-vector currents a_μ (isovector) and $a_\mu^{(s)}$ (isoscalar) (and not the corresponding vector currents) as these are the only external currents that are of interest in what follows. The last object in Eq. (30), D_μ, is the so-called chiral covariant derivative. At leading order, the axion only enters the model via these building blocks. At higher order, it also enters in the form of nonderivative interactions by means of terms involving the complex phase of the quark mass matrix.

In what follows, we only need the leading order pion-nucleon Lagrangian, which is given by

$$\mathcal{L}_{\pi N} = \bar{N} \left\{ i\slashed{D} - m_N + \frac{g_A}{2} \slashed{a} \gamma_5 + \frac{g_0^i}{2} \slashed{a}_i \gamma_5 \right\} N, \quad (31)$$

where $N = (p, n)^{\mathrm{T}}$ is an isodoublet containing the proton and the neutron spinors, m_N is the nucleon mass in the chiral limit, and g_A and the g_0^i's are the axial-vector and corresponding isoscalar coupling constants, all also in the chiral limit. Again, to the order we are working, we can identify these parameters with their physical values.

In Ref. [24], we already worked out and used the relevant vertices that can be derived from this Lagrangian and which are also needed for the present study. Denoting the momentum of an incoming axion with q_μ and setting b as the pion isospin index, one finds for the relevant vertices,

$$aNN : \frac{g_{aN}}{2f_a} \slashed{q} \gamma_5,$$
$$a\pi_b NN : i \frac{c_{u-d}}{4f_a F_\pi} \slashed{q} [\tau_3, \tau_b]. \quad (32)$$

The latter contact interaction is often ignored in studies of the aN reaction, which are mainly based on the former vertex, but has recently been included in the study of axion production in supernovae [35].

The axion-nucleon coupling appearing in Eq. (32) is a 2×2 matrix in isospin space defined as

$$g_{aN} = c_{u-d} g_A \tau_3 + c_i g_0^i \mathbb{1}, \quad (33)$$

from which one can directly read off the couplings of the axion to the proton, g_{ap}, and the neutron, g_{an}, respectively.

F. The Δ resonance in chiral perturbation theory

The free-field Lagrangian of the four Δ baryons is given by [36–41]

$$\mathcal{L}_\Delta = \bar{\Delta}_\mu \Lambda^{\mu\nu}(A) \Delta_\nu, \quad (34)$$

where

$$\Delta_\mu = \begin{pmatrix} \Delta_\mu^{++} \\ \Delta_\mu^+ \\ \Delta_\mu^0 \\ \Delta_\mu^- \end{pmatrix} \quad (35)$$

is the spin-$\frac{3}{2}$ and isospin-$\frac{3}{2}$ vector-spinor field, and

$$\Lambda^{\mu\nu}(A = -1) = -(i\slashed{\partial} - m_\Delta) + i(\gamma^\mu \partial^\nu + \gamma^\nu \partial^\mu - \gamma^\mu \slashed{\partial} \gamma^\nu) - m_\Delta \gamma^\mu \gamma^\nu. \quad (36)$$

Here, m_Δ denotes the mass of the Δ and A is a nonphysical parameter that for convenience has been set to -1. The propagator for the Δ with four-momentum p^μ is then given by

$$-i\frac{\slashed{p} + m_\Delta}{p^2 - m_\Delta^2} \left[g^{\mu\nu} - \frac{1}{3}\gamma^\mu \gamma^\nu + \frac{1}{3m_\Delta}(p^\mu \gamma^\nu - \gamma^\mu p^\nu) - \frac{2}{3m_\Delta^2} p^\mu p^\nu \right]. \quad (37)$$

The $\pi N\Delta$ and the $aN\Delta$ interactions are derived from the general leading-order interaction Lagrangian given by [37,42]

$$\mathcal{L}_{\mathrm{int.}} = \frac{g}{2} \bar{\Delta}_{\mu,i}(g^{\mu\nu} + z_0 \gamma^\mu \gamma^\nu) \langle \tau_i u_\nu \rangle N + \mathrm{H.c.}, \quad (38)$$

where H.c. stands for the Hermitian conjugate and $\langle \rangle$ denotes the trace in flavor space. Furthermore, we make use of the isospurion representation $\Delta_{\mu,i} = \mathcal{T}_i \Delta_\mu$ with the 2×4 isospin-$\frac{1}{2}$-to-isospin-$\frac{3}{2}$ transition matrices [37,43]

$$\mathcal{T}_1 = \frac{1}{\sqrt{6}} \begin{pmatrix} -\sqrt{3} & 0 & 1 & 0 \\ 0 & -1 & 0 & \sqrt{3} \end{pmatrix},$$
$$\mathcal{T}_2 = \frac{-i}{\sqrt{6}} \begin{pmatrix} \sqrt{3} & 0 & 1 & 0 \\ 0 & 1 & 0 & \sqrt{3} \end{pmatrix},$$
$$\mathcal{T}_3 = \sqrt{\frac{2}{3}} \begin{pmatrix} 0 & 1 & 0 & 0 \\ 0 & 0 & 1 & 0 \end{pmatrix}, \quad (39)$$

such that

$$\Delta_{\mu,1} = \frac{1}{\sqrt{2}} \begin{pmatrix} \frac{1}{\sqrt{3}}\Delta_\mu^0 - \Delta_\mu^{++} \\ \Delta_\mu^- - \frac{1}{\sqrt{3}}\Delta_\mu^+ \end{pmatrix},$$
$$\Delta_{\mu,2} = -\frac{i}{\sqrt{2}} \begin{pmatrix} \frac{1}{\sqrt{3}}\Delta_\mu^0 + \Delta_\mu^{++} \\ \Delta_\mu^- + \frac{1}{\sqrt{3}}\Delta_\mu^+ \end{pmatrix},$$
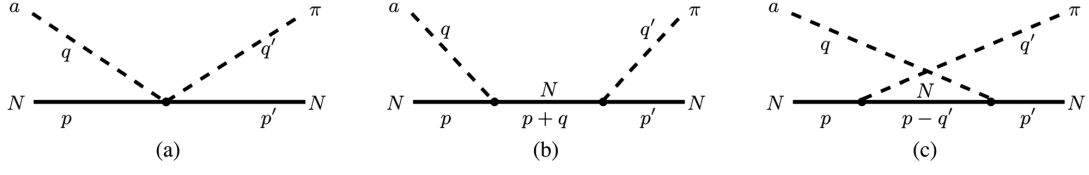$$\Delta_{\mu,3} = \sqrt{\frac{2}{3}} \begin{pmatrix} \Delta_\mu^+ \\ \Delta_\mu^0 \end{pmatrix}. \quad (40)$$

FIG. 1.   Tree-level contributions to $aN \to \pi N$ without the Δ intermediate state. (a) contact interaction, (b) s channel, and (c) crossed channel.

The interaction Lagrangian Eq. (38) contains two coupling constants g and z_0, the latter being an off shell parameter. N again denotes the nucleon doublet and u_μ has been given already above in Eq. (30). Note that this interaction Lagrangian only allows for isovector interactions with external axial currents a_μ, whereas isoscalar interactions with $a_{\mu,i}^{(s)}$ vanish as a consequence of the trace operation. This reflects what has been said already above; any $aN\Delta$ interaction must come with isospin violation, which is only present in a_μ, not in $a_{\mu,i}^{(s)}$.

III. RELEVANT DIAGRAMS AND THEIR CONTRIBUTIONS

A. Contact contribution and intermediate nucleon

Having set up the kinematic environment and the theoretical framework, we can now explore several contributions to the $aN \to \pi N$ scattering amplitude. We start with the tree-level contact and Born graphs shown in Fig. 1. The results can be obtained in a rather straightforward fashion by using the vertices of Eq. (32) and the πN vertex of the Lagrangian Eq. (31).

The contact interaction, Fig. 1(a), only gives a contribution to B^- and is free of any kinematic variable,

$$B_{1a}^- = \frac{c_{u-d}}{2 f_a F_\pi}. \tag{41}$$

This means that the contact interaction is solely present in the $ap \to \pi^+ n$ and $an \to \pi^- p$ processes, but absent in any process involving the neutral pion. For the diagrams of Figs. 1(b) and 1(c), one gets

$$A_{1b,1c}^+ = \frac{g_A^2 c_{u-d} m_N}{f_a F_\pi},$$

$$B_{1b,1c}^+(s,t) = -\frac{g_A^2 c_{u-d} m_N^2}{f_a F_\pi}\left(\frac{1}{s-m_N^2}-\frac{1}{u-m_N^2}\right),$$

$$A_{1b,1c}^{3+} = \frac{g_A g_0^i c_i m_N}{f_a F_\pi},$$

$$B_{1b,1c}^{3+}(s,t) = -\frac{g_A g_0^i c_i m_N^2}{f_a F_\pi}\left(\frac{1}{s-m_N^2}-\frac{1}{u-m_N^2}\right),$$

$$A_{1b,1c}^- = 0,$$

$$B_{1b,1c}^-(s,t) = -\frac{g_A^2 c_{u-d} m_N}{2 f_a F_\pi}\left[1+2m_N\left(\frac{1}{s-m_N^2}+\frac{1}{u-m_N^2}\right)\right], \tag{42}$$

where u needs to be understood as $u(s,t)$ via Eq. (5). In the Appendix, we give a different expression of these contributions in terms of the axion-nucleon coupling constants g_{an} and g_{ap} for each of the four possible $aN \to \pi N$ channels. However, for the study of the P_{33} partial wave, it is not expedient to rewrite them in terms of g_{an} and g_{ap}, because after forming the difference Eq. (14), one can nicely see that the isoscalar terms $\propto c_i$ stemming from $a_{\mu,i}^{(s)}$ drop out, leaving only the isospin violating portion $\propto c_{u-d}$ that originates from a_μ. This fact makes it easy to show (as will be done below) that in the case of the P_{33} partial wave the KSVZ axion can be treated as a special case of the DSFZ axion.

B. Intermediate Δ resonance

Including the Δ leads to the diagrams shown in Fig. 2. As the two diagrams are related by crossing, it is convenient to define

$$A_\Delta(s,t) = \frac{2g^2 c_{u-d}}{3 f_a F_\pi}\left\{\frac{2z_0}{3m_\Delta^2}[m_\Delta + (m_N + 2m_\Delta)z_0](s - m_N^2) + \frac{1}{s-\mu_\Delta^2}\left[(m_N + m_\Delta)\left(\frac{1}{2}[m_a^2 + M_\pi^2 - t] - \frac{1}{3}[s - m_N^2]\right)\right.\right.$$
$$\left.\left. - \frac{1}{6m_\Delta^2}\left((m_N + m_\Delta)([m_a^2 + M_\pi^2][s - m_N^2] + m_a^2 M_\pi^2) + m_a^2 M_\pi^2 m_\Delta + m_N(s - m_N^2)^2\right)\right]\right\}, \tag{43}$$

and

170
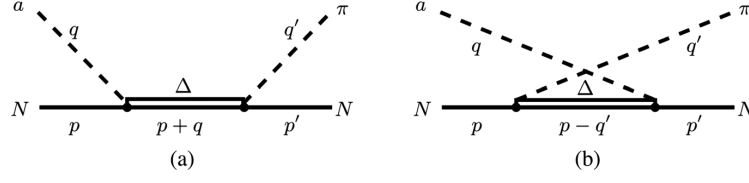
FIG. 2. Tree-level contributions to $aN \to \pi N$ with an intermediate Δ state. (a) s channel and (b) crossed channel.

$$B_\Delta(s,t) = \frac{2g^2 c_{u-d}}{3f_a F_\pi} \left\{ -\frac{z_0}{3m_\Delta^2} \left[m_a^2 + M_\pi^2 + 2(s - m_N^2)(1 + z_0) + 4m_N m_\Delta (1 + z_0) + 4m_N(m_N + m_\Delta)z_0 \right] \right.$$
$$+ \frac{1}{s - \mu_\Delta^2} \left[\frac{1}{2}[m_a^2 + M_\pi^2 - t] - \frac{1}{6}m_a^2 + \frac{1}{6m_\Delta}(m_N + m_\Delta)(4m_N m_\Delta - M_\pi^2) \right.$$
$$\left. \left. - \frac{1}{6m_\Delta^2} [(m_a^2 + M_\pi^2 + 2m_N m_\Delta)(s - m_N^2) + m_a^2(m_N m_\Delta + M_\pi^2) + (s - m_N^2)^2] \right] \right\}. \quad (44)$$

Here the axion mass terms are kept explicitly though they, being tiny for the standard QCD axion models, can be safely neglected.

Then one can combine both diagrams and obtains the following expressions

$$A_\Delta^+(s,t) = A_\Delta(s,t) + A_\Delta(u,t),$$
$$B_\Delta^+(s,t) = B_\Delta(s,t) - B_\Delta(u,t),$$
$$A_\Delta^-(s,t) = -\frac{1}{2}[A_\Delta(s,t) - A_\Delta(u,t)],$$
$$B_\Delta^-(s,t) = -\frac{1}{2}[B_\Delta(s,t) + B_\Delta(u,t)], \quad (45)$$

where again $u = u(s,t)$. Note that there is no contribution to T^{3+}. Equations (43) and (44) have a pole appearing at c.m. energies around the Δ mass squared. In order to circumvent any unnecessary subtleties related to this, we use a Breit-Wigner propagator with a complex mass squared

$$\mu_\Delta^2 = m_\Delta^2 - im_\Delta \Gamma_\Delta \quad (46)$$

with $m_\Delta \approx 1232$ MeV and $\Gamma_\Delta \approx 117$ MeV the Breit-Wigner mass and width of the Δ resonance. A more refined treatment could e.g., be given by including the Δ self-energy in the complex mass scheme, but that is not required here.

C. Pion rescattering

Another sort of diagram that contributes is shown in Fig. 3. As in the previous diagrams, the left (smaller) vertex leads to an axion-pion conversion (so this vertex basically comprises the contributions of Fig. 1). This pion consequently gets rescattered in the ordinary πN scattering. The

latter (larger) vertex treated in a proper way also includes contributions from the Δ baryon. As this is an often studied process, we can base the treatment of this diagram on previous results. In particular, we will adopt the method and results of Refs. [44,45].

The diagrams that contribute to the πN scattering at this order are basically the same as the ones discussed in the previous subsections, but with the axion replaced by another pion. Using Eqs. (11) and (17) leads to a projection to the P_{33} partial wave. We do not repeat the results for the diagrams here, they can be found in Ref. [44], Eqs. (3.4) and (3.9) [46]. Moreover, we also adopt the results for the renormalized chiral pion loops obtained in heavy baryon CHPT (HBCHPT) from [47] (which are needed for the unitarization, see below).

As the πN scattering above threshold and below the appearance of inelastic reactions fulfills the unitarity relation (here $W = \sqrt{s}$, the c.m. energy)

$$\text{Im} T_{l\pm}^I(W) = \frac{|\mathbf{q}|}{8\pi W} |T_{l\pm}^I(W)|^2, \quad (47)$$

the pole in the Δ propagator can be treated in a more systematic way than the one we used in Sec. III B for the $aN \to \pi N$ reaction. In particular, a suitable unitarization technique can be used to restore unitarity which is otherwise only fulfilled perturbatively in CHPT. The method used in Ref. [44] is the N/D method [48,49]. In a nutshell,
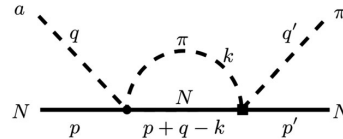
FIG. 3. The pion-rescattering diagram for $aN \to \pi N$.

it is based on the observation that the unitarity relation leads to a right-hand cut in the partial wave T-matrix such that one can write down a dispersion relation for the inverse amplitude with some extra terms which are free of any right-hand cuts. These can be matched to the amplitudes obtained from CHPT. This effectively corresponds to a resummation of the relevant diagrams. Possible double counting can be avoided by the matching procedure discussed in Ref. [45]. The integral of the dispersion relation can be performed analytically and is basically given by the known two-point loop function involving one pion and one nucleon,

$$g(s) = \frac{1}{16\pi^2} \left\{ a_0(\mu) + \left(1 - \frac{w}{m_N}\right) \log\left(\frac{M_\pi^2}{\mu^2}\right) - x_+ \log\left(\frac{x_+ - 1}{x_+}\right) - x_- \log\left(\frac{x_- - 1}{x_-}\right) \right\}, \quad (48)$$

at a renormalization scale μ. We take μ as the nucleon mass, and any change in μ can be reabsorbed by the subtraction constant $a_0(\mu)$. Furthermore, w is the c.m. pion energy and

$$x_\pm = \frac{s + m_N^2 - M_\pi^2}{2s} \pm \frac{1}{2s}\sqrt{\lambda(s, m_N^2, M_\pi^2)}. \quad (49)$$

The matching procedure for unitarizing the leading one-loop $\mathcal{O}(p^3)$ amplitude with the Δ resonance leads to

$$T_{\pi N}^{I,l\pm}$$
$$= \frac{1}{\left(T_{\text{tree}}^{I,l\pm} + T_{\text{loop}}^{I,l\pm} + T_\Delta^{I,l\pm} + \frac{2\sqrt{s}}{E_{\mathbf{p}}+m_N}(T_{\text{LO}}^{I,l\pm})^2 g(s)\right)^{-1} + g(s)}, \quad (50)$$

which indeed fulfills Eq. (47). Note that the tree contributions $T_{\text{tree}}^{I,l\pm}$ and $T_\Delta^{I,l\pm}$ for the resonance are taken as being the full relativistic ones, whereas $T_{\text{LO}}^{I,l\pm}$ is only the very leading-order HBCHPT amplitude.

Returning to pion axioproduction, we performed a full reanalysis of the phase shift $\delta_{l\pm}^I$ defined by

$$T_{l\pm}^I(W) = \frac{8\pi W}{|\mathbf{q}|} \exp(i\delta_{l\pm}^I) \sin(\delta_{l\pm}^I) \quad (51)$$

in order to use these results for the rescattering diagram and in order to determine accurate values for the coupling constants g and z_0 of Eq. (38) and a_0 of Eq. (48). The latter goal is achieved by fitting the resulting P_{33} phase shift to the results of the Roy-Steiner analysis of the πN scattering [50]. As input values we used the isospin-averaged nucleon mass $m_N = (m_n + m_p)/2 = 938.92$ MeV, the isospin-averaged pion mass $M_\pi = 138.03$ MeV, $F_\pi = 92.4$ MeV, and $m_\Delta = 1232$ MeV. The value of g_A is given below in
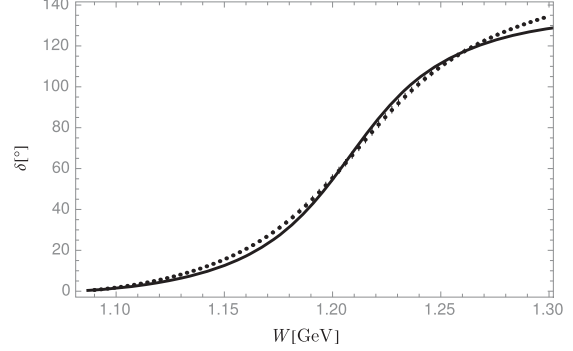
FIG. 4. The πN phase shift δ in the P_{33} channel (solid line) fitted to the results of the Roy-Steiner analysis (dots) from [50].

Sec. IV where we discuss the determination of the axion-baryon couplings, see Eq. (55). The fit to the phase shift values at $W \lesssim 1.3$ GeV yields

$$g = 1.249(16), \quad z_0 = -0.21(56), \quad a_0 = -0.959(12), \quad (52)$$

and is shown in Fig. 4.

Finally, the rescattering diagram is evaluated by

$$T_{\text{rescatt.}}^{33}(s) = \left(T_{ap\to\pi^0 p}^{33,\text{tree}}(s) g(s, M_{\pi^0}) - \frac{1}{\sqrt{2}} T_{ap\to\pi^+ n}^{33,\text{tree}}(s) g(s, M_{\pi^+}) \right) T_{\pi N}^{33}(s), \quad (53)$$

where $g(s, M_{\pi^{+,0}})$ is the pion-nucleon loop function Eq. (48) with the meson (nucleon) mass being the charged and neutral pion (neutron and proton) mass, respectively. $T_{aN\to\pi N}^{33,\text{tree}}$ denotes the partial wave projected amplitudes of Sec. III A and $T_{\pi N}^{33}$ the unitarized P_{33} partial wave amplitude just discussed. We consider the usage of the latter appropriate even though it is derived using on shell kinematics, as the off shell effects are certainly subleading [51].

The expression in the parentheses is the proper way of getting the isospin violating part of the amplitude, as discussed in Sec. II B, see Eq. (15), i.e., by taking the difference of the amplitudes and the difference in the charged and neutral pion/nucleon masses. If one neglects this mass difference, one might as well use Eq. (14) instead yielding

$$T_{\text{rescatt.}}^{33}(s) = T_{aN\to\pi N}^{33,\text{tree}}(s) g(s, M_\pi) T_{\pi N}^{33}(s), \quad (54)$$

where $T_{aN\to\pi N}^{33,\text{tree}}$ now is the $j = \frac{3}{2}$ projection of $T^{I=3/2}$, Eq. (14), and M_π is the isospin-averaged pion mass. In fact, this latter approximation gives an average deviation of only $\lesssim 2\%$ in comparison to Eq. (53), which is valid for the KSVZ axion and the DFSZ axion at $\sin^2\beta \lesssim 0.95$. Only for

values $\sin^2 \beta \to 1$ the deviation becomes more pronounced at c.m. energies $W \gtrsim 1.15$ GeV reaching a maximum of about 15%. This means that Eq. (54) is a very good approximation for the vast majority of cases.

IV. RESULTS

Let us take the last result of the previous section as a starting point for the discussion of the overall results of this study. If one indeed takes the approximation of equal pion/nucleon masses, then Eq. (12) causes that any dependence on the isoscalar couplings $g_0^i c_i$ is canceled and any dependence on the axion-nucleon coupling g_{aN} in this process reduces to a dependence on $g_A c_{u-d}$ only, which reflects that this part of the coupling enforces the isospin violation needed to enable the Δ resonance appearance. For the same reason, the diagrams of Fig. 2 with the explicit Δ solely depend on c_{u-d} and not on the c_i's. This has two consequences: First, the total amplitude for the DFSZ axion with $\sin^2 \beta$ in the interval [0, 1] and that for the KSVZ model will be $\propto c_{u-d}$; they have entirely the same shape, and only the magnitude changes as $\sin^2 \beta$ is varied. Second, as c_{u-d} only depends on the difference $X_u - X_d$, one can easily determine a value for $\sin^2 \beta$ such that $c_{u-d}^{\text{DFSZ}}(\sin^2 \beta) = c_{u-d}^{\text{KSVZ}}$, which is accomplished when $\sin^2 \beta = \frac{1}{2}$ [see Eq. (26)]. The $aN \to \pi N$ scattering amplitude in the P_{33} channel for the KSVZ axion is hence exactly the same as that for the DFSZ axion at $\sin^2 \beta = \frac{1}{2}$. As the deviation from this approximation is only $\lesssim 2\%$, this remains basically true even if one considers Eq. (53) instead of Eq. (54).

For the calculation of the final scattering amplitude, we make use of the nucleon matrix elements in order to determine the isovector and isoscalar axial-vector couplings

$$g_A = \Delta u - \Delta d,$$
$$g_0^{u+d} = \Delta u + \Delta d,$$
$$g_0^q = \Delta q, \quad \text{for } q = s, c, b, t, \tag{55}$$

where $s^\mu \Delta q = \langle p | \bar{q} \gamma^\mu \gamma_5 q | p \rangle$, with s^μ the spin of the proton. Of course, for the approximation discussed in the previous paragraph, only the value of g_A is of interest. For these matrix elements and z and w appearing in Eq. (26), we take the recent values from Ref. [52],

$$\Delta u = 0.847(50),$$
$$\Delta d = -0.407(34),$$
$$\Delta s = -0.035(13),$$
$$z = 0.485(19),$$
$$w = 0.025(1), \tag{56}$$

and ignore Δq for $q = c, b, t$.

In Fig. 5, we show the partial wave cross sections $\sigma_{aN \to \pi N}^{33}$ consisting of all the contributions discussed in Sec. III, for both with the approximation Eq. (54) and without it. Actually, the cross sections are multiplied by the factor f_a^2 in order to get rid of the unknown prefactor $1/f_a^2$. This unknown quantity also appears implicitly in the terms containing the axion mass in Eqs. (43) and (44), but has practically no effect as the axion mass $\propto 1/f_a$ can safely be neglected for the typical QCD axion window [Eq. (1)]. However, this prefactor has to be kept in mind when considering the strength of the amplitudes in Fig. 5.

As anticipated, the curves for different values of $\sin^2 \beta$ are identical up to the order of magnitude. As the absolute value of c_{u-d} is a linearly-decreasing function of $\sin^2 \beta$, the magnitude steadily decreases, which makes a DFSZ axion with $\sin^2 \beta \to 1$ the most unfavorable candidate for detection. As expected from the description at the end of the previous section, there is almost no visual deviation of the curves with approximation Eq. (54) and without it. Only for $\sin^2 \beta = 1$ this deviation becomes recognizable but is still a minor effect. Note that the figures for the limit values of $\sin^2 \beta = \{0, 1\}$ are given rather for illustrative purposes, as in realistic DFSZ models perturbative constraints from the heavy quark Yukawa couplings yield an allowed range [0.25, 170] for $\cot \beta$ [22] corresponding to approximately $\sin^2 \beta \in [0.00, 0.94]$.

As a result, there is indeed a considerable enhancement of the P_{33} partial wave cross section in the region of the Δ resonance, but this enhancement is considerably weaker than previously assumed by Carenza *et al.* [16], who estimated the cross section via $f_a^2 \sigma_{aN \to \pi N} \approx F_\pi^2 \sigma_{\pi N \to \pi N}$ taking a value of 100 mb for $\sigma_{\pi N \to \pi N}$ [53]. This estimation suggests a peak value $f_a^2 \sigma_{aN \to \pi N} \approx 1$ mb GeV^2. The discrepancy between the results of Fig. 5 and such estimation can be explained by the fact that $aN \to \pi N$ in the Δ sector is primarily an isospin breaking process, which always comes with an extra suppression. It is worthwhile to notice that the suppression of the isospin breaking here, characterized by the factor $(1 - z)/(1 + z) = (m_d - m_u)/(m_d + m_u) \approx 0.34$ for the model-independent part of c_{u-d} [see Eq. (27)], is much milder than that for usual isospin breaking in hadronic processes, characterized by $(m_d - m_u)/m_s$ or $(m_d - m_u)/\Lambda_{\text{QCD}}$. Thus, the results given in Ref. [16] are to be multiplied by a factor 10^{-1} to 10^{-5}, depending on the value of the model-dependent factor $\sin^2 \beta$, that is a suppression by at least one order of magnitude. Then the number of pions produced via $aN \to \pi N$ through the Δ resonance in a megaton water Cherenkov detector will be at most $\mathcal{O}(100)$ using the axion luminosity estimated in Ref. [16] for axions emitted from a supernova at 1 kiloparsec.

V. SUMMARY

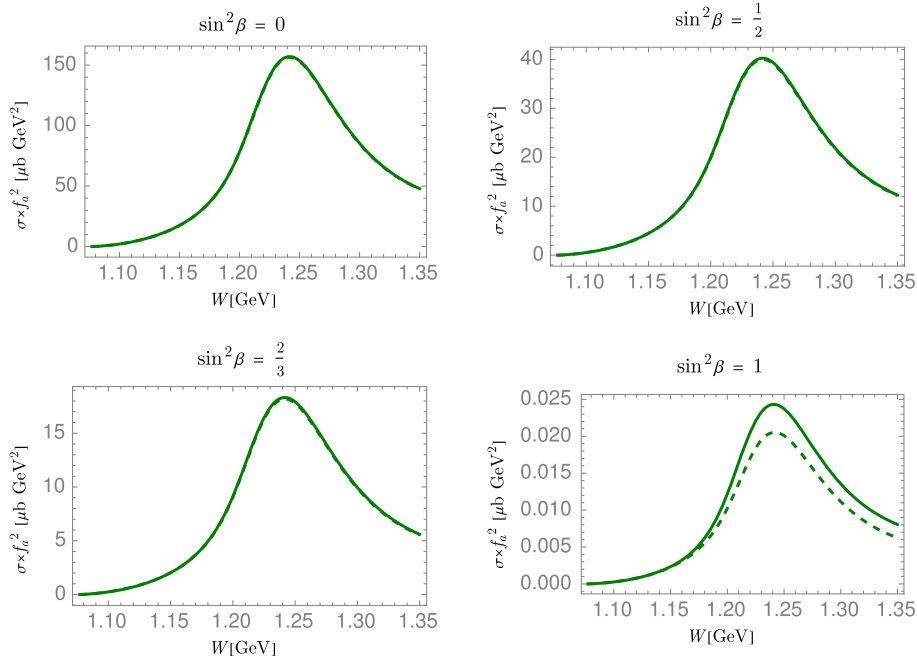In this study we presented an analysis of the pion axioproduction $aN \to \pi N$ with an intermediate Δ

FIG. 5.   The $aN \to \pi N$ partial wave cross section of the P_{33} channel versus the c.m. energy W for the DFSZ axion at different values of $\sin^2 \beta$ and the KSVZ axion (which corresponds to $\sin^2 \beta = \frac{1}{2}$, see main text). The dashed curve corresponds to the approximated case based on Eq. (54).

resonance. We included the Δ resonance in two different ways: First, we used the chiral interaction Lagrangian for the Δ to bring the axion explicitly into contact with the resonance, and, second, we used the well-known results of πN elastic scattering with Δ to include it implicitly in the form of the rescattering diagram in Fig. 3.

As the Δ is a spin-$\frac{3}{2}$ and isospin-$\frac{3}{2}$ particle, it shows its full leverage effect in the P_{33} partial wave, which is why we concentrated on a study of this particular partial wave. For the same reason, this interaction is essentially an isospin violating process, as the axion is an isosinglet. We have shown that an approximation that concentrates on this isospin violation and that neglects any isoscalar coupling, while at the same time ignoring the pion and nucleon isospin mass splittings, is still very accurate unless $\sin^2 \beta$ approaches 1 in the DFSZ axion model (where it still gives quite good results). In this way, it is shown that the partial wave amplitude for the KSVZ axion equals that for the DFSZ axion at $\sin^2 \beta = \frac{1}{2}$.

Finally, the enhancement of the amplitude anticipated by Carenza *et al.* [16] is indeed present in the region of the Δ resonance, although it is considerably weaker than their naive estimation by at least an order of magnitude. This is basically a consequence of the isospin breaking suppression which is much milder than that for usual isospin breaking hadronic processes. Therefore, it might be interesting to check whether other isospin-1/2 resonances such as the $N^*(1440)$ Roper resonance would provide an additional enhancement of the $aN \to \pi N$ cross section, as it is accessible without isospin breaking. The next step would hence be to investigate the impact of such resonances on the $aN \to \pi N$ reaction and consequently on the axion production in stellar objects, and whether this might be exploited to give fresh perspectives on experimental axion searches.

APPENDIX: AMPLITUDES OF THE LEADING-ORDER TREE GRAPHS

In this appendix we give the full expression of the leading-order tree graph amplitudes of the four $aN \to \pi N$ channels. Using the abbreviation

$$R_\mu = \frac{1}{2}(q_\mu + q'_\mu), \tag{A1}$$

the contact contribution reads

$$T^{1a}_{aN \to \pi^0 N} = 0, \tag{A2}$$

$$T^{1a}_{ap \to \pi^+ n} = \frac{c_{u-d}}{\sqrt{2}f_a F_\pi} \bar{u}(p') \slashed{R} u(p), \tag{A3}$$

$$T^{1a}_{an \to \pi^- p} = -\frac{c_{u-d}}{\sqrt{2}f_a F_\pi} \bar{u}(p') \slashed{R} u(p), \tag{A4}$$

where the superscript refers to Fig. 1. For the other two diagrams Figs. 1(b) and 1(c) one gets

$$T^{1b,1c}_{ap \to \pi^0 p} = \frac{g_A m_N g_{ap}}{f_a F_\pi} \bar{u}(p') \left\{ 1 - m_N \left(\frac{1}{s - m_N^2} - \frac{1}{u - m_N^2} \right) \slashed{R} \right\} u(p), \tag{A5}$$

$$T^{1b,1c}_{an \to \pi^0 n} = -\frac{g_A m_N g_{an}}{f_a F_\pi} \bar{u}(p') \left\{ 1 - m_N \left(\frac{1}{s - m_N^2} - \frac{1}{u - m_N^2} \right) \slashed{R} \right\} u(p), \tag{A6}$$

$$T^{1b,1c}_{ap \to \pi^+ n} = \frac{g_A}{\sqrt{2}f_a F_\pi} \bar{u}(p') \left\{ 2m_N g_0^i c_i - \left[g_A c_{u-d} + 2m_N^2 \left(\frac{g_{ap}}{s - m_N^2} - \frac{g_{an}}{u - m_N^2} \right) \right] \slashed{R} \right\} u(p), \tag{A7}$$

$$T^{1b,1c}_{an \to \pi^- p} = \frac{g_A}{\sqrt{2}f_a F_\pi} \bar{u}(p') \left\{ 2m_N g_0^i c_i + \left[g_A c_{u-d} - 2m_N^2 \left(\frac{g_{an}}{s - m_N^2} - \frac{g_{ap}}{u - m_N^2} \right) \right] \slashed{R} \right\} u(p). \tag{A8}$$

Here, g_{an} and g_{ap} are the usual axion-nucleon couplings given in Eq. (33).

[1] J. Preskill, M. B. Wise, and F. Wilczek, Cosmology of the invisible axion, Phys. Lett. **120B**, 127 (1983).

[2] L. F. Abbott and P. Sikivie, A cosmological bound on the invisible axion, Phys. Lett. **120B**, 133 (1983).

[3] M. Dine and W. Fischler, The not so harmless axion, Phys. Lett. **120B**, 137 (1983).

[4] J. Ipser and P. Sikivie, Are Galactic Halos Made of Axions?, Phys. Rev. Lett. **50**, 925 (1983).

[5] M. S. Turner, Early-Universe Thermal Production of Not-So-Invisible Axions, Phys. Rev. Lett. **59**, 2489 (1987); Erratum, Phys. Rev. Lett.**60**, 1101(E) (1988).

[6] L. D. Duffy and K. van Bibber, Axions as dark matter particles, New J. Phys. **11**, 105008 (2009).

[7] D. J. E. Marsh, Axion cosmology, Phys. Rep. **643**, 1 (2016).

[8] R. D. Peccei and H. R. Quinn, Conservation in the Presence of Pseudoparticles, Phys. Rev. Lett. **38**, 1440 (1977).

[9] R. D. Peccei and H. R. Quinn, Constraints imposed by CP conservation in the presence of pseudoparticles, Phys. Rev. D **16**, 1791 (1977).

[10] S. Weinberg, A New Light Boson?, Phys. Rev. Lett. **40**, 223 (1978).

[11] F. Wilczek, Problem of Strong P and T Invariance in the Presence of Instantons, Phys. Rev. Lett. **40**, 279 (1978).

[12] J. E. Kim, Weak Interaction Singlet and Strong CP Invariance, Phys. Rev. Lett. **43**, 103 (1979).

[13] M. A. Shifman, A. I. Vainshtein, and V. I. Zakharov, Can confinement ensure natural CP invariance of strong interactions?, Nucl. Phys. **B166**, 493 (1980).

[14] M. Dine, W. Fischler, and M. Srednicki, A simple solution to the strong CP problem with a harmless axion, Phys. Lett. **104B**, 199 (1981).

[15] A. R. Zhitnitsky, On possible suppression of the axion hadron interactions. (In Russian), Sov. J. Nucl. Phys. **31**, 260 (1980).

[16] P. Carenza, B. Fore, M. Giannotti, A. Mirizzi, and S. Reddy, Enhanced Supernova Axion Emission and its Implications, Phys. Rev. Lett. **126**, 071102 (2021).

[17] We use the term axioproduction in analogy to terms like electroproduction or photoproduction. Pion axioproduction hence means pion production induced by axions.

[18] T. Fischer, P. Carenza, B. Fore, M. Giannotti, A. Mirizzi, and S. Reddy, Observable signatures of enhanced axion

emission from protoneutron stars, Phys. Rev. D **104**, 103012 (2021).

[19] J. E. Kim, Light pseudoscalars, particle physics and cosmology, Phys. Rep. **150**, 1 (1987).

[20] J. E. Kim and G. Carosi, Axions and the strong *CP* problem, Rev. Mod. Phys. **82**, 557 (2010); Erratum, Rev. Mod. Phys. **91**, 049902(E) (2019).

[21] Z.-Y. Lu, M.-L. Du, F.-K. Guo, U.-G. Meißner, and T. Vonk, QCD θ-vacuum energy and axion properties, J. High Energy Phys. 05 (2020) 001.

[22] L. Di Luzio, M. Giannotti, E. Nardi, and L. Visinelli, The landscape of QCD axion models, Phys. Rep. **870**, 1 (2020).

[23] G. Grilli di Cortona, E. Hardy, J. Pardo Vega, and G. Villadoro, The QCD axion, precisely, J. High Energy Phys. 01 (2016) 034.

[24] T. Vonk, F.-K. Guo, and U.-G. Meißner, Precision calculation of the axion-nucleon coupling in chiral perturbation theory, J. High Energy Phys. 03 (2020) 138.

[25] T. W. Donnelly, S. J. Freedman, R. S. Lytel, R. D. Peccei, and M. Schwartz, Do axions exist?, Phys. Rev. D **18**, 1607 (1978).

[26] D. B. Kaplan, Opening the axion window, Nucl. Phys. **B260**, 215 (1985).

[27] M. Srednicki, Axion couplings to matter. 1. *CP* conserving parts, Nucl. Phys. **B260**, 689 (1985).

[28] H. Georgi, D. B. Kaplan, and L. Randall, Manifesting the invisible axion at Low-energies, Phys. Lett. **169B**, 73 (1986).

[29] S. Chang and K. Choi, Hadronic axion window and the big bang nucleosynthesis, Phys. Lett. B **316**, 51 (1993).

[30] N. Fettes and U.-G. Meißner, Towards an understanding of isospin violation in pion nucleon scattering, Phys. Rev. C **63**, 045201 (2001).

[31] M. Hoferichter, B. Kubis, and U.-G. Meißner, Isospin violation in low-energy pion-nucleon scattering revisited, Nucl. Phys. **A833**, 18 (2010).

[32] Note the typo in Ref. [24], Eq. (3.16). $\tilde{u}_{\mu,i}$, which corresponds to $u_{\mu,i}$ in the present paper, is of course not $\propto \tau_3$, but $\propto \mathbb{1}$.

[33] S. Weinberg, Phenomenological lagrangians, Physica A (Amsterdam) **96A**, 327 (1979).

[34] V. Bernard, N. Kaiser, and U.-G. Meißner, Chiral dynamics in nucleons and nuclei, Int. J. Mod. Phys. E **04**, 193 (1995).

[35] K. Choi, H. J. Kim, H. Seong, and C. S. Shin, Axion emission from supernova with axion-pion-nucleon contact interaction, J. High Energy Phys. 02 (2022) 143.

[36] E. E. Jenkins and A. V. Manohar, Chiral corrections to the baryon axial currents, Phys. Lett. B **259**, 353 (1991).

[37] H.-B. Tang and P. J. Ellis, Redundance of Δ-isobar parameters in effective field theories, Phys. Lett. B **387**, 9 (1996).

[38] T. R. Hemmert, B. R. Holstein, and J. Kambor, Heavy baryon chiral perturbation theory with light deltas, J. Phys. G **24**, 1831 (1998).

[39] V. Pascalutsa and D. R. Phillips, Effective theory of the $\Delta(1232)$ resonance in Compton scattering off the nucleon, Phys. Rev. C **67**, 055202 (2003).

[40] C. Hacker, N. Wies, J. Gegelia, and S. Scherer, Including the Delta(1232) resonance in baryon chiral perturbation theory, Phys. Rev. C **72**, 055203 (2005).

[41] H. Krebs, E. Epelbaum, and U.-G. Meißner, On-shell consistency of the Rarita-Schwinger field formulation, Phys. Rev. C **80**, 028201 (2009).

[42] H. Krebs, E. Epelbaum, and U.-G. Meißner, Redundancy of the off-shell parameters in chiral effective field theory with explicit spin-3/2 degrees of freedom, Phys. Lett. B **683**, 222 (2010).

[43] V. Pascalutsa, M. Vanderhaeghen, and S. N. Yang, Electromagnetic excitation of the Delta(1232)-resonance, Phys. Rep. **437**, 125 (2007).

[44] U.-G. Meißner and J. A. Oller, Chiral unitary meson baryon dynamics in the presence of resonances: Elastic pion nucleon scattering, Nucl. Phys. **A673**, 311 (2000).

[45] J. A. Oller and U.-G. Meißner, Chiral dynamics in the presence of bound states: Kaon nucleon interactions revisited, Phys. Lett. B **500**, 263 (2001).

[46] As the diagrams of Fig. 2 and the corresponding diagrams of πN scattering are basically the same, the result of Ref. [44] can also be found by replacing $m_a \to M_\pi$ in Eqs. (43) and (44), adjusting of course the coupling constants in front.

[47] N. Fettes, U.-G. Meißner, and S. Steininger, Pion—nucleon scattering in chiral perturbation theory. 1. Isospin symmetric case, Nucl. Phys. **A640**, 199 (1998).

[48] G. F. Chew and S. Mandelstam, Theory of low-energy pion pion interactions, Phys. Rev. **119**, 467 (1960).

[49] J. A. Oller, Unitarization technics in hadron physics with historical remarks, Symmetry **12**, 1114 (2020).

[50] M. Hoferichter, J. Ruiz de Elvira, B. Kubis, and U.-G. Meißner, Roy–Steiner-equation analysis of pion–nucleon scattering, Phys. Rep. **625**, 1 (2016).

[51] M. Mai and U.-G. Meißner, New insights into antikaon-nucleon scattering and the structure of the Lambda(1405), Nucl. Phys. **A900**, 51 (2013).

[52] Y. Aoki *et al.*, FLAG review 2021, arXiv:2111.09849.

[53] The $\pi^+ p$ elastic cross section is the largest around the Δ resonance region, of about 100 mb [54].

[54] P. A. Zyla *et al.* (Particle Data Group), Review of particle physics, Prog. Theor. Exp. Phys. **2020**, 083C01 (2020).

176

Acknowledgments